



A University of Sussex DPhil thesis

Available online via Sussex Research Online:

<http://sro.sussex.ac.uk/>

This thesis is protected by copyright which belongs to the author.

This thesis cannot be reproduced or quoted extensively from without first obtaining permission in writing from the Author

The content must not be changed in any way or sold commercially in any format or medium without the formal permission of the Author

When referring to this work, full bibliographic details including the author, title, awarding institution and date of the thesis must be given

Please visit Sussex Research Online for more information and further details

University of Sussex

Investigation of The Sn-P Bond and Related Studies

Submitted for the degree of DPhil

September 2010

Steven Mark Wilcock

I hereby declare that the studies described in this thesis are the sole work of the author, and have not been previously submitted, either in the same or any other form, for a degree to this or any other university.

Steven Mark Wilcock

Acknowledgements

First and foremost I would like to thank Gerry Lawless for all his help and advice over the past four years, without which none of this would have been possible. I wish him the best of luck in America and feel sure the department will be a poorer place for his absence. I'd also like to thank John Nixon whose insights both in and out of group meetings were invaluable and with whom, if all goes to plan, I shall hopefully be able to collaborate further. Also deserving a special mention is Martyn Coles, if only for the sheer number of roles he's played in my university career (personal tutor, MChem supervisor, 2nd DPhil supervisor, Christmas bowling rival, etc...), truly a man for all seasons.

I owe a huge debt of thanks to all the following friends and colleagues that have kept me going through the process. To my good friend Bill, a fellow of infinite jest, of most excellent fancy, and a kindred spirit with whom I could happily converse indefinitely on myriad topics. To my two long term office mates Ben, whose facial hair officially makes him less trustworthy and more flammable than me, and Dan, who despite all the trouble he's put me to has helped me in so many ways, especially in my final week. To Zoë, who over the past few years has become barely recognisable as the timid little girl who was too scared to eat lunch with me when we first met, and Joy, who's been alongside me since the very beginning nearly eight years ago and has provided some much needed consistency throughout the whole process. To my former group members Ian, who's been a fantastic help for all manner of things in the lab (you're on your own with the glovebox from now on), Chris, who convinced me that getting a doctorate was well within my reach, and Matt, who helped me find my feet in the early days and then abandoned me after about six weeks. Thanks to all the various

undergrads who didn't help my productivity at all but made the time a lot more fun. Fran, who was endlessly entertaining whether at the cinema, laughing at fat children on the bus or providing unique artwork for my lab bench. Róisín, whose irrepressible nature and flair with a paint pen has left the face of our office permanently altered. My Arab friends Dana and Juman, who assure me my birthday is celebrated annually in their homeland as a national holiday. Thanks to Krissy, who put a roof over my head when I would otherwise have been homeless, and Tara, Gemma and Caroline for putting up with me for a month (and again, sorry for not helping with your luggage Tara). Thanks to all my longer serving housemates who helped me get away from work at the end of the day, Matt, Vicki, Nic and Liz, all of whom made temporary houses feel like homes.

I would also like to thank all those people who've made a far more practical contribution to my work. To Iain for all his NMR help, both in running spectra and explaining the finer points. To Ali for the mass spec and Peter and Martyn (again) for the X-ray diffraction. Thanks to Dave, Gill and Billy for keeping me well supplied, to Mick and Fran for letting me steal all manner of equipment from the teaching labs and to Roger and Ken for making a broken vacuum line mean a lost morning and not a lost week.

Finally I'd like to thank my parents. Without them I wouldn't be where I am today, they not only supplied me with the brilliant genes I possess, but have supported me throughout everything I've done and with only a minimum of nagging (which I'm aware must have taken a huge amount of self restraint).

Abstract

This thesis reports the synthesis and analysis of a number of organometallic compounds, focusing primarily on novel structures containing Sn and P atoms.

Chapter 1 contains a literature review examining the different structural and bonding properties and reactions of C_4H_4 , P_4 and $P_2C_2R_2$.

Chapter 2 describes the ability of the $P_2C_2^tBu_2$ ligand to cause a reductive elimination in Sn(IV) species. Several different products from the reaction between Me_2SnCl_2 and $Cp_2Zr(P_2C_2^tBu_2)$ are determined, and mechanisms for their interconversion are proposed. The synthesis of $Sn(P_2C_2Ad_2)$ is reported along with its unprecedentedly low frequency ^{119}Sn NMR spectroscopic chemical shift.

Chapter 3 contains attempts to produce transition metal complexes with phosphalkyne based ligands. The crystal structure of a complex containing Fe and Zr centres with two $P_2C_2Ad_2$ rings is reported along with analysis of its paramagnetism. Mechanisms for the exchange of $P_2C_2R_2$ rings and chlorides are also proposed.

Chapter 4 details the synthesis of a range of Cp_nSnI_m species and a comparison of their solid and solution state structures using X-ray diffraction and NMR spectroscopy. Reactions between these compounds and $P(SiMe_3)_3$ or $LiP(SiMe_3)_2$ are performed in order to explore the possibility of forming a Sn-P multiple bond.

Chapter 5 outlines the synthesis of bicyclic systems based on $C_6H_4-1,2-(PH_2)_2$ and Sn and Ge dialkyls. The effect of alkyl group bulk on product structure is investigated.

Chapter 6 explores the reaction between $C_6H_4-1,2-(PH_2)_2$ and $P(SiMe_3)_3$ in which an exchange of H and $SiMe_3$ groups occurs. The mechanism of the reaction is elucidated by the introduction of a catalytic proton source.

Contents

Acknowledgements	i
Abstract	iii
Contents	iv
List of Abbreviations.....	viii
Chapter 1	1
A Literature Review on the Structure and Bonding of C_4H_4 , P_4 and $P_2C_2R_2$	1
Chapter 2	25
Sn Complexes Containing the $P_2C_2R_2$ Ligand	25
2.1: Introduction.....	25
2.2: Results and Discussion	34
Reaction of $Cp_2Zr(P_2C_2^tBu_2)$ with Me_2SnCl_2	35
Reaction of $Cp_2Zr(P_2C_2^tBu_2)$ with two equivalents of Me_2SnCl_2	41
Synthesis of Product C (2.3)	48
Synthesis of $[Me_2Sn(P_2C_2^tBu_2)]_2$ (2.4).....	59
Attempted Reaction of $Cp_2Zr(P_2C_2Ad_2)$ with Me_2SnCl_2	64
Reaction of $Cp_2Zr(P_2C_2Ad_2)$ with $SnCl_2$	65
2.3: Conclusions.....	68
References	69

Chapter 3	71
The Synthesis of Transition-Metal Phosphaalkyne Complexes.....	71
3.1: Introduction.....	71
3.2: Results and Discussion	81
Reaction of $\text{TiCl}_4 \cdot 2\text{THF}$ with $\text{Cp}_2\text{Zr}(\text{P}_2\text{C}_2^t\text{Bu}_2)$	82
Reaction of $\text{TiCl}_3 \cdot 3\text{THF}$ with $\text{Cp}_2\text{Zr}(\text{P}_2\text{C}_2\text{Ad}_2)$	83
Reaction of Cp_2TiCl_2 with Mg and AdCP	84
Reaction of product B with C_2Cl_6	89
Reaction of FeCl_2 with $\text{Cp}_2\text{Zr}(\text{P}_2\text{C}_2\text{Ad}_2)$	92
3.3: Conclusions.....	99
References	100
 Chapter 4	 104
Investigating Cyclopentadienyl Tin Halides as Potential Precursors for $\text{Sn}=\text{P}$ Bonds.	104
4.1: Introduction.....	104
4.2: Results and Discussion	114
Synthesis of Cp^*SnI_3 (4.1).....	114
Synthesis of $\text{Cp}^{\text{Me}^4}_2\text{SnI}_2$ (4.2).....	116
Reaction between KCp^* , SnI_4 and $\text{P}(\text{SiMe}_3)_3$	119
Synthesis of Cp^sSnI_3 (4.4)	125
Reaction Between Cp^sSnI_3 and $\text{P}(\text{SiMe}_3)_3$	128
Reaction Between Cp^sSnI_3 and $\text{LiP}(\text{SiMe}_3)_2$	130
4.3: Conclusions.....	134
References	135

Chapter 5	137
Using Bis(phosphino)benzene to Produce New Group 14 Heterocycles.....	137
5.1: Introduction.....	137
5.2: Results and Discussion	147
Synthesis of $C_6H_4-1,2-P_2(\mu-SnMe_2)(\mu^2-Sn_2Me_4)$ (5.1)	148
Synthesis of $C_6H_4-1,2-(PH)_2(\mu-Sn^tBu_2)$ (5.2)	158
Synthesis of $C_6H_4-1,2-(PH)_2(\mu-GeMe_2)$ (5.3)	167
5.3: Conclusions.....	171
References	172
 Chapter 6	 174
The Exchange of Protons and Trimethylsilyl Groups Between Phosphines.....	174
6.1: Introduction.....	174
6.2: Results and Discussion	180
6.3: Conclusions.....	194
 Experimental	 196
General Details.....	196
Starting materials	198
Experimental Procedures	200
Synthesis of $Me_2Sn(P_2C_2^tBu_2)SnMe_2Cl_2$ (2.1).....	200
Synthesis of $Me_2Sn(P_2C_2^tBu_2)$ (2.2).....	201
Synthesis of $Me_2SnCl(P_2C_2^tBu_2)H$ (2.3)	202
Synthesis of $[Me_2Sn(P_2C_2^tBu_2)]_2$ (2.4).....	203
Synthesis of $Sn(P_2C_2Ad_2)$ (2.5).....	204

Synthesis of $\text{TiCp}_2(\text{AdCP})_3$ (3.1)	204
Synthesis of $\text{ZrCp}(\text{P}_2\text{C}_2\text{Ad}_2)\text{Cl}_2\text{Fe}(\text{P}_2\text{C}_2\text{Ad}_2)$ (3.3)	205
Evans' Method NMR Spectroscopic Study of $\text{CpZr}(\text{P}_2\text{C}_2\text{Ad}_2)\text{Cl}_2\text{Fe}(\text{P}_2\text{C}_2\text{Ad}_2)$..	206
Synthesis of $\text{Cp}^{\text{Me}^4}_2\text{SnI}_2$ (4.2).....	206
Synthesis of Cp^*SnI (4.3)	207
Synthesis of $\text{Cp}^{\text{S}}\text{SnI}_3$ (4.4)	208
Synthesis of $\text{C}_6\text{H}_4\text{P}_2(\text{SnMe}_2)_3$ (5.1).....	209
Synthesis of $\text{C}_6\text{H}_4\text{P}_2(\text{SnMe}_2)(\text{SnMe}_2\text{Cl})_2$ (5.1b)	210
Synthesis of $\text{C}_6\text{H}_4(\text{PH})_2\text{Sn}^t\text{Bu}_2$ (5.2)	211
Synthesis of $\text{C}_6\text{H}_4(\text{PH})_2\text{GeMe}_2$ (5.3).....	212
Substituent exchange between $\text{Bn}(\text{PH}_2)_2$ and $\text{P}(\text{SiMe}_3)_3$	214
References	215

List of Abbreviations

Ad	Adamantyl
Å	Angstrom(s) = 10^{-10} m
Benzene-d ⁶	C ₆ D ₆
BM	Bohr magneton = 9.27402×10^{-24} J T ⁻¹
ⁿ Bu	<i>Normal</i> -butyl
^t Bu	<i>Tertiary</i> -butyl
Cp	C ₅ H ₅
Cp*	C ₅ Me ₅
Cp ^{Me4}	C ₅ Me ₄ H
Cp ^S	C ₅ Me ₄ (SiMe ₂ ^t Bu)
δ	Chemical shift
d	Doublet
DME	Dimethoxyethane
DMF	Dimethylformamide
E	Undefined main group element
EI	Electron impact
Et	Ethyl
{ ¹ H}	¹ H decoupled
IR	Infrared
<i>J</i>	Spin-spin coupling constant
kcal	Kilocalorie(s)
m	Multiplet
M	Undefined metal

M^+	Parent molecular ion
MVS	Metal vapour synthesis
Me	Methyl
ml	Millilitre(s)
$\nu_{1/2}$	Resonance width at half maximum height
NMR	Nuclear magnetic resonance
Ph	Phenyl
R	Undefined organic substituent
s	Singlet
$^{117/119}\text{Sn}$	Average of ^{117}Sn and ^{119}Sn isotopes
t	Triplet
THF	Tetrahydrofuran ($\text{C}_4\text{H}_8\text{O}$)
THF- d^8	Deuterated tetrahydrofuran ($\text{C}_4\text{D}_8\text{O}$)
TMS	Tetramethylsilane
u	Atomic mass unit(s)
X	Undefined substituent

Chapter 1

A Literature Review on the Structure and

Bonding of C_4H_4 , P_4 and $P_2C_2R_2$

When the aromatic nature of benzene was identified over 100 years ago, it sparked the imaginations of synthetic chemists to produce other carbon-based aromatic systems. The features defining an aromatic system are well known, *i.e.*, the presence of a planar, cyclic system with a delocalisation of $4n + 2$ electrons resulting in an inherent stability and uniformity of bonding around the ring. The first attempts were directed towards the synthesis of both eight and four membered rings. Whilst cyclooctatetraene was produced with relative ease, cyclobutadiene posed a multitude of challenges. With respect to its molecular orbitals the four p_z orbitals of each C combine to produce one bonding orbital, one anti-bonding orbital and two degenerate non-bonding orbitals. These molecular orbitals contain four electrons, the lowest energy (bonding) orbital is fully populated and each of the degenerate non-bonding orbitals contains one unpaired electron. (Figure 1.1)¹

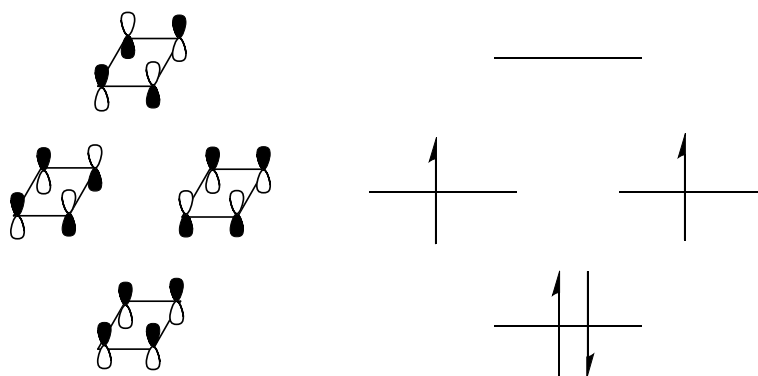


Figure 1.1: Frontier molecular orbitals of cyclobutadiene (simplified)

This di-radical nature coupled with the strained geometry of the four-membered ring result in an inherently unstable molecule which reacts almost immediately upon formation, either in the presence of additional reagents, or in their absence, will rapidly dimerise to form tricyclooctadiene.² The transient nature of cyclobutadiene made structural analysis of the molecule impossible and debate over whether it adopted a square or rectangular structure remained unresolved for several decades. Eventually, the advent of matrix isolation techniques meant that single molecules of cyclobutadiene could be trapped and studied by infrared spectroscopy which identified its alternate single- and double-bonded structure.³

In the interim, however, organometallic chemists followed a different route. In 1956, Longuet-Higgins and Orgel predicted that cyclobutadiene could be stabilised within the coordination sphere of a transition metal in a similar fashion to the already known cyclopentadienyl ligands.⁴ The stabilisation they predicted would be achieved by increasing the number of π -electrons from four to six. Thus both would meet the Hückel criterion of $4n + 2$ electrons and would have a stable aromatic system. For the cyclopentadienyl ligand this involves a formal transfer of one electron from the metal centre whereas filling each of the two non-bonding orbitals of the cyclobutadienyl ligand requires two. Their predictions were quickly proved correct from experimentally isolated complexes containing substituted cyclobutadienyl ligands such as tetraphenylcyclobutadieneirontricarbonyl (I),⁵ tetramethylcyclobutadienenickel chloride (II),⁶ and cyclobutadieneirontricarbonyl (III).⁷ (Figure 1.2)

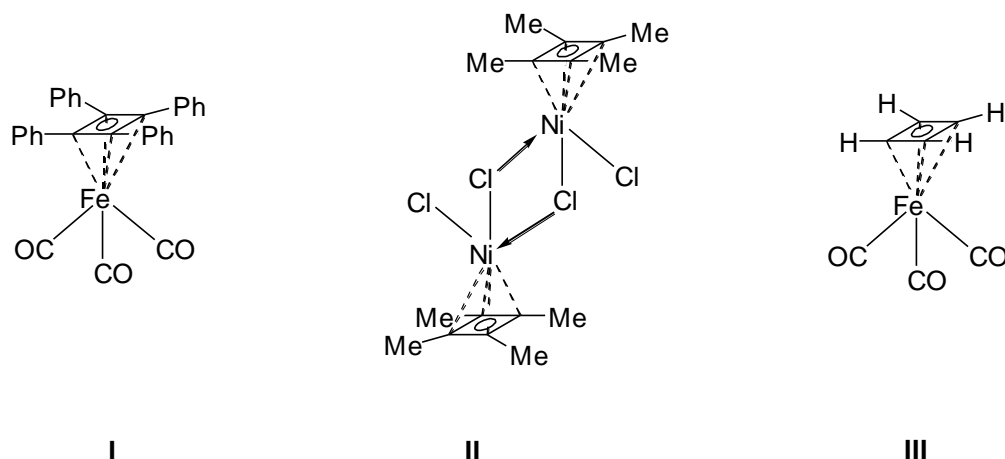
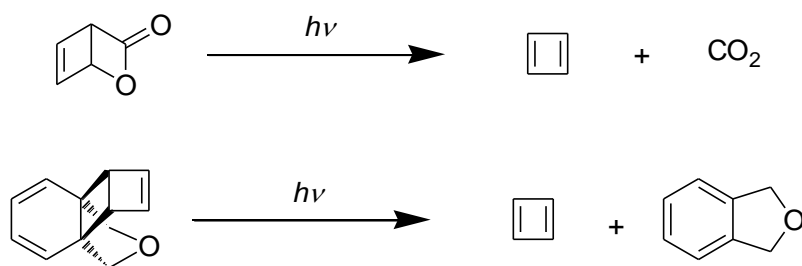


Figure 1.2: Early cyclobutadienyl complexes

All three of these complexes have since been shown by single crystal X-ray diffraction to have four equal length ring C-C bonds indicating that they are in fact aromatic.⁸⁻¹⁰

Since they were first produced around fifty years ago, *circa* 500 molecular structures have been published featuring an aromatised cyclobutadienyl metal fragment. In comparison, there are currently over 38,500 structures based on a metal coordinated cyclopentadiene.¹¹ This discrepancy is due to the relative instability of the cyclobutadiene precursor. Whilst the typical Diels-Alder dimerisation of the cyclopentadiene molecules¹² can be prevented by converting them into aromatic alkali metal salts, there is no equivalent stabilisation technique for their cyclobutadienyl analogues, unless they possess multiple substituents such as ester or phenyl groups to disperse the double negative charge.¹³ This is why the cyclobutadienyl ring must be produced *in situ*, usually by elimination reactions from larger molecules, prior to coordination to a metal centre.^{3,14} (Scheme 1.1)



Scheme 1.1: Examples of cyclobutadiene formed via photolysis

The complications which arise from this *in situ* step, such as the reactivity of any side products, make the cyclobutadienyl ligand far less attractive to synthetic organometallic chemists.

In spite of these intrinsic difficulties, or maybe because of them, cyclobutadiene continues to fascinate theoretical and synthetic chemists alike. Whilst it may not have the same ubiquitous appeal as cyclopentadienyl, complexes containing cyclobutadienyl groups are still regularly reported.^{15,16} One area of research involving cyclobutadiene that has proven even more fertile in recent years however, is the calculation of its thermochemical properties, specifically its antiaromaticity.¹⁷ As previously mentioned, cyclobutadiene is a very unstable molecule, but this instability is due to multiple factors and determining the contribution from each remains a challenge. It was not until 2006 that an accurate value was determined for the heat of formation of cyclobutadiene at $429 \pm 16 \text{ kJmol}^{-1}$,¹⁸ in turn leading to a calculation of a total destabilisation energy of $316 \pm 16 \text{ kJmol}^{-1}$.¹⁷ This value though is an inseparable mix of both ring strain factors and antiaromaticity. The notion of ring strain serves more as a description of effects than a property that can be easily assigned to any particular steric feature. In the case of cyclobutadiene there appear to be two predominant factors which are responsible for the ring strain,¹⁷ the most obvious being found in the C-C-C bond angles. The ideal angle for sp^2 hybridised carbon atoms would be 120° , but the rectangular shape of the ring

means that all of the angles are 90° , representing a considerable deviation. The second major cause of ring strain is due to the close proximity of the two localised π -bonds. In a molecule of cyclobutadiene, the double bonds are forced closer to each other than in any other molecule.¹⁹ The repulsion between these two π -bonds is believed to be the reason that the calculated length of the single bonds is 0.1 \AA longer than the open chain butadiene.²⁰ These two steric strains contribute to a significant portion of the overall destabilisation energy of cyclobutadiene, but the exact figure is unknown. As a result, estimates of the antiaromatic contribution to the destabilisation energy are subject to a large degree of uncertainty, with reported values ranging from 44 kJmol^{-1} to 230 kJmol^{-1} ,^{21,22} with no definitive method yet established to determine a single value.

Before the advent of data from molecular structure studies or IR spectroscopy, it was proposed that C_4H_4 molecule might have a tetrahedral structure.²³ With all the evidence now available this may seem like a completely unfeasible premise, but it is not entirely illogical. In numerous instances it has been shown that the isolobal relationship between the CH fragment and a phosphorus atom allows one to substitute for the other.²⁴ Therefore, considering the tetrahedral structure of white phosphorus - P_4 (IV), the existence of tetrahedrane (V) seems entirely plausible. It has been well established, however, that the two molecules do not form analogous structures. Whilst some sterically protected tetrahedranes are known,²⁵ the unsubstituted form is not, and neither is free tetraphosphacyclobutadiene (VI) (although as with cyclobutadiene (VII), the aromatic dianion has been captured on a metal centre with the associated aromaticity providing the stabilisation).²⁶

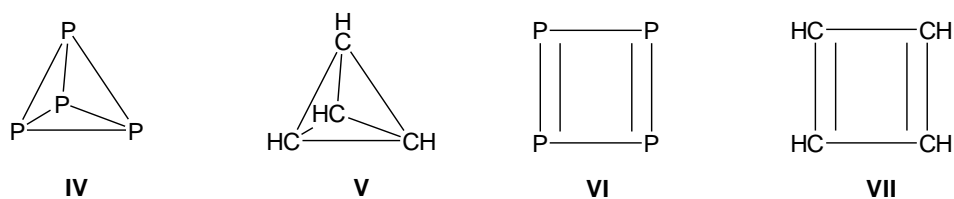


Figure 1.3: The differing structures of C_4H_4 and P_4 , with their theoretical analogues

There are a number of factors which are likely contribute to this disparity between the possible isomers, such as bond length and orbital hybridisation, but the structure seems to ultimately be determined by balancing the energy difference between the saturated and unsaturated forms and the increased strain of the three membered over the four membered rings. In both instances the tetrahedral structure is more strained than the planar diene. However, because the two π bonds of the diene are weaker than the two σ bonds of the tetrahedral structure, the sum of the bond energies diene would suggest a relatively higher energy state.²⁷

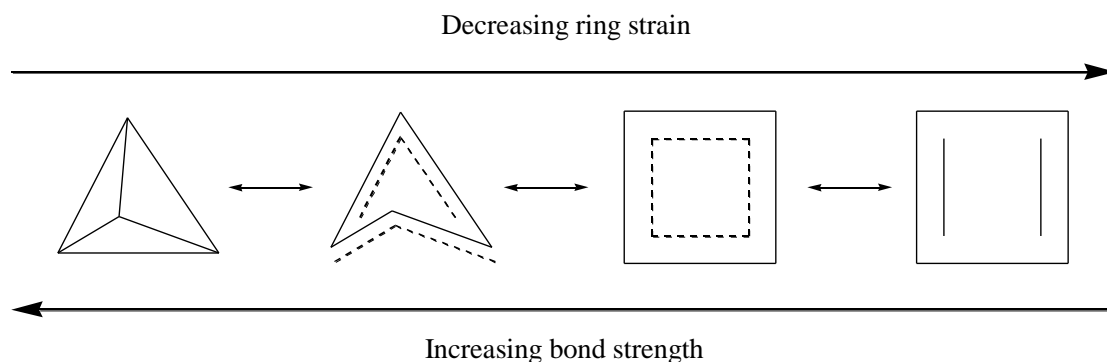
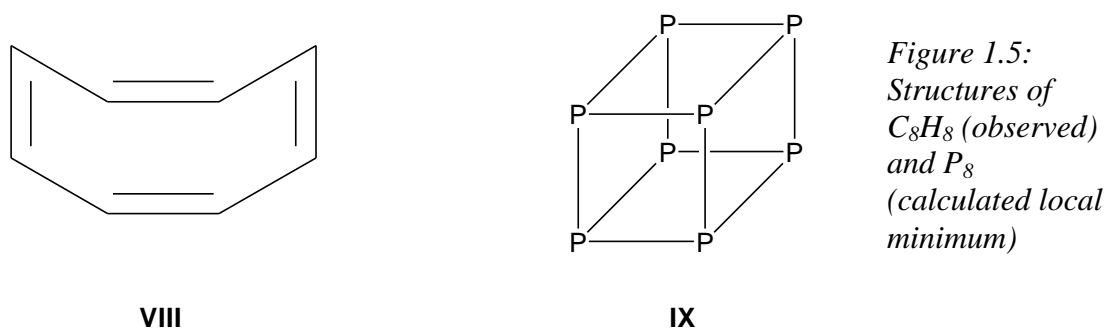


Figure 1.4: Tautomerisation between structures of P_4/C_4H_4 and the relevant driving forces.

Because the difference between the energies of σ and π bonds increases down the periodic table as p-orbital overlap decreases, the increased energy of the P based diene is too great to be offset by the reduction in ring strain.²⁸ Conversely, in the case of carbon the bond energy difference is less than experienced with P, ultimately meaning

that the diene structure is adopted due to its favourable geometry.²⁹ The tendency for phosphorus based molecules to form saturated cages rather than the unsaturated rings favoured by the equivalent CH molecules is also evident in the eight membered systems, cyclooctatetraene (VIII)³⁰ and the P₈ phosphorus cube (IX) which is calculated to lie at a local energy minimum.³¹ (Figure 1.5)



Some of this structural dissimilarity can also be found in the relevant metal complexes. The existence of cyclobutadienyl complexes has already been discussed and it has been shown that the P₄ can be aromatised in forming a metal complex.²⁶ However, there are examples of the tetrahedral P₄ bound to a metal³² through the breaking of one of the P-P bonds in what can be viewed as an oxidative addition. No analogous compounds of C₄H₄ are known.

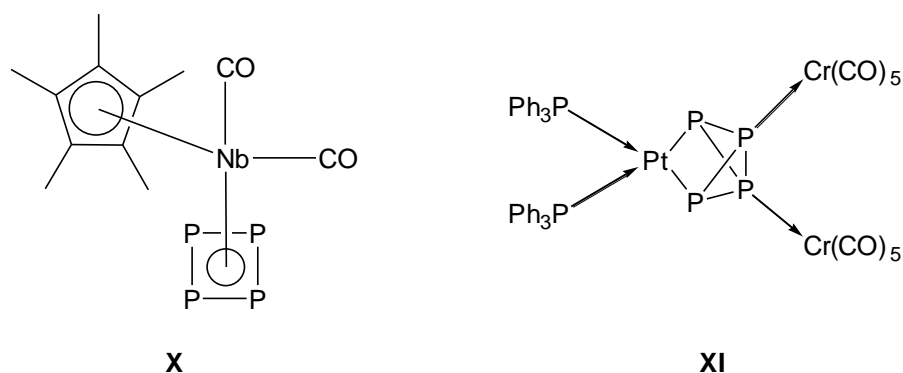
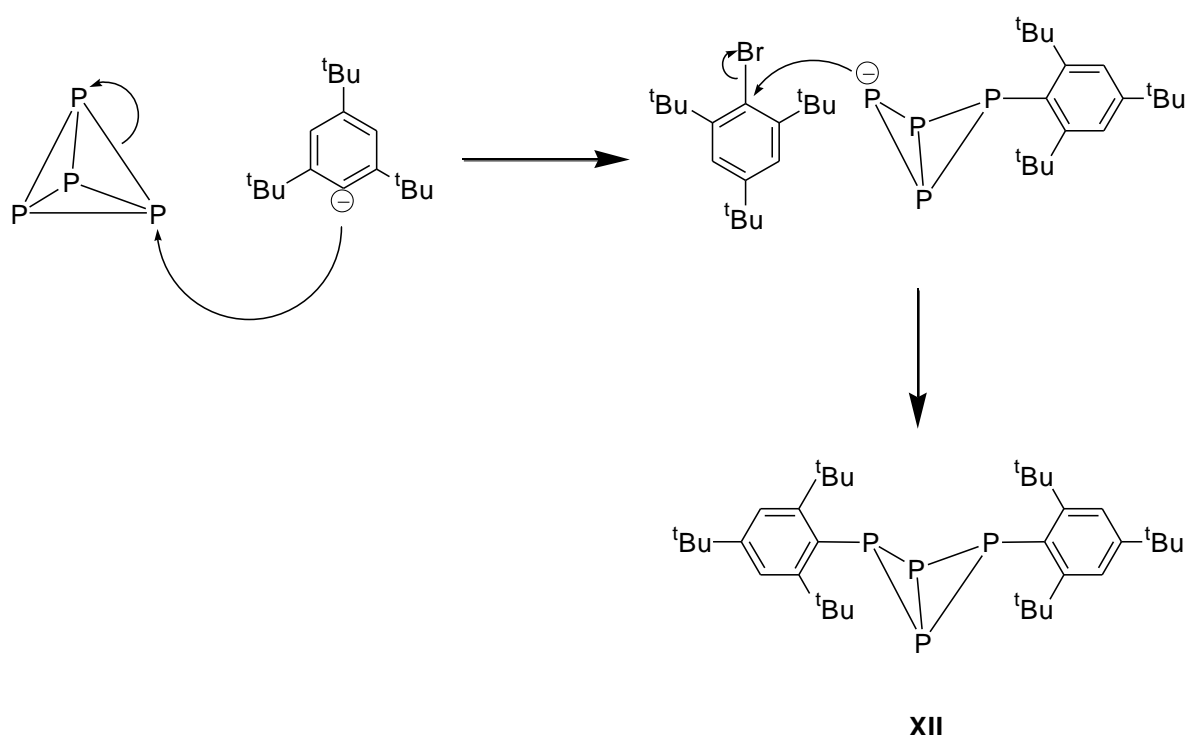


Figure 1.6: Planar and tetrahedral P₄ complexes

In addition to the formation of transition metal complexes, the activation of P_4 by main group compounds has been widely explored.³³ The P_4 unit is most susceptible to nucleophilic attack by negatively charged species which breaks one of the bonds, opening the tetrahedron to form the butterfly-like structure. Using a bulky nucleophile and electrophile the P_4 can be trapped in this open form.³⁴ (Scheme 1.2)



Scheme 1.2: Activation of P_4 by bulky aryl nucleophile and electrophile.

Without the steric stabilisation though, repeated attack on the P_4 unit is more commonly observed, leading to the formation of a mixture of P_1 species.³⁵ For example, the reaction between P_4 and sodium hydroxide will ultimately yield hydrogen, phosphine and sodium hypophosphite.

Perhaps more interesting though are the activations by low coordinate main group atoms. Compounds such as carbenes or monovalent group 13 elements can be

viewed as either possessing a lone pair of electrons and an unoccupied orbital,³⁶ or having both a positive and negative charge. This dual nature allows them to act both as nucleophile and electrophile, in theory enabling the activation of P_4 without additional quenching reagents by inserting into the P-P bond and forming what could be described as a bridged butterfly structure.³³ Subsequent reactions then convert this into a variety of different forms determined by the activating element and its substituents. In the case of monovalent aluminium, for example, using the bulky nacnac ligand $[HC(CMeN(2,6-iPr_2C_6H_3))_2Al]$ causes an insertion into two bonds forming opposite edges of the tetrahedron.³⁷ This leaves the phosphorus atoms in a puckered four membered ring between the two aluminium atoms. If a less bulky substituent such as Cp^* is used, the result is a complete separation of the phosphorus atoms into the alternating P-Al structure shown, where the Cp^* ligands are η^5 apart from those of the aluminium atoms bound to three phosphorus atoms which are η^1 .³⁸ (Figure 1.7)

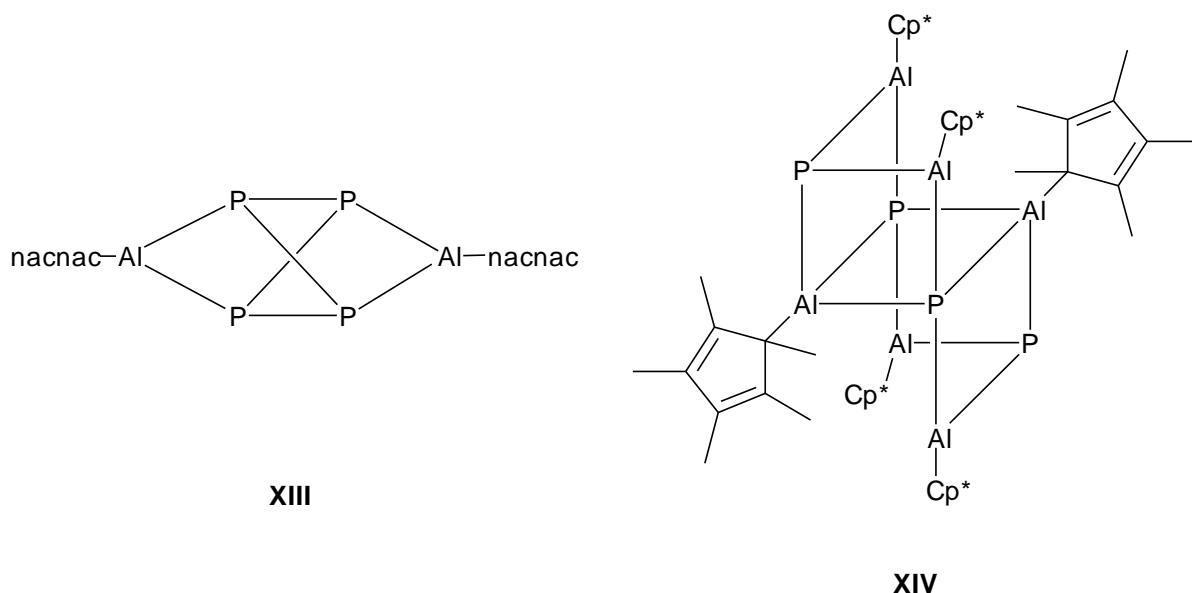


Figure 1.7: Products of insertion of monovalent aluminium species into P_4 .

In a similar fashion, the monovalent gallium species $\text{Ga}_4[\text{C}(\text{SiMe}_3)_3]_4$ has been shown to insert into three of the bonds around a single phosphorus to produce a structure similar to nortricyclane.³⁹ This is in contrast to the behaviour of the fully oxidised Ga(III) compound ${}^t\text{Bu}_3\text{Ga}$ which no longer possessing the potential to undergo an oxidative addition by insertion into the P-P bond, adds across the bond.⁴⁰ This opens the tetrahedron to form the butterfly structure as previously seen, but as the Ga is a Lewis acid the lone pair of electrons on the newly formed alkyl phosphorus coordinates to it forming a bridged structure. (Figure 1.8)

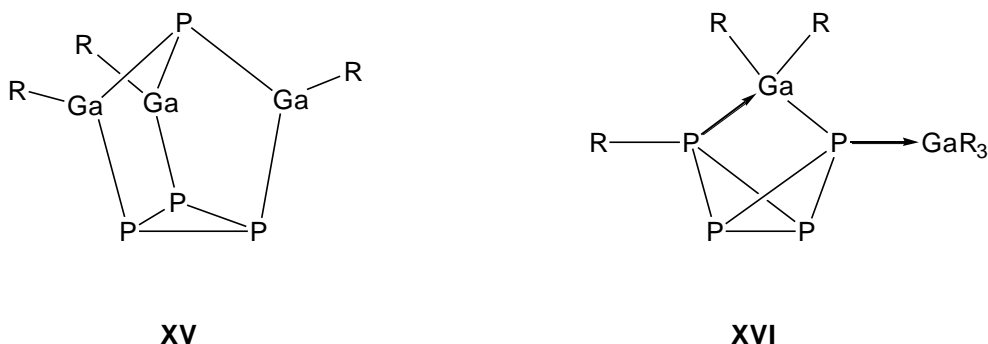
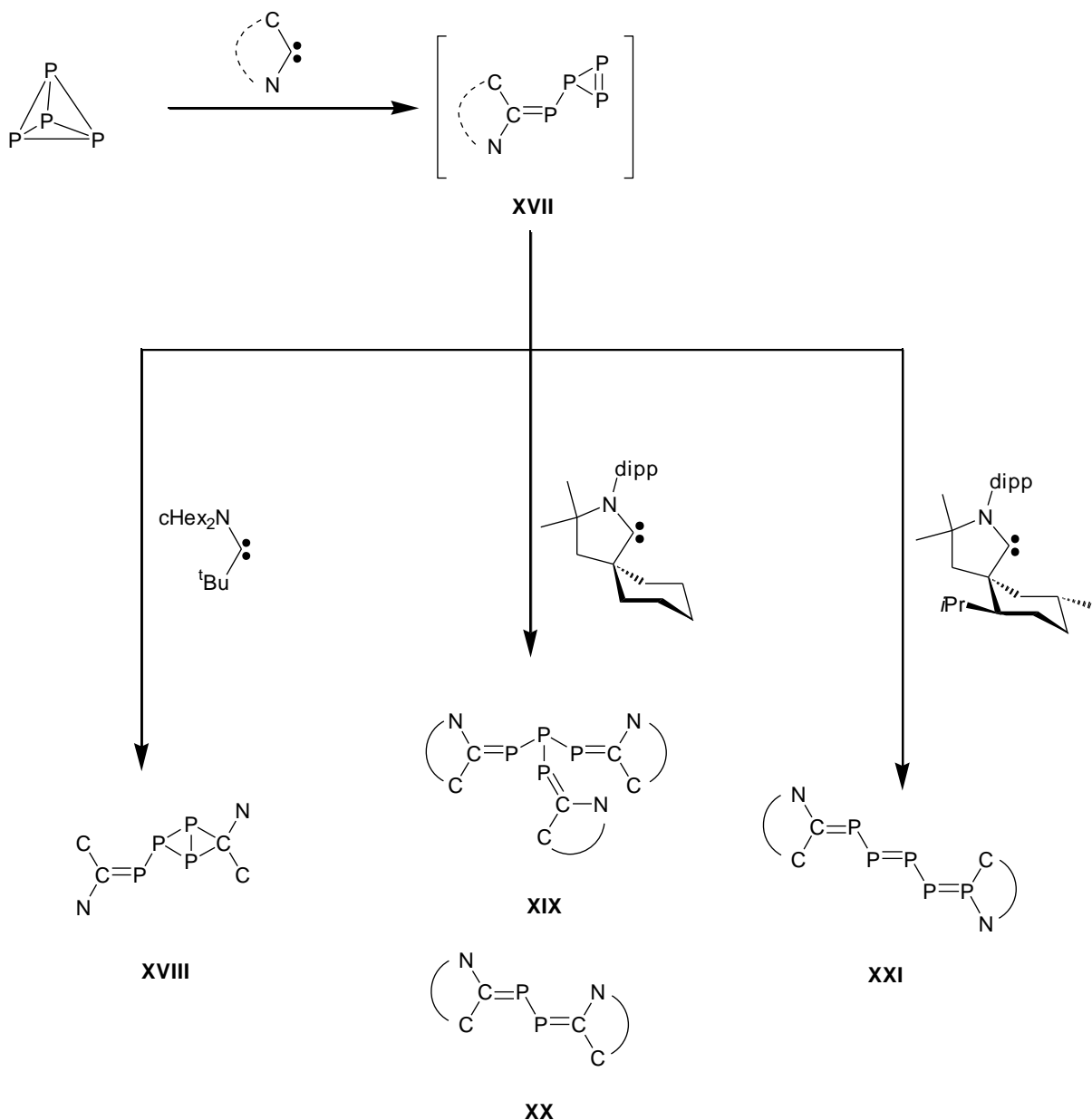


Figure 1.8: Products of P_4 activation by gallium centred reagents.

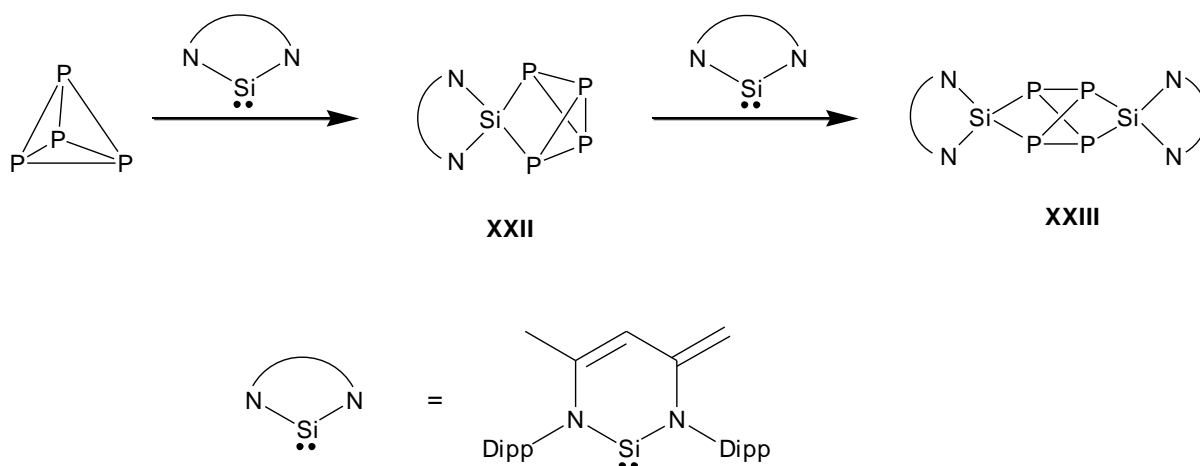
Unlike the monovalent group 13 compounds, the tendency of carbenes is not to insert into the P-P bonds. Instead the carbon forms a double bond with one of the phosphorus atoms, opening the tetrahedron into a three membered ring with a P=C side chain. The effect of subsequent carbene attacks is largely dependent on the identity of the carbon substituents, often either adding across a P-P bond or opening the ring to form chains.^{41,}
⁴² (Scheme 1.3)



Scheme 1.3: Reactions between P_4 and different carbenes.

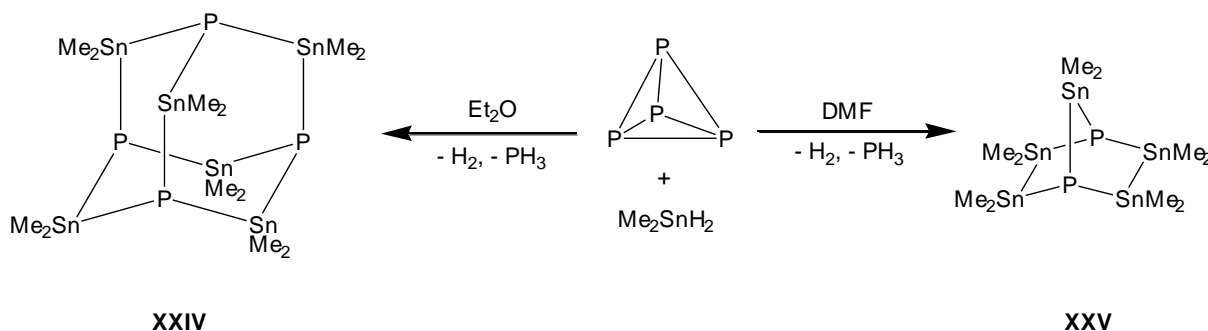
The fact that carbenes typically form $C=P$ double bonds rather than maintaining the cage structure seems to be due to the nucleophilic nature of the carbenes as opposed to other electrophilic reagents.⁴³ Despite being from the same group, electrophilic silylenes behave far more like the aluminium and gallium examples than the carbenes. Possibly the best examples of this are the results by Driess *et al* in 2007,⁴⁴ in which a cyclic silylene is shown to insert into one of the $P-P$ bonds to form the now familiar bridged

butterfly structure which may be followed by the insertion of a second silylene molecule into the bond opposite the first, producing a structure reminiscent of (XIII). (Scheme 1.4)



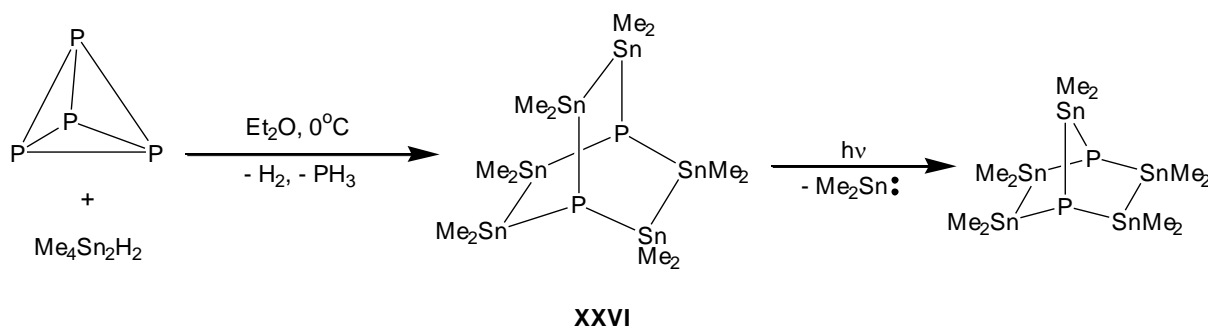
Scheme 1.4: Activation of P_4 by silylenes.

Much of the study into the activation of P_4 by Sn species has concerned methyltin hydrides, which undergo a reductive elimination *in situ* to produce a transient stannylene group. Depending on the reaction conditions, dimethyltin dihydride can be used to form either an adamantane like structure by insertion into each of the six P-P bonds, or a norbornane like structure by fragmenting the P_4 unit and just bridging between two P atoms.⁴⁵ (Scheme 1.5)



Scheme 1.5: Insertion of stannylenes into P_4 .

A similar reaction using tetramethyldistannane has been shown to yield a bicyclooctane analogue (XXVI) in which two phosphorus atoms are connected by three distannyl bridges. Because the Sn-Sn bond is already present before the reaction, there is no need for the organic base (DMF) which was previously required to prevent the formation of (XXIV) when using dimethyltin dihydride. When exposed to light, however, (XXVI) will eject dimethylstannylene to form (XXV).⁴⁶ (Scheme 1.6)

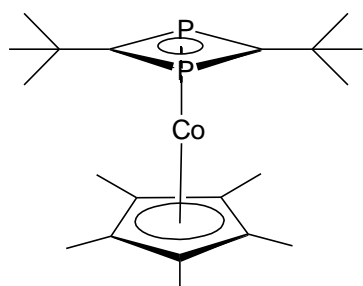


Scheme 1.6: Activation of P₄ by tetramethylstannene, followed by photolysis.

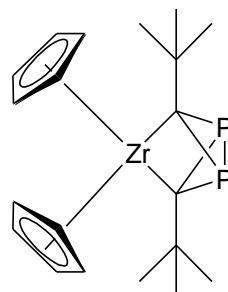
These examples serve to further illustrate the inherent reactivity differences between P₄ and C₄H₄. Whilst the activated P₄ clusters in these examples are often doubly reduced, none of them adopt an aromatic ring structure over the saturated polycyclic forms.

Bearing these widely differing activities in mind, an obvious progression of research leads to the following question; how would a molecule comprised of a mixture of P and C fragments behave? Would it resemble the relatively stable tetrahedron of phosphorus or the reactive anti-aromatic ring of cyclobutadiene? And how would it bond to a metal centre? Answers to these questions first started appearing in 1986 when two papers^{47,48} emerged describing the cyclodimerisation of a phosphalkyne by transition metal (most notably cobalt) complexes. These reactions result in new

complexes containing a four membered ring with alternating phosphorus and carbon atoms. The ring was found to be planar with all P-C bonds of equal length and coordinated η^4 to the metal centre, indicating the same aromatisation experienced by the P_4 and C_4 rings. The fact that the mixed atom ring can act in a similar fashion to that witnessed in both extremes should come as no surprise and, in and of itself, tells us little about the nature of the ring. These complexes do, however, show that a $P_2C_2R_2$ ring could be synthesised relatively trivially and opened up the field for further study. These initial papers were followed up a year later with reports of another dimerisation of the $^t\text{BuCP}$, this time using a Zr centre.⁴⁹ Unlike the previous examples the $P_2C_2R_2$ system in this case was not a square planar ring but instead formed the opened tetrahedral type structure observed for (XI), with additional bonds formed between the two P and the two C bound to the Zr centre.



XXVII



XXVIII

Figure 1.9: Different structures of the phosphalkyne dimer formed on metal centres.

This ligation mode of the $P_2C_2R_2$ unit affords the phosphorus atoms the saturated nature they favour, while the presence of the zirconium atom between the carbon atoms results in a lower ring strain than if it were a tetrahedron. Since these early examples, the $P_2C_2R_2$ moiety has been used in several further complexes with a variety of different

transition metals, substituent groups and other ligands,⁵⁰⁻⁵⁴ but to date (XXVIII) remains the only example displaying the tetrahedron type structure on a transition metal centre.

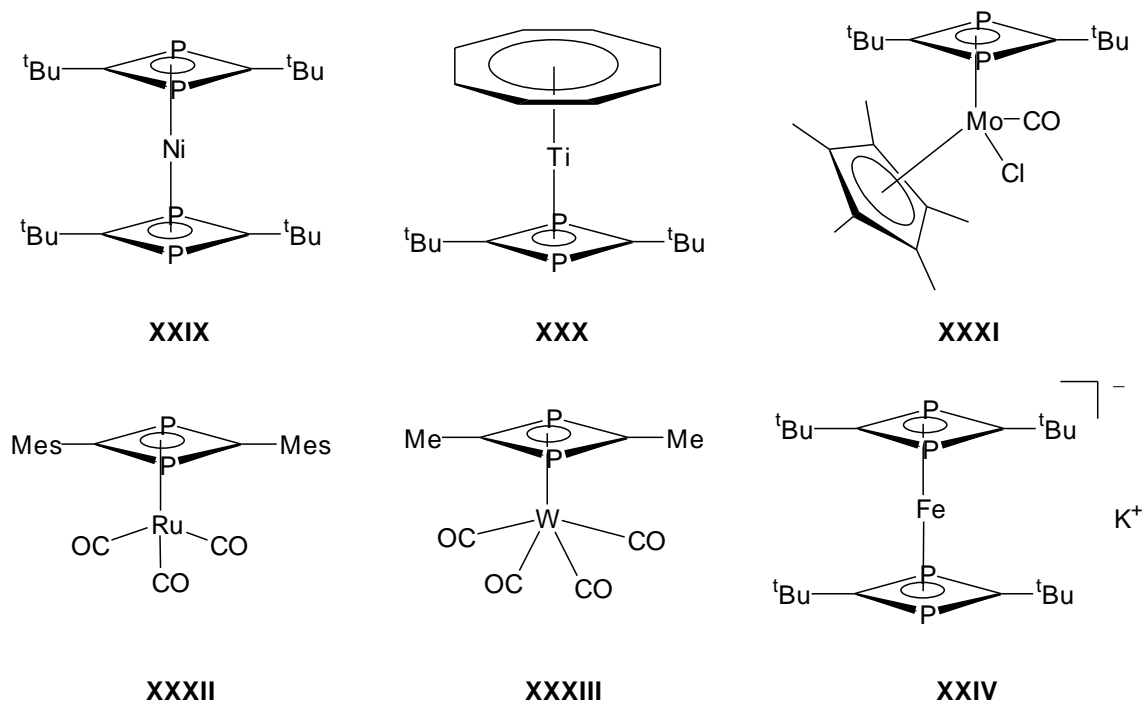
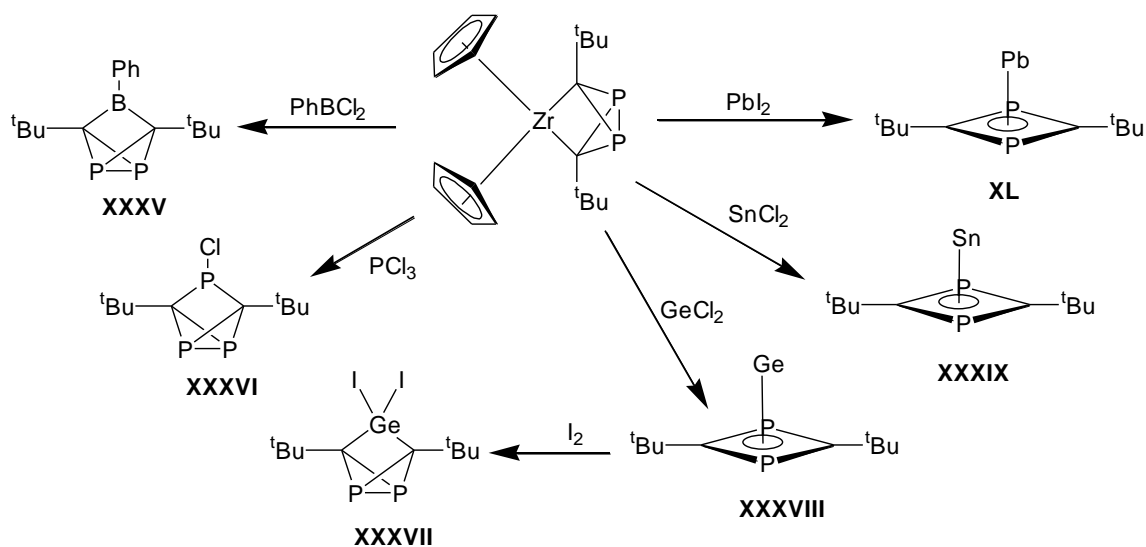


Figure 1.10: Selected transition metal diphosphacyclobutadiene complexes

From these examples the $P_2C_2R_2$ ring does not seem to exhibit any behaviour that has not been observed for P_4 compounds, but this is no longer the case when the ring is removed from the transition metal. Several papers have been published which detail reactions between (XXVIII) and different main group halides, forming zirconocene dihalide and transferring the $P_2C_2R_2$ unit onto the new centre. Once transferred the $P_2C_2R_2$ unit adopts a number of different structures depending on the new metal centre. In some cases, such as the reactions with $PhBCl_2$ and PCl_3 ,⁵⁵ it will retain the structure it held in the Zr complex. In contrast, reactions with $SnCl_2$ ⁵⁶ and PbI_2 ⁵⁷ form planar ring complexes while the products of reactions with $GeCl_2$ varied in structure depending on the ultimate oxidation state of the Ge.⁵⁷



Scheme 1.7: Transfer of the P_2C_2 ring to main group elements

The most substantial move towards a cyclobutadienyl like structure is seen in the reaction with $SbCl_3$.⁵⁸ This results in a planar $P_2C_2R_2$ ring with one double bond and the antimony atom forming a three membered ring on the opposite side, producing an analogue of the housene⁵⁹ molecule.



Scheme 1.8: Transfer of the $P_2C_2R_2$ ring onto antimony

The presence of a discrete double bond is far more reminiscent of the cyclobutadiene structure than any seen with a P_4 fragment. This suggests, as might well be expected,

the bonding interactions of the $P_2C_2R_2$ ring occupy something of a middle ground between cyclobutadiene and P_4 , capable of adopting structures which closely resemble those of either of the single element analogues depending on the molecular environment.

The previous examples illustrate well the variable structure of the $P_2C_2R_2$ ring when bound to another atom or coordinated to a metal centre but provide no indication as to how it exists as a separate entity, just the neutral ring without any other atoms to stabilise it. At a glance, two obvious possibilities present themselves. If the ring behaves like P_4 , then (holding with the tBu system as it is one of the more commonly used) it would form bis(*tert*-butyl)diphosphatetrahedrane. On the hand, it could form bis(*tert*-butyl)diphosphacyclobutadiene the analogue of C_4H_4 .

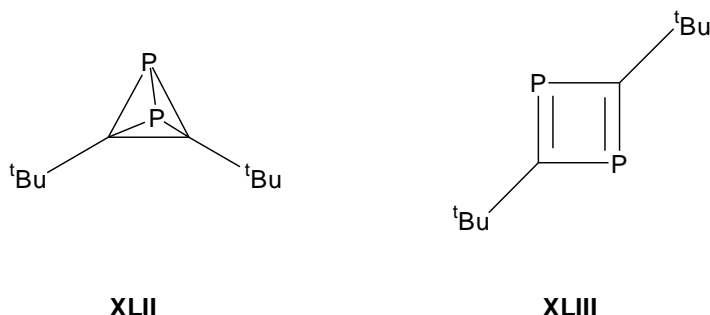
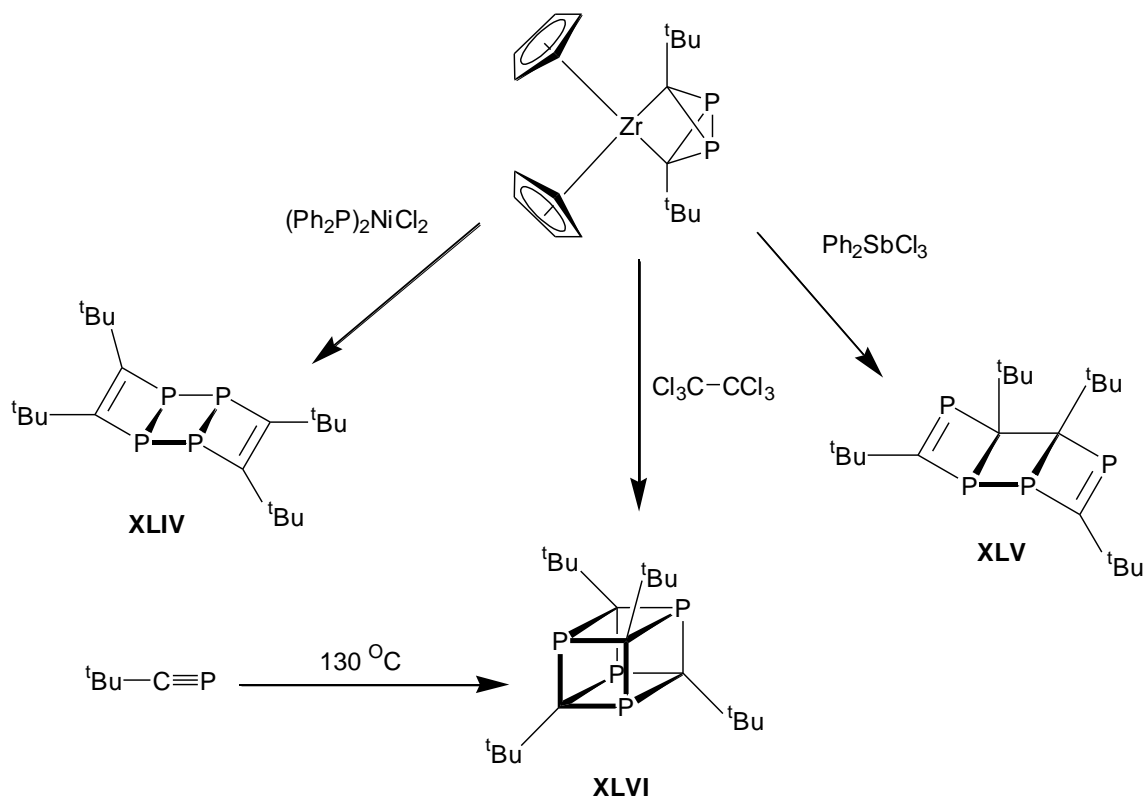


Figure 1.11: Possible free P_2C_2 structures

Given that P_4 and C_4tBu_4 ²⁵ both exist as tetrahedral molecules, one could be forgiven for supposing that (XLII) would be the adopted structure, but in reality this does not seem to be the case. As previously mentioned, the P_4 tetrahedron is favoured over the diene because of the relatively weak P-P π -bonds.²⁸ The tetra-*tert*-butyltetrahedrane on the other hand is stabilised by the steric “corset effect”,²⁵ whereby the tetrahedral shape offers the maximum separation of the bulky alkyl groups. The P-P bonds have been replaced by P-C bonds, in which the energy difference between σ -bonds and π -bonds is not as great,⁶⁰ and without the 3rd and 4th tBu groups the maximum separation is actually

across the diagonal of the planar ring rather than in the tetrahedron. Ironically, by combining halves of two molecules that stabilised the tetrahedron in different ways, both effects have been nullified resulting in the probable favouring of the dienyl structure.

As in the case of cyclobutadiene, (XLIII) is a highly reactive species and so as yet has not been observed directly. Its presence can be inferred though by examining the products of its dimerisation reactions. These often take the form of tetraphosphatricyclooctadienes (tetraphosphaladderenes), demonstrating the analogy with cyclobutadiene. However, while the cyclobutadiene ring is comprised solely of carbon atoms and so can only form one dimer, the two different atoms of the $P_2C_2R_2$ ring mean that different isomers of the dimer can be formed by different reactions⁶¹⁻⁶³ (Scheme 1.9). (In the case of XLIV, the ring is transferred to the nickel centre and undergoes a rearrangement before being released).



Scheme 1.9: Products of $P_2C_2R_2$ ring dimerisations.

Thus far the 1,3,5,7-tetraphosphaladderene has not been observed, quite possibly because it converts easily into the tetraphosphacubane (XLVI) through a 2+2 cyclisation.⁶³ This is in contrast to the behaviour of the solely carbon tricyclooctadiene which, if anything, will decompose to a cyclooctatetraene.¹ Once again, this illustrates the ability of the $P_2C_2R_2$ ring to alternate between mimicking the structures of the entirely C or P based analogues depending on the molecular environment.

Previous computational models have disagreed with experimental evidence, suggesting that the most commonly seen P_4C_4 structure, (XLVI), is actually the least thermodynamically stable, and that the 1,3-diphosphacyclobutadiene (XLIII) is similarly disfavoured over other four membered species.⁶³

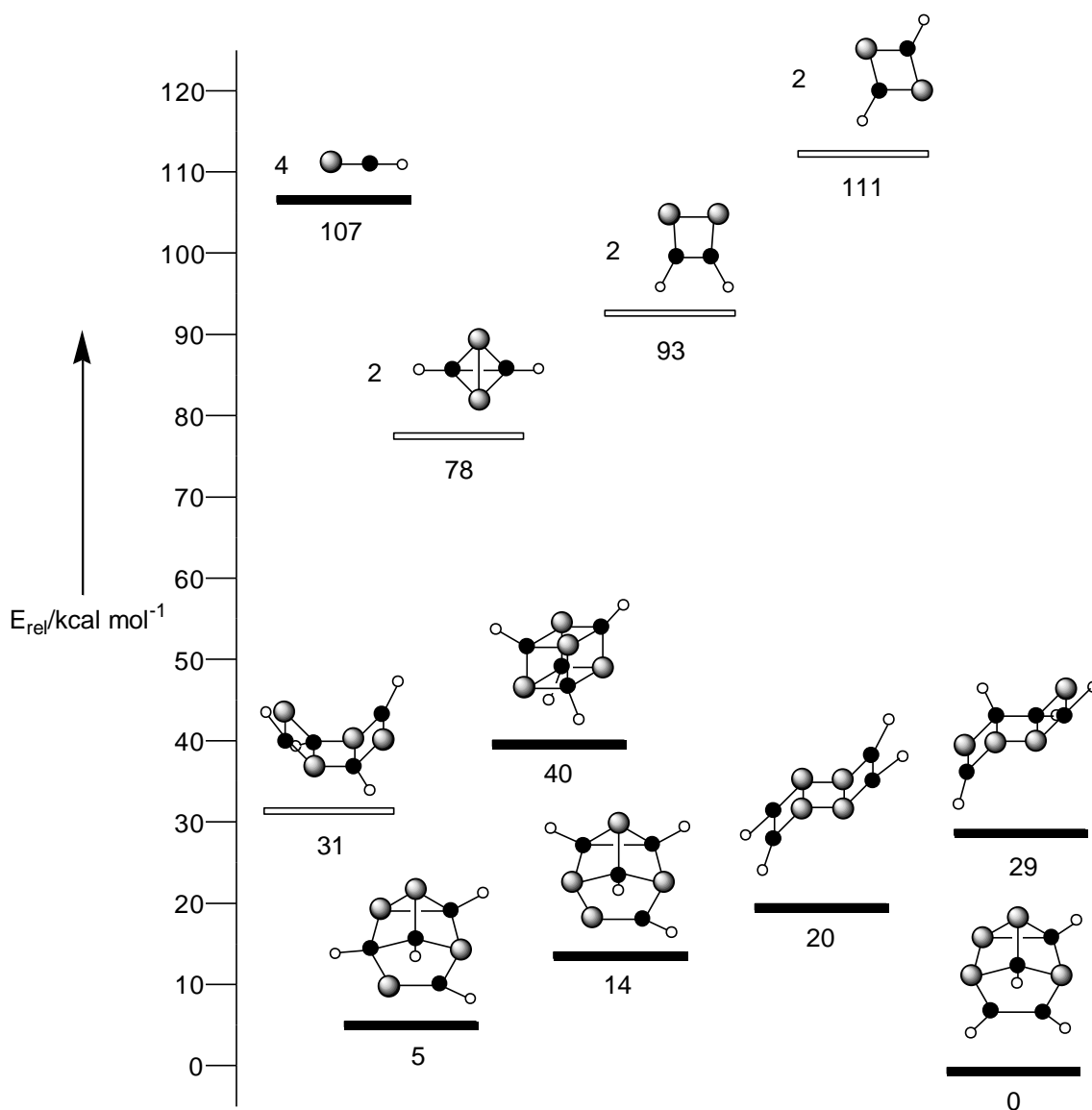


Figure 1.12: Relative energies of HCP oligomers. Black = C, Gray = P, White = H ⁴⁸
 Black bar = known structure, White bar = postulated

The reason for this discrepancy may well be a result of the decision to model the simpler phosphaacetylene rather than *tert*-butylphosphaalkyne. By using a considerably smaller group on the carbon atom, structures such as (XLIII) and (XLVI) which offer the maximum separation of carbon substituents will not be as advantageous as the real world analogues.

References

1. Stone, F. G. A., West, R., Maitlis, P. M., *Advances in Organometallic Chemistry*, 1966, **4**, 95
2. Bally, T., Bernhard, S., Matzinger, S., Roulin, J-L., Sastry, G. N., Truttman, L., Zhendong Z., Marcinek A., Adamus J., Kaminski R., Gebicki J., Williams F., Guo-Fei C., Fölscher M. P., *Chem. Eur. J.*, 2000, **6**, 858
3. Masamune, S., Souto-Bachiller F. A., Machiguchi T., Bertie J. E., *J. Am. Chem. Soc.*, 1978, **100**, 4889
4. Longuet-Higgins, H. C., Orgel, L. E., *J. Chem. Soc. (London)*, 1956, 1969
5. Hübel, W., Braye, E. H., *J. Inorg. Nucl. Chem.*, 1959, **10**, 250
6. Criegee, R., Schroeder, G., *Angew. Chem.*, 1959, **71**, 70
7. Emerson, G. F., Watts, L., Pettit, R., *J. Am. Chem. Soc.*, 1965, **87**, 131
8. Dodge, R.P., Schomaker, V., *Nature*, 1960, **186**, 798
9. Dunitz, J. D., Mez, H. C., Mills, O. S., Shearer, H. M. M., *Helv. Chim. Acta.*, 1962, **45**, 647
10. Harvey, P. D., Schaefer, W. P., Gray, H. B., Gilson, D. F. R., Butler, I. S., *Inorg. Chem.*, 1988, **27**, 57
11. Cambridge Structural Database, 2010
12. Karpyak, N. M., Makitra, R. G., Marshalok, G. A., Pal'chikova, O. Y., Yatchishin, I. I., *Russian Journal of General Chemistry*, 2005, **75**, 1712
13. McKee, M. L., von Ragué Schleyer, P., Balci, M., *J. Phys. Chem. A*, 2000, **104**, 1246
14. Newton, M. D., Krantz, A., Lin, Y., *J. Am. Chem. Soc.*, 1973, **95**, 2744
15. Boñaga, L. V. R., Han-Cheng, Z., Moretto A. F., Hong, Y., Gauthier, D. A., Jian, L., Leo, G. C., Maryanoff, B. E., *J. Am. Chem. Soc.*, 2005, **127**, 3473

16. Nomura, M., Fujii, T., Kajitani, M., *Organometallics*, 2009, **28**, 3776
17. Bally, T., *Angew. Chem. Int. Ed.*, 2006, **45**, 6616
18. Fattahi, A., Liz, L., Tian, Z., Kass, S. R., *Angew. Chem. Int. Ed.*, 2006, **45**, 4984
19. Politzer, P., Grice, M. E., Murray, J. S., Seminario, J. M., *Can. J. Chem.*, 1993, **71**, 1123
20. Levchenko, S. V., Krylov, A. I., *J. Chem. Phys.*, 2004, **120**, 175
21. Mo, J., Schleyer, P. von R., *Chem. Eur. J.*, 2006, **12**, 2009
22. Deniz, A. A., Peters, K. S., Snyder, G. L., *Science*, 1999, **286**, 1119
23. Lipscomb, W. N., *Tetrahedron Letters*, 1959, **18**, 20
24. Dillon, K. B., Mathey, F., Nixon, J. F., *Phosphorus: The Carbon Copy* 1998
25. Maier, G., *Angew. Chem. Int. Ed. Engl.*, 1988, **27**, 309
26. Scherer, O. J., Vondung, J., Wolmoershäuser, G., *Angew. Chem. Int. Ed. Engl.*, 1989, **28**, 1355
27. Heslop, R. B., Jones, K., *Inorganic Chemistry: A Guide To Advanced Study*, 1976, 412-415
28. Baird, N. C., *Can. J. Chem.*, 1984, **62**, 341
29. Glukhovtsev, M. N., Pross, A., Laiter, S., *J. Phys. Chem.*, 1995, **99**, 6828
30. Steitwieser, A., Heathcock, C. H., Kosower, E. M., *Introduction to Organic Chemistry*, 4th Ed., 1992, 654
31. Trinquier, G., Daudey, JP., Kohima, N., *J. Am. Chem. Soc.*, 1985, **107**, 7210
32. Scheer, M., Dargatz, M., Ruffńska, A., *J. Organomet. Chem.*, 1992, **440**, 327
33. Scheer, M., Balázs, G., Seitz, A., *Chem. Rev.*, 2010, **110**, 4236
34. Riedel, R.; Hausen, H.-D.; Fluck, E. *Angew. Chem., Int. Ed. Engl.*, 1985, **24**, 1056.
35. Rauhut, M. M., Bernheimer, R., Semsel, A. M., *J. Org. Chem.*, 1963, **28**, 478

36. Kirmse, W., *Carbene Chemistry – 2nd Ed.*, 1971
37. Peng, Y., Fan, H., Zhu, H., Roesky, H. W., Magull, J., Hughes, C. H., *Angew. Chem., Int. Ed.*, 2004, **43**, 3443
38. Dohmeier, C., Schnöckel, H., Robl, C., Schneider, U., Ahlrichs, R., *Angew. Chem., Int. Ed. Engl.*, 1994, **33**, 199
39. Uhl, W., Beuter, M. *Chem. Commun.*, 1999, 771
40. Power, M. B., Barron, A. R. *Angew. Chem., Int. Ed. Engl.*, 1991, **30**, 1353
41. Back, O., Kuchenbeiser, G., Donnadiou, B., Bertrand, G. *Angew., Chem., Int. Ed.*, 2009, **48**, 5530
42. Masuda, J. D., Schoeller, W. W., Donnadiou, B., Bertrand, G. *Angew., Chem., Int. Ed.*, 2007, **46**, 7052
43. Schoeller, W. W. *Phys. Chem. Chem. Phys.*, 2009, **11**, 5273
44. Xiong, Y., Yao, S., Brym, M., Driess, M. *Angew. Chem., Int. Ed.*, 2007, **46**, 4511
45. Mathiasch, B., Dräger, M. *Angew. Chem., Int. Ed. Engl.*, 1978, **17**, 767
46. Dräger, M., Mathiasch, B. *Angew. Chem., Int. Ed. Engl.*, 1981, **20**, 1029
47. Hitchcock, P. B., Maah, M. J., Nixon, J. F., *Chem. Commun.*, 1986, 737
48. Binger, P., Milczarek, R., Mynott, R., Regitz, M., Rösch W., *Angew. Chem. Int. Ed. Engl.*, 1986, **25**, 644
49. Binger, P., Biedenbach, B., Krüger, C., Regitz, M., *Angew. Chem. Int. Ed. Engl.*, 1987, **26**, 764.
50. Binger, P., Glaser, G., Albus, S., Kruger, C., *Chem. Ber.*, 1995, **128**, 1261
51. Himmel, D., Seitz, M., Scheer, M., *Z. Anorg. Allg. Chem.*, 2004, **630**, 1220
52. Jones, C., Schulten, C., Stasch, A., *Dalton Trans.*, 2006, 3733

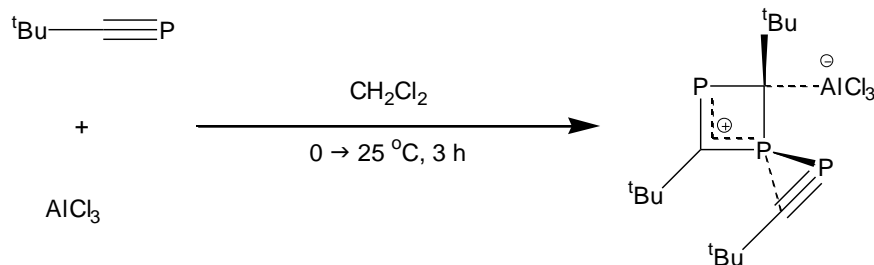
53. Wettling, T., Wolmoershäuser, G., Binger, P., Regitz, M., *Chem. Commun.*, 1990, 1541
54. Wolf, R., Slootweg, J. C., Ehlers, A. W., Hartl, F., de Bruin, B., Lutz, M., Spek, A. L., Lammertsma, K., *Angew. Chem. Int. Ed. Engl.*, 2009, **48**, 3104
55. Binger, P., Wettling, T., Schneider, R., Zurmühlen, F., Bergsträsser, U., Hoffmann, J., Maas, G., Regitz, M., *Angew. Chem. Int. Ed. Engl.*, 1991, **30**, 207
56. Francis, M. D., Hitchcock, P. B., *Chem. Commun.*, 2002, 86
57. Francis, M. D., Hitchcock, P. B., *Organometallics*, 2003, **22**, 2891
58. Fish, C., Green, M., Jeffery, J.C., Kilby, R. J., Lynam, J. M., McGrady, J. E., Pantazis, D. A., Russel, C. A., Willans, C. E., *Angew. Chem. Int. Ed. Engl.*, 2006, **45**, 6685
59. Hsu, S. L., Andrist, A. H., Gierke, T. D., Benson, R. C., Flygare, W. H., Baldwin, J. E., *J. Am. Chem. Soc.*, 1970, **92**, 5250
60. Chow, A. R., Beaudet, R. A., *J. Phys. Chem.*, 1989, **93**, 421
61. Geissler, B., Barth, S., Bergsträsser, U., Slany, M., Durkin, J., Hitchcock, P. B., Hofmann, M., Binger, P., Nixon, J. F., von Ragué Schleyer, P., Regitz, M., *Angew. Chem. Int. Ed. Engl.*, 1995, **34**, 484
62. Fish, C., Green, M., Kilby, R. J., McGrady, J. E., Pantazis, D. A., Russel, C. A., *Dalton Trans.*, 2008, 3753
63. Wettling, T., Schneider, J., Wagner, O., Kreiter, C. G., Regitz, M., *Angew. Chem. Int. Ed. Engl.*, 1989, **28**, 1013

Chapter 2

Sn Complexes Containing the $P_2C_2R_2$ Ligand

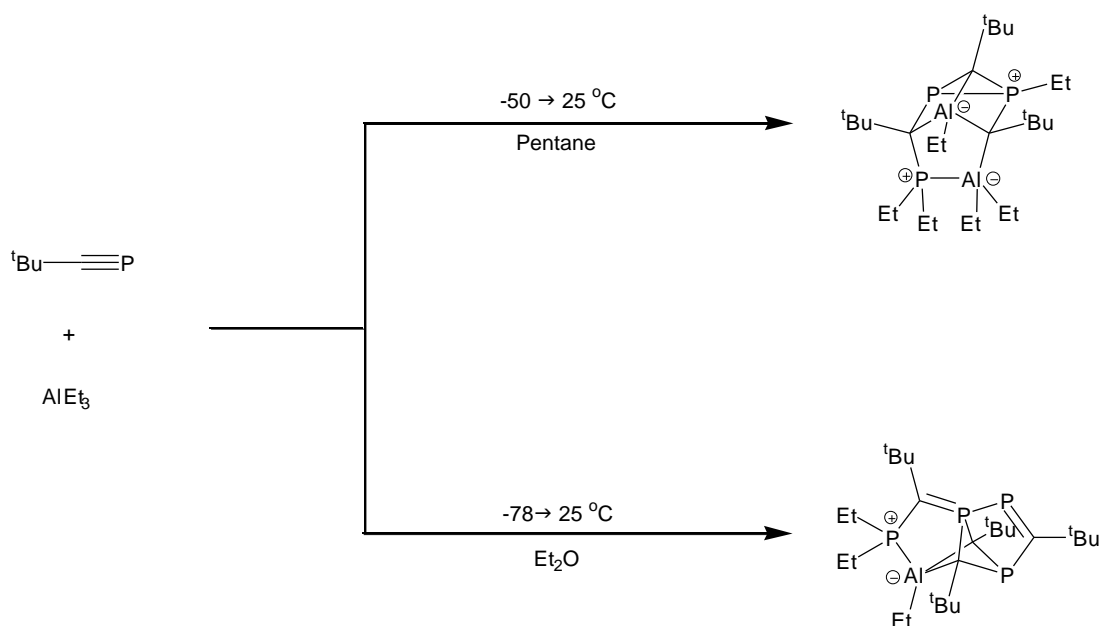
2.1: Introduction

Although there are many reports featuring a phosphaaalkyne dimer bound to a main group element,¹ it is rarely the case that the dimerisation occurs *in situ*, as is frequently observed for transition metals (*vide* Chapter 3). The reaction in which two equivalents of phosphaaalkyne are coupled using aluminium trichloride, in fact produced a bicyclic trimer.² (Scheme 2.1)



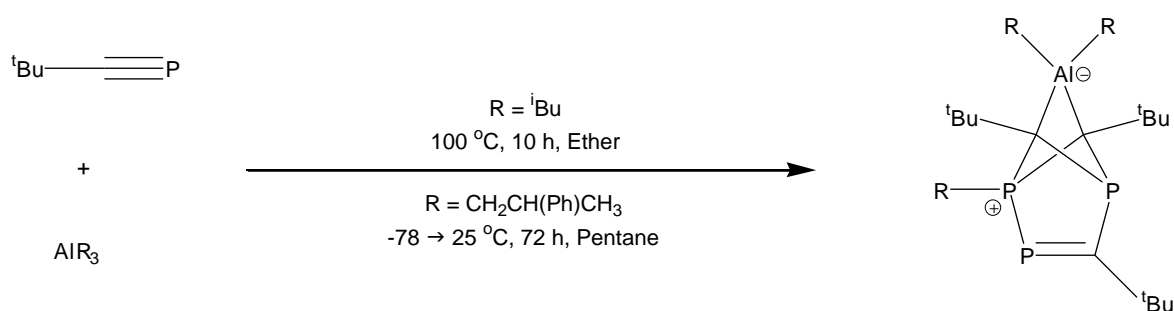
Scheme 2.1: Coupling of phosphaaalkyne by $AlCl_3$

Subsequently, similar reactions were performed in the following years using aluminium (and later gallium) trialkyls. Initially it was observed that the reaction employing triethylaluminium produced a trimer or tetramer (incorporating two and one aluminium centres respectively) depending on the reaction conditions.³ (Scheme 2.2)



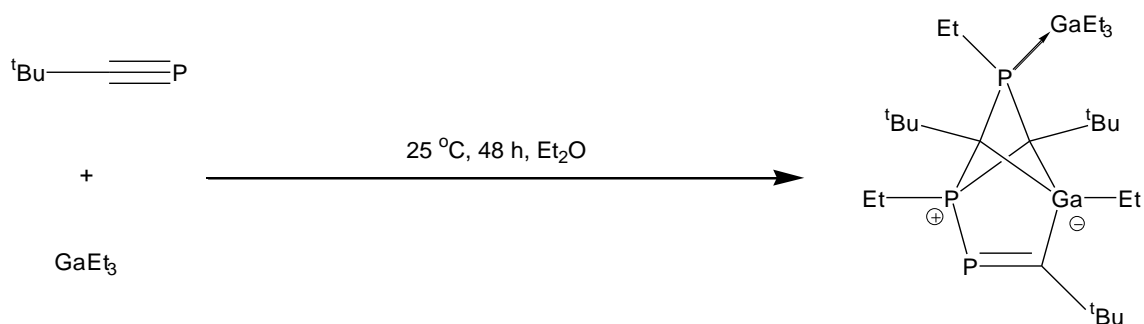
Scheme 2.2: Coupling of phosphalkyne by AlEt_3 under varying conditions

Later research showed that by replacing the ethyl groups with *iso*-butyl or 2-phenylpropyl groups afforded a different trimeric structure containing a single dialkyl aluminium moiety.⁴ (Scheme 2.3)



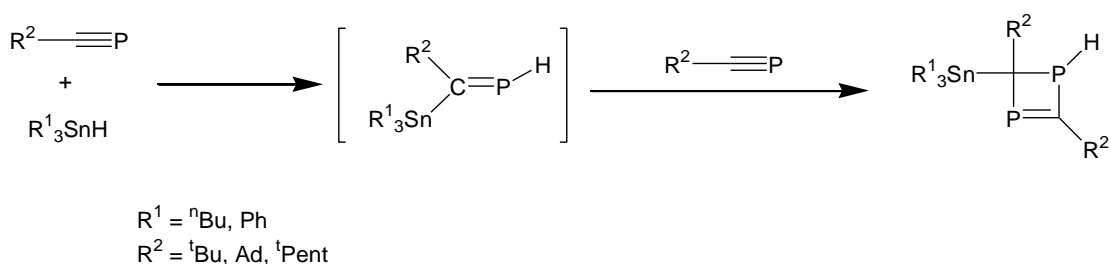
Scheme 2.3: Coupling of phosphalkyne by bulky trialkyl aluminium species

In the same article, triethylgallium was reported to afford a similar product as the bulkier dialkyl aluminium analogues but the relative positions of the phosphorus and metal atom were different. (Scheme 2.4)



Scheme 2.4: Coupling of phosphalkyne by GaEt_3

In addition to these two reports employing Al and Ga, the only other reported dimerisation resulted from the activation of an excess of phosphalkyne by one of two trialkyltin hydrides.⁵ The authors postulated the formation of a stannyl phosphalkene intermediate which then proceeded to react with a further equivalent of the phosphalkyne to produce a diphosphacyclobutene. (Scheme 2.5)



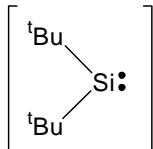
Scheme 2.5: Coupling and hydrostannylation of phosphalkynes using trialkyl tin hydrides

Although the analogous reactions using dialkyl tin dihydrides were reported to give the similar diphosphacyclobutenes, these were apparently unstable with respect to an unspecified decomposition rendering their isolation impossible. Using dialkyltinchlorohydrides on the other hand produced stable products, but in addition to the dimer, a tetramer was formed containing a dialkyltin moiety inserted into one of the P-C bonds of a tetraphosphacubane. (Scheme 2.6)



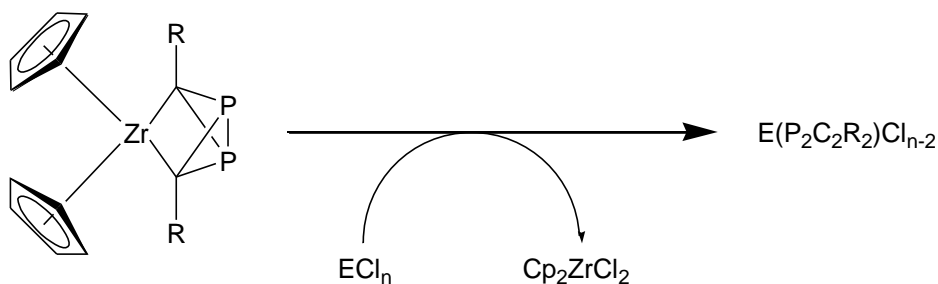
Scheme 2.6: Coupling of phosphalkyne using dialkyltin hydrochlorides

Finally, there is a single example of a 1:1 phosphaaalkyne complex of a main group element which was synthesised when ^tBuCP was employed to trap a photolytically generated silylene.⁶ (Scheme 2.7) The complex contained a three membered P-C-Si ring with a carbon-phosphorus double bond.



Scheme 2.7: Trapping of silylene using phosphalkynes

Almost all reported syntheses of $P_2C_2R_2$ complexes of main group elements have employed $Cp_2Zr(P_2C_2R_2)$ in conjunction with the corresponding main group chloride. (Scheme 2.8)



Scheme 2.8: Synthesis of $P_2C_2R_2$ complexes of main group elements

Many of these complexes along with their respective molecular structures have been discussed in the introductory literature review but some additional detail will be presented here. In complexes such as those of Ge(II), Sn(II) and Pb(II),^{7,8} the molecular structure displayed may be described as a $P_2C_2R_2$ ring bound η^4 to the metal centre. It may, however, be more accurately described as a five-atom, Wadeian, *nido*-cluster,⁹ adopting the expected square-base, pyramidal structure. The frontier orbitals of such clusters are formed from a combination of p_x , p_y and sp -hybrid orbitals of the metal and the π orbitals of appropriate symmetry of the $P_2C_2R_2$ ring (Figure 2.1)

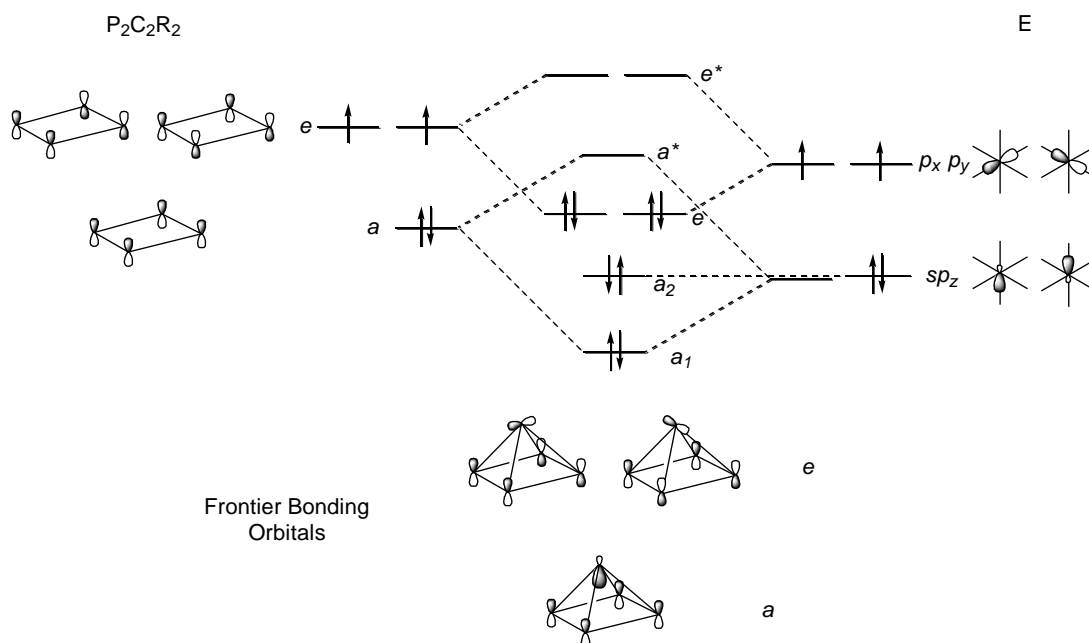


Figure 2.1: Frontier orbitals of $EP_2C_2R_2$ clusters ($E = Ge, Sn$ or Pb)

This same structure is also predicted for the isoelectronic cationic analogues of the phosphorus, arsenic and antimony.^{10,11} (Figure 2.2)

Theoretical calculations on the all possible cluster isomers possible *e.g.* with either C-C, P-P, or C-P bonded species have shown that the synthetically isolated species is not always the most stable, but is determined to some extent by the nature of the existing structure of the $P_2C_2R_2$ group bound to the Zr centre and to kinetic barriers preventing its rearrangement.¹¹

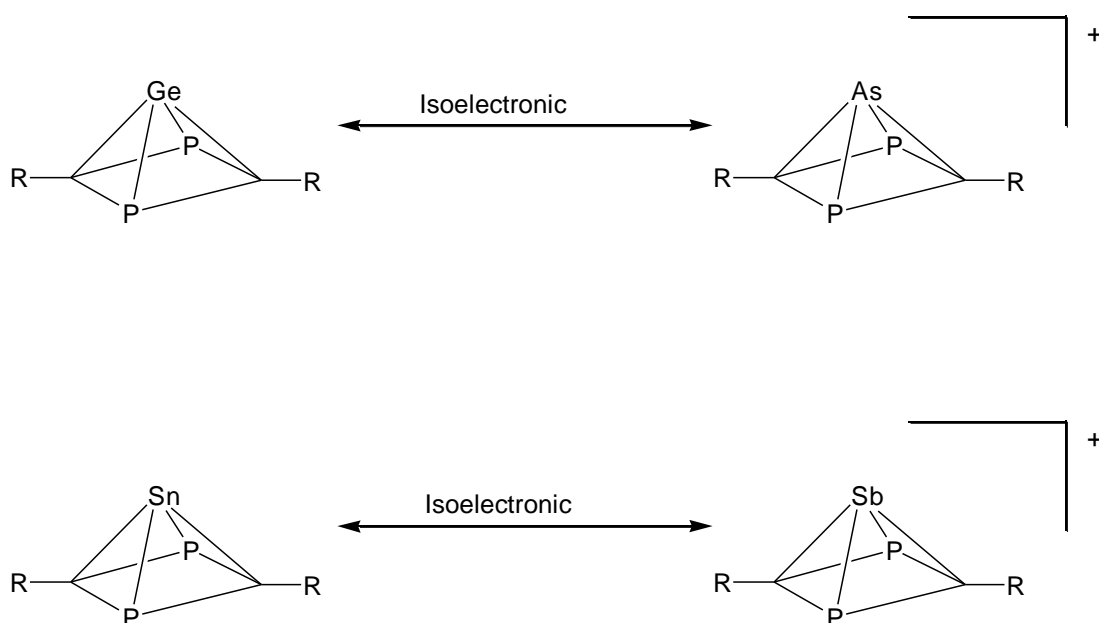
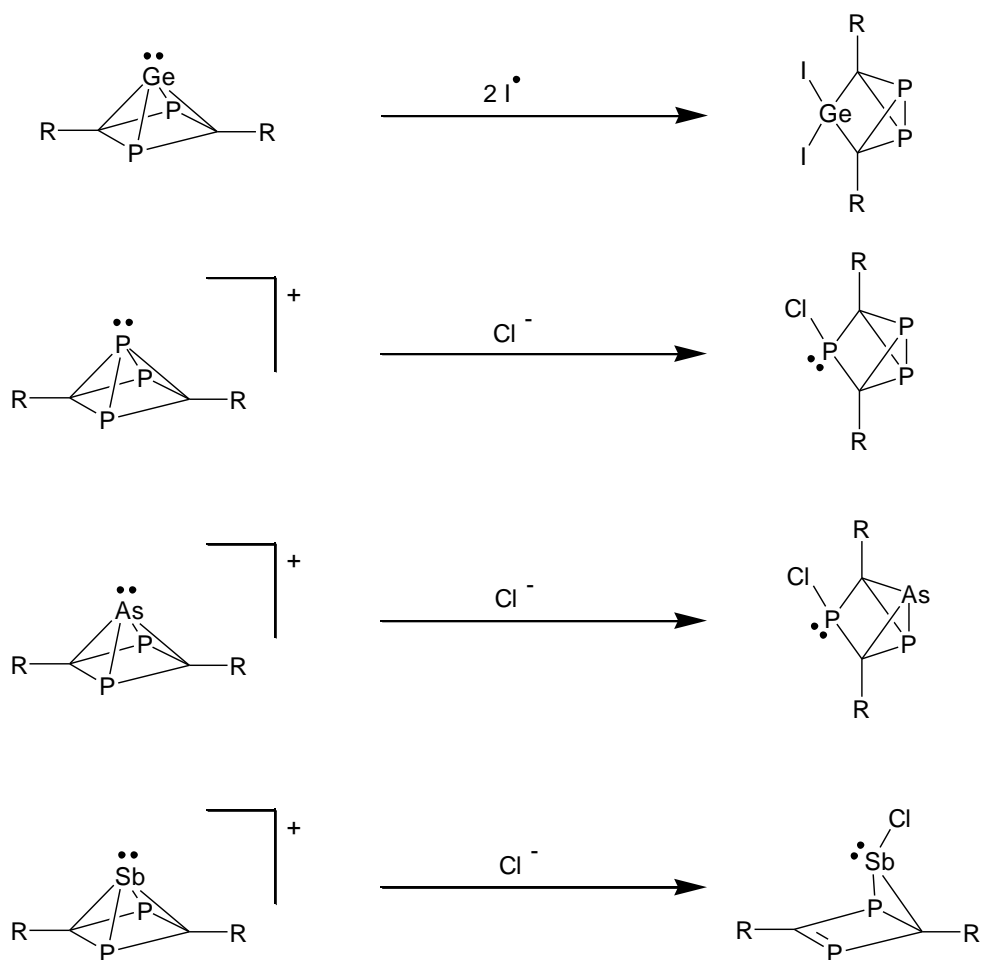


Figure 2.2: Isoelectronic relationship between neutral group 14 and anionic group 15 clusters

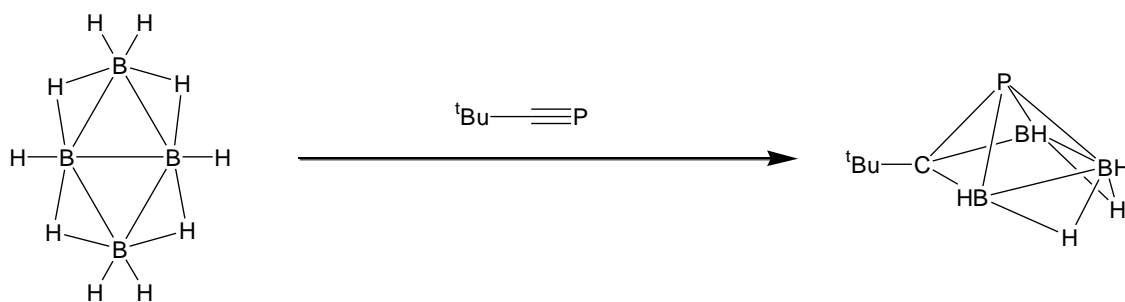
In order for Wade's rules to be applicable the atoms must be sp -hybridised. A change in structure is thus to be expected when the apical atom breaks this condition *e.g.* changing from Ge(II) to Ge(IV). Although the Ge(IV) centre also formally uses two electrons to bond to the $P_2C_2R_2$ unit, the new orbital rearrangement requires this bonding to be composed of two discrete σ -bonds rather than the three delocalised cluster bonds. Similar structural alterations are observed for the neutral group 15 analogues. Thus, although the number of bonding electrons remains the same as their cationic counterparts, the population of what was previously an unoccupied orbital requires that the atom is rehybridised and the molecular structure becomes non-Wadeian structure.^{8,10-12} (Scheme 2.9)



Scheme 2.9: Molecular structures displayed by selected main group derivatives of $(\text{P}_2\text{C}_2\text{R}_2)$ as a function of oxidation state.

To date, it is noteworthy that the equivalent Sn(IV) and Pb(IV) non-Wadeian structures have not been reported.

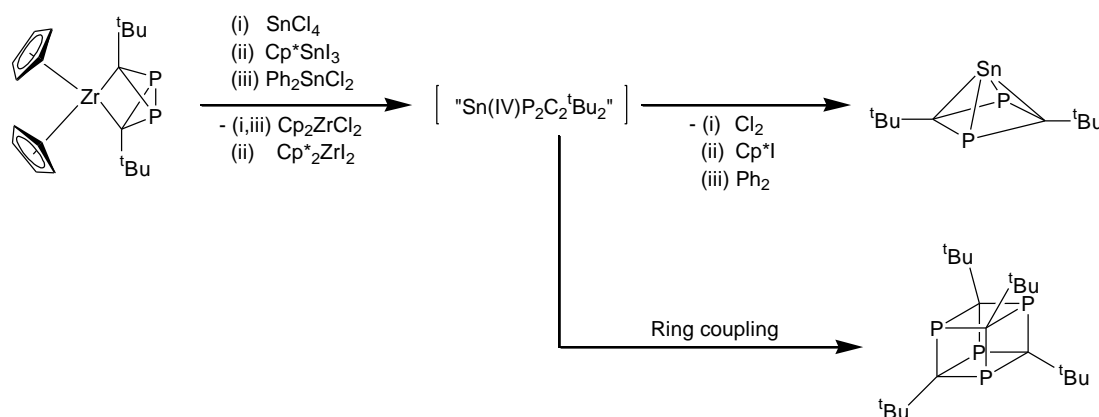
Wadeian cluster formation has also been reported the novel phosphacarbaborane $2\text{-}^t\text{Bu-1,2-PCB}_3\text{H}_5$ which was isolated from the reaction of $^t\text{BuCP}$ with B_4H_{10} .¹³ (Scheme 2.10)



Scheme 2.10: Reaction of B_4H_{10} with ${}^t\text{BuCP}$

2.2: Results and Discussion

In an attempt to synthesise a Sn(IV) analogue of the previously reported Sn(II) species, $\text{Sn}(\text{P}_2\text{C}_2^t\text{Bu}_2)$,⁹ a series of reactions using $\text{Cp}_2\text{Zr}(\text{P}_2\text{C}_2^t\text{Bu}_2)$ and several tin reagents of the general formula $\text{R}_n\text{SnX}_{4-n}$ ($\text{R} = \text{Ph}$, Cp , or Me and $\text{X} = \text{Cl}$, or I) were performed. For the majority of these reactions the only product identified by $^{31}\text{P}\{^1\text{H}\}$ NMR spectroscopy was $\text{Sn}(\text{P}_2\text{C}_2^t\text{Bu}_2)$, or on occasion a mixture containing a high proportion of $\text{Sn}(\text{P}_2\text{C}_2^t\text{Bu}_2)$, and the previously characterised tetraphosphacubane, $(\text{P}_4\text{C}_4^t\text{Bu}_4)$.¹⁴ All Sn(IV) intermediates which may have been formed during these reactions were unstable with respect to reductive elimination, presumably arising from a radical coupling of the two of the ligands, although the by-products were not identified. (Scheme 2.11)

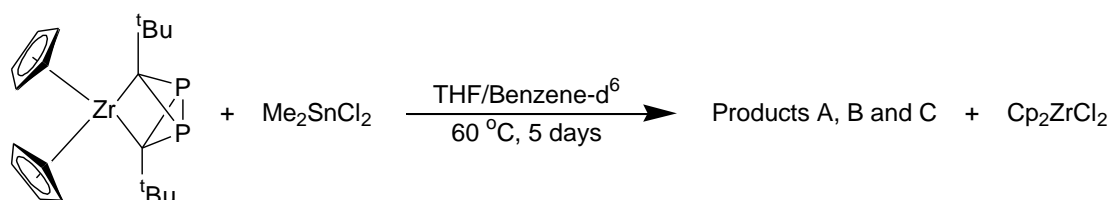


Scheme 2.11: Proposed formation of $\text{Sn}(\text{P}_2\text{C}_2^t\text{Bu}_2)$ and $\text{P}_4\text{C}_4^t\text{Bu}_4$

After the continued reduction of the Sn(IV) reagents, Me_2SnCl_2 was chosen as an alternative reagent as the methyl groups would be less prone to radical formation and thus less likely to form the stable Sn(II) product. This strategy succeeded in avoiding

the formation, $\text{Sn}(\text{P}_2\text{C}_2^t\text{Bu}_2)$, and instead, depending on the conditions, three different Sn(IV) compounds could be produced.

Reaction of $\text{Cp}_2\text{Zr}(\text{P}_2\text{C}_2^t\text{Bu}_2)$ with Me_2SnCl_2



Scheme 2.12: Reaction of $\text{Cp}_2\text{Zr}(\text{P}_2\text{C}_2^t\text{Bu}_2)$ with Me_2SnCl_2

An initial reaction using a 1:1 stoichiometry was performed in an NMR tube using a mixture of THF and benzene- d^6 (*circa* 9:1). The mixture was heated to $60\text{ }^\circ\text{C}$ for five days after which time the $^{31}\text{P}\{^1\text{H}\}$ NMR spectrum was recorded. This spectrum indicated that three products had been formed a ratio of *circa* 2:0.9:0.7. (Figure 2.3) The resonances attributable to each of the three products were assigned on the basis of the values determined for their respective integrals and coupling constants. The ^{31}P NMR spectroscopy data for these compounds is displayed in Table 2.1, with P^{i} and P^{ii} denoting the higher and lower frequency chemical shifts respectively of each compound.

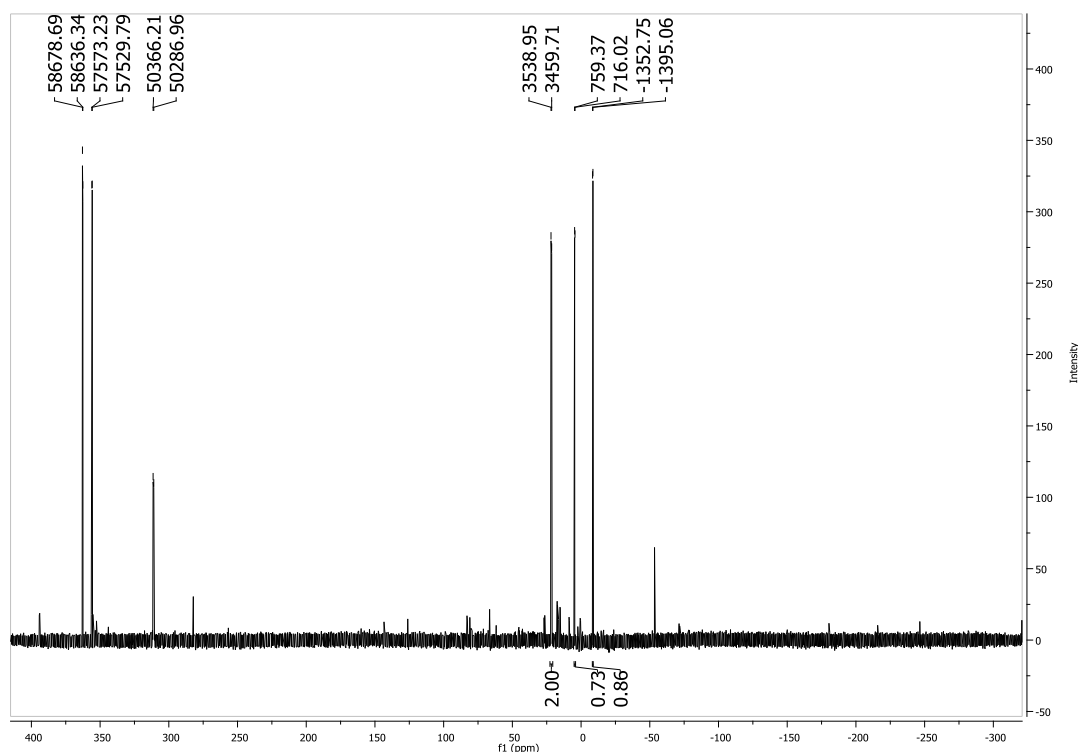


Figure 2.3: $^{31}\text{P}\{^1\text{H}\}$ NMR spectrum of the products of reaction of Me_2SnCl_2 with $\text{Cp}_2\text{Zr}(\text{P}_2\text{C}_2^t\text{Bu}_2)$

Each product was observed as pairs of doublets indicating that all three contained two chemically inequivalent phosphorus atoms. Thus the possibility any of these products having a “butterfly-type” structure, as observed for the zirconocene precursor, was ruled out. The $^{31}\text{P}\{^1\text{H}\}$ NMR spectrum also showed only a very slight trace of $\text{Sn}(\text{P}_2\text{C}_2^t\text{Bu}_2)$ at δ 143.4, illustrating that the majority of the Me_2SnCl_2 starting material had not been reduced.

Product	Relative Integral	P^i			P^{ii}			$J P^I-P^{II}$ /Hz
		δ	$J P-^{119}Sn$ /Hz	$J P-^{117}Sn$ /Hz	δ	$J P-^{119}Sn$ /Hz	$J P-^{117}Sn$ /Hz	
A	0.37	311.2 (broad)	124	Unresolved	21.4	1635 46	1560 Unresolved	80
B	1.0	355.8	242	231	4.6	1310	1252	43
C	0.43	362.5	-	-	-8.2	17	Unresolved	42

Table 2.1: Compiled NMR spectroscopic data for products A, B and C

The $^{119}\text{Sn}\{^1\text{H}\}$ NMR spectrum of the mixture showed that the resonances of all three products displayed chemical shifts between δ 0 and 150, also indicating the retention of the Sn(IV) centre. (Figure 2.4)

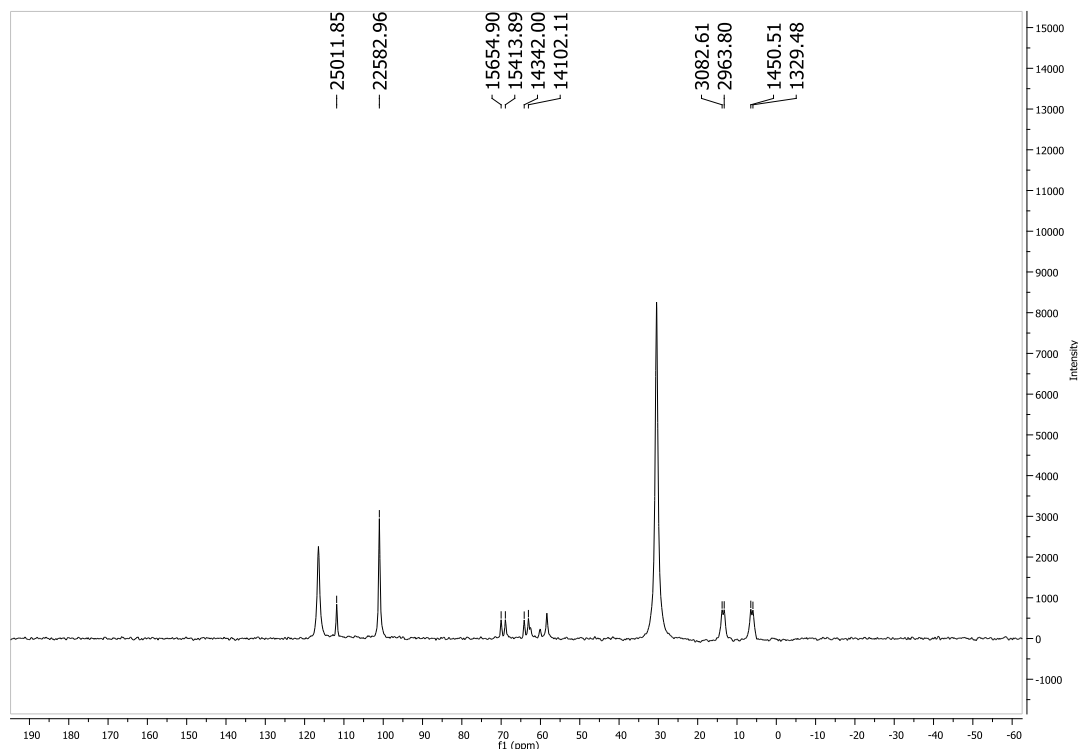
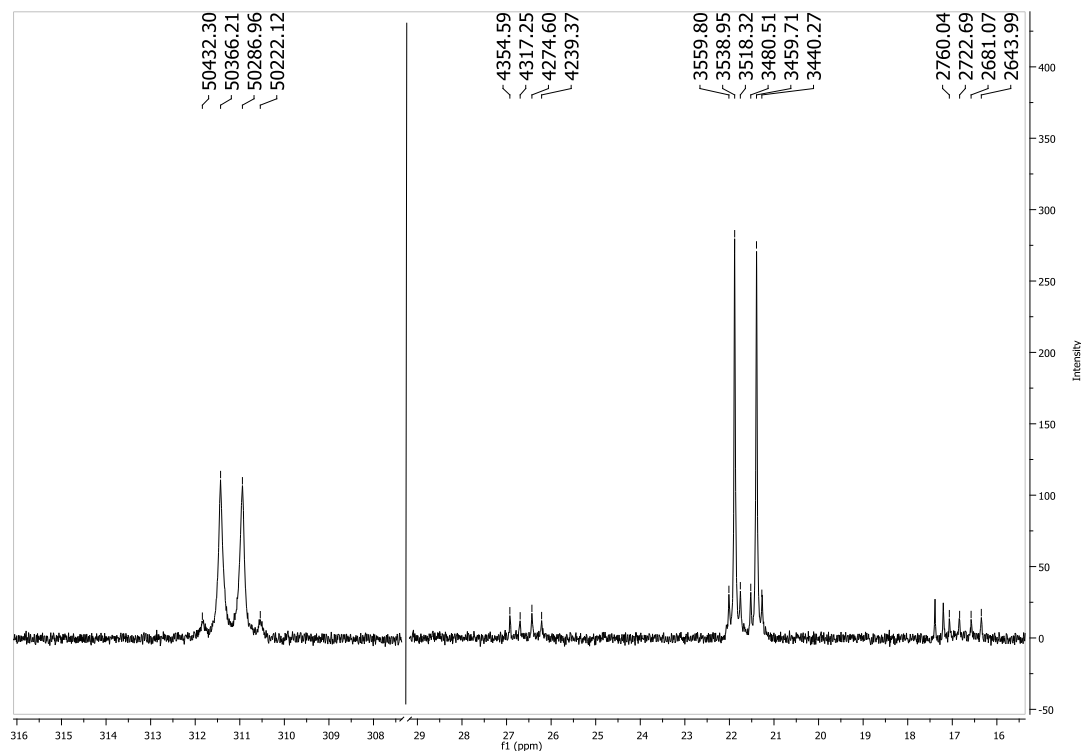


Figure 2.4: $^{119}\text{Sn}\{^1\text{H}\}$ NMR spectrum of the products of reaction of Me_2SnCl_2 with $\text{Cp}_2\text{Zr}(\text{P}_2\text{C}_2^t\text{Bu}_2)$

The $^{119}\text{Sn}\{^1\text{H}\}$ NMR spectrum also showed two significant impurities at δ 30 and 118. The resonance at δ 30 corresponded to Me_2SnCl_2 while the resonance at δ 118 was attributed to an unidentified decomposition product of Me_2SnCl_2 , *e.g.*, $(\text{Me}_2\text{ClSn})_2$ or $(\text{Me}_2\text{ClSn})_2\text{O}$. The nature of this decomposition was not pursued.

For product A, the value determined for the J_{P-P} was 80 Hz, which was notably almost double that determined for the other two products. (Figure 2.5)



*Figure 2.5: Expanded $^{31}\text{P}\{^1\text{H}\}$ NMR spectrum of product A
(trace impurity visible as doublet at δ 17.3)*

In the $^{31}\text{P}\{^1\text{H}\}$ NMR spectrum, both resonances attributed to product A displayed Sn satellites. Although the $^{117}\text{Sn}/^{119}\text{Sn}$ satellites could not be resolved for the resonance at δ 311, a value of 124 Hz was determined for their average which is in the range typically observed for $^2J_{P-Sn}$ couplings. The second resonance at δ 21 displayed much larger Sn-P couplings and indeed the $^{117}\text{Sn}/^{119}\text{Sn}$ satellites were resolved. The much larger values of 1635 and 1560 Hz measured for the $^{31}\text{P}-^{119}\text{Sn}/^{117}\text{Sn}$ couplings respectively indicated a $^1J_{Sn-P}$. In addition to this coupling to one Sn centre a second set of satellites with a value of 37 Hz were observed. These were attributed to a coupling arising from a second Sn centre. This assignment was supported by the observation that the $^{119}\text{Sn}\{^1\text{H}\}$ NMR

spectrum of the mixture contained an additional resonance that had the same relative integral as the resonance assigned to the first Sn centre associated with product A. Furthermore the line-width associated with this ^{119}Sn resonance at δ 101 ($\nu_{1/2} = 91$ Hz), ruled out the observation of the expected doublet for which a coupling constant of 37 Hz would be present. (Figure 2.6)

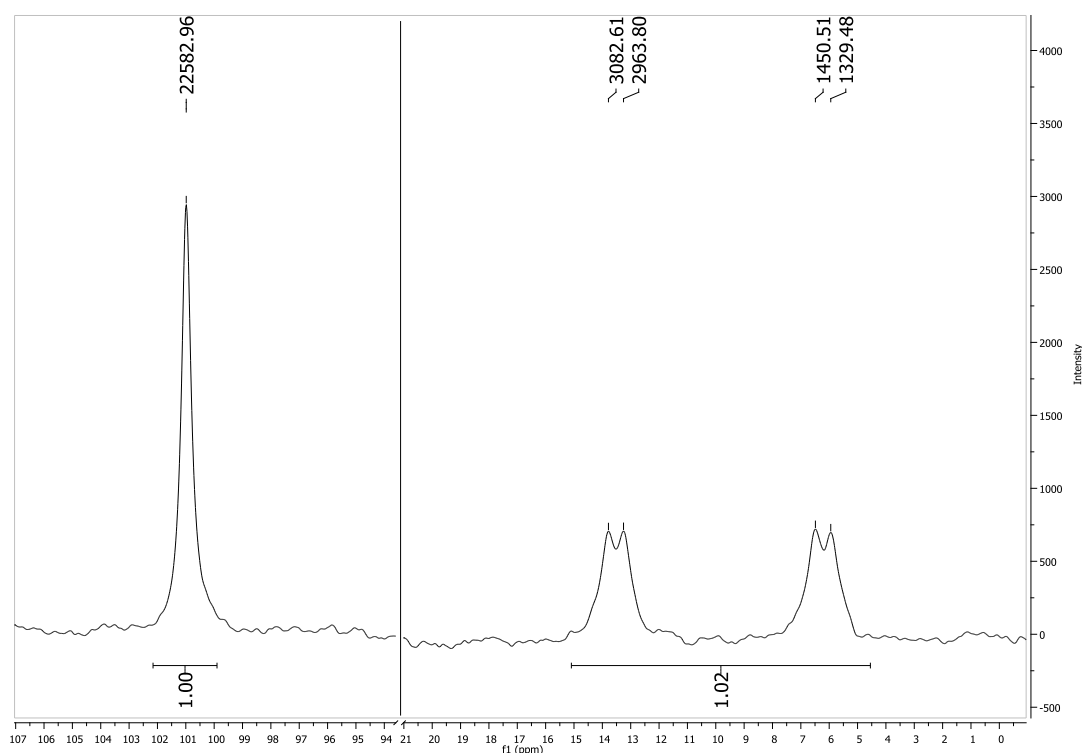


Figure 2.6: Expanded $^{119}\text{Sn}\{^1\text{H}\}$ NMR spectrum of product A

Having postulated that product A contained a second Sn centre, an attempt was made to synthesise it selectively using two equivalents of Me_2SnCl_2 .

Reaction of $\text{Cp}_2\text{Zr}(\text{P}_2\text{C}_2^t\text{Bu}_2)$ with two equivalents of Me_2SnCl_2

The reaction of $\text{Cp}_2\text{Zr}(\text{P}_2\text{C}_2^t\text{Bu}_2)$ with two equivalents of Me_2SnCl_2 was carried out in a mixture of THF and benzene- d^6 (circa 9:1). The mixture was heated to 50 °C for 5 days in the absence of light. Product A was synthesised in approximately 85% yield (as determined from the integration of the resonances in the $^{31}\text{P}\{^1\text{H}\}$ NMR spectrum) along with traces of products B and C. (Figure 2.7)

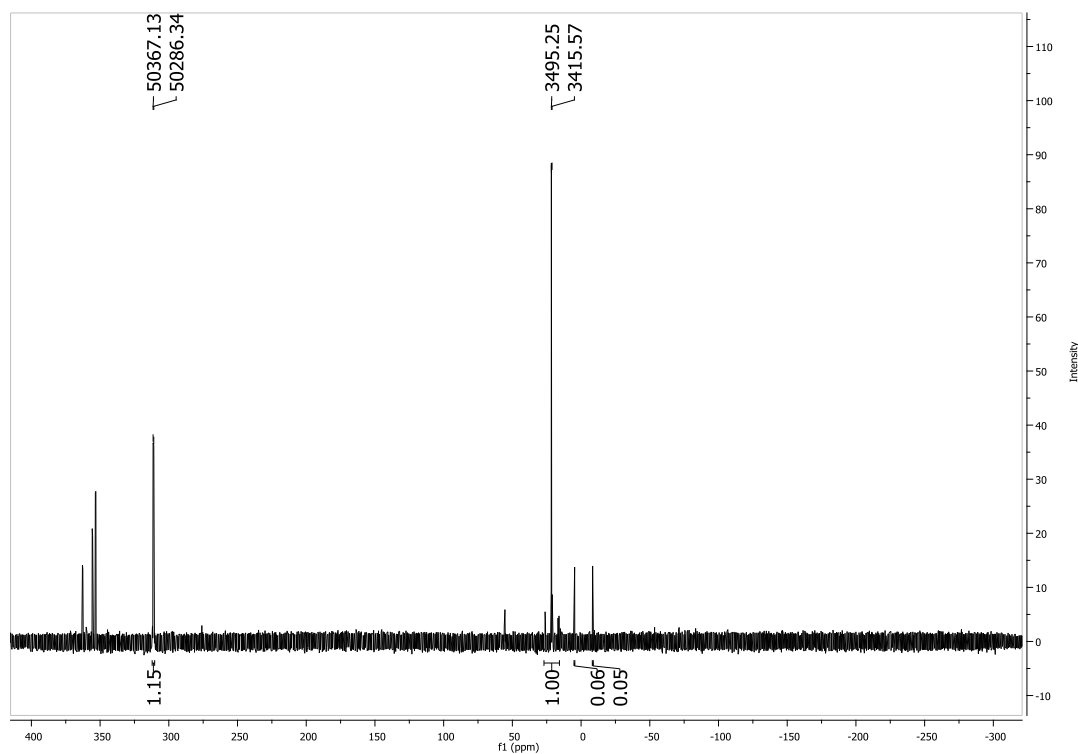


Figure 2.7: $^{31}\text{P}\{^1\text{H}\}$ NMR spectrum of product A

The ^1H NMR spectrum of product A displayed four resonances with an integral ratio of 9:9:6:6 (Figure 2.8)

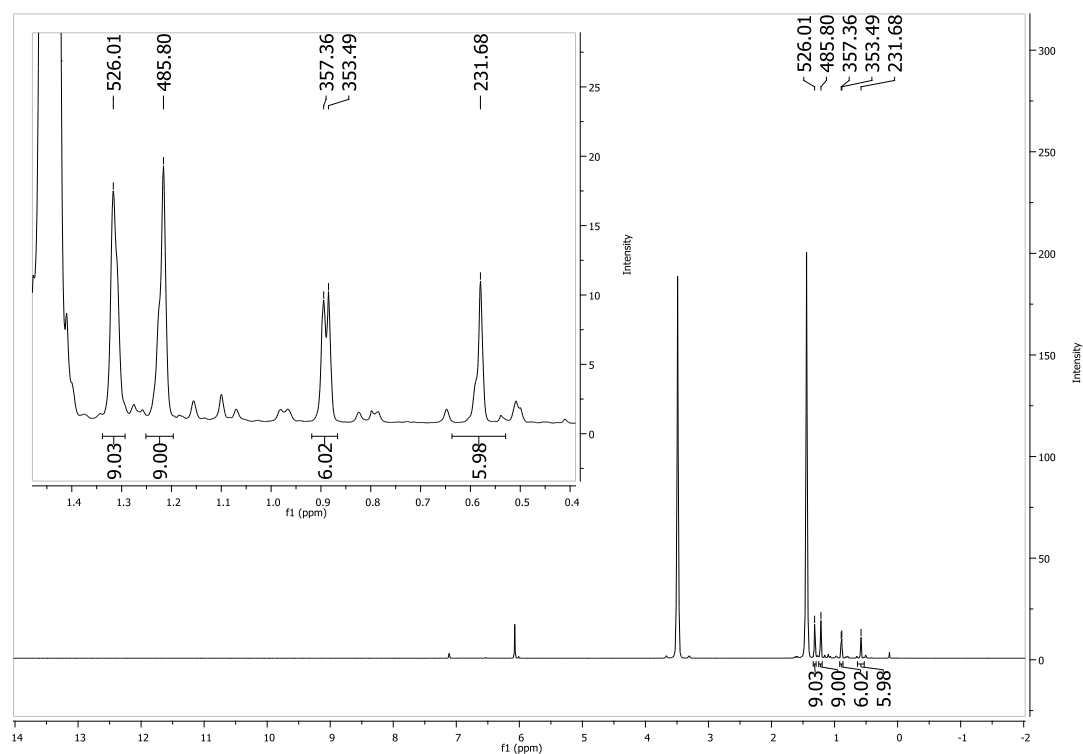


Figure 2.8: ^1H NMR spectrum of product A

Chemical Shift	Relative Integral	$J\ ^1\text{H}-^{31}\text{P}/\text{Hz}$	$^2J\ ^1\text{H}-^{117/119}\text{Sn}/\text{Hz}$
1.32	9	-	-
1.22	9	-	-
0.89	6	4	57
0.58	6	-	58

Table 2.2: ^1H NMR spectroscopic data for product A

The resonances at δ 1.32 and 1.22 were assigned, based on their integrals and chemical shifts, to the presence of two inequivalent ^tBu groups. Both of the resonances at δ 0.89 and 0.58 possessed Sn satellites and although the $^{117/119}\text{Sn}$ individual couplings could not be resolved this further confirmed the presence of a second Me_2Sn moiety in

product A. (Table 2.2) A molecular structure for product A which is consistent with the NMR spectroscopic data is shown in Figure 2.9.

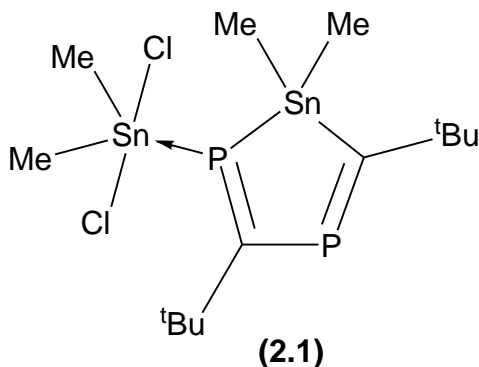
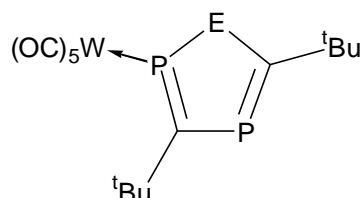


Figure 2.9: Proposed molecular of product A (2.1)

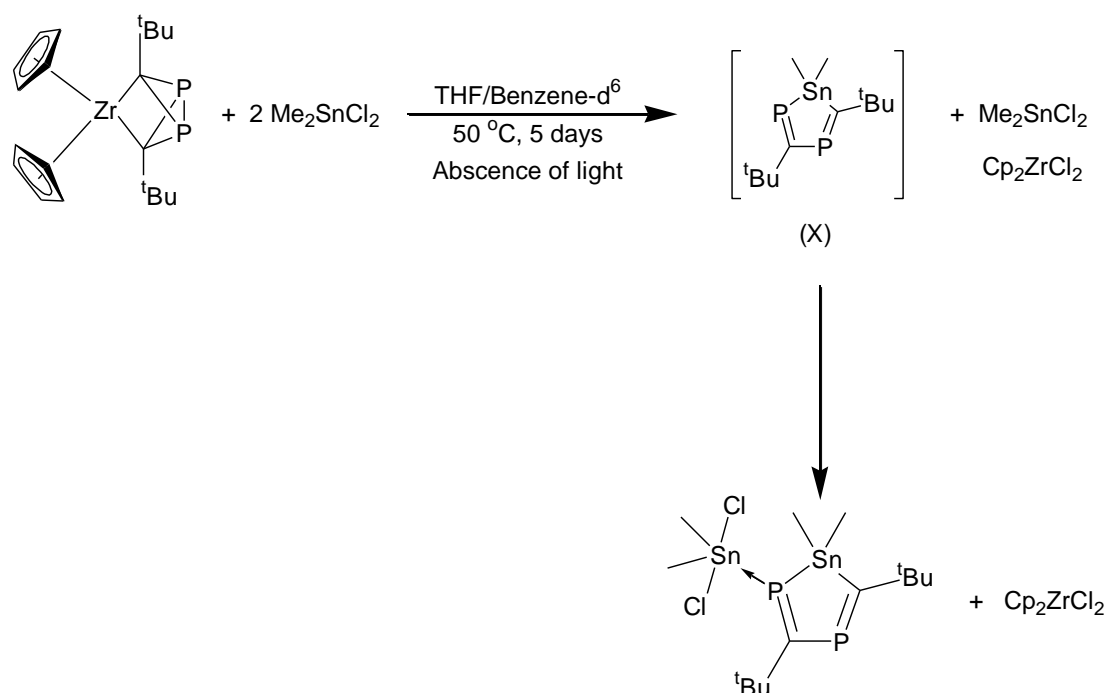
The nature of the SnCPCP ring would render the Me groups which are projected above and below this plane chemically equivalent in the ^1H NMR spectrum. The introduction of a second Me_2Sn group within product A is proposed to derive from the coordination of the ring P atom adjacent to the first Sn centre, for which two sets of Sn satellites were observed in the $^{31}\text{P}\{^1\text{H}\}$ NMR spectrum of A. This coordination is also responsible for the large value of the $^2J_{\text{P-P}}$ detected for this resonance, since similarly increased couplings have been observed for other P-C ring systems (containing S,¹⁵ Se¹⁶ or Te¹⁷) upon W centres.¹⁸ (Figure 2.10)



E	S	Se	Te
$^2J_{\text{P-P}}$ Without $\text{W}(\text{CO})_5$	49.5 Hz	49.1 Hz	50.8 Hz
$^2J_{\text{P-P}}$ With $\text{W}(\text{CO})_5$	62.5 Hz	64.0 Hz	66.1 Hz

Figure 2.10: Increased $^2J_{\text{P-P}}$ couplings due to coordination to $\text{W}(\text{CO})_5$

Since the uncoordinated SnCPCP ring was not observed in the ^{31}P NMR or ^{119}Sn NMR spectra it was postulated that this precursor (X) is unstable without the effect of the second Sn centre. (Scheme 2.13)



Scheme 2.13: Synthesis of product A

Whilst product A could be synthesised selectively, product B could only be obtained from the reaction of $\text{Cp}_2\text{Zr}(\text{P}_2\text{C}_2\text{tBu}_2)$ with one equivalent of Me_2SnCl_2 , as outlined in Scheme 2.12. The value of the P-P coupling constant of 43 Hz observed for product B is a value characteristic of a $^2J_{\text{P-P}}$ coupling around a $\text{P}_2\text{C}_2\text{R}_2$ ring.⁵ (Figure 2.11)

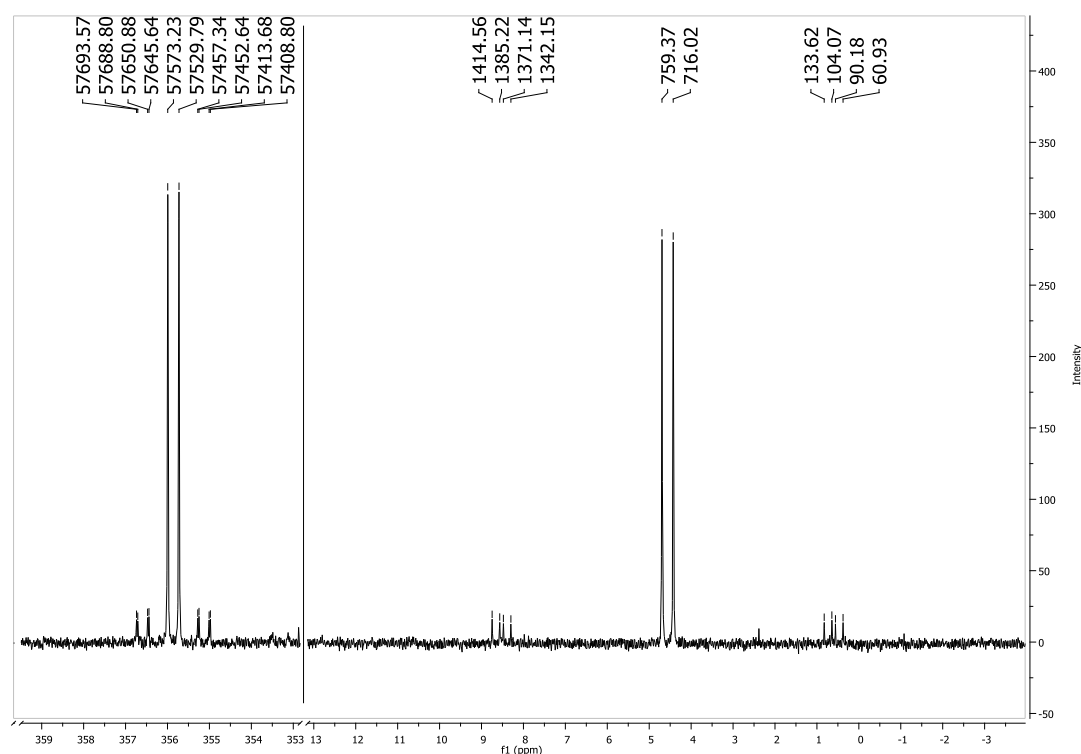


Figure 2.11: Expanded $^{31}\text{P}\{^1\text{H}\}$ NMR spectrum of product B

The chemical shifts of the resonances observed at *circa* δ 350 and 0 are typically displayed by unsaturated and saturated phosphorus atoms respectively. Both resonances displayed $^{117}\text{Sn}/^{119}\text{Sn}$ satellites. For the resonance at δ 356 the measured values of 231 and 242 Hz for the ^{31}P - $^{117}\text{Sn}/^{119}\text{Sn}$ coupling constants are typical of a $^2J_{\text{P-Sn}}$ coupling. On the other hand for the resonance at δ 5 the much higher values of 1252 and 1310 Hz determined for the ^{31}P - $^{117}\text{Sn}/^{119}\text{Sn}$ coupling constants respectively are typical of a $^1J_{\text{P-Sn}}$ coupling. These coupling constants were also observable in the $^{119}\text{Sn}\{^1\text{H}\}$ NMR spectrum resonance attributed to this product which was observed at δ 67 as a doublet of doublets. (Figure 2.12)

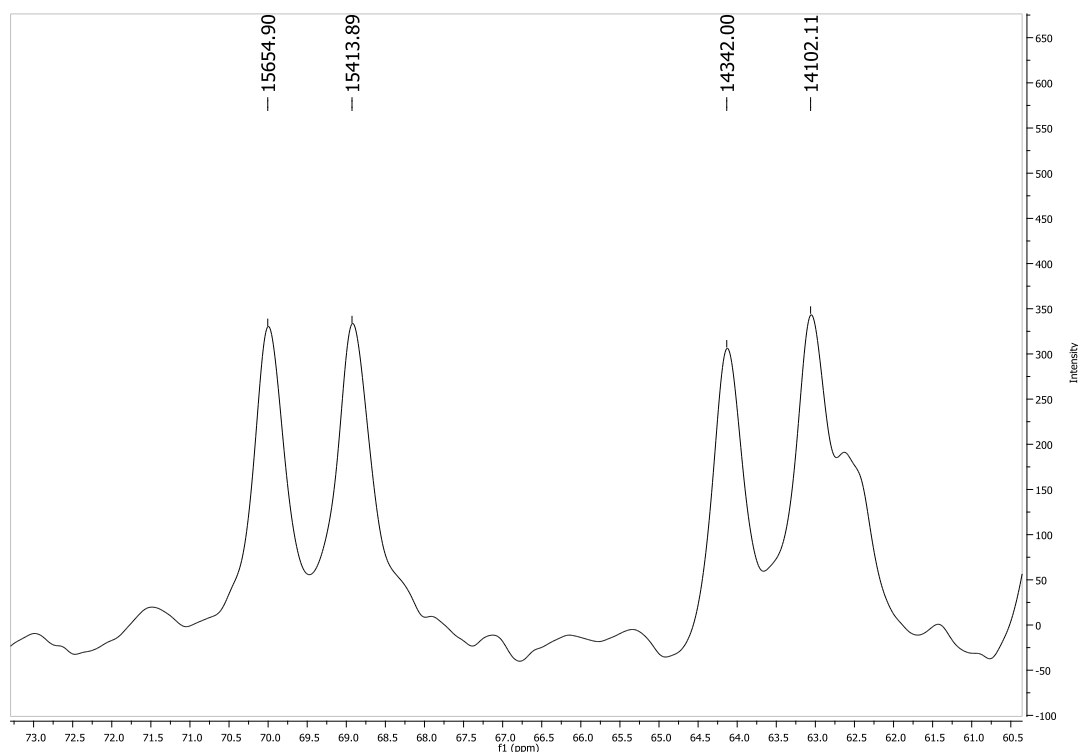


Figure 2.12: Expanded $^{119}\text{Sn}\{^1\text{H}\}$ NMR spectrum of product B (unidentified impurity visible as a shoulder at δ 62.5)

For product B a molecular structure which is consistent with the NMR spectroscopic data is shown in Figure 2.13.

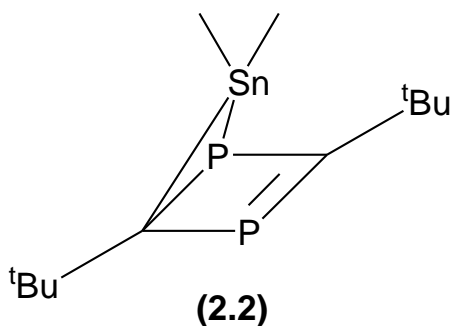
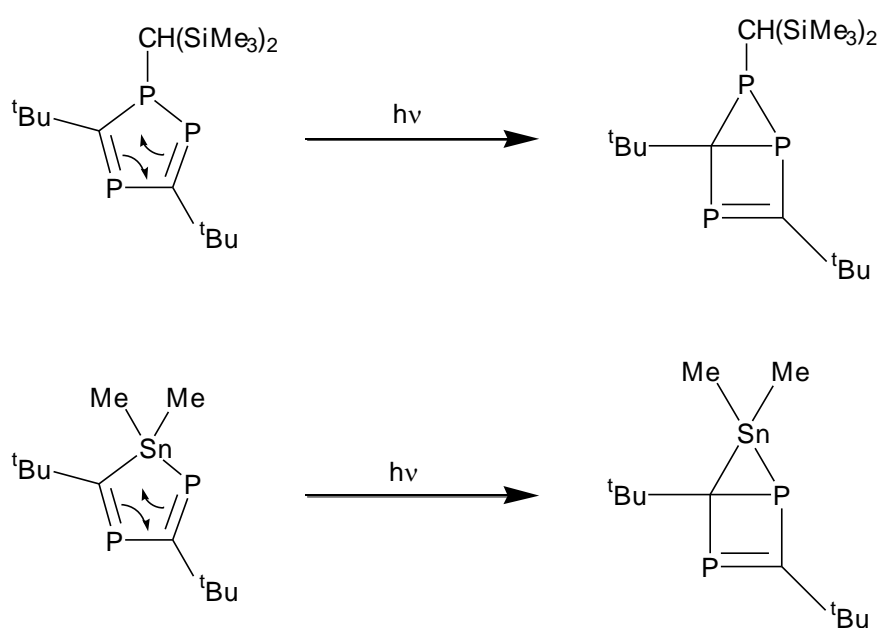


Figure 2.13: Proposed molecular structure of product B (2.2)

This molecular structure is a Sn analogue of the bicyclic product identified from the reaction of $\text{Cp}_2\text{Zr}(\text{P}_2\text{C}_2^t\text{Bu}_2)$ and SbCl_3 ¹² (*vide* Chapter 1, Scheme 1.8). As no X-ray

diffraction data is available for product B, no comparison of bond lengths and angles can be made with $\text{SbCl}(\text{P}_2\text{C}_2^t\text{Bu}_2)$, it is interesting to note, however, that whilst the $^{31}\text{P}\{^1\text{H}\}$ NMR spectrum of product B indicates the two expected P environments, that of $\text{SbCl}(\text{P}_2\text{C}_2^t\text{Bu}_2)$ shows only one. This suggests a far greater degree of fluxionality in the Sb-P bonds than in the Sn-P bonds. The proposal of this molecular structure for product B is based on two observations. Firstly, the identification of the five-membered Me_2SnCPCP ring motif within product A which, in our opinion, is made relatively stable by the presence of the second Sn centre. Clearly, the structure proposed for product B could be a precursor for product A. Secondly, it has been reported that the triphosphole, $\text{P}_3\text{C}_2^t\text{Bu}_2\text{CH}(\text{SiMe}_3)_2$,¹⁹ which possesses an analogous five-membered ring motif as the structure proposed for the precursor X, but with $\{(\text{Me}_3\text{Si})_2\text{CH}\}\text{P}$ in place of the Me_2Sn group, underwent an electrocyclication to form the triphospha-bicyclopentene when exposed to sunlight over several days.²⁰ (Scheme 2.14) Given the similarities between the two systems it is postulated that the equivalent reaction is the source of product B.

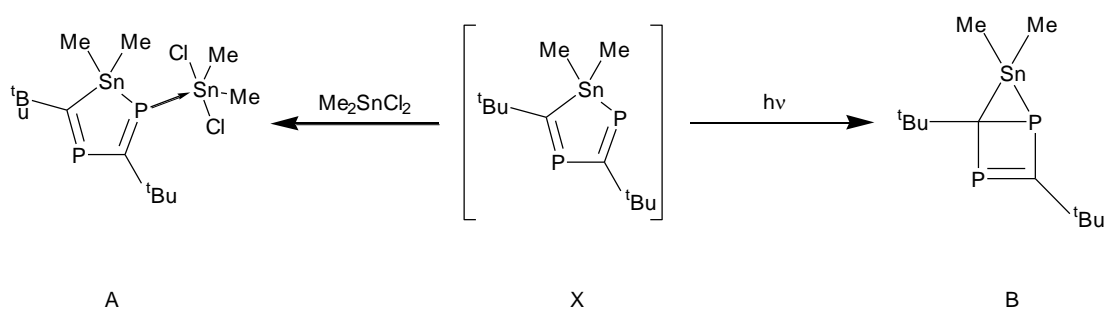


Scheme 2.14: Electrocyclisations of triphosphole and $\text{Me}_2\text{Sn}(\text{P}_2\text{C}_2^t\text{Bu}_2)$

This reaction is, in effect, an analogue of the well-established photochemical 2+2 cycloadditions which are common in organic chemistry.²¹

This shared precursor of products A and B explains their concomitant production, and accounts for the conditions required to increase the proportion of product A formed.

(Scheme 2.15)



Scheme 2.15: Formation of products A and B from precursor X

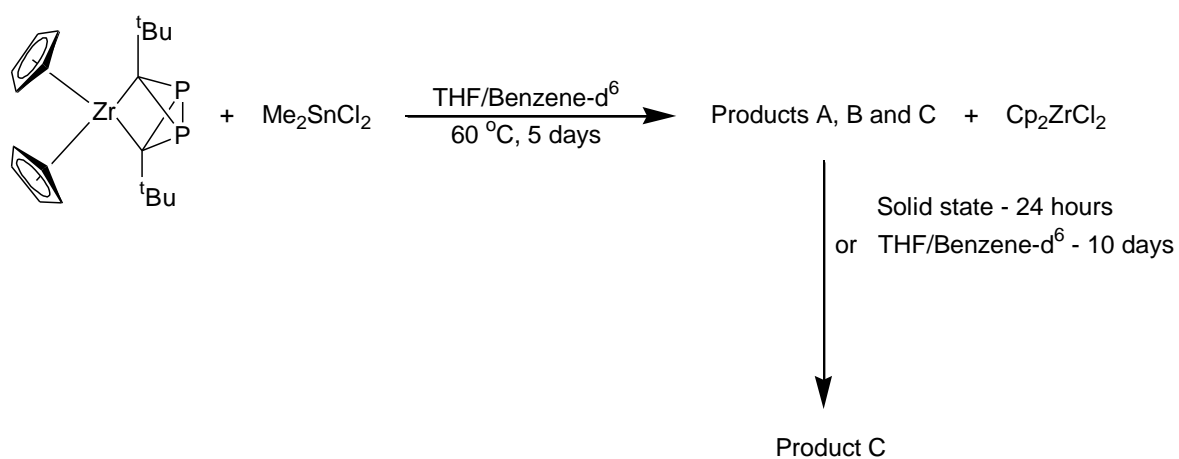
Synthesis of Product C (2.3)

Method 1:

When the solvent was removed *in vacuo* from solutions containing the mixture of products A, B and C and the resulting yellow solid was left to stand at ambient temperature for 24 hours in the light, the resonances observed in the $^{31}\text{P}\{^1\text{H}\}$ NMR spectra assigned to products A and B were no longer visible, while those assigned to product C were still present along with a trace amount of a new product. (Figure 2.14) That product C had increased in concentration was determined from measurements of the signal to baseline noise ratio (s/n) determined from a series of $^{31}\text{P}\{^1\text{H}\}$ NMR spectra, which increased from 25.6 to 144.5.

Method 2:

Similarly when a THF/benzene-d⁶ solution containing the mixture of products A, B and C was maintained at ambient temperature for 10 days in the light, the only the resonances arising from product C were observed in the ³¹P{¹H} NMR spectra of these solutions. (Figure 2.14)



Scheme 2.16: Synthesis of product C

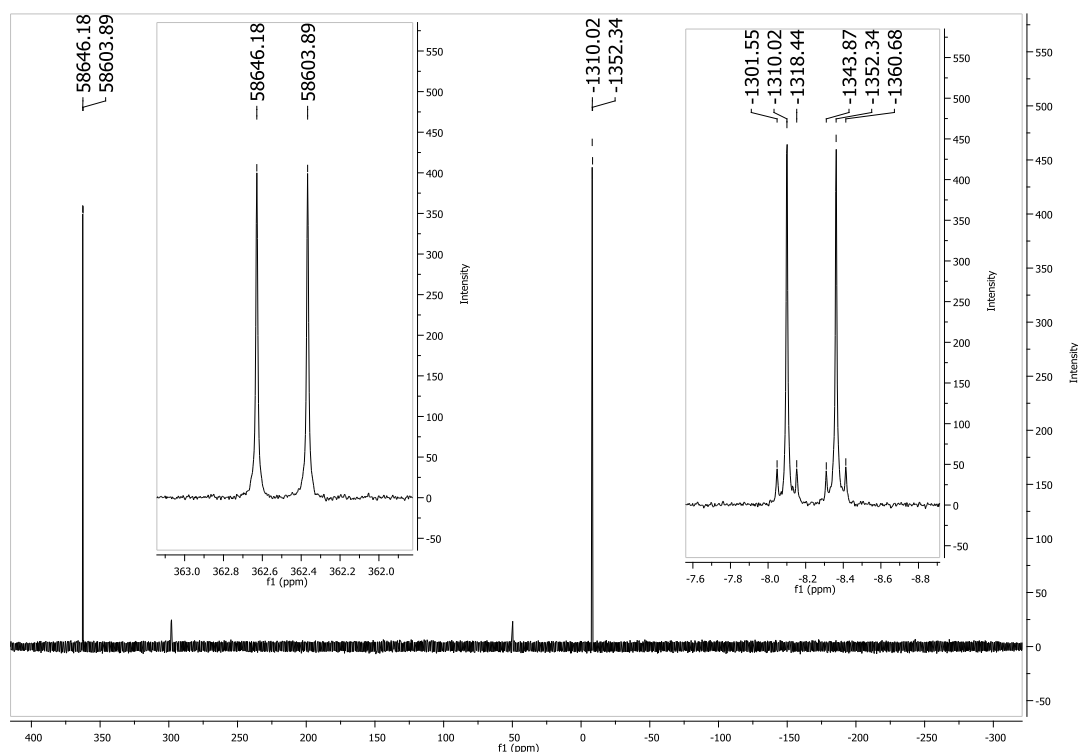


Figure 2.14: $^{31}\text{P}\{^1\text{H}\}$ NMR spectrum product C

The two resonances were observed as a pair of doublets with a $^2J_{\text{P-P}}$ of 42 Hz. The resonance at δ -8 showed $^{117/119}\text{Sn}$ satellites with a coupling constant value of 17 Hz, but there was no sign of $^{117/119}\text{Sn}$ satellites for the resonance at δ 363.

A mass spectrum of product C, obtained *via* method 1 revealed that the parent ion possessed a mass of 386 u which was consistent with a formula for product C of $\text{Me}_2\text{Sn}(\text{P}_2\text{C}_2^t\text{Bu}_2)\text{HCl}$. (Figure 2.15) The major fragments at 351 and 201 indicated the loss of the Cl first, followed by the Me_2Sn group, leaving a $\text{H}(\text{P}_2\text{C}_2^t\text{Bu}_2)_2$ which then underwent further fragmentation. The presence of the Sn and Cl atoms in the appropriate fragments was also confirmed by the isotopic splitting patterns.

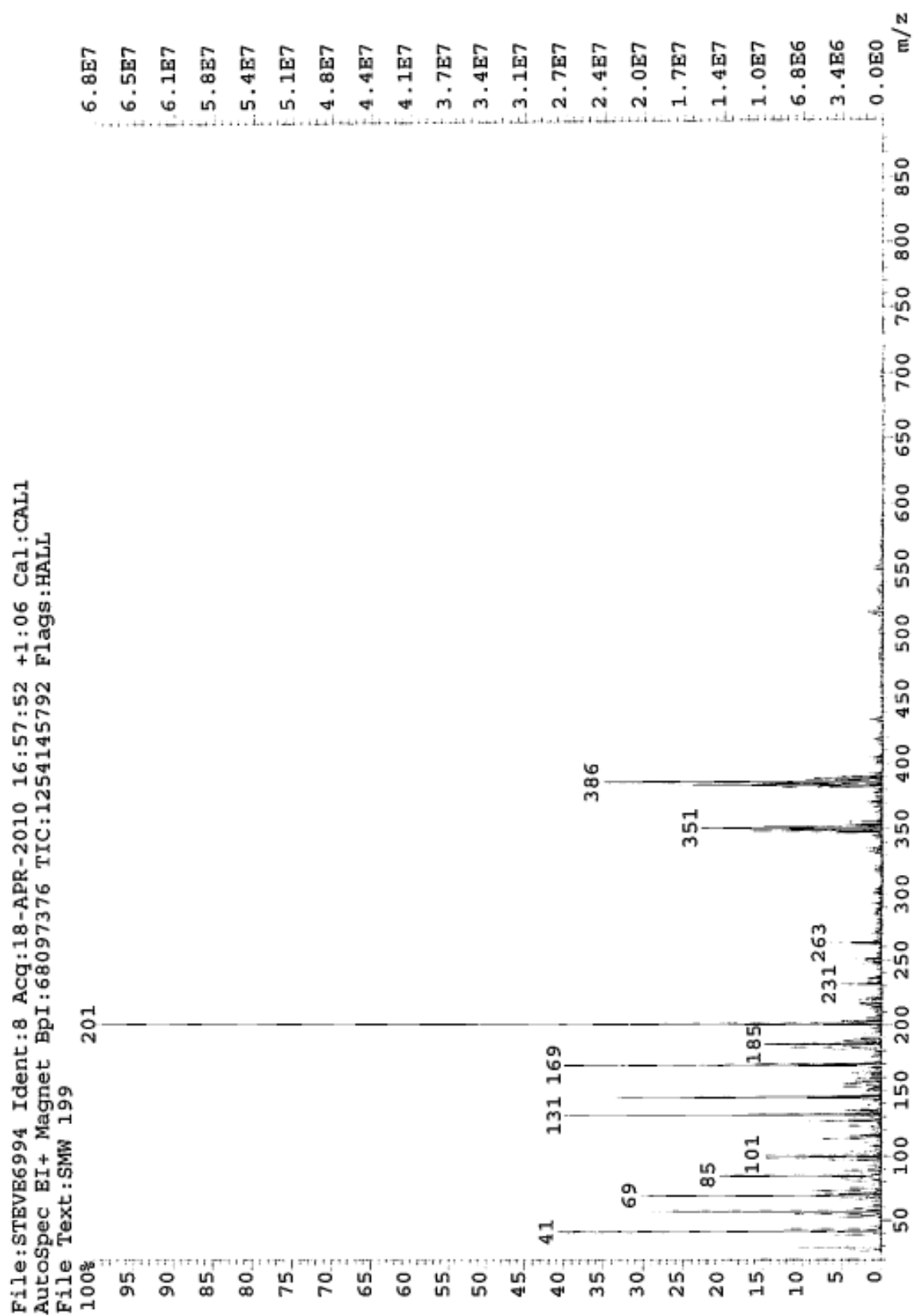


Figure 2.15: Mass spectrum of product C

In order to confirm the presence of this additional proton and ascertain its location within the molecular structure of product C, a proton coupled ^{31}P NMR spectrum was obtained. (Figure 2.16)

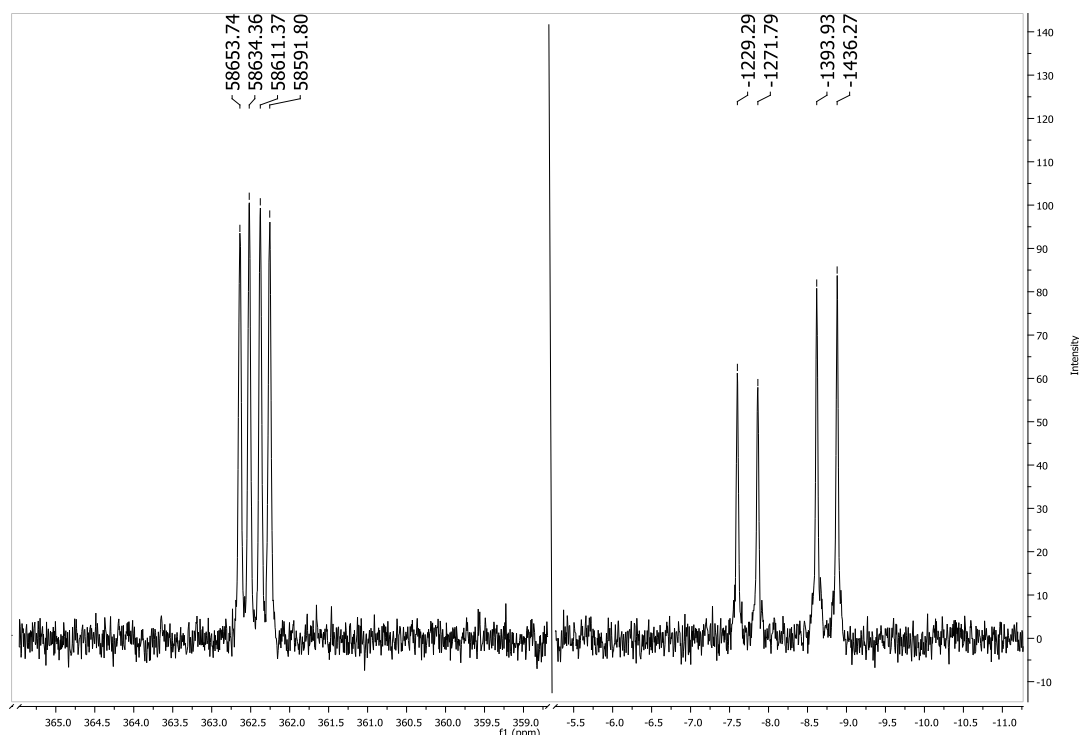


Figure 2.16: ^{31}P NMR spectrum product C

In this spectrum each of the two resonances which were observed previously as doublets in $^{31}\text{P}\{^1\text{H}\}$ NMR spectrum now appeared as doublets of doublets. For the resonance at δ -8 a ^{31}P - ^1H coupling constant value of 165 Hz was determined which is typical of $^1J_{\text{P-H}}$. For the second resonance at δ 363 a much smaller value of 20 Hz was determined for the ^{31}P - ^1H coupling, a value which is typical of $^3J_{\text{P-H}}$ coupling. The ^1H NMR spectrum revealed a corresponding doublet of doublets centred at δ 6.70. Combining the value of the chemical shift, the ^{31}P - ^1H couplings, and the relative integral ratios confirmed product C contained a protonated P centre. (Figure 2.17) The complete ^1H NMR spectroscopic data for product C is shown in Table 2.3.

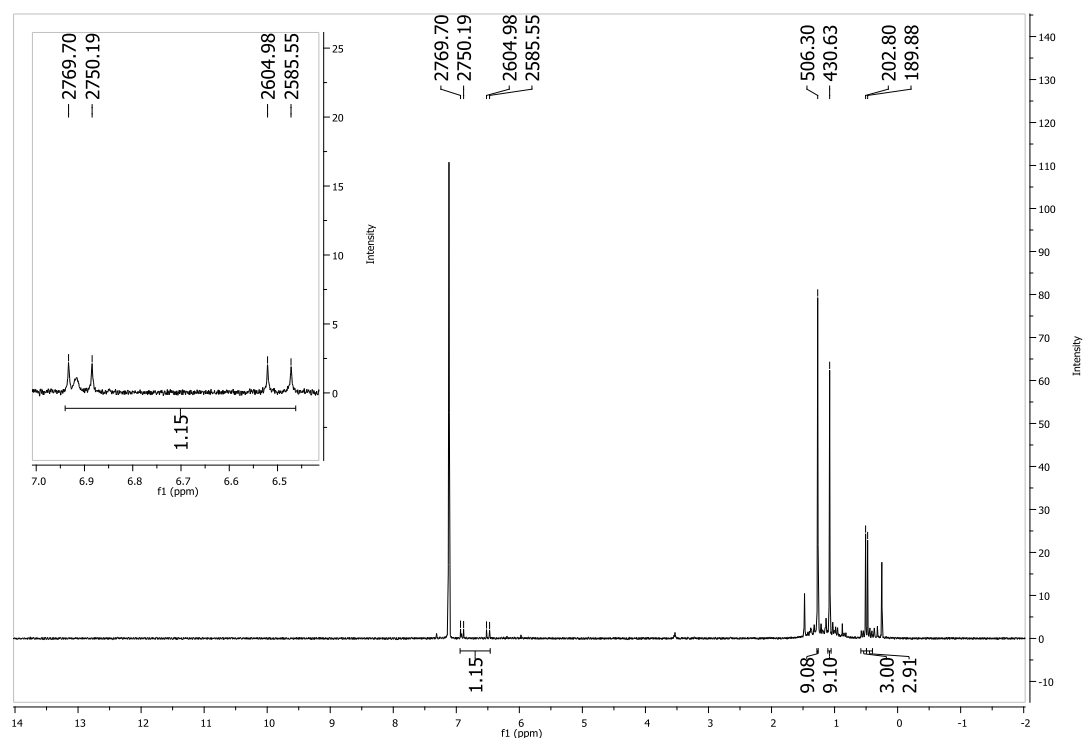


Figure 2.17: ^1H NMR spectrum product C

Chemical Shift	Relative Integral	$J^{1\text{H}-^{31}\text{P}}/\text{Hz}$	$J^{1\text{H}-^{117/119}\text{Sn}}/\text{Hz}$
6.70	1	165, 20	-
1.27	9	-	-
1.08	9	-	-
0.51	3	-	54
0.48	3	-	54

Table 2.3: ^1H NMR data for Product C

The $^{119}\text{Sn}\{^1\text{H}\}$ NMR spectrum of product C showed a single, broad resonance at δ 112. (Figure 2.18)

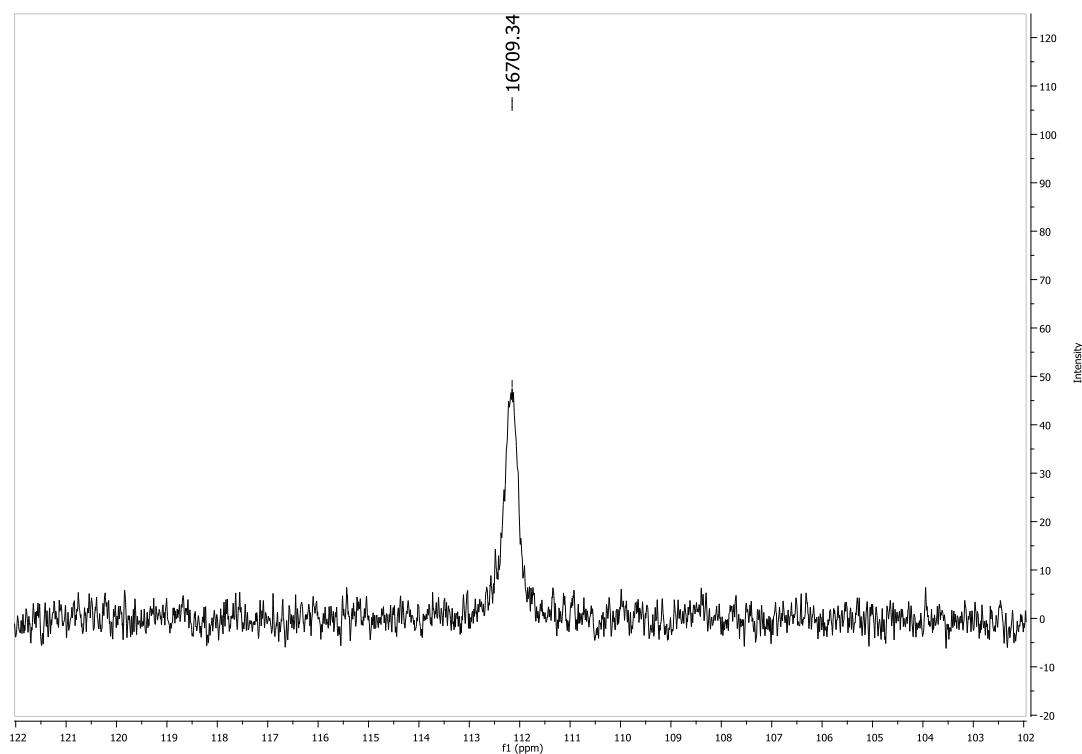


Figure 2.18: $^{119}\text{Sn}\{^1\text{H}\}$ NMR spectrum $\text{Me}_2\text{SnCl}(\text{P}_2\text{C}_2^t\text{Bu}_2)\text{H}$

The proposed molecular structures of product C based on the NMR spectroscopic data and mass spectrometric data is shown in Figure 2.19.

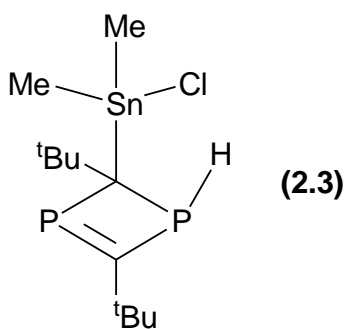


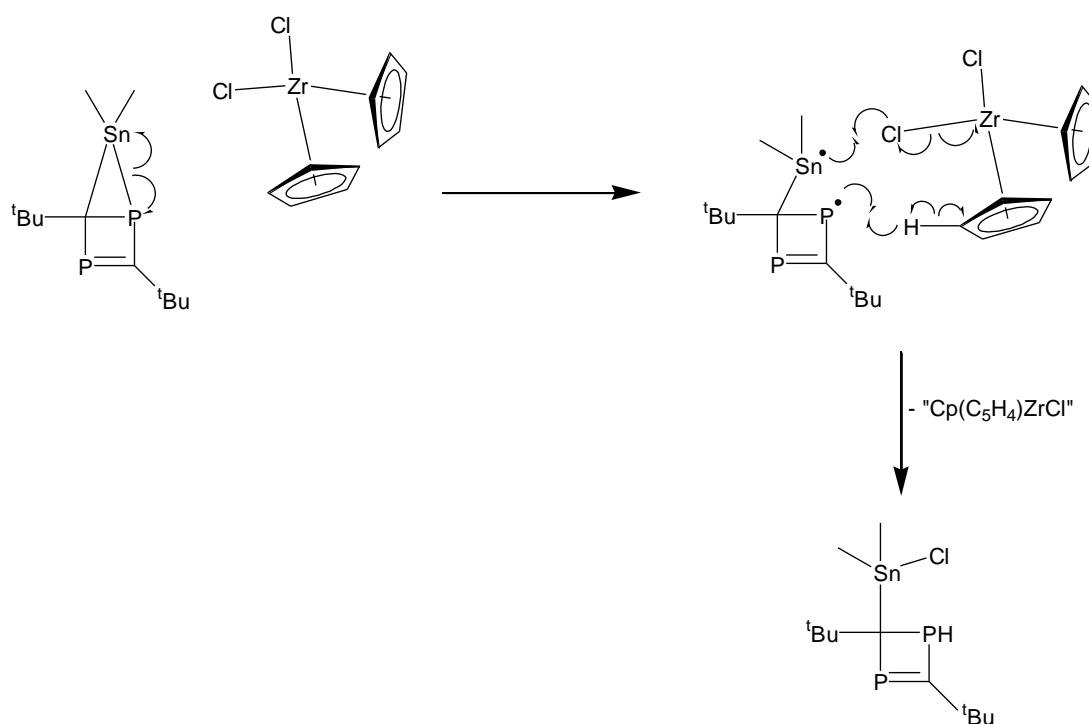
Figure 2.19: Proposed molecular structure of product C (2.3)

The structure proposed for product C is that a square planar P_2C_2 ring with one of the P atoms protonated and its adjacent C atom bearing a SnMe_2Cl group. The

proposed structure is analogous to products isolated from the hydrostannylation reactions of Regitz *et al.*⁵ (*vide supra*, Scheme 2.6) Although such structures should display $^2J_{\text{P-Sn}}$ couplings of *circa* 100-300 Hz, the greatest Sn-P coupling detected in the $^{31}\text{P}\{^1\text{H}\}$ NMR spectrum was the 17 Hz coupling to the protonated P. The reduced coupling could arise from two factors. Firstly, if the angle between the Sn and P dipoles is close to 90° , which is likely given similar structures previously observed,⁵ or secondly, since the angles of the square planar ring imply a high level of p-orbital character in the bonding orbitals, the value of any $^2J_{\text{P-Sn}}$ coupling would also be reduced.²² Ordinarily, the unsaturated P atom might be expected to couple to the Sn more strongly than the saturated P as the sp^2 hybridisation has a higher proportion of s-orbital character than the sp^3 . This was not observed in this case, indicating that the angle between the dipoles of the Sn and unsaturated P was much closer to 90° .

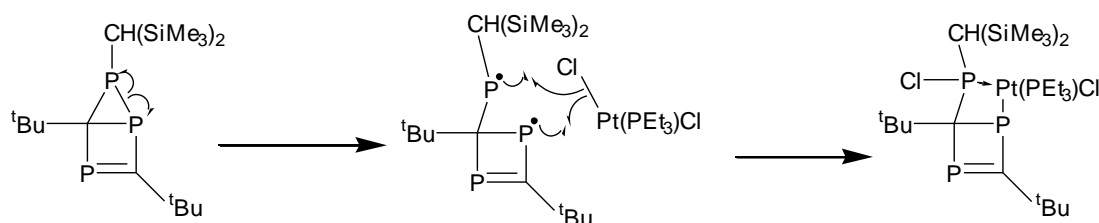
Product C is proposed to arise as a result of the interaction between $\text{Me}_2\text{Sn}(\text{P}_2\text{C}_2^t\text{Bu}_2)$ and the Cp_2ZrCl_2 which was generated as a by-product during the reaction between $\text{Cp}_2\text{Zr}(\text{P}_2\text{C}_2^t\text{Bu}_2)$ and Me_2SnCl_2 . The possibility of the H and Cl originating from a second equivalent of Me_2SnCl_2 was discounted for two reasons. Firstly, the production of product C was seen to be greatest towards the end and after the initial reaction of $\text{Cp}_2\text{Zr}(\text{P}_2\text{C}_2^t\text{Bu}_2)$ with Me_2SnCl_2 , which correlated to an increased concentration of Cp_2ZrCl_2 but a decreased concentration of Me_2SnCl_2 . Secondly, a lack of acidic protons available from Me_2SnCl_2 means that after the abstraction of the chloride the SnMe_2Cl moiety would likely bind to the P atom of the ring (which was not observed) or couple with a second equivalent to form $(\text{Me}_2\text{ClSn})_2$. This would leave the P centred radical to abstract a proton from another source, probably the solvent, but performing the reaction in THF-d^8 showed no evidence of a deuterated product.

The reaction was accelerated by exposure to sunlight and thus was proposed to proceed *via* a radical mechanism involving the homolytic fission of the Sn-P bond. The chloride would then be transferred from the Zr onto the Sn leaving an unpaired electron on the P which is thought to abstract a proton from the Cp ring, although the ultimate fate of the Zr complex is unknown. (Scheme 2.17)



Scheme 2.17: Proposed abstraction of HCl from Cp_2ZrCl_2 by $\text{Me}_2\text{Sn}(\text{P}_2\text{C}_2^t\text{Bu}_2)$ to form $\text{Me}_2\text{SnCl}(\text{P}_2\text{C}_2^t\text{Bu}_2)\text{H}$

This proposed reaction presents another similarity between the behaviours of $\text{Me}_2\text{Sn}(\text{P}_2\text{C}_2^t\text{Bu}_2)$ and triphosphabicyclopentene. The triphosphabicyclopentene has been shown to undergo a reaction with $[\text{PtCl}_2(\text{PEt}_3)]_2$ in which the P-P bond was broken, a chloride was transferred to P with the $\text{CH}(\text{SiMe}_3)_2$ substituent and Pt was bound between the P atoms.²⁰ (Scheme 2.18) This differs from the reaction depicted in Scheme 2.13 only in that, due to the sterically unhindered Pt centre and lack of acidic protons, the Pt has bound to the P rather than transferring a H.



Scheme 2.18: Reaction of $P_3C_2^tBu_2CH(SiMe_3)_2$ with $[PtCl_2(PEt_3)_2]$

Although in some ways the $Me_2Sn(P_2C_2^tBu_2)$ and triphoshabicyclopentene systems appear very similar, a major difference in the activity of these compounds arose in the [1,3]-sigmatropic rearrangement. In the case of the triphoshabicyclopentene, $^{31}P\{^1H\}$ NMR spectroscopy reportedly showed a transition in which the phosphorus atoms of the ring became equivalent, indicating that it was the P-P bonds that were fluxional, with the P-C bond maintained throughout.^{20,23} In the $^{31}P\{^1H\}$ NMR spectrum of $Me_2Sn(P_2C_2^tBu_2)$ such a pattern was not observed. Instead there appeared to be a pair of doublets with a coupling constant value of 60 Hz displayed at δ 353 and 56 with different degrees of broadening, suggesting a possible fluxional state. (Figure 2.20)

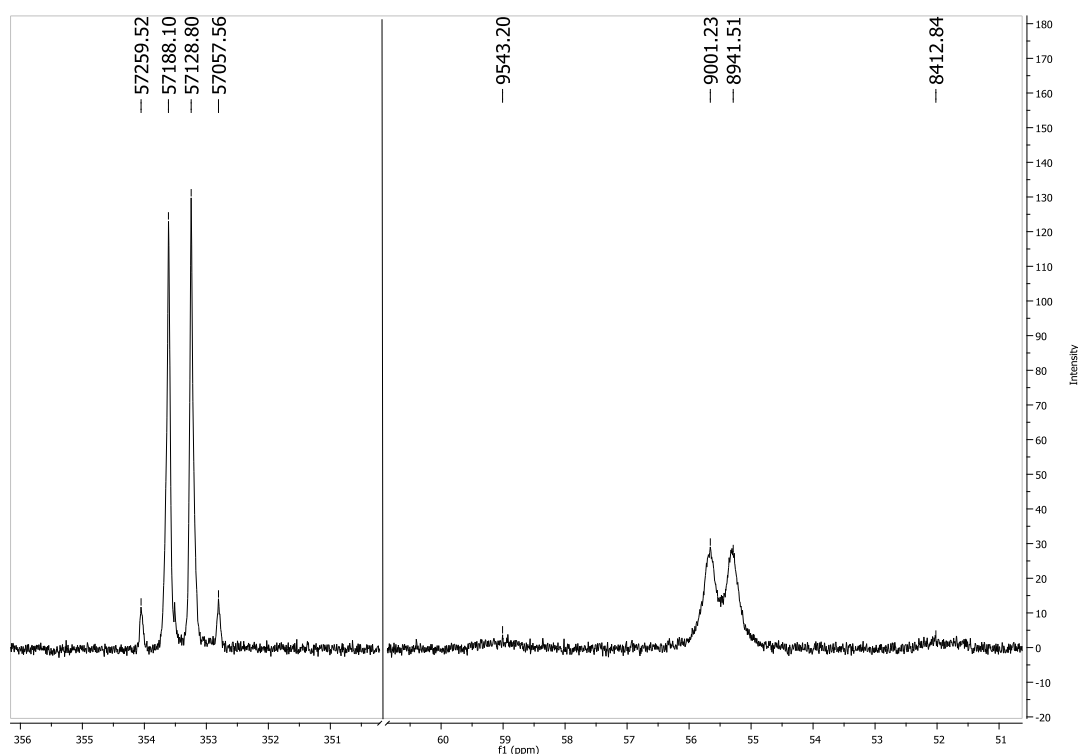


Figure 2.20: Expanded $^{31}\text{P}\{^1\text{H}\}$ NMR spectrum postulated as $\text{Me}_2\text{Sn}(\text{P}_2\text{C}_2^t\text{Bu}_2)$ during [1,3]-sigmatropic rearrangement

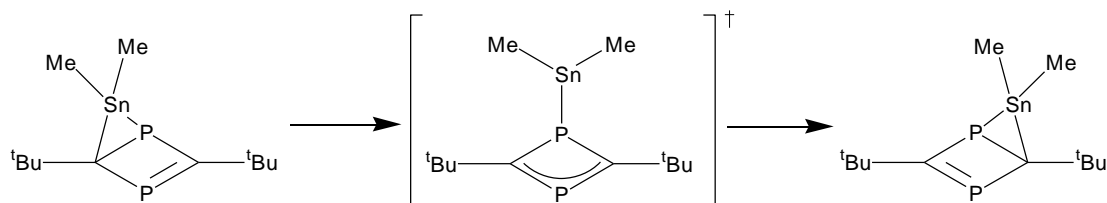
The resonance at δ 56 shows a far greater broadening and a higher value of coupling constant to $^{117/119}\text{Sn}$ than that at δ 353. (Table 2.4)

Chemical Shift	$J^{31}\text{P}-^{117/119}\text{Sn}/\text{Hz}$	Line-width
353.4	69	8
55.5	1079	40

Table 2.4: $^{31}\text{P}\{^1\text{H}\}$ NMR data postulated as $\text{Me}_2\text{Sn}(\text{P}_2\text{C}_2^t\text{Bu}_2)$ during [1,3]-sigmatropic rearrangement

This indicated that if these resonances are the result of a [1,3]-sigmatropic rearrangement transition state, the resonance at δ 56 corresponds to the P bound directly to the Sn atom and therefore undergoing the greater change in chemical shift during the

rearrangement. This suggests that the Sn-C bonds were fluxional in this example.
(Scheme 2.19)



Scheme 2.19: [1,3]-sigmatropic rearrangement of $\text{Me}_2\text{Sn}(\text{P}_2\text{C}_2^t\text{Bu}_2)_2$

This is an unexpected result in light of the fact that the decomposition product of $\text{Me}_2\text{Sn}(\text{P}_2\text{C}_2^t\text{Bu}_2)_2$ showed that the Sn-P bond had been broken. The reason for this apparent discrepancy is not known, but it may be the case that the rearrangement must be arrested by the coordination of one of the P atoms to a metal centre (as observed for the triphospha-bicyclopentene²⁰) before the Sn-P bond cleavage can take place.

Synthesis of $[\text{Me}_2\text{Sn}(\text{P}_2\text{C}_2^t\text{Bu}_2)]_2$ (2.4)

The $^{31}\text{P}\{^1\text{H}\}$ NMR spectra of product C showed a small impurity with resonances at δ 297.8 and 49.2. (Figure 2.21)

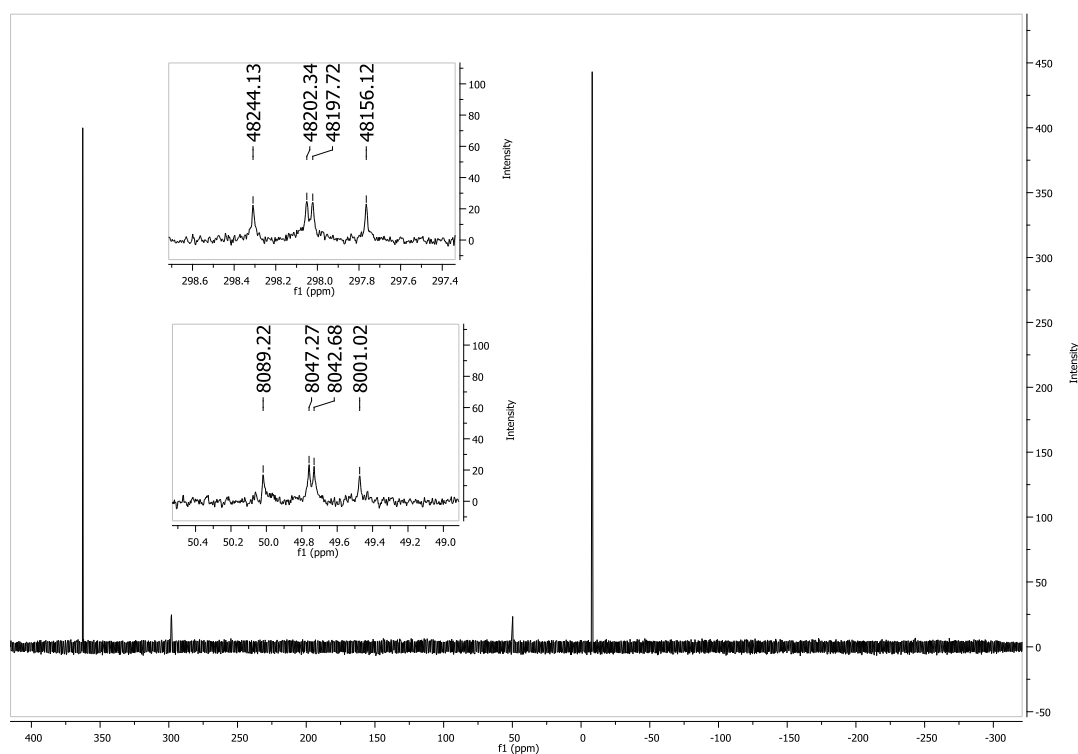


Figure 2.21: $^{31}\text{P}\{^1\text{H}\}$ NMR spectrum of product C with focus on the trace impurity

Unlike products A, B and C, these resonances appeared as doublets of doublets, each with P-P coupling constants with values of 46 Hz and 42 Hz. This indicates a system containing four P atoms in pairs which were chemically equivalent but not magnetically equivalent. This was postulated to arise from a dimerisation of the $\text{Me}_2\text{Sn}(\text{P}_2\text{C}_2^t\text{Bu}_2)$ molecule, a fact which was later confirmed by single crystal X-ray diffraction. (Figure 2.22)

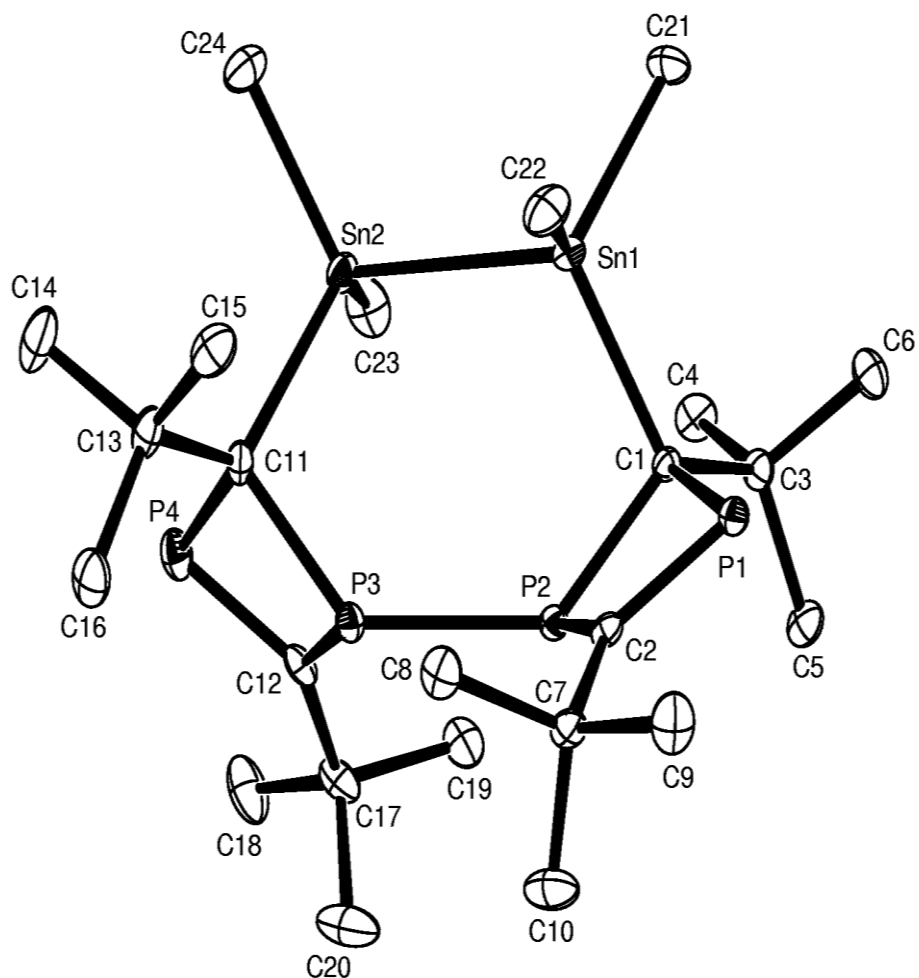


Figure 2.22: ORTEP molecular structure of $[\text{Me}_2\text{Sn}(\text{P}_2\text{C}_2^t\text{Bu}_2)]_2$ (**2-4**) (*H* atoms omitted for clarity)

Selected Bond Lengths [\AA]	
Sn1-Sn2	2.7609(3)
Sn1-C1	2.212(2)
C1-P1	1.869(3)
C1-P2	1.891(3)
P1-C2	1.699(3)
P2-C2	1.795(3)
P2-P3	2.1999(9)
C1-C3	1.564(3)
C2-C7	1.518(3)
Sn2-C11	2.211(3)
C11-P3	1.891(3)
C11-P4	1.871(3)
P4-C12	1.701(3)
P3-C12	1.794(3)
C11-C13	1.553(4)
C12-C17	1.513(4)

Selected Bond Angles [$^\circ$]	
Sn2-Sn1-C1	108.27(6)
Sn1-C1-P1	106.02(11)
Sn1-C1-P2	110.40(11)
Sn1-C1-C3	115.88(16)
P1-C1-P2	88.59(11)
C1-P2-C2	83.97(11)
C1-P1-C2	87.33(12)
P1-C2-P2	97.44(12)
P1-C2-C7	129.67(19)
P2-C2-C7	132.04(19)
C1-P2-P3	129.40(8)
C2-P2-P3	111.45(8)
Sn1-Sn2-C11	108.71(7)
Sn2-C11-P3	109.42(11)
C11-P3-P2	129.43(9)
C11-P4-C12	87.04(12)
P3-C12-P4	97.33(14)
C11-P3-C12	83.82(12)

This compound appeared to be a second decomposition product of $\text{Me}_2\text{Sn}(\text{P}_2\text{C}_2^t\text{Bu}_2)$ in which an absence of Cp_2ZrCl_2 meant that after the proposed radical cleavage of the Sn-P bond the compound coupled with a second equivalent of $\text{Me}_2\text{Sn}(\text{P}_2\text{C}_2^t\text{Bu}_2)$, forming the Sn-Sn and P-P bonds. Therefore, in order to attempt to synthesise a larger sample for better analysis, a sample of the products from the reaction of $\text{Cp}_2\text{Zr}(\text{P}_2\text{C}_2^t\text{Bu}_2)$ with two equivalents of Me_2SnCl_2 was prepared as described (*vide supra*) but the solvent system was altered so that the poorly coordinating solvent (benzene- d_6) was in higher proportion (*circa* 90 %) so as to limit the effective presence of the Cp_2ZrCl_2 . After being exposed to sunlight for 14 days to promote the radical cleavage, approximately 1/3 of the $\text{Me}_2\text{Sn}(\text{P}_2\text{C}_2^t\text{Bu}_2)$ had been converted to the dimer, allowing a more detailed $^{31}\text{P}\{^1\text{H}\}$ NMR spectroscopic analysis. (Figure 2.23)

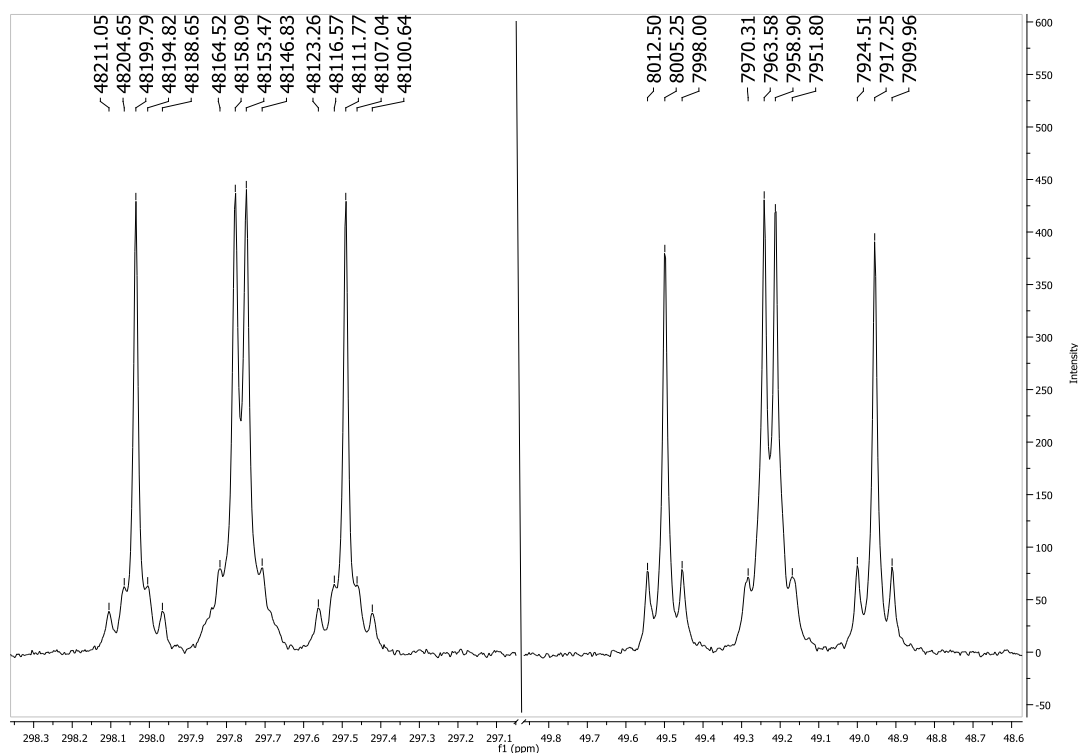


Figure 2.23: Expanded $^{31}\text{P}\{^1\text{H}\}$ NMR spectrum of $[\text{Me}_2\text{Sn}(\text{P}_2\text{C}_2^t\text{Bu}_2)]_2$

The magnetic inequivalence of the two halves of the dimer results in a considerable second order effect which, along with the multiple 2J and 3J couplings, makes the

resonances broader and more complex. This additional complexity is just as evident, if not more so, in the $^{119}\text{Sn}\{^1\text{H}\}$ NMR spectrum. (Figure 2.24)

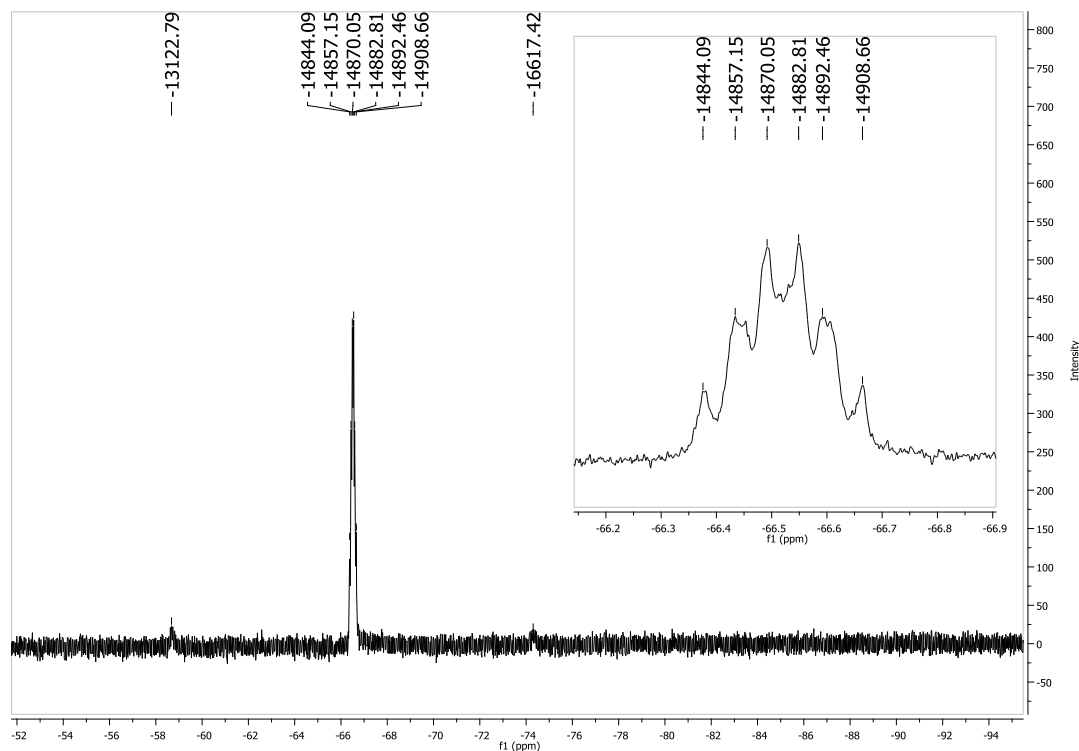


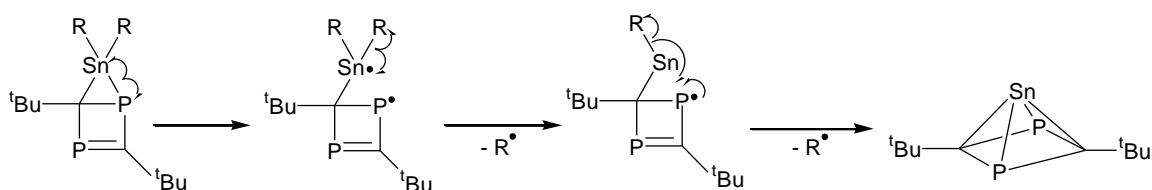
Figure 2.24: $^{119}\text{Sn}\{^1\text{H}\}$ NMR spectrum of $[\text{Me}_2\text{Sn}(\text{P}_2\text{C}_2^t\text{Bu}_2)]_2$

The broadness and degree of coupling made any analysis of the Sn-P relationship from this resonance incredibly difficult, but the $^1J^{117}\text{Sn}$ satellites were detectable with a coupling constant value of 3495 Hz. The NMR spectroscopic data for $[\text{Me}_2\text{Sn}(\text{P}_2\text{C}_2^t\text{Bu}_2)]_2$ is outlined in Table 2.5.

P1, P4		P2, P3		$J^{31\text{P}-^{31}\text{P}}$ /Hz	$^{119}\text{Sn } \delta$	$J^{119}\text{Sn} - ^{117}\text{Sn}$ /Hz
^{31}P δ	$J^{31\text{P}-\text{Sn}}$ /Hz	^{31}P δ	$J^{31\text{P}-\text{Sn}}$ /Hz			
297.91	22.35 10.04	49.51	14.69	46.42 41.95	-66.52	3495

Table 2.5: $^{31}\text{P}\{^1\text{H}\}$ and $^{119}\text{Sn}\{^1\text{H}\}$ NMR spectroscopic data of $[\text{Me}_2\text{Sn}(\text{P}_2\text{C}_2^t\text{Bu}_2)]_2$

This decomposition pathway initiated by the radical cleavage of the Sn-P bond is also postulated to be responsible for the reductive elimination reactions outlined in Scheme 2.11. It is thought that once the Sn radical has been formed, one of the substituents is lost to form a stable Sn(II) centre. This is then attacked by the unpaired electron of the ring which in turn caused the ejection of the second substituent and affords $\text{Sn}(\text{P}_2\text{C}_2^t\text{Bu}_2)$. (Scheme 2.20)



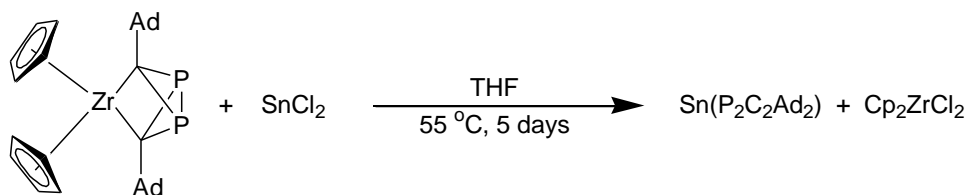
Scheme 2.20: Potential mechanism for the radically initiated formation of $\text{Sn}(\text{P}_2\text{C}_2^t\text{Bu}_2)$

Attempted Reaction of $\text{Cp}_2\text{Zr}(\text{P}_2\text{C}_2\text{Ad}_2)$ with Me_2SnCl_2

Although the reaction between $\text{Cp}_2\text{Zr}(\text{P}_2\text{C}_2^t\text{Bu}_2)$ and Me_2SnCl_2 proceeded with little difficulty, the analogous reaction using Ad groups instead of ^tBu was almost nonexistent. After heating a 1:1 reaction mixture at 60 °C in THF for seven days (by which point the equivalent ^tBu reaction would be complete) the $^{31}\text{P}\{^1\text{H}\}$ NMR spectrum showed minimal product formation, with the emerging resonances closely resembling those seen from the ^tBu analogue. Given the slow progress of the reaction it was decided that further study of this reaction would not be advantageous.

Reaction of $\text{Cp}_2\text{Zr}(\text{P}_2\text{C}_2\text{Ad}_2)$ with SnCl_2

$\text{Cp}_2\text{Zr}(\text{P}_2\text{C}_2\text{Ad}_2)$ and SnCl_2 were heated to 55 °C in THF for five days, causing the mixture to change colour from orange to yellow. (Scheme 2.21)



Scheme 2.21: Reaction of $\text{Cp}_2\text{Zr}(\text{P}_2\text{C}_2^t\text{Bu}_2)$ with SnCl_2

The $^{31}\text{P}\{^1\text{H}\}$ NMR spectrum of the product showed a single resonance at δ 140.2 which displayed $^{117}\text{Sn}/^{119}\text{Sn}$ satellites with coupling constant values of 291 and 305 Hz respectively. (Figure 2.25)

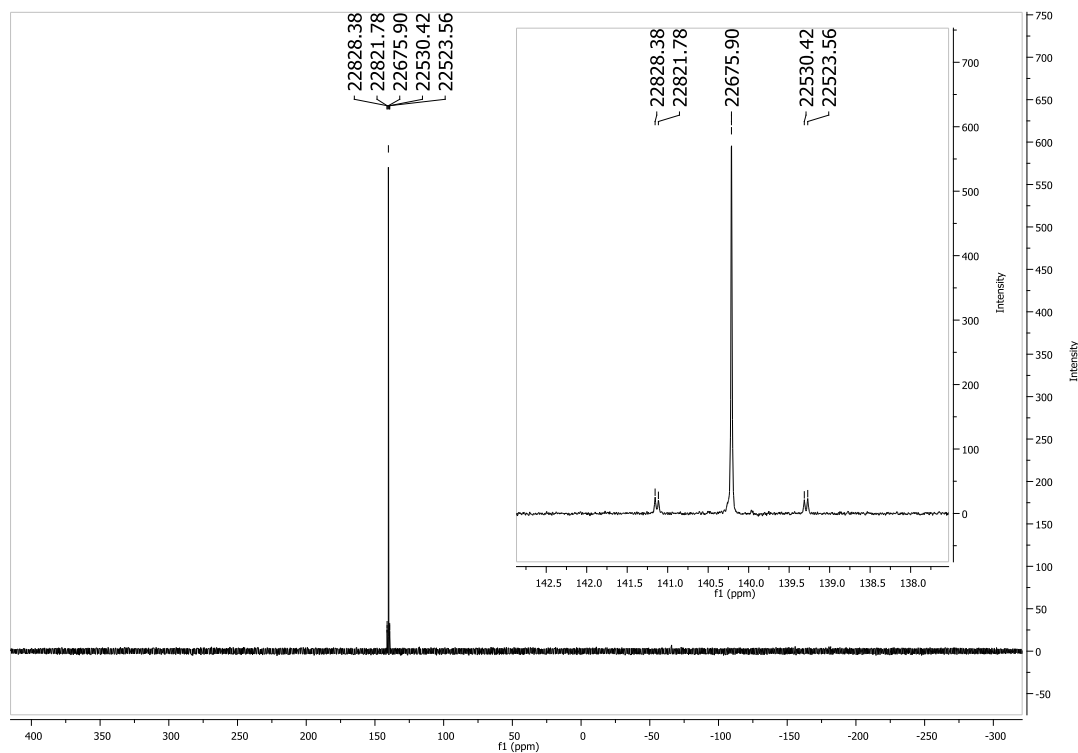


Figure 2.25: $^{31}\text{P}\{^1\text{H}\}$ NMR spectrum of $\text{Sn}(\text{P}_2\text{C}_2\text{Ad}_2)$

This $^{31}\text{P}\{^1\text{H}\}$ NMR spectrum closely resembled that of $\text{Sn}(\text{P}_2\text{C}_2^t\text{Bu}_2)$, which displayed a chemical shift of δ 144.9 and $^{117}\text{Sn}/^{119}\text{Sn}$ satellites with coupling constant values of 284 Hz and 296 Hz respectively.⁸ Based on this data and the similarity of the reagents and reaction conditions it was proposed that the product is $\text{Sn}(\text{P}_2\text{C}_2\text{Ad}_2)$. (Figure 2.26)

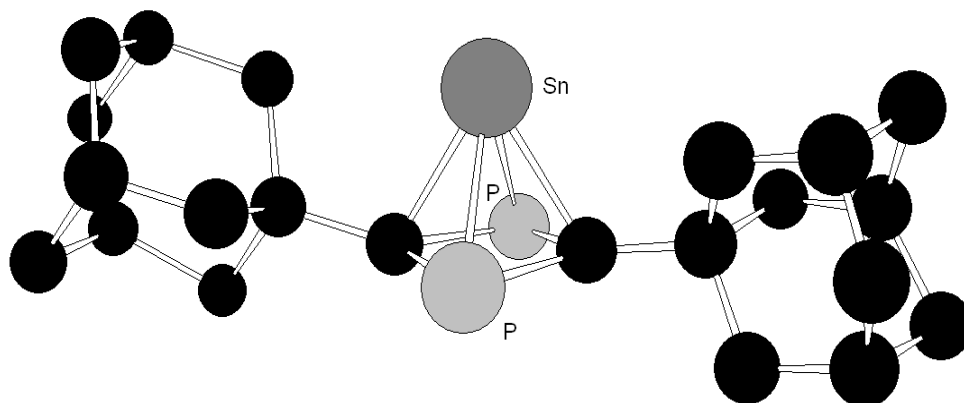


Figure 2.26: Proposed structure of $\text{Sn}(\text{P}_2\text{C}_2\text{Ad}_2)$ (2.5)

The most noteworthy feature though came from the $^{119}\text{Sn}\{^1\text{H}\}$ NMR spectroscopic data. Whilst the $^{119}\text{Sn}\{^1\text{H}\}$ NMR spectroscopic resonance of the ^tBu analogue has a chemical shift of δ -2129, that of the Ad complex was observed at δ -2405, displaying the expected triplet splitting due to the two coupling P atoms. (Figure 2.27)

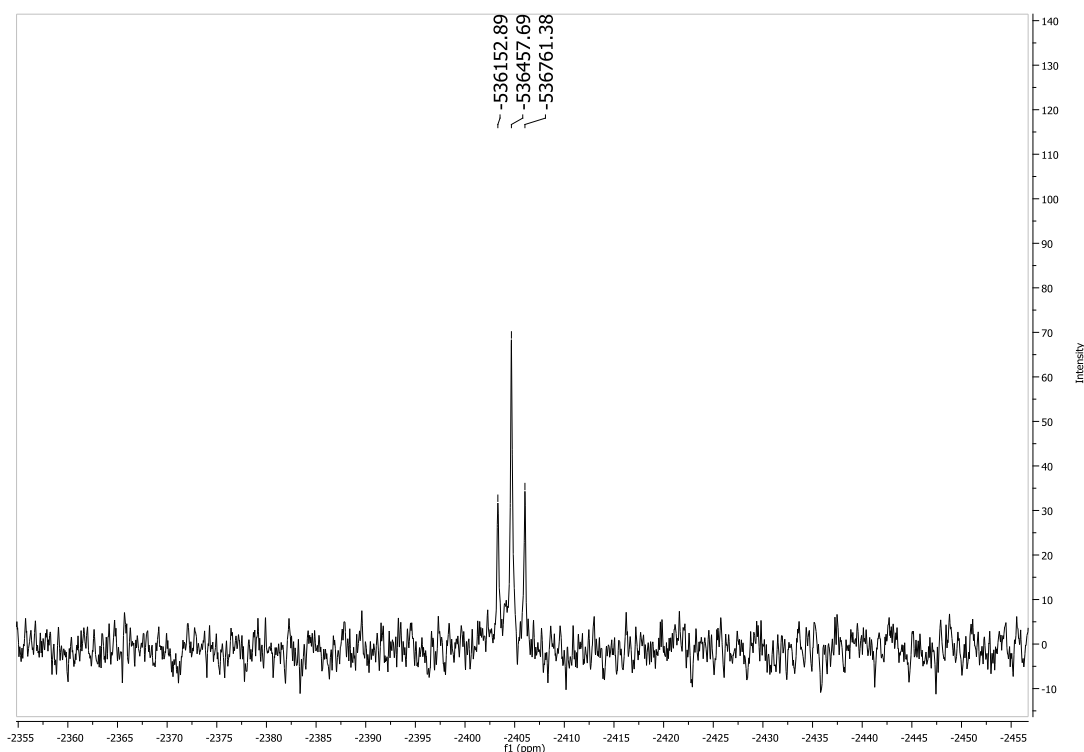


Figure 2.27: Expanded $^{119}\text{Sn}\{^1\text{H}\}$ NMR spectrum of $\text{Sn}(\text{P}_2\text{C}_2\text{Ad}_2)$

Compound	^{31}P δ	^{119}Sn δ	$J_{\text{P-Sn}}$
$\text{Sn}(\text{P}_2\text{C}_2\text{Ad}_2)$	140.2	-2405	305
$\text{Sn}(\text{P}_2\text{C}_2^t\text{Bu}_2)$	144.9	-2129	296

Table 2.6: $^{31}\text{P}\{^1\text{H}\}$ and $^{119}\text{Sn}\{^1\text{H}\}$ NMR spectroscopic data for $\text{Sn}(\text{P}_2\text{C}_2\text{R}_2)$ complexes

Particularly low frequency NMR spectroscopy shifts are a recognised feature of the apical atom in *nido*-clusters of this form,¹³ but comparison with collections of $^{119}\text{Sn}\{^1\text{H}\}$ NMR spectroscopic data^{24,25} suggests that this could be the lowest frequency shift measured to date. The next lowest frequency found was that of $[\text{Cp}^t\text{Bu}_2\text{Sn}][\text{BF}_4]$ reported to be δ -2337.7,²⁶ a compound which can also be thought of as a *nido*-cluster with an apical Sn atom.

2.3: Conclusions

The initial reactions in this chapter indicate one point quite clearly; compounds of the formula $R_2Sn(P_2C_2^tBu_2)$ are generally unstable with respect to reductive elimination. Upon further study it was determined that the cause of this instability was rooted in the Sn-P bond and its propensity towards radical cleavage. It was found that by using Me groups as the substituents the reductive elimination could be prevented affording two related products, but over time the reactive Sn-P bond would cause either dimerisation or the abstraction of HCl from other reagents depending on the conditions. The chemistry of this system was found to be very similar to that of previously reported triphospholes, which exhibit analogous structures that can be interconverted through a light-induced electrocyclisation.

Similar reactions using the $P_2C_2Ad_2$ ring showed almost no reaction whatsoever, but the compound $Sn(P_2C_2Ad_2)$ was produced using $SnCl_2$. This compound exhibited an incredibly low frequency chemical shift in the ^{119}Sn NMR spectrum, significantly lower than that of its tBu analogue. The reason for this difference is unclear, especially in view of the fact that the ^{31}P NMR spectra of all the related compounds show almost no difference between the two analogues.

References

1. See Chapter 1
2. Breit, B., Bergsträsser, U., Maas, G., Regitz, M., *Angew. Chem. Int. Ed. Engl.*, 1992, **31**, 1055
3. Breit, B., Hoffmann, A., Bergsträsser, U., Ricard, L., Mathey, F., Regitz, M., *Angew. Chem. Int. Ed. Engl.*, 1994, **33**, 1491
4. Hoffmann, A., Mack, A., Goddard, R., Binger, P., Regitz, M., *Eur. J. Inorg. Chem.*, 1998, 1597
5. Schmitz, M., Göller, R., Bergsträsser, U., Leininger, S., Regitz, M., *Eur. J. Inorg. Chem.*, 1998, 227
6. Schäffer, A., Weidenbruch, M., Saak, W., Pohl, S., *Angew. Chem. Int. Ed. Engl.*, 1987, **26**, 776
7. Francis, M. D., Hitchcock, P. B., *Organometallics*, 2003, **22**, 2891
8. Francis, M. D., Hitchcock, P. B., *Chem. Commun.*, 2002, 86
9. Shriver, D. F., Atkins, P. W., *Inorganic Chemistry*, 3rd Ed., 2002, 342
10. Lynam, J. M., Copsey, C. M., Green, M., Jeffrey, J. C., MacGrady, J. E., Russell, C. A., Slattery, J. M., Swain, A. C., *Angew. Chem. Int. Ed. Engl.*, 2003, **42**, 2778
11. Fish, C., Green, M., Jeffrey, J. C., Killby, R. J., Lynam, J. M., MacGrady, J. E., Pantazis, D. A., Russell, C. A., Williams, C. E., *Chem. Commun.*, 2006, 1375
12. Fish, C., Green, M., Jeffery, J. C., Kilby, R. J., Lynam, J. M., McGrady, J. E., Pantazis, D. A., Russel, C. A., Willans, C. E., *Angew. Chem. Int. Ed. Engl.*, 2006, **45**, 6685
13. Condick, P. N., Fox, M. A., Greatrex, R., Jones, C., Ormsby, D. L., *Chem. Commun.*, 2002, 1448

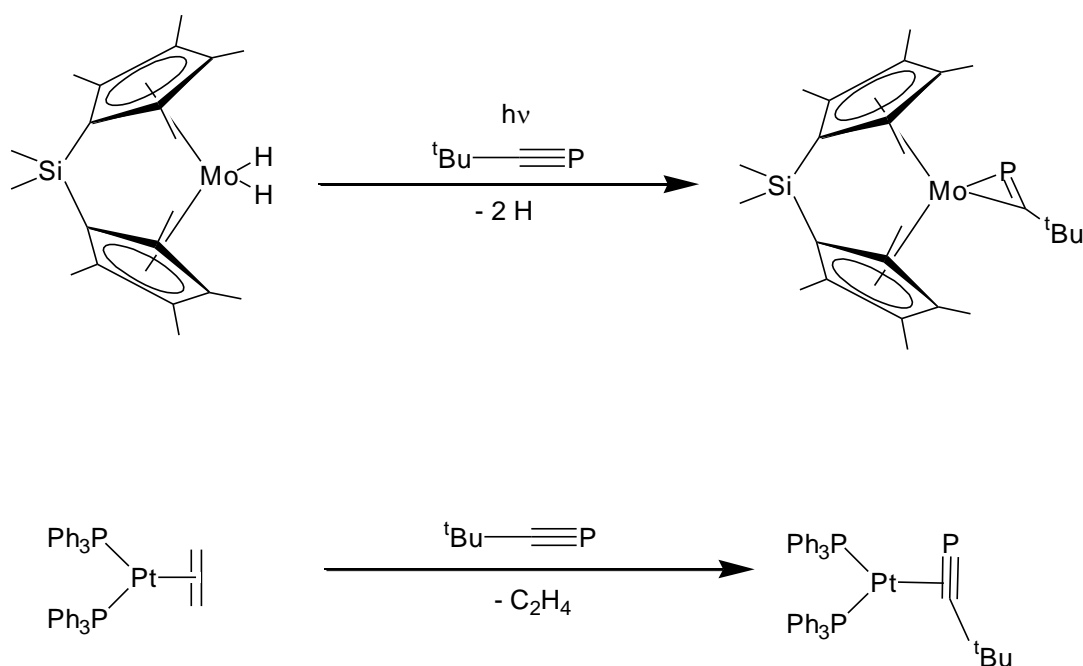
14. Wettling, T., Schneider, J., Wagner, O., Kreiter, C. G., Regitz, M., *Angew. Chem. Int. Ed. Engl.*, 1989, **28**, 1013
15. Dietz, J., Schmidt, T., Renner, J., Bergsträsser, U., Tabellion, F., Preuss, F., Binger, P., Heydt, H., Regitz, M., *Eur. J. Org. Chem.*, 2002, 1664
16. Caliman, V., Hitchcock, P. B., Nixon, J. F., Sakaya, N., *Bull. Soc. Chim. Belg.*, 1996, **105**, 675
17. Francis, M. D., Jones, C., Morley, C. P., *Tet. Lett.*, 1999, **40**, 3815
18. Francis, M. D., Hibbs, D. E., Hitchcock, P. B., Hursthouse, M. B., Jones, C., Mackewitz, T., Nixon, J. F., Nyulászi, L., Regitz, M., Sakarya, N., *J. Organomet. Chem.*, 1999, **580**, 156
19. Cloke, F. G. N., Hitchcock, P. B., Hunnable, P., Nixon, J. F., Nyulászi, L., Niecke, E., Thelen, V., *Angew. Chem. Int. Ed. Engl.*, 1998, **37**, 1083
20. Caliman, V., Hitchcock, P. B., Nixon, J. F., *Chem. Commun.*, 1998, 1537
21. Clayden, J., Greeves, N., Warren, S., Wothers, P., *Organic Chemistry*, 2001, p927
22. Mosher, M. D., Ojha, S., *J. Chem. Educ.*, 1998, **75**, 888
23. Bachrach, S. M., Caliman, V., Nixon, J. F., *J. Chem. Soc. Chem. Commun.*, 1995, 2395
24. Webb, G. A., Wrackmeyer, B., *Ann. R. NMR S.*, 1985, **16**, 73
25. Davis, A. G., Gielen, M., Pannell, K. H., Tiekink, E. R. T., Wrackmeyer, B., *Tin Chemistry: Fundamentals, Frontiers and Applications*, 2008, 17
26. Jutzi, P., Dickbreder, R., *J. Organomet. Chem.*, 1989, **373**, 301

Chapter 3

The Synthesis of Transition-Metal Phosphaalkyne Complexes

3.1: Introduction

The most common examples of metal complexes containing a coordinated phosphaaalkyne unit are those which have a single RCP ligand. The addition of further equivalents is restricted by either the electron count of the resulting complex or the steric demands imposed by the other substituents.^{1,2} (Scheme 3.1)



Scheme 3.1: Selected examples of transition metal phosphaaalkyne complexes

Whereas the analogous nitrile ligands coordinate to metals through the nitrogen lone pair, the phosphaaalkyne has been shown, in the vast majority of cases, to coordinate in an η^2 fashion through the π -orbitals of the multiple bond. Photoelectron spectroscopic studies have revealed that the HOMO of a phosphaaalkyne is the π -bonding orbital,³ and

that these electrons are used in the metal-ligand bonding. Instances of η^1 -coordination have been reported in complexes which contain other bulky ligands which prevent the η^2 -coordination mode being adopted.⁴ It is also possible for η^2 -coordinated phosphalkyne ligands to act as bridging ligands *via* the P lone pair.⁵ (Figure 3.1)

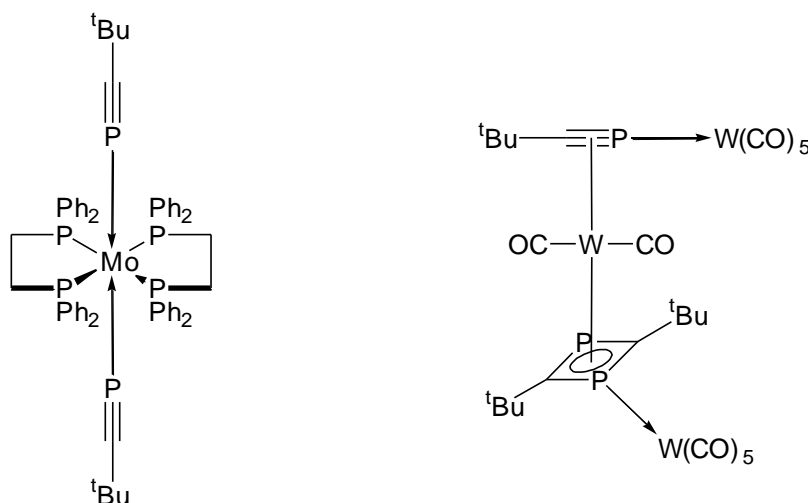
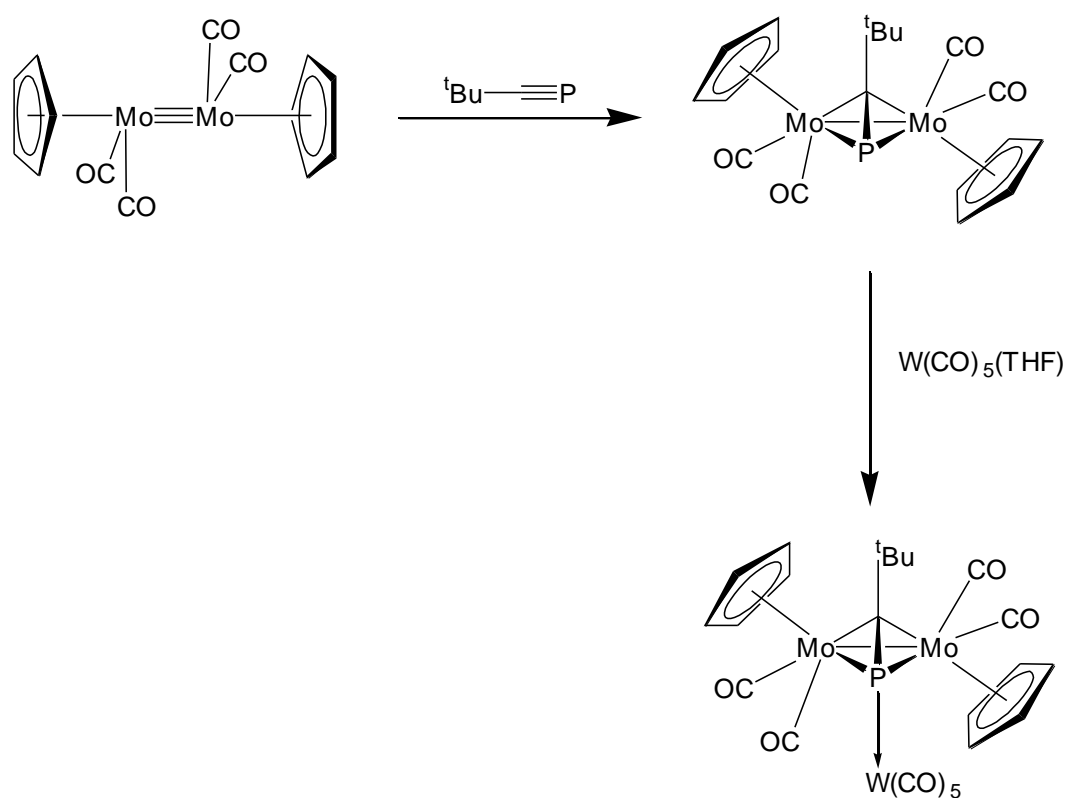


Figure 3.1: Complexes containing phosphalkyne ligands displaying η^1 - and η^1, μ^1 -coordination modes

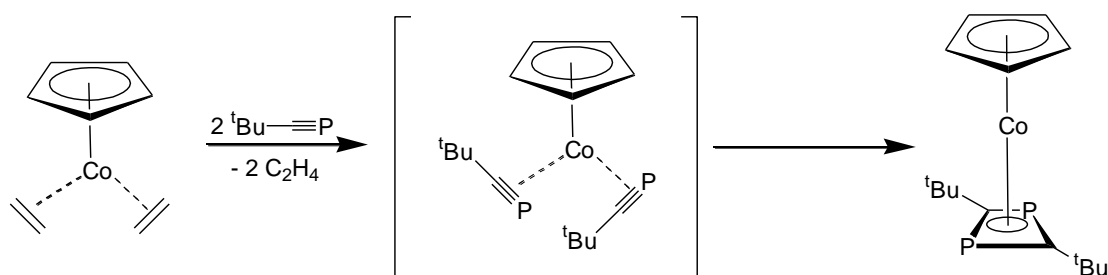
In addition to the μ^1 bridging mode, phosphalkynes may adopt an η^2, μ^2 ligating mode, in which each of two pairs of π electrons is donated to a different metal centre.⁶ As this ligating mode does not involve the phosphorus lone pair, it is available for coordination to a third metal centre.⁷ (Scheme 3.2)



Scheme 3.2: Formation of a complex containing $t\text{BuCP}$ bridging three metal centres

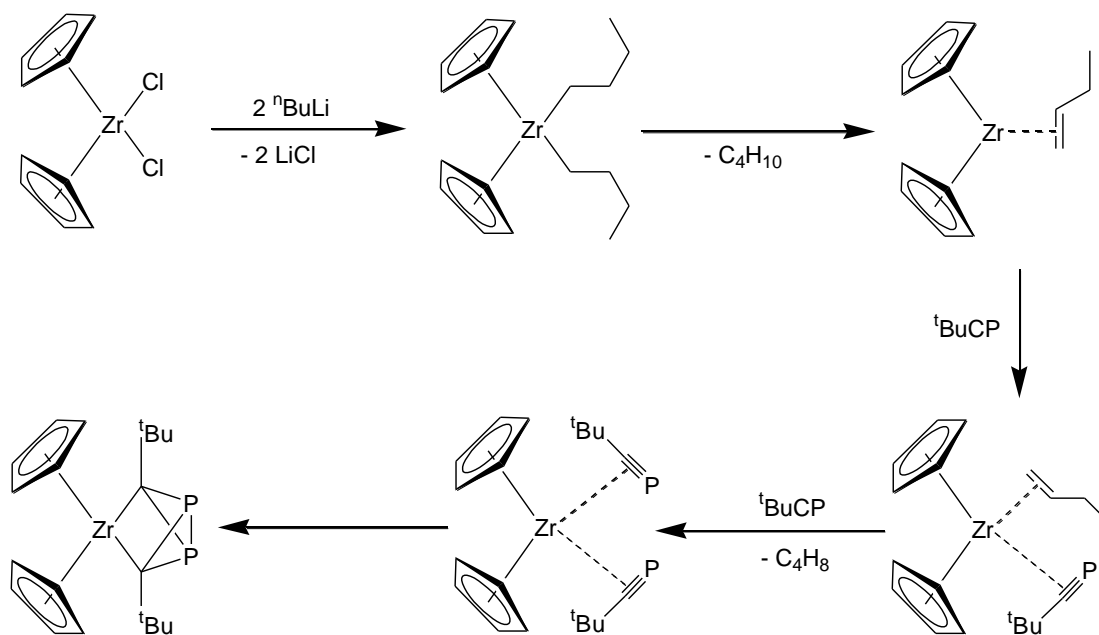
Many transition metal complexes featuring $\text{P}_2\text{C}_2\text{R}_2$ ligands have also been synthesised. Since earliest reports,^{8,9} the dimerisation of phosphalkynes within the coordination sphere of a transition metal has become a reaction repeated many times, with examples found using metals from Group 4¹⁰ to Group 10¹¹ and from the first-¹², second-¹³ and third-row¹⁴ d-block elements.

A synthetic route commonly employed for these derivatives is based on the displacement of multiple L-type ligands such as C_2H_4 ⁹ or CO ¹⁵ by the appropriate equivalents of RCP , their subsequent dimerisation, and concomitant oxidation of the metal centre by two. (Scheme 3.3)



Scheme 3.3: Formation of a $t\text{BuCP}$ dimer on a cobalt centre

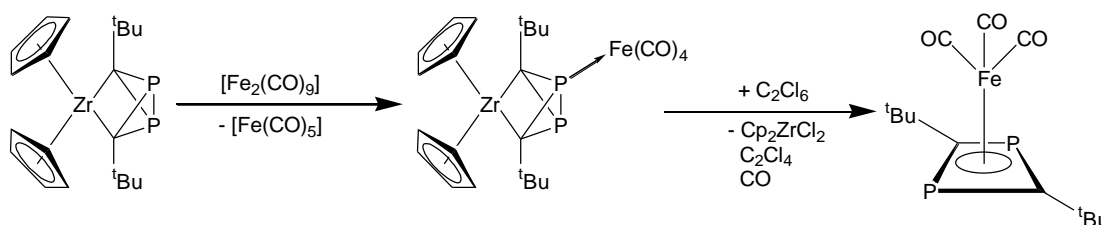
For certain metals for which no obvious low oxidation state starting material is available a precursor containing a metal centre in higher e.g. Cp_2ZrCl_2 can be used. This can be reduced *in situ* prior to the introduction of the phosphalkyne. In the synthesis of $\text{Cp}_2\text{Zr}(\text{P}_2\text{C}_2\text{R}_2)$,¹³ the reduction is normally achieved using $n\text{BuLi}$,¹⁶ which di-alkylates the Zr to provide an intermediate which is unstable with respect to β -elimination, affording butane and a butene η^2 -bound to the Zr. This rearrangement facilitates coordination of the first phosphalkyne while subsequent displacement of the butene permits coordination of the second. Finally, dimerisation occurs. (Scheme 3.4)



Scheme 3.4: Formation of the tetrahedral $t\text{BuCP}$ dimer from Cp_2ZrCl_2

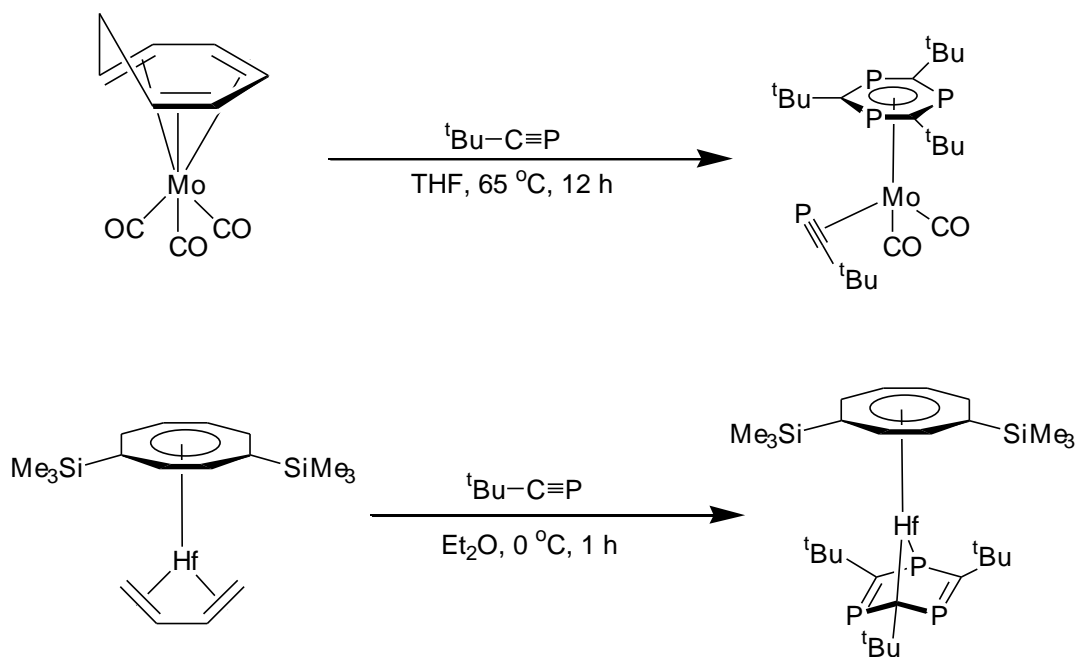
To date, the $\text{ZrCp}_2(\text{P}_2\text{C}_2\text{R}_2)$ derivatives are the only transition metal complexes for which the molecular structure of the complexed dimer is not square planar.

Whilst $\text{Cp}_2\text{Zr}(\text{P}_2\text{C}_2\text{R}_2)$ complexes have been used as $\text{P}_2\text{C}_2\text{R}_2$ transfer reagents for numerous main group elements,¹⁷⁻²⁰ they have rarely been employed for transition metals. A single report occurs in the literature detailing the use of $\text{Cp}_2\text{Zr}(\text{P}_2\text{C}_2^t\text{Bu}_2)$ for the synthesis of $\text{Fe}(\text{P}_2\text{C}_2^t\text{Bu}_2)(\text{CO})_3$.¹⁶ (Scheme 3.5) Rather than choosing FeCl_2 as the source of Fe, the carbonyl $\text{Fe}_2(\text{CO})_9$ was selected along with C_2Cl_6 to enable the formation of Cp_2ZrCl_2 .



Scheme 3.5: Transfer of the $t\text{BuCP}$ dimer from Zr to Fe

Sometimes the coupling of phosphalkynes by a transition metals produces trimers, $\text{P}_3\text{C}_3\text{R}_3$ rather than a dimer.^{10,21-23} Again their synthesis involves displacement of L-type ligands from a metal coordination sphere, (Scheme 3.6) but unlike the dimers, the trimers do not necessarily alter the oxidation state of the metal as the six membered ring may exist as in three structural isomers including one planar aromatic, neutral species. (Figure 3.2)



Scheme 3.6: Formation of tBuCP trimers on Mo and Hf

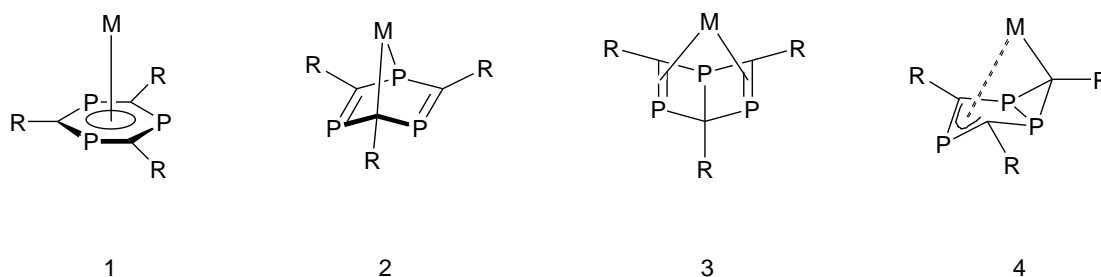
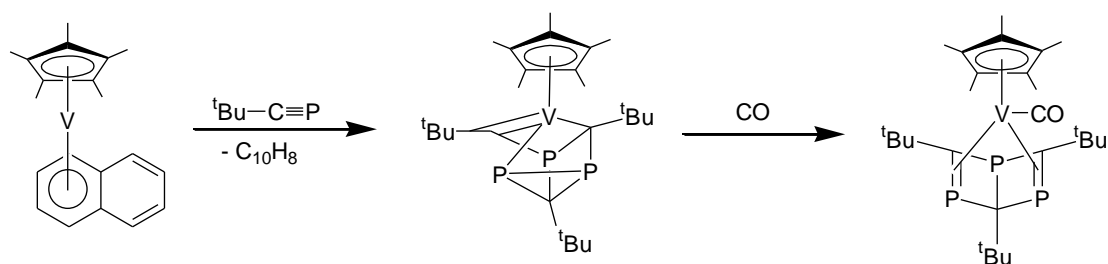


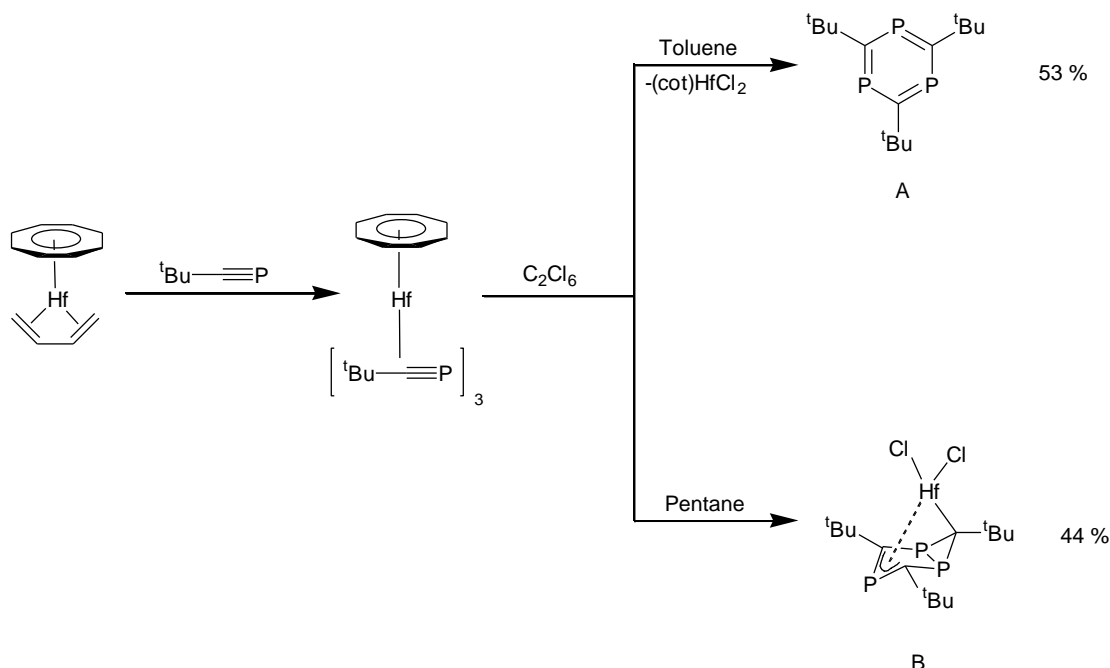
Figure 3.2: Bonding modes of $\text{P}_3\text{C}_3\text{R}_3$

There have been a small number of complexes reported featuring phosphalkyne trimers derived from bicyclic ring systems (bonding modes [3] and [4]). One of the earliest examples of a phosphalkyne trimerisation reported a Dewar-benzene trimer formed on a V centre.²⁴ (Scheme 3.7)



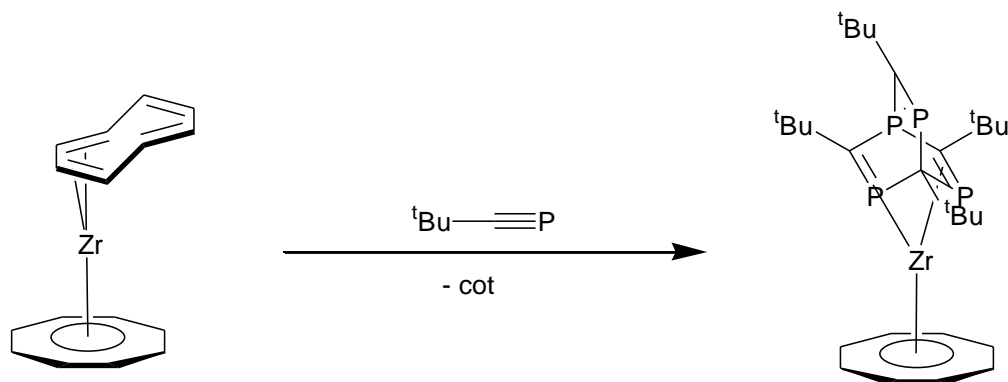
Scheme 3.7: Formation of the Dewar-benzene ^tBuCP trimer on a vanadium centre

In addition to the complex with bonding mode [2] shown in Scheme 3.6, some Hf-based trimers have also been synthesised by displacement of a butadiene ligand from [Hf(η-C₈H₈)(η-C₄H₆)]. Simply combining ^tBuCP with the complex resulted in a trimer of unknown structure, but its subsequent reaction with C₂Cl₆ in toluene afforded triphosphabenzene A, while in pentane the Hf complex B was produced.²¹ (Scheme 3.8)



Scheme 3.8: Formation of an uncharacterised ^tBuCP trimer on hafnium and its reactions with hexachloroethane

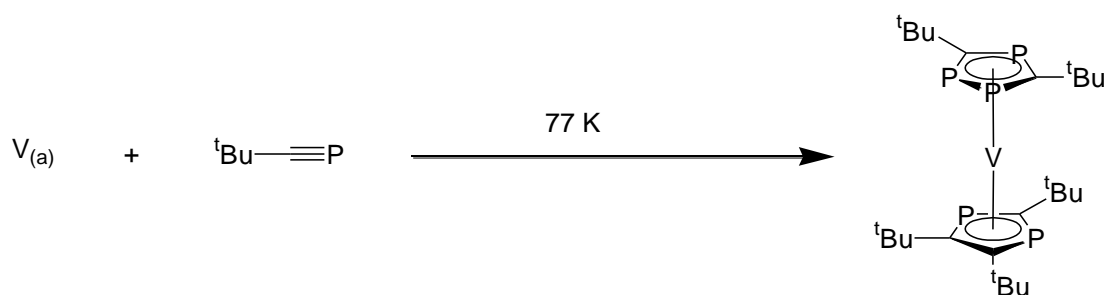
One possible factor accounting for the rarity of $P_3C_3R_3$ complexes may be the tendency for a fourth phosphalkyne to add across the $P_3C_3R_3$ unit in a $4 + 2$ addition producing a tetraphosphabarrelene.¹⁰ (Scheme 3.9)



Scheme 3.9: Formation of $P_4C_4R_4$ by a Zr centre

As the fourth equivalent of phosphalkyne adds to the uncoordinated face of the $P_3C_3R_3$ ring there is very little increase in the steric demands of the resulting $P_4C_4R_4$ ligand but electronically it is an L_2 ligand, rather than an L_3 . Preventing the addition of the fourth phosphalkyne unit through steric or electronic saturation is not a trivial endeavour.

Whilst the synthesis of phosphalkyne based analogues of cyclobutadiene and benzene may be relatively straightforward to envisage *via* the coupling reactions discussed above, a synthetic route to an analogue of the ubiquitous cyclopentadienyl ligand is less obvious. In order to form an odd-numbered ring the triple bond of one phosphalkyne would need to be cleaved. In 1995 it was reported that cocondensation of V atoms with $tBuCP$ afforded a pentaphosphavanadocene with one $P_2C_3tBu_3$ and one $P_3C_2tBu_2$ ring.²⁵(Scheme 3.10)



Scheme 3.10: Formation of a $P_2C_3^tBu_3$ and $P_3C_3^tBu_3$ rings on vanadium by MVS

This route has also provided several transition metal complexes featuring three-, four-, five- and six-membered rings.²⁶⁻²⁹ (Figure 3.3)

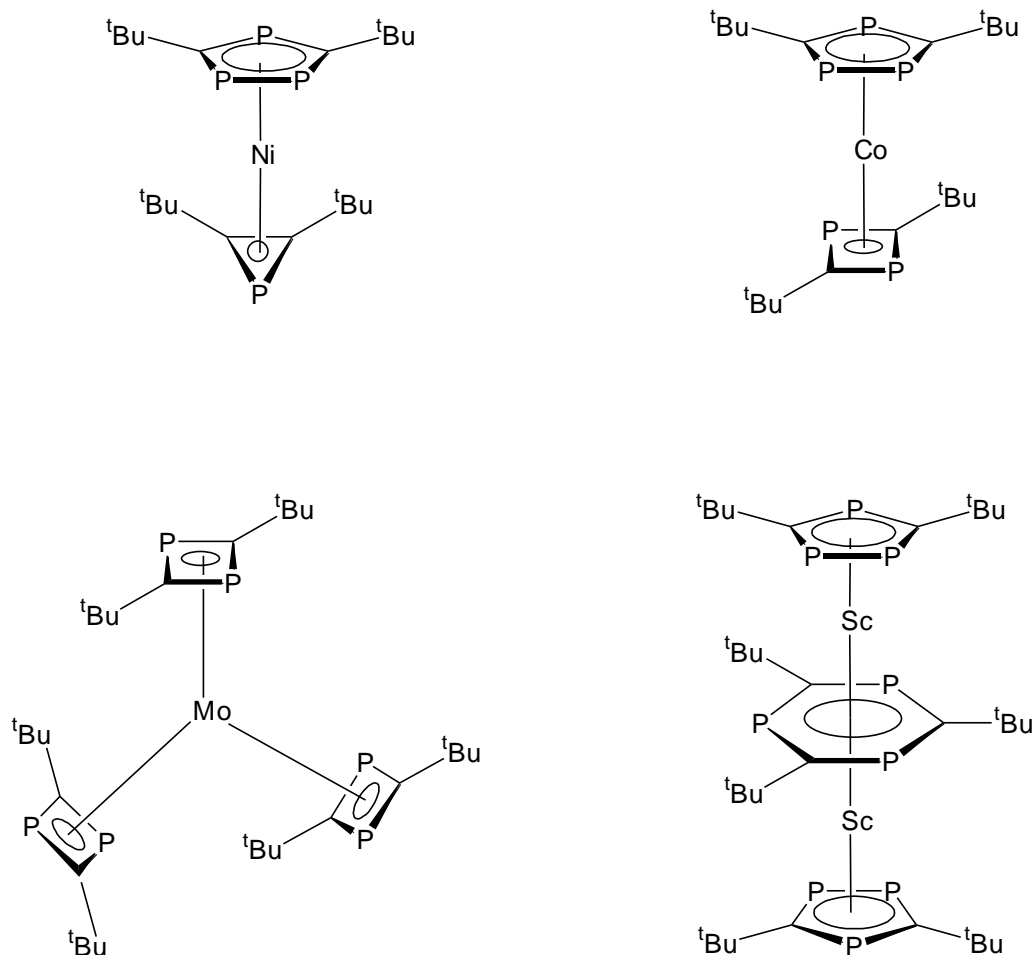


Figure 3.3: A range of transition metal complexes containing different ring systems based on $tBuCP$ synthesised by MVS

Complexes have been reported in which phosphalkynes were coordinated η^2 - to Ti centres featuring other sterically demanding ligands.^{30,31} (Figure 3.4)

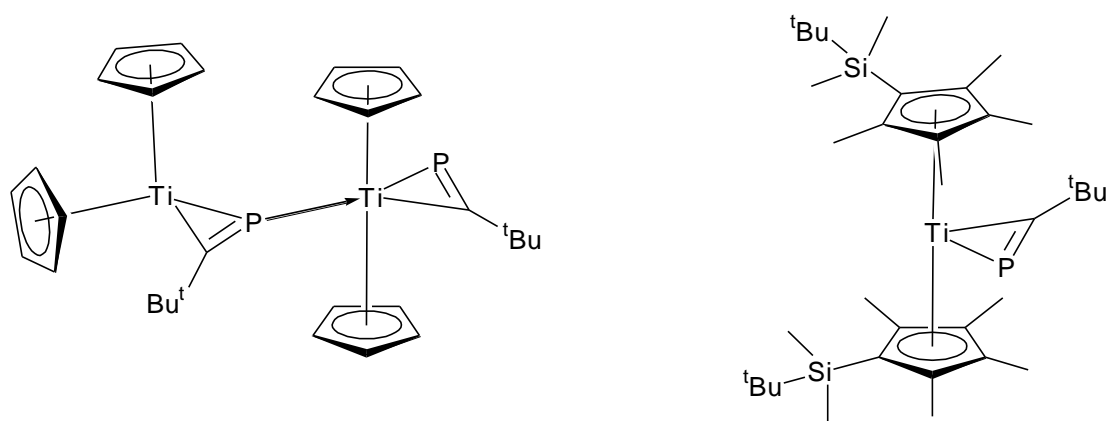


Figure 3.4: Known Ti complexes with coordinated ${}^t\text{BuCP}$

A different reaction reported by Binger *et al*³² involving the reduction of Cp_2TiCl_2 with ${}^n\text{BuLi}$ and then the addition of ${}^t\text{BuCP}$ afforded a product in which three ${}^t\text{BuCP}$ units had undergone addition reactions with one of the Cp rings. (Figure 3.5)

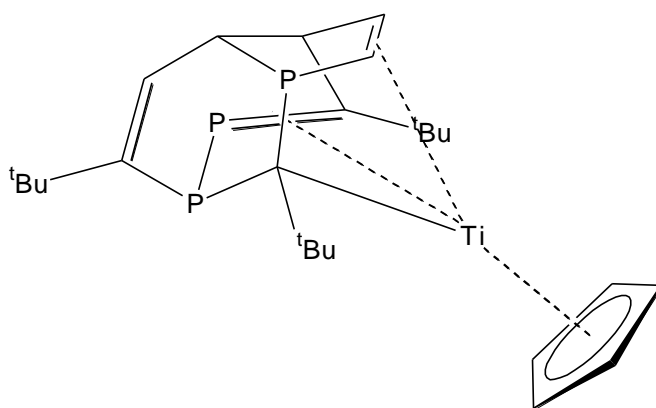


Figure 3.5: Previously reported structure of $\text{TiCp}_2({}^t\text{BuCP})_3$ formed from the reaction between Cp_2TiCl_2 , ${}^n\text{BuLi}$ and ${}^t\text{BuCP}$

As yet, however, no Ti complex has been reported featuring solely phosphalkyne based ligands. The initial reaction detailed in the following Results and Discussion section attempts to use the well established $P_2C_2R_2$ /dichloride exchange reaction employing $Cp_2Zr(P_2C_2R_2)$ to synthesise a complex with the formula $Ti(P_2C_2R_2)_2$. (Figure 3.6)

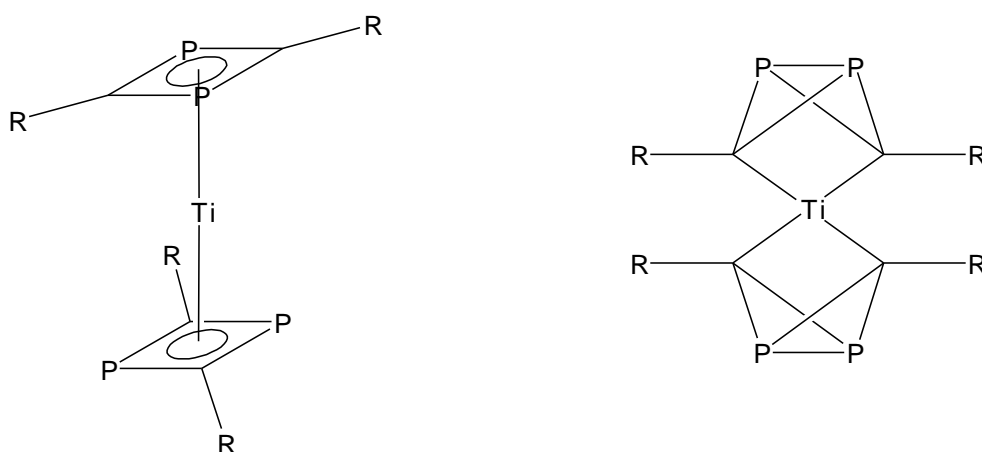
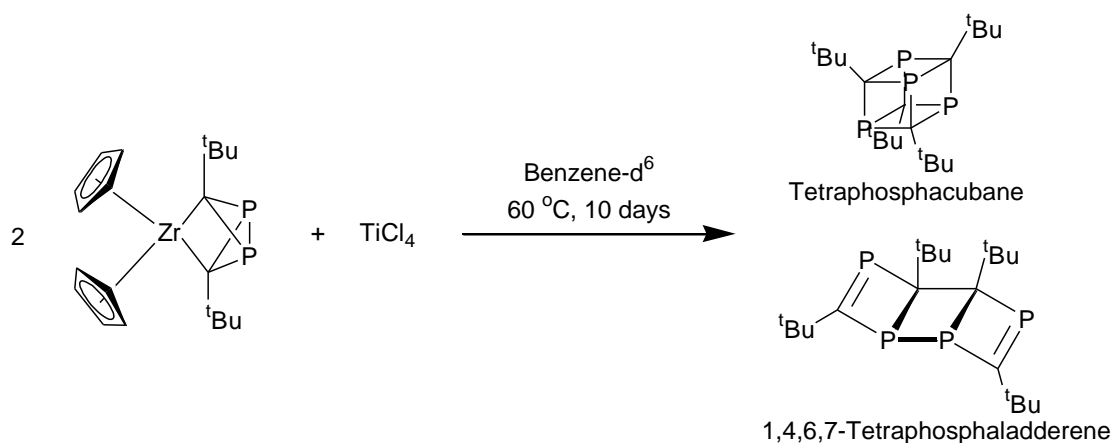


Figure 3.6: Potential Ti complexes containing two $P_2C_2R_2$ rings

3.2: Results and Discussion

Reaction of $\text{TiCl}_4 \cdot 2\text{THF}$ with $\text{Cp}_2\text{Zr}(\text{P}_2\text{C}_2^t\text{Bu}_2)$

A reaction was carried out employing $\text{TiCl}_4 \cdot 2\text{THF}$ and two equivalents of $\text{Cp}_2\text{ZrP}_2\text{C}_2^t\text{Bu}_2$ in benzene- d^6 and heated to 60 °C for ten days, with the desired product possessing two $\text{P}_2\text{C}_2^t\text{Bu}_2$ rings coordinated to the Ti centre. The product of this reaction as determined by $^{31}\text{P}\{^1\text{H}\}$ NMR spectroscopy was predominantly a mixture of tetramers namely, tetraphosphacubane (at δ 257)³³ and its isomer 1,4,6,7-tetraphosphaladderene (at δ 397 and 43).³⁴ (Scheme 3.11)

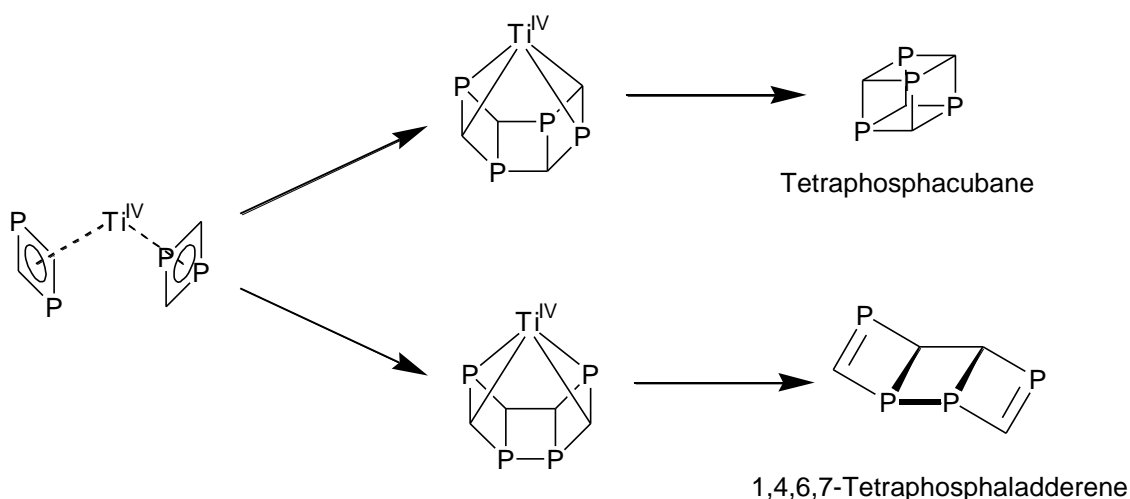


Scheme 3.11: Reaction of $\text{Cp}_2\text{Zr}(\text{P}_2\text{C}_2^t\text{Bu}_2)$ with TiCl_4

Compound	Chemical Shift	$J_{\text{P-P}}/\text{Hz}$
Tetraphosphacubane	257	-
1,4,6,7-Tetraphosphaladderene (pos.1, 4)	397	29
1,4,6,7-Tetraphosphaladderene (pos.6, 7)	43	29

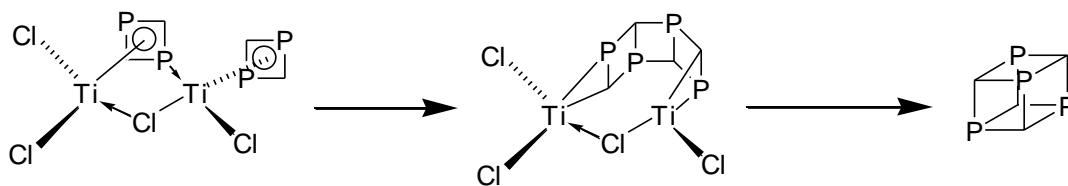
Table 3.1: $^{31}\text{P}\{^1\text{H}\}$ NMR spectroscopic data for selected $^t\text{BuCP}$ tetramers

A possible mechanism for this reaction could initially involve the transfer of two $\text{P}_2\text{C}_2^t\text{Bu}_2$ rings to the Ti followed by a coupling the rings and a reductive elimination. (Scheme 3.12)



Scheme 3.12: Proposed mechanism for the formation of phosphaaalkyne tetramers (^tBu groups omitted for clarity)

Alternatively, the coupling could arise as the result of a bridging interaction between two Ti centres after the addition of just one ring to each. (Scheme 3.13)

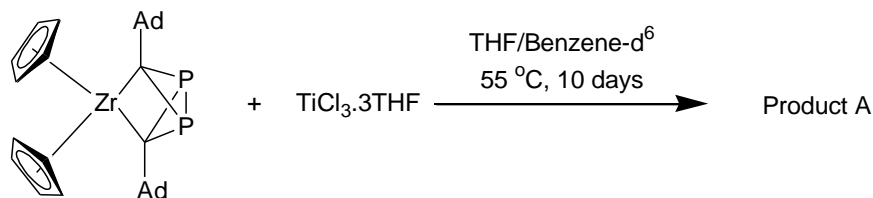


Scheme 3.13: Alternative proposed mechanism for the formation of phosphaaalkyne tetramers (^tBu groups omitted for clarity)

Reaction of $\text{TiCl}_3 \cdot 3\text{THF}$ with $\text{Cp}_2\text{Zr}(\text{P}_2\text{C}_2\text{Ad}_2)$

In an attempt to prevent formation of the tetramers, TiCl_3 was employed instead of TiCl_4 and a single equivalent of $\text{Cp}_2\text{ZrP}_2\text{C}_2\text{Ad}_2$ was added. The reagents were

combined in an NMR tube with a mixture of THF and benzene-d⁶ and heated to 55 °C.
(Scheme 3.14)



Scheme 3.14: Reaction between $\text{Cp}_2\text{Zr}(\text{P}_2\text{C}_2\text{Ad}_2)$ and TiCl_3

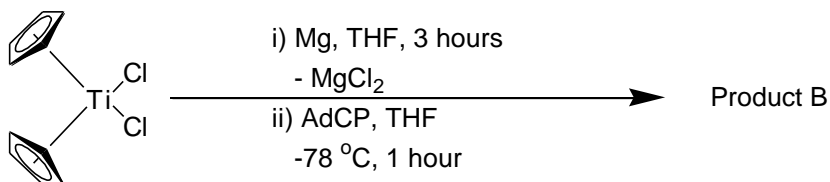
During the course of this reaction $^{31}\text{P}\{^1\text{H}\}$ NMR spectroscopy revealed a gradual disappearance of the resonance attributable to $\text{Cp}_2\text{Zr}(\text{P}_2\text{C}_2\text{Ad}_2)$ but not the appearance of any new resonance. The reaction was performed in a sealed NMR tube and as no solid precipitate was observed it is reasonable to conclude that the complete absence of any ^{31}P resonances arose from the proximity of the P atoms to the paramagnetic Ti(III) centre. This in turn indicated that limiting the addition to one $\text{P}_2\text{C}_2\text{R}_2$ ring per Ti centre the tetramer formation could be avoided.

Following this, a reaction using Cp_2TiCl_2 was investigated. This system was employed as the diamagnetic Ti(IV) oxidation state would allow NMR spectroscopic analysis, while the two Cp ligands prevent the addition of a second $\text{P}_2\text{C}_2\text{R}_2$ ring.

Reaction of Cp_2TiCl_2 with Mg and AdCP

A sample of Cp_2TiCl_2 was reduced by stirring with activated Mg in THF for three hours by which point the mixture had turned from red to light blue/green. The

reduced species was then filtered from the Mg into a THF solution containing two equivalents of AdCP at -78 °C, causing a colour change to dark green. (Scheme 3.15)



Scheme 3.15: Reaction between Cp_2TiCl_2 , Mg and AdCP

The resulting product displayed a $^{31}\text{P}\{^1\text{H}\}$ NMR spectrum (Figures 3.7 and 3.8) which showed three resonances in a 1:1:1 ratio at δ -50, -129 and -191 (along with some AdCP at δ -68). This indicated the formation a complex containing three inequivalent P atoms.

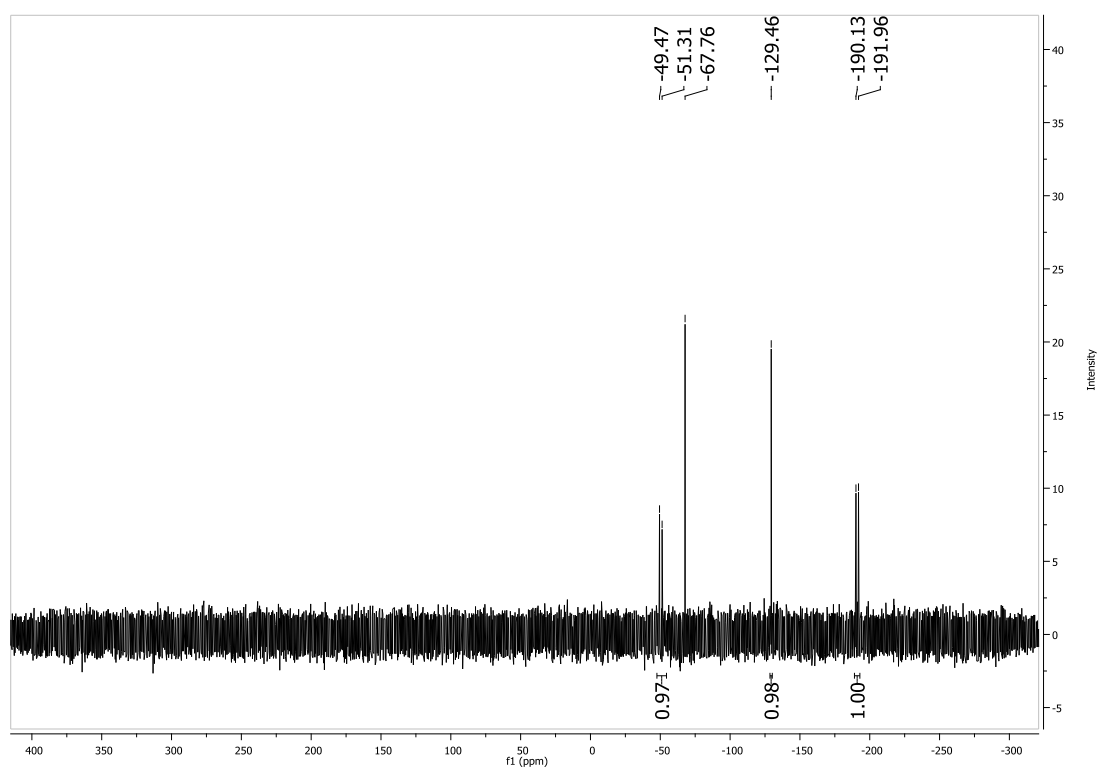


Figure 3.7: $^{31}\text{P}\{^1\text{H}\}$ NMR spectrum of the reaction mixture of Cp_2TiCl_2 and AdCP

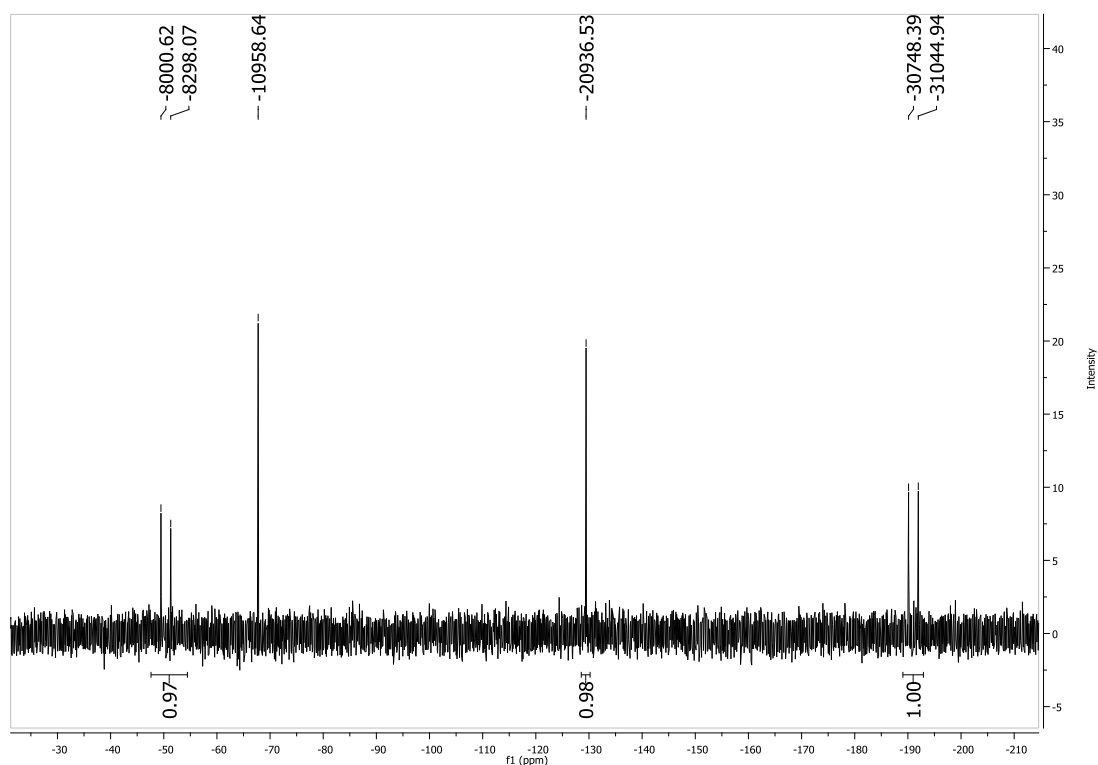


Figure 3.8: Expanded $^{31}\text{P}\{^1\text{H}\}$ NMR spectrum of $\text{Cp}_2\text{Ti}(\text{AdCP})_3$ and AdCP

These chemical shifts are compared with those of related compounds in Table 3.2. Unfortunately, no NMR spectroscopic data was available for the product depicted in Figure 3.5.

Compound	^{31}P δ (solvent)	Temp. / $^\circ\text{C}$	Ref.
Product B	-50.4, -129.5, -191.0 (C_6D_6)	30	This work
$[\text{Ti}(\eta\text{-Cp}^S)_2(\eta^2\text{-PC}^t\text{Bu})]$	587.6 (C_6D_6)	25	31
$[\text{Ti}(\eta\text{-Cp})_2(\eta^2\text{-PC}^t\text{Bu})(\text{PMe}_3)]$	122.7 (C_7D_8)	-30	30
$\{\text{Ti}(\eta\text{-Cp})_2(\eta^2\text{-PC}^t\text{Bu})\}$	431.6 ($\text{C}_4\text{D}_8\text{O}$)	-40	30
$[\{\text{Ti}(\eta\text{-Cp})_2(\eta^2\text{-PC}^t\text{Bu})\}_2]$	438.4, 73.5 ($\text{C}_4\text{D}_8\text{O}$)	-105	30
$[\text{Ti}(\eta\text{-C}_8\text{H}_8)(\eta\text{-P}_2\text{C}_2^t\text{Bu}_2)]$ (PCPC ring)	214.5 (C_7D_8)	32	35
$[\text{Ti}(\eta\text{-C}_8\text{H}_8)(\eta\text{-P}_2\text{C}_2^t\text{Bu}_2)]$ (PPCC ring)	133.6 (C_7D_8)	32	35

Table 3.2: $^{31}\text{P}\{^1\text{H}\}$ NMR spectroscopic data for Ti-phosphaalkyne complexes

This clearly shows that the ^{31}P chemical shifts of product B are greatly removed from those reported for any of the previously observed complexes listed. This implies that none of the AdCP units in product B are coordinated as either an $\eta^2\text{-PCAd}$ or as an $\eta^4\text{-P}_2\text{C}_2\text{Ad}_2$ ring.

The resonances at δ -50 and -191 appeared as doublets with a coupling constant value of 297 Hz. This falls in the region typical for a P-P single bond, indicating a P-P coupled dimer which was anticipated given the bulk of the Ad substituents. The third resonance was a singlet and thus implies the presence of another AdCP ligand. The presence of three equivalents of AdCP per Ti centre was also supported by the mass spectral data. (Figure 3.9) A parent ion of 714 u was observed which is approximately consistent with a formulation of $\text{Cp}_2\text{Ti}(\text{PCAd})_3$ (ideally 712 u). Another major ion was observed at 536 u which corresponded to the loss of a 178 u *i.e.* an AdCP ligand.

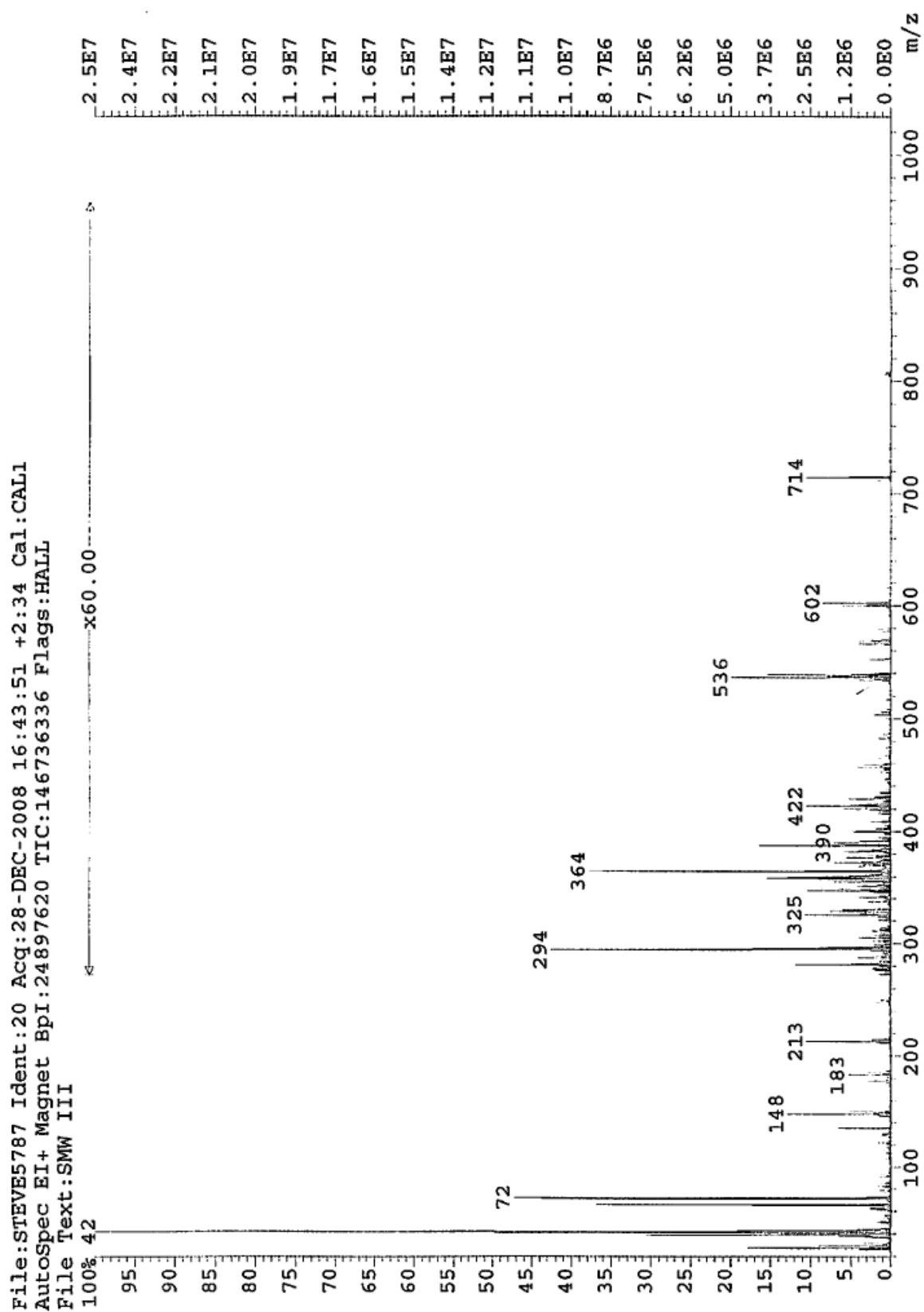


Figure 3.9: Mass spectrum of $\text{Cp}_2\text{Ti}(\text{AdCP})_3$

A speculated structure of product B is shown in Figure 3.10, possessing a phosphalkyne bound η^1 (corresponding to the $^{31}\text{P}\{^1\text{H}\}$ NMR spectroscopic resonance at δ -129) and a PPCC ring bound η^2 (corresponding to the resonances at δ -50 and δ -191). These atypical bonding modes may account for the considerable difference between the chemical shifts observed in the $^{31}\text{P}\{^1\text{H}\}$ NMR spectrum of product B and previously reported Ti complexes containing similar ligands.

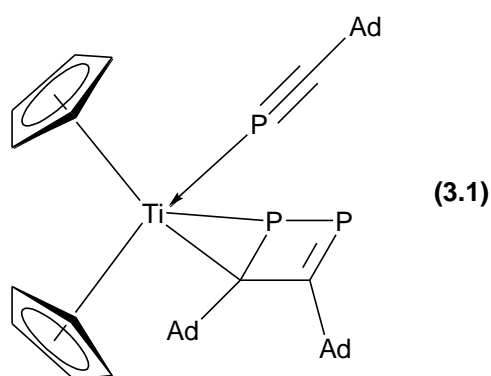
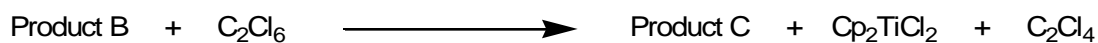


Figure 3.10: Postulated molecular structure of product B (3.1)

The high solubility of this compound meant that no crystals could be obtained for X-ray diffraction, making and suggested structure largely speculative. It is also still unclear as to why the P of the phosphalkyne shows no coupling to those of the PPCC ring.

Reaction of product B with C_2Cl_6

In an attempt to chlorinate the Ti centre and liberate the phosphalkyne based products, an excess C_2Cl_6 was added to a sample of the product in benzene- d_6 at ambient temperature, changing the colour from green to red. (Scheme 3.16)



Scheme 3.16: Reaction of product B with C₂Cl₆

The $^{31}\text{P}\{^1\text{H}\}$ NMR spectrum of the product of this reaction (Figures 3.11 and 3.12) showed three resonances (still accompanied by the free AdCP), one of which showed coupling to both of the others, suggesting that all three AdCP units were now joined.

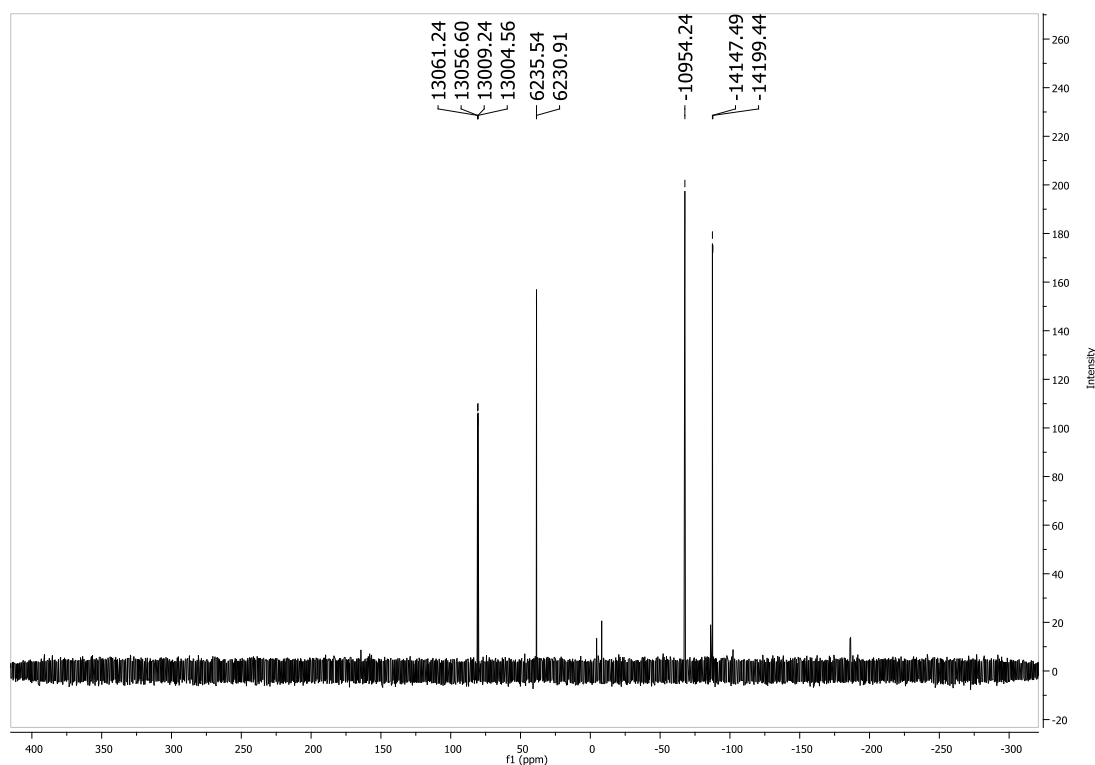


Figure 3.11: $^{31}\text{P}\{^1\text{H}\}$ NMR spectrum of the product formed by the reaction of $\text{Cp}_2\text{Ti}(\text{AdCP})_3$ and C_2Cl_6 , plus unreacted AdCP

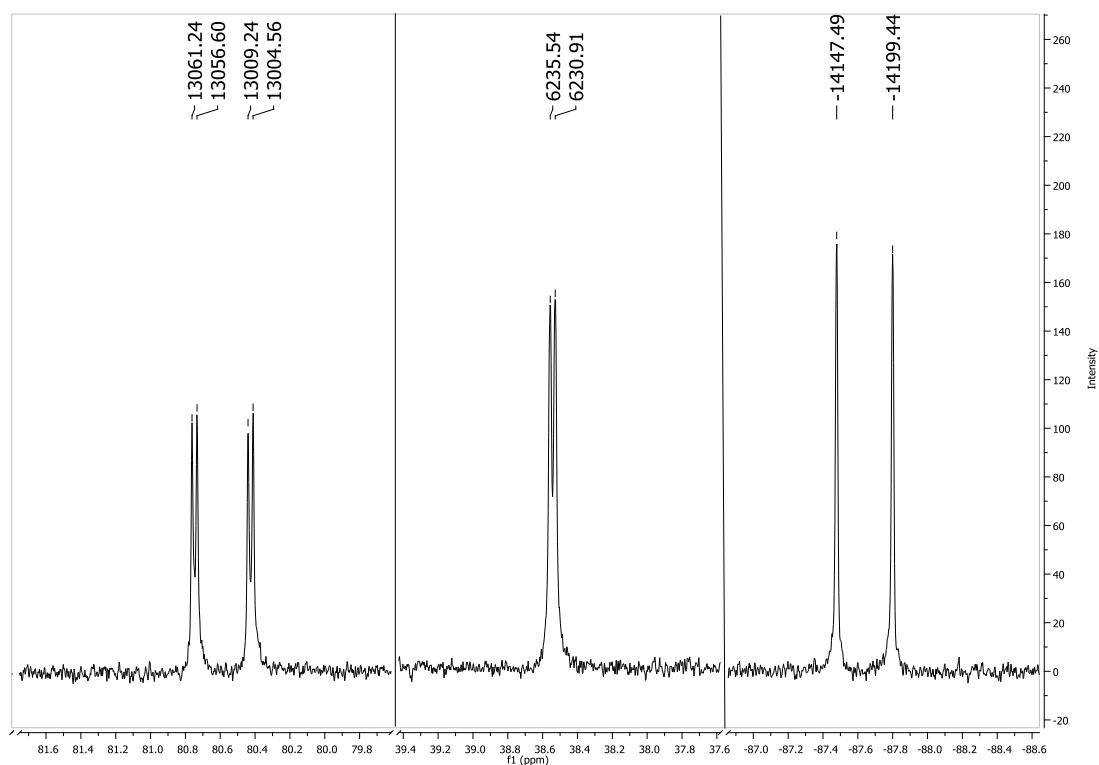


Figure 3.12: Expanded $^{31}\text{P}\{^1\text{H}\}$ NMR spectrum of the product of the reaction between $\text{Cp}_2\text{Ti}(\text{AdCP})_3$ and C_2Cl_6

The coupling constants of *circa* 50 Hz and 5 Hz are indicative of 2J and 3J couplings respectively, indicating that not only were the three AdCP units coupled in product C, but that the P-P bond indicated by the $^{31}\text{P}\{^1\text{H}\}$ NMR spectrum of product B has been broken. As with product B, no definitive structure for product C could be assigned, but one possibility given the small values of the coupling constants would be an open chain of three AdCP units, terminated by Cl atoms from the excess C_2Cl_6 . (Figure 3.13)

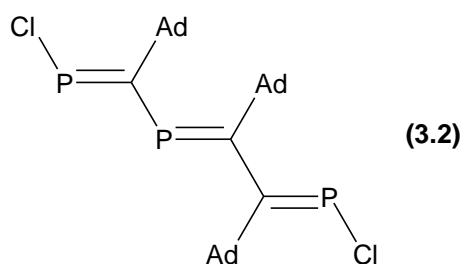
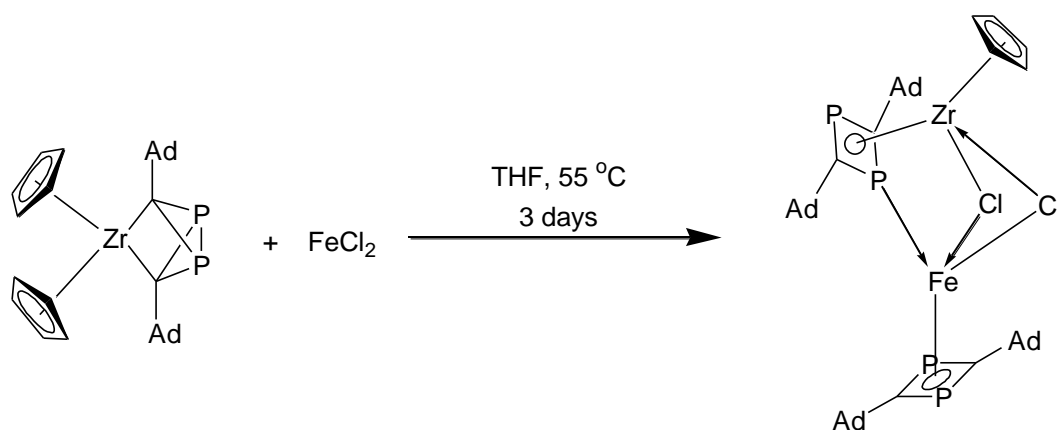


Figure 3.13: Postulated structure of product C (3.2)

After the reactions of the Ti compounds, the potential to form other complexes incorporating the $P_2C_2R_2$ ligand and different first row transition metals was investigated. Given that Fe(II) centres have been shown to coordinate $P_2C_2R_2$ rings in an η^4 fashion in complexes such as $Fe(P_2C_2^tBu_2)(CO)_3$,³⁶ a reaction was undertaken to ascertain whether an Fe analogue of the established $Sn(P_2C_2R_2)^{16}$ complexes could be produced, without the need for additional ligands.

Reaction of $FeCl_2$ with $Cp_2Zr(P_2C_2Ad_2)$

Using a preparation similar to that of $Sn(P_2C_2Ad_2)$, $FeCl_2$ was combined with one equivalent of $Cp_2Zr(P_2C_2Ad_2)$ in THF, degassed and heated to 55 °C for three days. (Scheme 3.17)



Scheme 3.17: Reaction of $Cp_2Zr(P_2C_2Ad_2)$ and $FeCl_2$

This reaction afforded a brown solution from which dark-purple, square plate crystals were formed. The molecular structure was determined by a single crystal X-ray

diffraction study and shown to contain both Fe and Zr metal centres as well as two $\text{P}_2\text{C}_2\text{Ad}_2$ rings. (Figure 3.14)

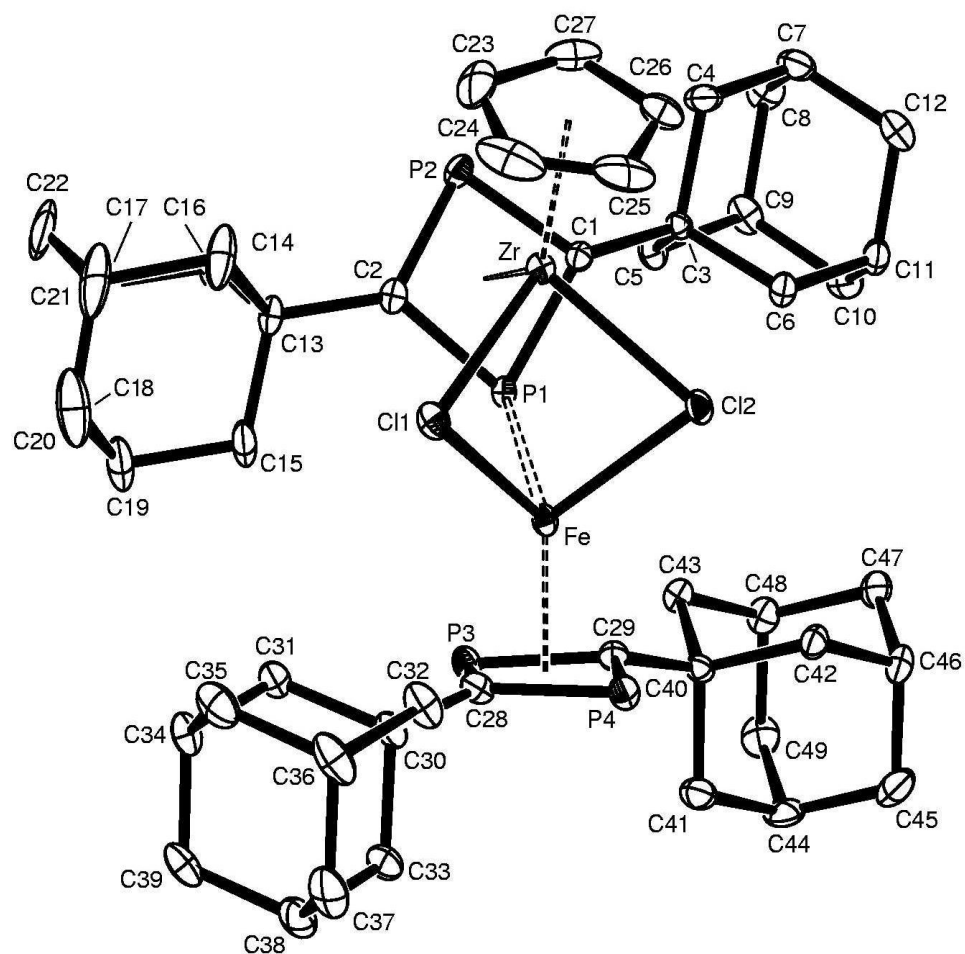


Figure 3.14: ORTEP molecular structure of $\text{CpZr}(\text{P}_2\text{C}_2\text{Ad}_2)\text{Cl}_2\text{Fe}(\text{P}_2\text{C}_2\text{Ad}_2)$ (**3.3**) (*H* atoms omitted for clarity)

Selected Bond Lengths [\AA]	
Zr-Cl1	2.4997(12)
Zr-Cl2	2.5133(12)
Fe-Cl1	2.3651(13)
Fe-Cl2	2.3600(12)
Zr-P1	2.6523(12)
Zr-P2	2.771(12)
Zr-C1	2.338(4)
Zr-C2	2.571(4)
Fe-P1	2.4074(13)
Fe-P3	2.3041(13)
Fe-P4	2.3145(14)
Fe-C28	2.174(5)
Fe-C29	2.102(5)
Zr-C23	2.511(5)
Zr-C24	2.514(6)
Zr-C25	2.520(5)
Zr-C26	2.520(5)
Zr-C27	2.529(5)

Selected Bond Angles [$^\circ$]	
Zr-Cl1-Fe	74.32(2)
Zr-Cl2-Fe	74.49(2)
Zr-P1-Fe	
Cl1-Zr-Cl2	83.79(4)
Cl1-Fe-Cl2	90.22(4)
C1-P1-C2	81.2(2)
C1-P2-C2	84.4(2)
P1-C1-P2	93.9(2)
P1-C2-P2	97.2(2)
C28-P3-C29	80.7(2)
C28-P4-C29	81.1(2)
P3-C28-P4	99.6(2)
P3-C29-P4	98.2(2)
C27-C23-C24	106.7(6)
C23-C24-C25	108.2(6)
C24-C25-C26	109.2(6)
C25-C26-C27	108.8(8)
C26-C27-C23	107.1(6)

Comparison with literature values for Zr-C(Cp) bond lengths³⁷ showed them to be typical for a Cp ligand coordinated to a Zr(IV) centre. Similarly the Zr-Cl and Fe-Cl bond lengths were in the range expected for bridging Cl to the respective metals,^{38,39} and the Fe-P bonds were similar to the handful of previously reported examples of complexes containing P₂C₂R₂ rings coordinated to Fe centres.^{12,36,40} A comparison of the bonding between Zr and the P₂C₂Ad₂ was not possible as no previous examples of η^4 coordination to Zr have been reported. The P₂C₂Ad₂ ring adopts this near planar coordination mode (P1 deviated by 0.431 Å) due to the enhanced stability of its aromaticity. In the starting material, Cp₂Zr(P₂C₂Ad₂) the η^4 coordination mode is not possible due to the available orbitals of the metal centre. The Cp₂Zr fragment possesses three orbitals available for bonding, all of which lie in a plane between the Cp rings and do not provide the necessary overlap with the orbitals of the planar P₂C₂R₂ ring to allow a bonding interaction.

The paramagnetic nature of this product, was evident from its NMR spectra. Employing the Evans' method⁴¹ gave a value of three for the number of unpaired electrons in this bimetallic complex.

Although no NMR spectrum of the product could be obtained, ³¹P{¹H} NMR spectra run of the reaction after two days revealed a pair of doublets at δ -97.6 and 366.6, the latter being much broader, with a coupling of 47 Hz. (Figure 3.15)

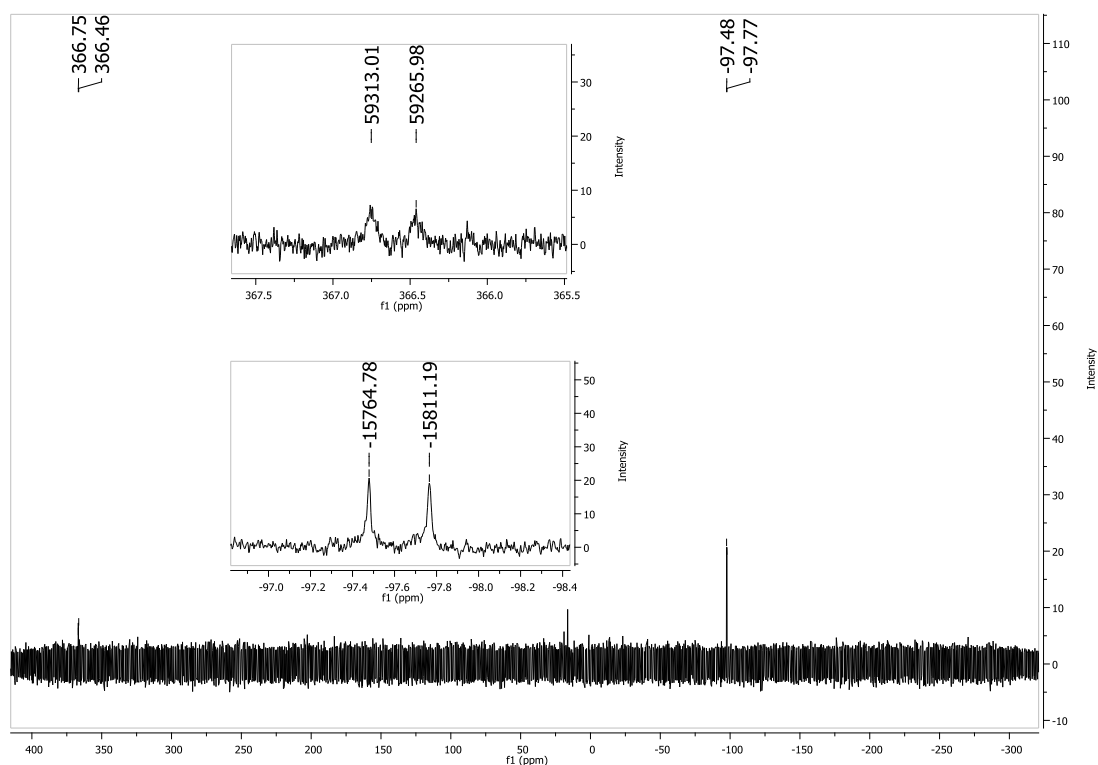
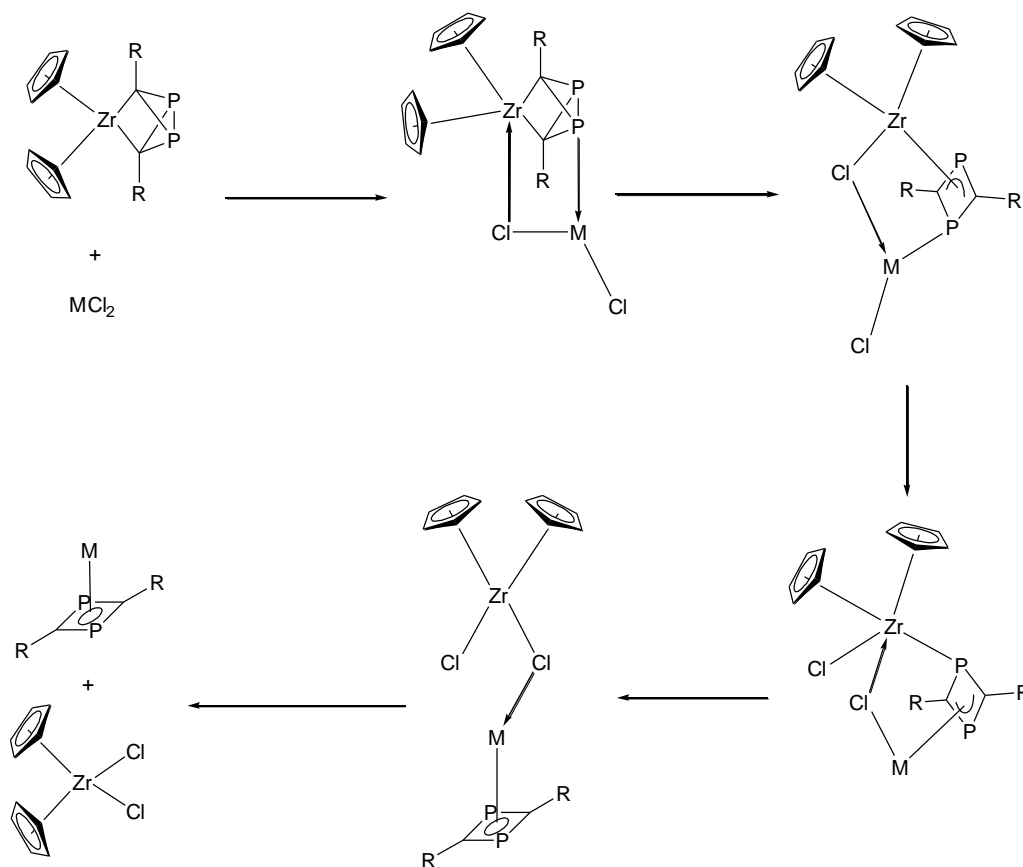


Figure 3.15: $^{31}\text{P}\{^1\text{H}\}$ NMR spectrum of the intermediate in the reaction of $\text{Cp}_2\text{Zr}(\text{P}_2\text{C}_2\text{Ad}_2)$ with FeCl_2

Given the low intensity and broad nature of these resonances it is postulated that these resonances correspond to an intermediate species in which the phosphorus atoms are no longer equivalent. The chemical shift value of δ 366 is typical for an unsaturated P atom, implying that the P-P bond of $\text{Cp}_2\text{Zr}(\text{P}_2\text{C}_2\text{Ad}_2)$ is broken.

Examining the molecular structure of the dimer, in particular the presence of bridging Cl and a $\text{P}_2\text{C}_2\text{Ad}_2$ ring it is tempting to propose a general mechanism for the Cl/ $\text{P}_2\text{C}_2\text{R}_2$ ring exchange. Initial coordination of a Cl lone pair from MCl_2 to the Zr and from one of the P atoms to the M leads to the formation a dimer. As the bridging Cl transfers to the Zr the P-P bond of the coordinated $\text{P}_2\text{C}_2\text{R}_2$ group breaks and the ring shifts towards the incoming M centre, with its coordination mode to M switching from L- to X-type.

If this process is repeated then the second Cl is transferred to the zirconium and the $P_2C_2R_2$ ring would move completely to the M centre. Finally, the dative M-Cl bond dissociate, affording Cp_2ZrCl_2 and the new $MP_2C_2R_2$ system. (Scheme 3.18) This mechanism would account for the products observed in reactions in which main group halides are employed and which are by far more numerous than their transition metal analogues (*vide* Chapter 2).

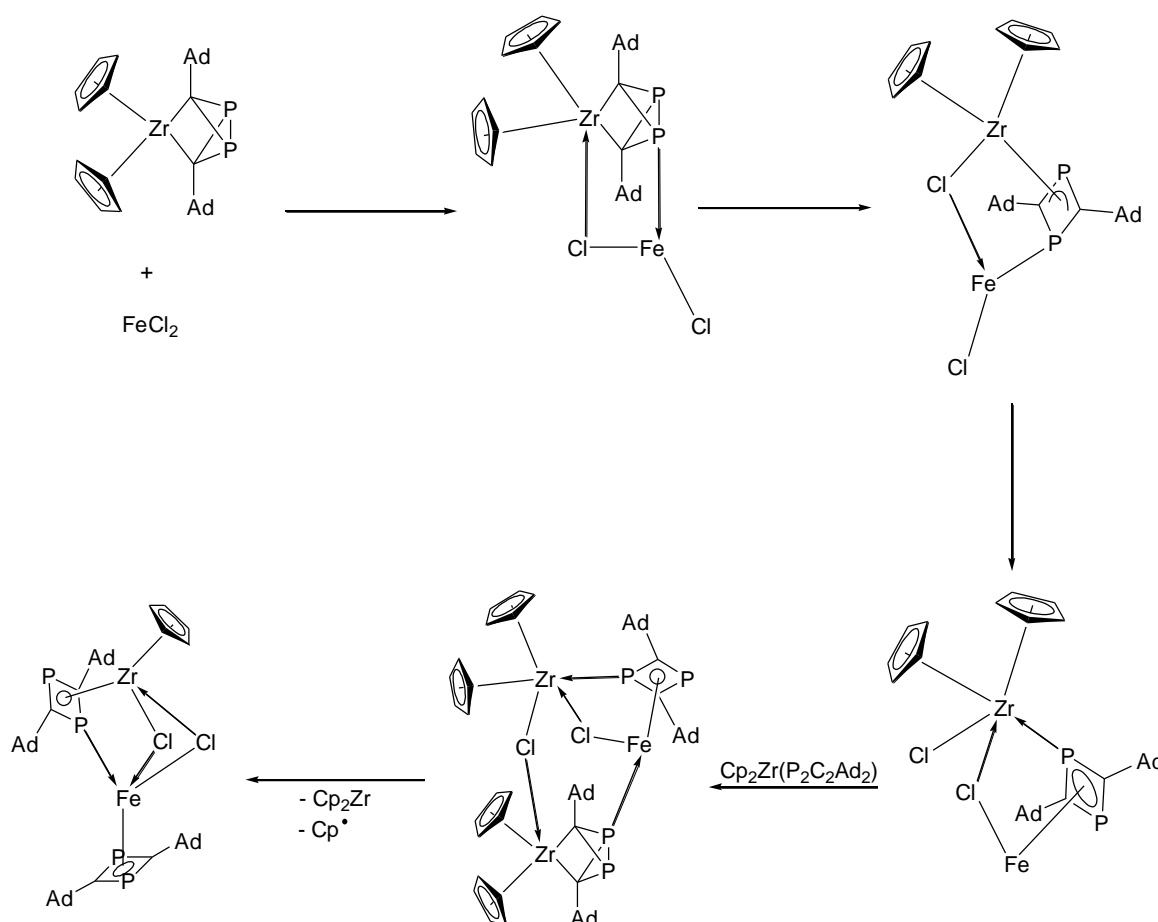


Scheme 3.18: Proposed general mechanism for the $P_2C_2R_2$ /dichloride exchange

Clearly this is not the mechanism operating when $FeCl_2$ is the metal halide. Unlike its main group analogues for which any redox process must be a two-electron event, Fe can undergo a single electron transfer process. If the formal oxidation states of the metal centres in the product are assigned as Zr(IV) and Fe(III) then an one electron oxidation

of the Fe has occurred. The presence of the second $P_2C_2Ad_2$ group in the dimer implies that reaction with a second equivalent of $Cp_2Zr(P_2C_2Ad_2)$ must be involved.

It is the ability of Fe to support a +3 oxidation state that permits the $P_2C_2Ad_2$ ring to coordinate η^4 without the requirement for the Fe centre to transfer a second Cl. The resulting chloro-bridged compound then coordinated to a second equivalent of the zirconium reagent *via* the Cl. However, since the transfer of the second $P_2C_2Ad_2$ ring would require the Fe to adopt an unfavourable +4 oxidation state the progress was arrested before this could happen. Instead, it is postulated that the chloride donation prompted the loss of a Cp radical which (along with the loss of Cp_2Zr) afforded the product. (Scheme 3.19)



Scheme 3.19: Proposed mechanism for the formation of $ZrCp(P_2C_2Ad_2) Cl_2Fe(P_2C_2Ad_2)$

3.3: Conclusions

The reactions of $\text{Cp}_2\text{Zr}(\text{P}_2\text{C}_2\text{R}_2)$ with TiCl_3 and TiCl_4 indicate that the transfer of the $\text{P}_2\text{C}_2\text{R}_2$ ligand from Zr to Ti is achievable, but that the presence of two rings on the metal centre leads to an unstable state in which the rings are lost and combined into molecules of tetraphosphacubane.

By reducing Cp_2TiCl_2 and combining with AdCP a compound was formed with the proposed formula of $\text{Cp}_2\text{Ti}(\text{AdCP})_3$. The structure of this complex could not be determined but it is clear that there is a marked difference between this and the analogous reaction involving Zr which dimerises the phosphaaalkyne into the butterfly structure.

The reaction between $\text{Cp}_2\text{Zr}(\text{P}_2\text{C}_2\text{Ad}_2)$ and FeCl_2 produced a paramagnetic complex containing both metal centres bridged by chlorides and a $\text{P}_2\text{C}_2\text{Ad}_2$ ring. The molecular structure of this complex helped to formulate the proposed mechanism, not just for its own synthesis, but also for the general $\text{P}_2\text{C}_2\text{R}_2/2\text{Cl}$ exchange reactions that have provided the principal theme of this and the previous chapter.

References

1. Churchill, D., Shin, J. H., Hascall, T., Hahn, J. M., Bridgewater, B. M., Parkin, G., *Organometallics*, 1999, **18**, 2403
2. Burckett-St. Laurent, J. C. T. R., Hitchcock, P. B., Kroto, H. W., Nixon, J. F., *J. C. S. Chem. Comm.*, 1981, 1142
3. Nixon, J. F., *Coord. Chem. Rev.*, 1995, **145**, 201
4. Hitchcock, P. B., Maah, M. J., Nixon, J. F., Zora, J. A., Leigh, G. J., Abubakar, M., *Angew. Chem., Int. Ed. Engl.*, 1987, **26**, 474
5. Kramkowski, P., Scheer, M., *Eur. J. Inorg. Chem.*, 2000, 1869
6. Becker, G., Herrmann, W. A., Kalcher, W., Kriechbaum, G. W., Pahl, C., Wagner, C. T., Ziegler, M. L., *Angew. Chem., Int. Ed. Engl.*, 1983, **22**, 413
7. Burckett-St. Laurent, J. C. T. R., Hitchcock, P. B., Kroto, H. W., Meidine, M. F., Nixon, J. F., *J. Organomet. Chem.*, 1982, **238**, C82
8. Hitchcock, P. B., Maah, M. J., Nixon, J. F., *Chem. Commun.*, 1986, 737
9. Binger, P., Milczarek, R., Mynott, R., Regitz, M., Rösch W., *Angew. Chem. Int. Ed. Engl.*, 1986, **25**, 644
10. Binger, P., Leininger, S., Stannek, J., Gabor, B., Mynott, R., Bruckmann, J., Krüger, C., *Angew. Chem. Int. Ed. Engl.*, 1995, **34**, 2227
11. Wettling, T., Wolmoershäuser, G., Binger, P., Regitz, M., *Chem. Commun.*, 1990, 1541
12. Böhm, D., Knoch, F., Kummer, S., Schmidt, U., Zenneck, U., *Angew. Chem. Int. Ed. Engl.*, 1995, **34**, 198
13. Binger, P., Biedenbach, B., Krüger, C., Regitz, M., *Angew. Chem. Int. Ed. Engl.*, 1987, **26**, 764.

14. Scheer, M., Schuster, K., Budzichowski, T. A., Chisholm, M. H., Streib, W. E.,
J. Chem. Soc. Chem. Commun. 1995, 1671
15. Jones, C., Schulten, C., Stasch, A., *Dalton Trans.*, 2006, 3733
16. Wettling, T., Geissler, B., Barth, S., Schneider, R., Binger, P., Regitz, M.,
Angew. Chem. Int. Ed. Engl., 1992, **31**, 758
17. Binger, P., Wettling, T., Schneider, R., Zurmühlen, F., Bergsträsser, U.,
Hoffmann, J., Maas, G., Regitz, M., *Angew. Chem. Int. Ed. Engl.*, 1991, **30**, 207
18. Francis, M. D., Hitchcock, P. B., *Organometallics*, 2003, **22**, 2891
19. Francis, M. D., Hitchcock, P. B., *Chem. Commun.*, 2002, 86
20. Fish, C., Green, M., Jeffery, J.C., Kilby, R. J., Lynam, J. M., McGrady, J. E.,
Pantazis, D. A., Russel, C. A., Willans, C. E., *Angew. Chem. Int. Ed. Engl.*,
2006, **45**, 6685
21. Binger, P., Stutzmann, S., Stannek, J., Günther, K., Phillips, P., Mynott, R.,
Bruckmann, J., Krüger, C., *Eur. J. Inorg. Chem.*, 1999, 763
22. Barron, A. R., Cowley, A. H., *Angew. Chem. Int. Ed. Engl.*, 1987, **26**, 907
23. Binger, P., Glaser, G., Stannek, J., Leininger, S., *Phosphorus Sulfur Silicon
Relat. Elem.*, 1996, **109/110**, 149
24. Milczarek, R., Rüsseler, W., Binger, P., Jonas, K., Angermund, K., Krüger, C.,
Regitz, M., *Angew. Chem. Int. Ed. Engl.*, 1987, **26**, 908
25. Cloke, F. G. N., Flower, K. R., Hitchcock, P. B., Nixon, J. F., *J. Chem. Soc.
Chem. Commun.*, 1995, 1659
26. Avent, A. G., Cloke, F. G. N., Flower, K. R., Hitchcock, P. B., Nixon, J. F.,
Vickers, D. M., *Angew. Chem. Int. Ed. Engl.*, 1994, **33**, 2330
27. Cloke, F. G. N., Flower, K. R., Hitchcock, P. B., Nixon, J. F., Vickers, D. M., *J.
Organomet. Chem.*, 2001, **625**, 212

28. Cloke, F. G. N., Flower, K. R., Hitchcock, P. B., Nixon, J. F., *J. Chem. Soc. Chem. Commun.*, 1994, 498
29. Arnold, P. L., Cloke, F. G. N., Nixon, J. F., *Chem. Commun.*, 1998, 797
30. Binger, P., Biedenbach, B., Herrmann, A. T., Langhauser, F., Betz, P., Goddard, R., Krüger, C., *Chem. Ber.*, 1990, **123**, 1617
31. Aazam, E. S., Thesis, 2001
32. Binger, P., Barth, S., Biedenbach, B., Haas, J., Herrmann, A. T., Milczarek, R., Schneider, R., *Phosphorus Sulfur Silicon Relat. Elem.*, 1993, **77**, 1
33. Wettling, T., Schneider, J., Wagner, O., Kreiter, C. G., Regitz, M., *Angew. Chem. Int. Ed. Engl.*, 1989, **28**, 1013
34. Geissler, B., Barth, S., Bergsträsser, U., Slany, M., Durkin, J., Hitchcock, P. B., Hofmann, M., Binger, P., Nixon, J. F., von Ragué Schleyer, P., Regitz, M., *Angew. Chem. Int. Ed. Engl.*, 1995, **34**, 484
35. Binger, P., Glasser, G., Albus, S., Krueger, C., *Chem. Ber.*, 1995, **128**, 1261
36. Heinemann, F. W., Kummer, S., Seiss-Brandl, U., Zenneck, U., *Organometallics*, 1999, **18**, 2021
37. (a) Hunter, W. E., Hrcir, D. C., Bynum, R. V., Penttilä, R. A., Atwood, J. L., *Organometallics*, 1983, **2**, 750 (b) Urazowski, I. F., Ponomaryev, V. I., Nifant'ev, I. E., Lemonovskii, D.A., *J. Organomet. Chem.*, 1989, **368**, 287 (c) King, W. A., Di Bella, S., Gulino, A., Lanza, G., Fragalà I. L., Stern, C. L., Marks, T. J., *J. Am. Chem. Soc.*, 1999, **121**, 355 (d) Prout, K., Cameron, T. S., Forder, R. A., Critchley, A. R., Denton, B., Rees, G. V., *Acta Crystallogr., Sect. B: Struct. Crystallogr. Cryst. Chem.*, 1974, **30**, 2290
38. (a) Schweder, B., Görls, H., Walther, D., *Inorg. Chim. Acta*, 1999, **286**, 14 (b) LoCoco, M. D., Zhang, X., Jordan, R. F., *J. Am. Chem. Soc.*, 2004, **126**, 15231

39. (a) Cotton, F.A., Luck, R. L., Son, K.A., *Inorg. Chim. Acta*, 1991, **184**, 177 (b) Sun, J.S., Zhao, H., Ouyang, X., Clérac, R., Smith, J. A., Clemente-Juan, J. M., Gómez-García, C., Coronado, E., Dunbar, K. R., *Inorg. Chem.*, 1999, **38**, 5841
40. Wolf, R., Slootweg, C., Ehlers, A. W., Hartl, F., de Bruin, B., Lutz, M., Spek, A. L., Lammertsma, K., *Angew. Chem. Int. Ed.*, 2009, **48**, 3104
41. (a) Evans, D. F., *J. Chem. Soc.*, 1959, 2003 (b) Evans, D. F., Fazakerley, G. V., Phillips, R. F., *J. Chem. Soc. A.*, 1971, 1931 (c) De Buysser, K., Herman, G. G., Bruneel, E., Hoste, S., Van Dreissche, I., *Chem. Phys.*, 2005, **315**, 286

Chapter 4

Investigating Cyclopentadienyl Tin Halides as Potential Precursors for $\text{Sn}\equiv\text{P}$ Bonds

4.1: Introduction

When the first phosphalkyne was synthesised almost fifty years ago by Gier¹ it marked the beginning of a great deal of interest, not just into phosphalkynes, but in multiple bonding between main group elements.²

For heavier main group elements, there is an increasing tendency for the lower of the two available oxidation states to become more stable, resulting from the inert pair effect³ and a consequential reduction in the number of bonds formed by the heavier elements. In the case of the group 14 elements, for example, alkynes are ubiquitous whereas there is a relative dearth of germyl and stannyl analogues. For many years, this behaviour led to an accepted “double-bond rule”² which stated that multiple bonds of heavy main group atoms could not exist stably. The explanation proposed was that as an atom becomes larger, there is lessening of the overlap between the p-orbitals,⁴ thus making the formation of π -bonds ever more difficult and favouring the single bond and two lone pairs configuration. (Figure 4.1)

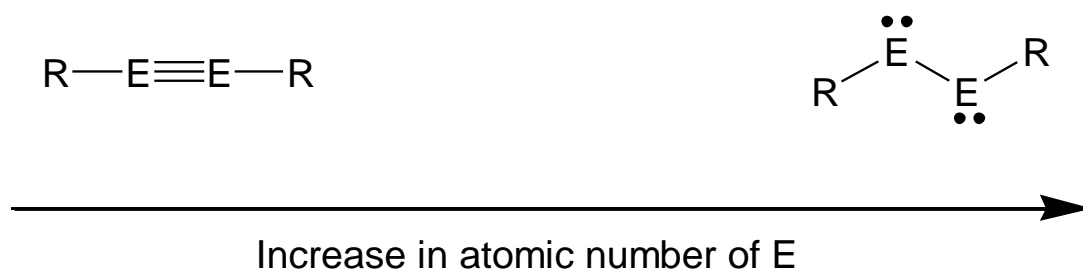


Figure 4.1: The inert pair effect. (E = group 14 element)

The inert pairs and bent geometries of low-coordinate compounds of heavy, main-group elements arises as a result of increased mixing of the π and σ^* orbitals of the central bond, due to the decrease in their energy separation as the atomic number of E increases. This mixing of orbitals lowers the energy of the π orbital increasing the stability of the molecule, but in doing so transforms the bonding orbital into a non-bonding orbital.² (Figure 4.2)

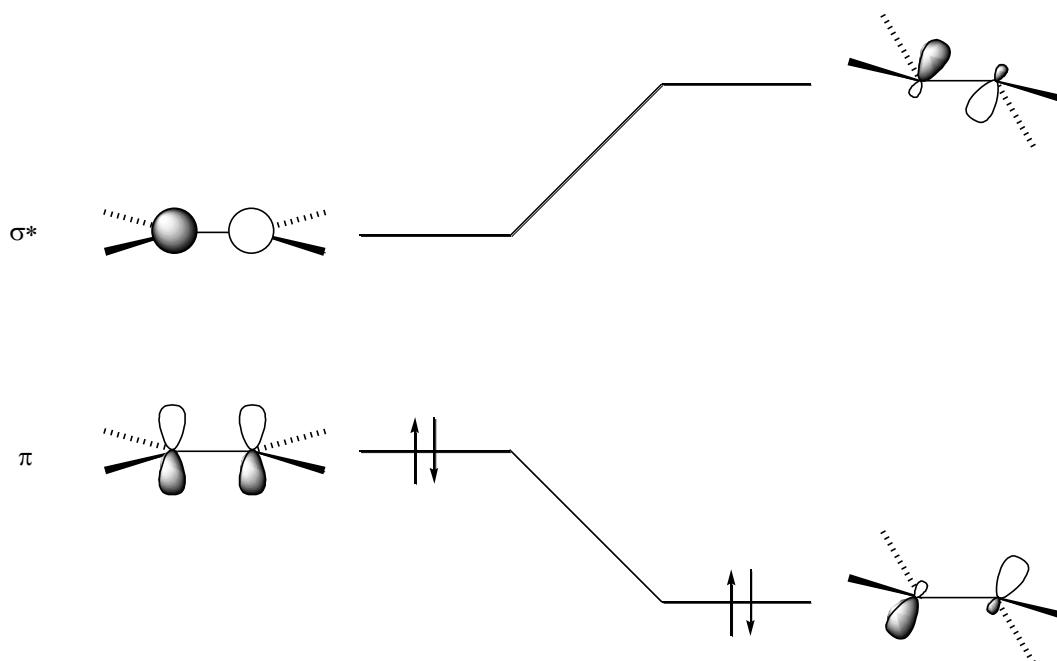
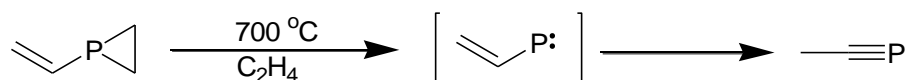


Figure 4.2: Mixing of π and σ^* orbitals in heavy element alkene analogues

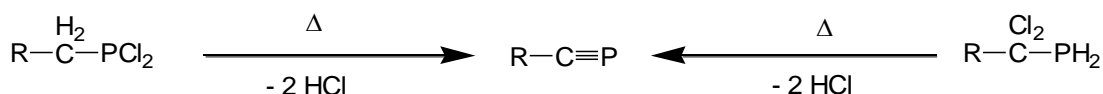
These facts make the synthesis of heavier main group multiple bonds much more challenging than their first row congeners, although still achievable through judicious use of substituent groups.

The first phosphalkyne, HCP, was produced by passing phosphine through an arc struck between graphite electrodes at reduced pressure for several hours.¹ This caused a reaction between the phosphine and the carbon, producing HCP and HCCH in a 1:4 ratio as well as traces of H₂CCH₂. HCP readily polymerises, which was later found to be a common property of phosphalkynes, which resulted in the colourless gas changing to a black solid unless stored at very low temperatures (≤ 124 °C) and/or pressures. Since then, phosphalkynes containing different alkyl and aryl substituents have been reported⁵ by a variety of methods. For example, flash vacuum thermolysis of 1-vinylphosphirane at 700 °C has been employed to produce MeCP *via* a vinylphosphidine intermediate.⁶ (Scheme 4.1)



Scheme 4.1: Formation of MeCP by flash vacuum thermolysis

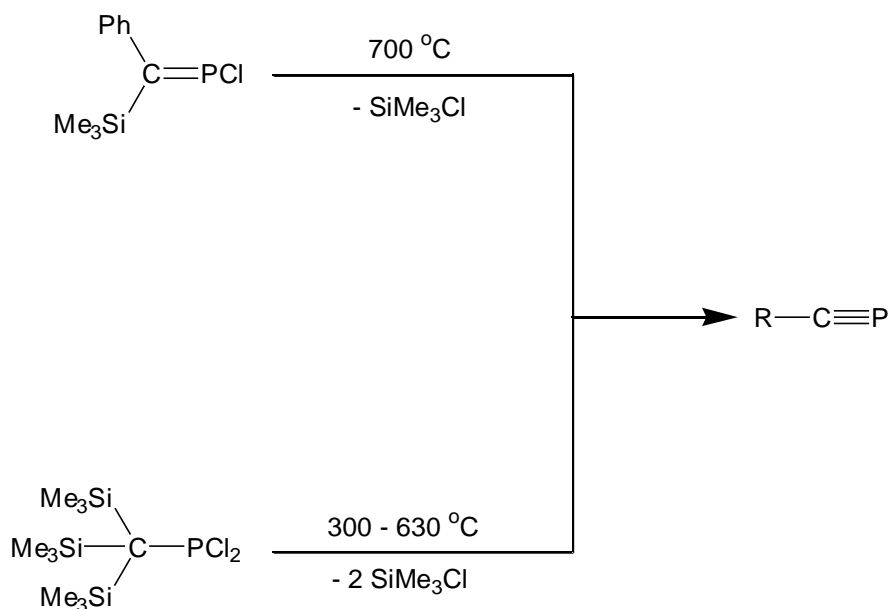
A more widely used synthesis employs the elimination of adjacent atoms or groups across a C-P bond as a greater range of substituents on the carbon atom *e.g.* the elimination of HCl, from dichlorophosphaalkanes⁷ and dichloroalkylphosphines.⁸ (Scheme 4.2)



Scheme 4.2: Formation of phosphalkyne by elimination of HCl

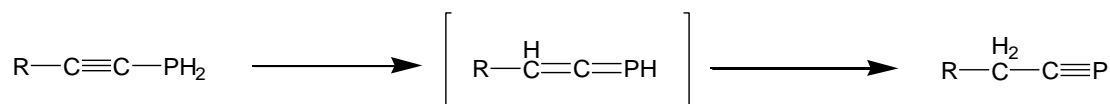
Flash vacuum pyrolysis of chloro(phenyl(trimethylsilyl)methyl)phosphine was reported to afford phenylphosphaalkyne.⁹ while pyrolysis of dichloro(tris(trimethylsilyl)methyl)phosphine afforded trimethylsilyllphosphaalkyne.¹⁰ (Scheme 4.3)

As shown in Scheme 4.2 the H and Cl atoms may originate on either the C or P elements whereas the trimethylsilyl groups depicted in Scheme 4.3 are always based on the carbon centre.



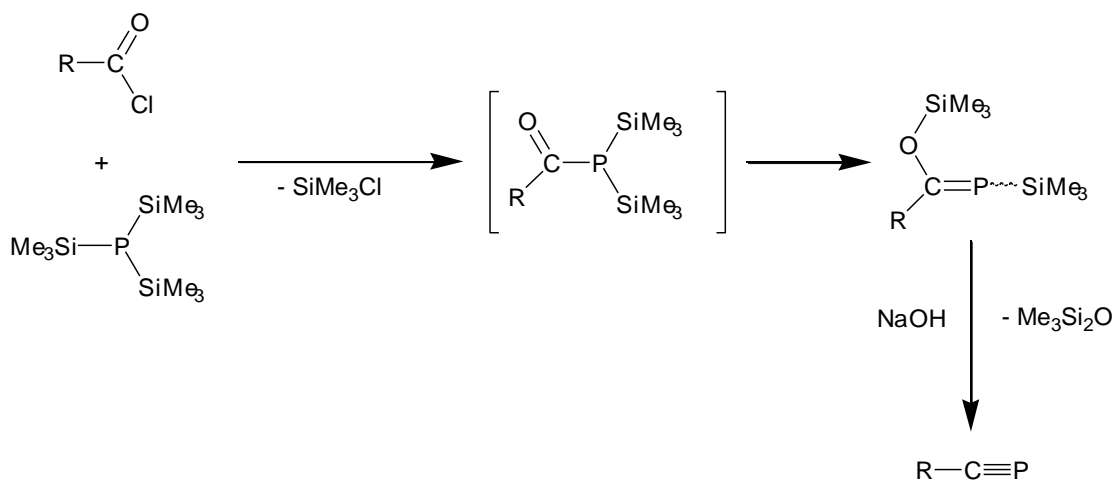
Scheme 4.3: Formation of phosphaalkyne via the elimination of SiMe₃Cl

This method, however, provided product of low yields and purities. Good yields may be obtained when the desired phosphaalkyne contains a primary or secondary carbon is bound to the C atom and thus can be synthesised *via* a Lewis base catalysed rearrangement of the corresponding alkynyl phosphine.¹¹ (Scheme 4.4)



Scheme 4.4: Formation of phosphalkyne by rearrangement of its alkynyl phosphine

Perhaps the most frequently employed method for the preparation of phosphalkynes involves the elimination of hexamethyldisiloxane.¹² (Scheme 4.5) The initial step of this synthesis combines $\text{P}(\text{SiMe}_3)_3$ and an appropriate acyl halide. A molecule of trimethylsilyl chloride is eliminated to create the carbon phosphorus bond. This is quickly followed by a migration of a trimethylsilyl group from the P to the O of the carbonyl group, providing the $\text{C}=\text{P}$. Addition of base subsequently catalyses the elimination of the hexamethyldisiloxane thus forming the $\text{C}\equiv\text{P}$



Scheme 4.5: Formation of phosphalkyne by elimination of hexamethyldisiloxane

This method affords high yields under relatively mild conditions, hence its wide appeal. It was using this method that, in 1981, the first kinetically stabilised phosphalkyne, $^t\text{BuC}\equiv\text{P}$, was synthesised.¹² Unlike HCP which polymerised readily, $^t\text{BuC}\equiv\text{P}$ could be stored, without decomposition at ambient temperatures and pressures. The ^tBu

substituent hinders access to the reactive $\text{C}\equiv\text{P}$ moiety which is required for polymerisation to occur. Although twenty years elapsed between the synthesis of HCP and $^t\text{BuC}\equiv\text{P}$ the isolation of the latter prompted the publication of several analogues such as the adamantyl¹³ and 2,4,6-tri-*tert*-butylphenyl (Mes*).¹⁴ (Figure 4.3)

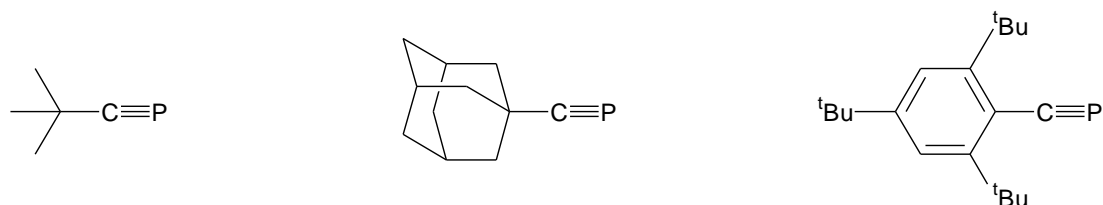
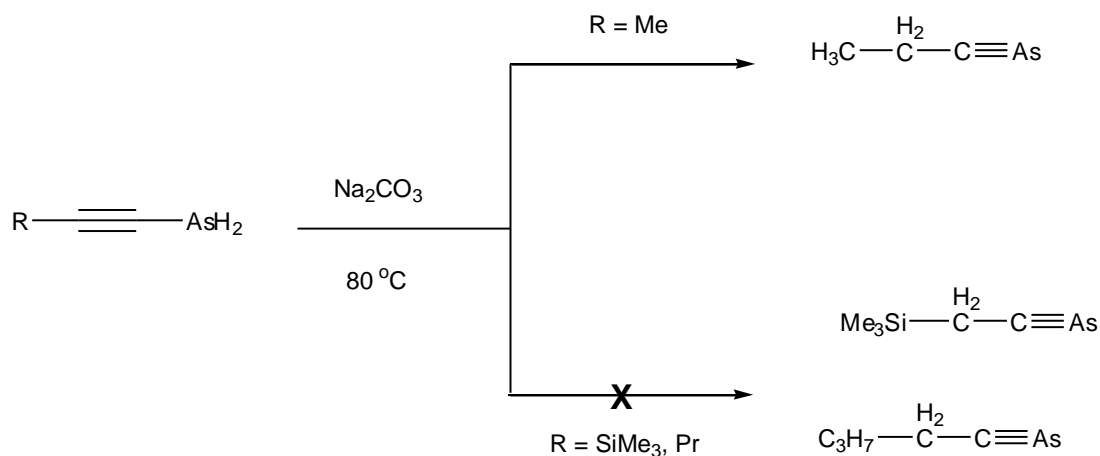


Figure 4.3: Selected kinetically stabilised phosphalkynes

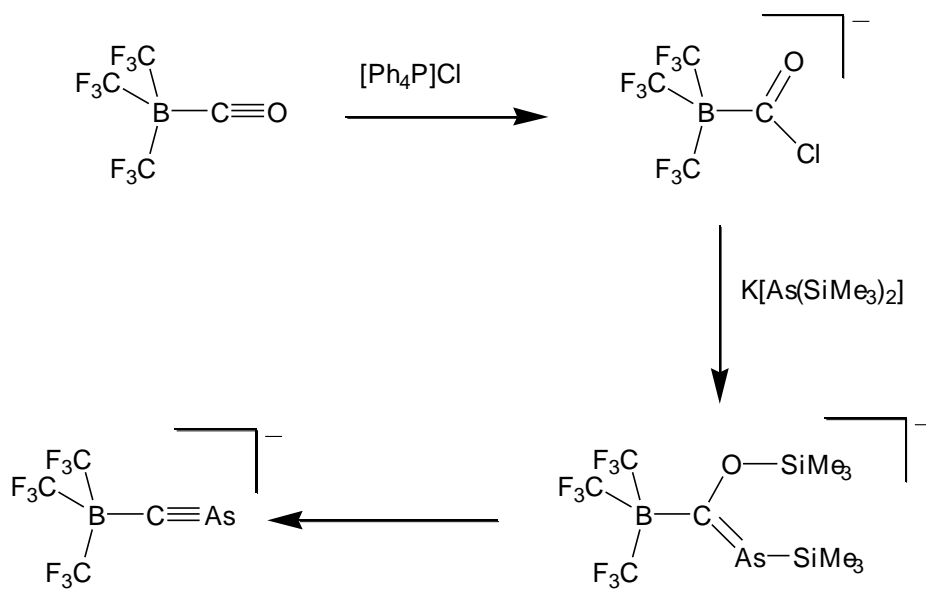
Once a family of stable phosphalkynes had been established, investigators turned to elements other than P to search for further examples of $\text{C}\equiv\text{E}$

The arsaalkynes² were subsequently explored but only a handful of examples have, to date, been identified, and only one of these, Mes* $\text{C}\equiv\text{As}$, is stable as a neutral species.¹⁵ This was formed *via* the route outlined in Scheme 4.5. Others such as Me $\text{C}\equiv\text{As}$ were prepared *via* the Lewis base catalysed rearrangement depicted in Scheme 4.4 but rapidly decomposes, with a half-life of only one hour at 0 °C.¹⁶ After having synthesised ethynylarsine, sodium carbonate was used at 80 °C to induce a rearrangement to the Me $\text{C}\equiv\text{As}$. This method was later used to synthesise the third example, Et $\text{C}\equiv\text{As}$, but failed for the synthesis of the ^nBu and $(\text{Me}_3\text{Si})\text{CH}_2$ analogues.¹⁷ (Scheme 4.6)



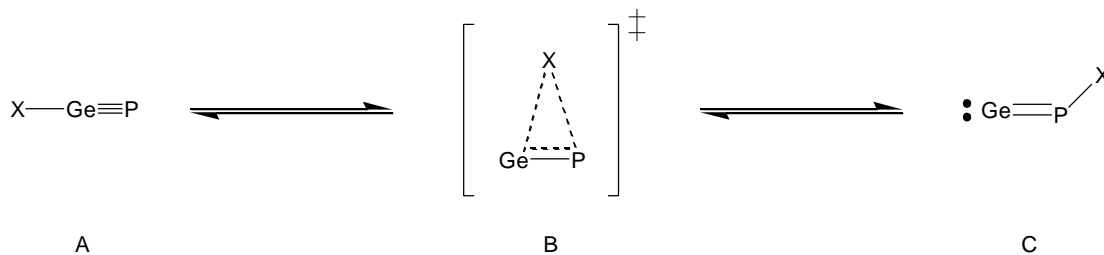
Scheme 4.6: Formation of arsaalkynes by base catalysed rearrangement of an alkyne

More recently, an anionic tris(trifluoromethyl)borosarsaalkyne was synthesised.¹⁸ as outlined in Scheme 4.7.



Scheme 4.7: Formation of an arsaalkyne trialkylborane complex by elimination of (SiMe₃)₂O

Currently, there are no examples of molecules containing a triple bond between a heavier group 14 and 15 element, although some theoretical reports have appeared regarding the effect of different substituents, X, on the stability of $\text{Ge}\equiv\text{P}$.¹⁹ (Scheme 4.8)



Scheme 4.8: Theoretical equilibrium between Ge(IV) and Ge(II) multiply bonded phosphorus species

B3LYP calculations were used to show that the doubly bonded form (C) is intrinsically more thermodynamically stable, but the triply bonded molecule (A) lies at a local minimum on the potential energy surface and could be stabilised kinetically. The authors also revealed that A was stabilised by the presence of π -donating, electronegative groups, whilst the reverse was true for C.

Two years later, another calculation was reported for the $\text{XSn}\equiv\text{P}$ analogue.²⁰ The overall conclusion this time was that the electronic properties of X could not be tailored to make the triply bonded form more thermodynamically stable than the doubly bonded form. The use of very bulky aryl substituents such as $\text{C}_6\text{H}_3\text{-2,6-[C}_6\text{H}_2\text{-2,4,6-C(SiH}_3)_3\text{]}_2$ was calculated to provide an energy minimum for the triply bonded species. (Figure 4.4)

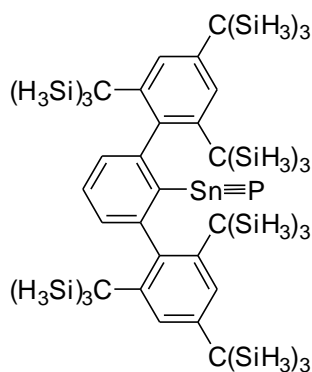


Figure 4.4: Theoretically stable $\text{Sn}\equiv\text{P}$ species

This calculation showed $\text{XSn}\equiv\text{P}$ to be more stable than $\text{Sn}=\text{P}-\text{X}$ by approximately 20.71 kcal/mol, and around 22.80 kcal/mol less than the associated 2+2 dimer.

Although the elusive $\text{RSn}\equiv\text{P}$ molecule could supposedly be stabilised by employing a suitable ligand, this does present its own set of problems. Because the ligand is designed to block any oligomerisation of the $\text{Sn}\equiv\text{P}$ moiety by virtue of its bulk, it is difficult to envisage a route *via* a suitable Sn(IV) precursor a difficulty which is compounded by the necessity of requiring a $\text{Sn}-\text{P}$ bond-forming step in the synthesis. One possible remedy would be to use an ambidentate ligand, which when bonding to the Sn in one mode would maintain the bulk of the ligand away from the Sn centre thus facilitating the $\text{Sn}-\text{P}$ bond formation step. But would then adopt its second ligation mode in which the bulk of the ligand would protect the multiple bond after its subsequent formation. It is well established that the cyclopentadienyl ligand when bonded to Sn(IV) centres binds in an η^1 fashion while for its Sn(II) analogues an η^5 mode is adopted.²¹⁻²⁴ (Figure 4.5)

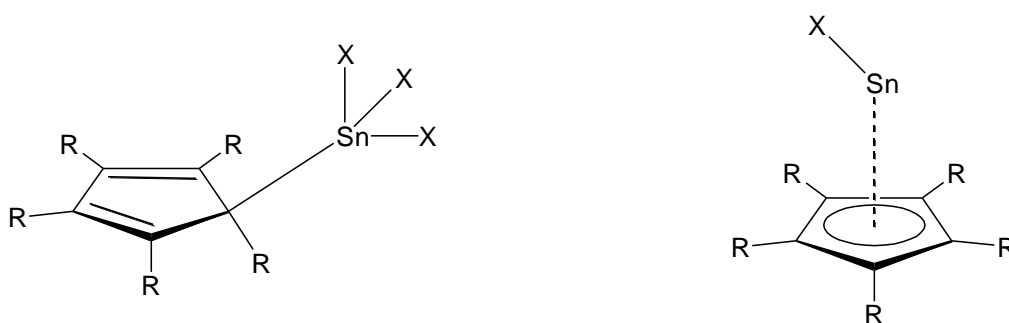
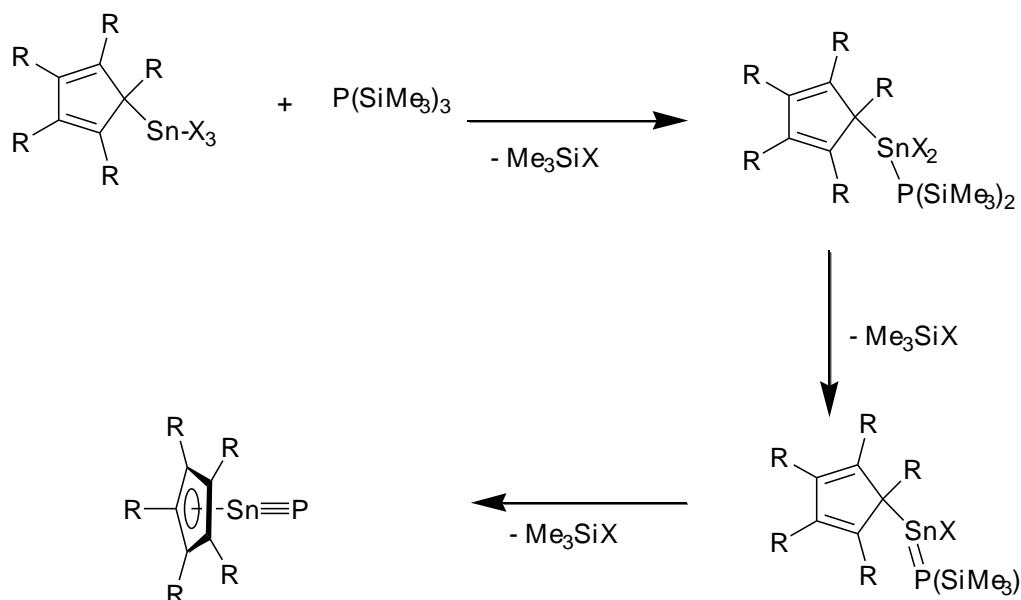


Figure 4.5: Cp bonding modes in Sn(IV) and Sn(II) complexes

Thus a route employing a CpSnX_3 and $\text{P}(\text{SiMe}_3)_3$ to afford $\text{CpSn}\{\text{P}(\text{SiMe}_3)_2\}\text{X}_2$ was proposed. Subsequent sequential elimination of two equivalents of Me_3SiX could then provide $\text{CpSn}\equiv\text{P}$. (Scheme 4.9)



Scheme 4.9: Proposed synthetic route to $\text{CpSn}\equiv\text{P}$

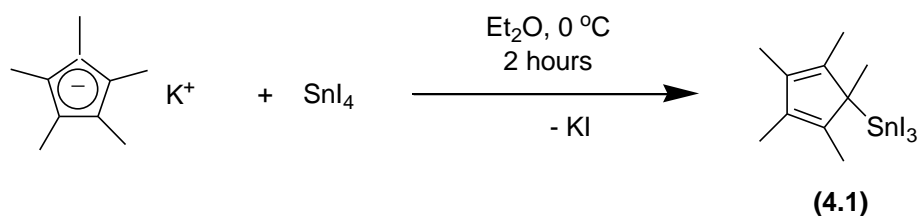
Whilst, a common method for synthesising phosphalkynes involves starting with an acylchloride and elimination of hexamethyldisiloxane, a similar route using analogous Sn reagents was thought unlikely to be successful. In addition to the weaker π -bonds being formed, the SnO bond is much stronger than the corresponding CO bond (approximately 530 and 360 kJmol^{-1} respectively),²⁵ making the elimination of siloxane far less likely.

4.2: Results and Discussion

A number of attempts were made to synthesise molecules which could potentially act as precursors to SnP multiple bonds by sequential eliminations of trimethylsilyl halides. To begin with, reactions between a variety of Sn chlorides and $\text{P}(\text{SiMe}_3)_3$ were attempted, but this invariably resulted in the formation of insoluble black/brown solids which were most likely some mixture of polymers and/or clusters. Postulating that this was caused by too rapid and uncontrolled an elimination of SiMe_3Cl , the decision was made to use iodides instead of chlorides, as they would be less reactive towards the SiMe_3 groups. To this end, attempts were made to add different Cp derivatives to Sn iodides, with varying levels of success.

Synthesis of Cp^*SnI_3 (4.1)

The first of these was the synthesis of Cp^*SnI_3 , synthesised from SnI_4 and KCp^* stirred for two hours in Et_2O at 0°C . (Scheme 4.10)



*Scheme 4.10: Synthesis of Cp^*SnI_3*

The product was crystallised as dark red needles which were used for X-ray diffraction. (Figure 4.6) This complex had previously been reported as a product of the reaction between Cp^*_2SnI and HgI_2 in benzene.²⁶

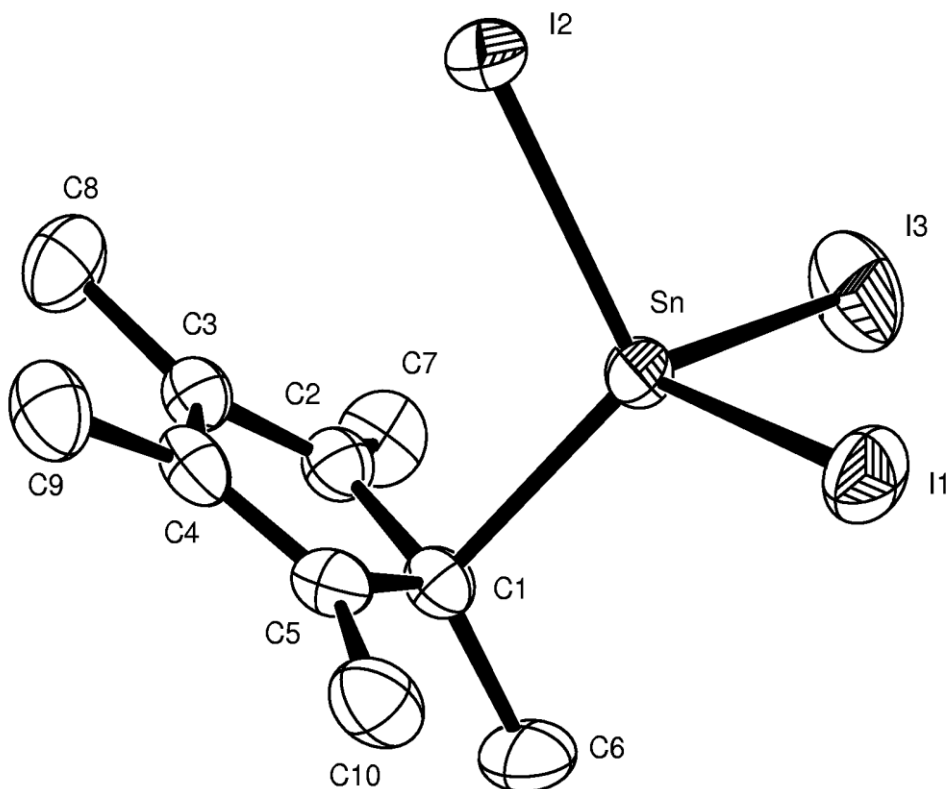


Figure 2.6: ORTEP molecular structure of Cp^*SnI_3 (H atoms omitted for clarity)

Selected Bond Lengths [\AA]	
C1-Sn	2.216(5)
C1-C2	1.494(8)
C2-C3	1.361(8)
C3-C4	1.459(8)
C4-C5	1.341(9)
C5-C1	1.500(8)
C1-C6	1.519(8)
Sn-I1	2.6986(6)
Sn-I2	2.6763(6)
Sn-I3	2.6962(6)

Selected Bond Angles [$^\circ$]	
Sn-C1-C2	96.9(4)
Sn-C1-C5	98.0(3)
Sn-C1-C6	111.0(4)
C2-C1-C5	104.6(5)
C1-C2-C3	107.9(5)
C2-C3-C4	109.1(5)
C3-C4-C5	110.3(5)
C4-C5-C1	107.9(5)
C1-Sn-I1	114.57(15)
I1-Sn-I2	105.290(19)
I2-Sn-I3	107.73(2)
I1-Sn-I3	103.77(2)

The solid state molecular structure showed that ring is bound η^1 to the Sn, with observably different C-C bond lengths representative of localised single and double bonds. The ^1H NMR spectrum showed only one resonance at δ 1.65 and with $^{117/119}\text{Sn}$

satellites with a coupling constant value of 75 Hz (the separate satellites of the different isotopes were unresolved), indicating that the position of the Sn relative to the ring is fluxional and, while the ring is still η^1 , the Sn is shifting around all five carbon atoms. (Figure 4.7)

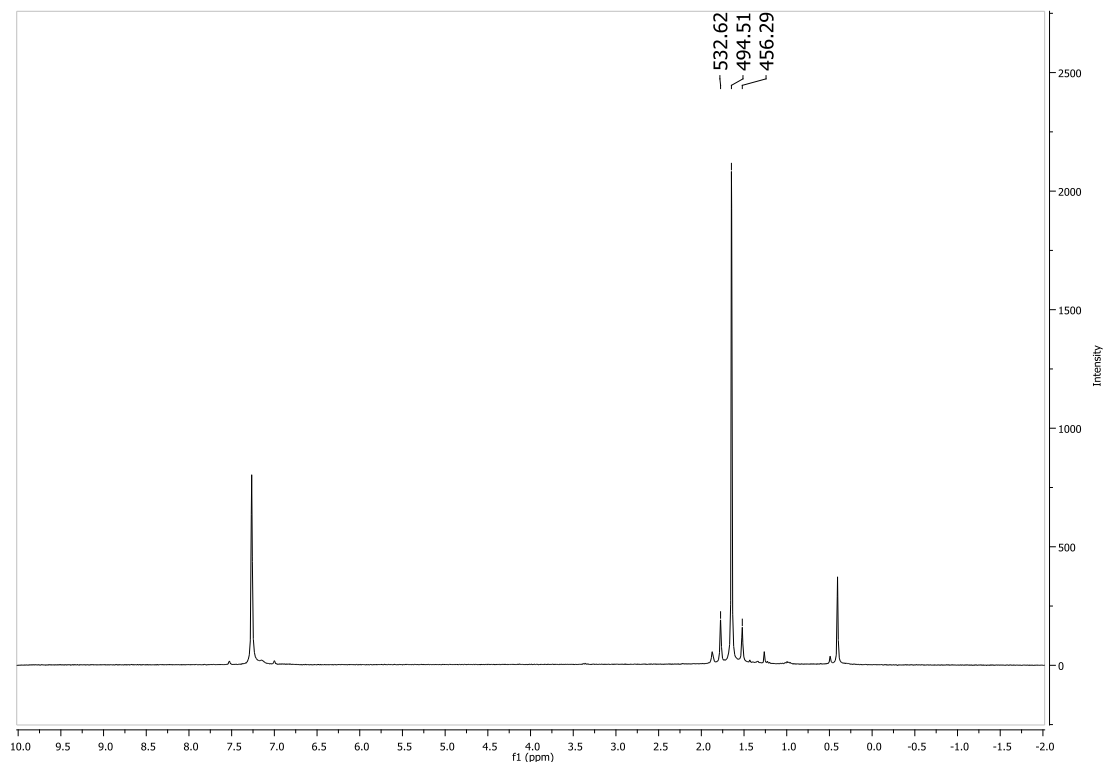


Figure 4.7: ^1H NMR spectrum of Cp^*SnI_3

Synthesis of $\text{Cp}^{\text{Me}4}_2\text{SnI}_2$ (4.2)

Following the successful synthesis of Cp^*SnI_3 , the reaction of SnI_4 with one equivalent $\text{LiCp}^{\text{Me}4}$ was performed, stirring the reagents for two hours in diethyl ether at $0\text{ }^\circ\text{C}$. In this instance, however, the result was the formation of the $\text{Cp}^{\text{Me}4}_2\text{SnI}_2$, as shown by X-ray diffraction analysis of the crystalline product. (Figure 4.8) It is unclear whether the two rings were added to the Sn from the outset or if there was a scrambling

of ligands subsequent to the initial reaction, but the Cp^{Me4} was evidently insufficiently bulky to deter the addition of a second ring.

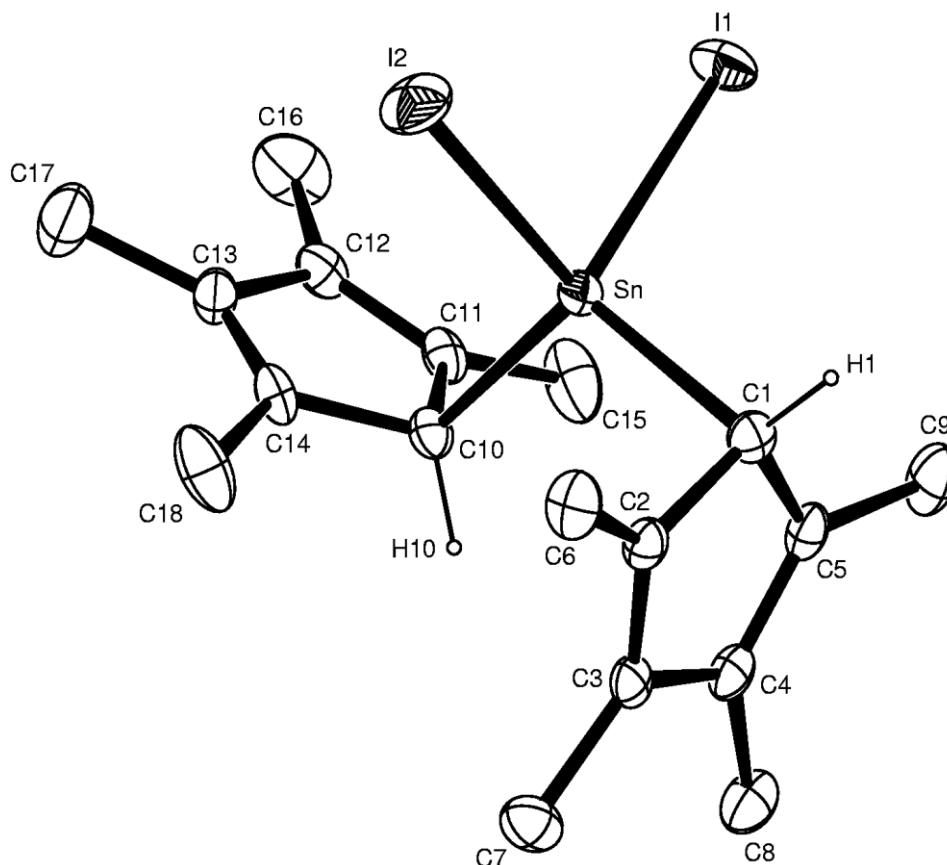


Figure 4.8: ORTEP molecular structure of $\text{Cp}^{\text{Me4}}_2\text{SnI}_2$ (H atoms omitted for clarity)

Selected Bond Lengths [\AA]	
C1-Sn	2.202(5)
C1-C2	1.473(8)
C2-C3	1.360(8)
C3-C4	1.445(8)
C4-C5	1.363(8)
C5-C1	1.479(8)
Sn-C10	2.205(5)
C10-C11	1.483(8)
C11-C12	1.347(9)
C12-C13	1.465(9)
C13-C14	1.338(9)
C14-C10	1.484(8)
Sn-I2	2.7101(6)

Selected Bond Angles [$^\circ$]	
Sn-C1-C2	98.3(4)
Sn-C1-C5	98.9(3)
C1-Sn-C10	113.6(2)
C2-C1-C5	105.5(5)
C1-C2-C3	108.1(5)
C2-C3-C4	109.0(5)
C3-C4-C5	109.8(5)
C4-C5-C1	107.3(5)
Sn-C10-C11	103.8(4)
Sn-C10-C14	104.8(4)
C14-C10-C11	104.0(5)
C1-Sn-I1	109.08(15)
C1-Sn-I2	111.22(16)

(continued overleaf)

Sn-I1	2.7170(6)
-------	-----------

C10-Sn-I1	112.01(16)
C10-Sn-I2	111.19(16)
I1-Sn-I2	98.778(19)

As in the case of Cp^*SnI_3 , the X-ray crystal structure of $\text{Cp}^{\text{Me}^4}\text{SnI}_2$ showed an η^1 coordination of the Cp^{Me^4} rings, with equivalent bond lengths and angles showing similar values between the two structures. The ^1H NMR spectrum of $\text{Cp}^{\text{Me}^4}\text{SnI}_2$ showed three resonances corresponding to the single proton on the ring and the two different Me environments. (Figure 4.9) All three resonances exhibit $^{117/119}\text{Sn}$ satellites but with widely differing values of coupling constant. (Table 4.1)

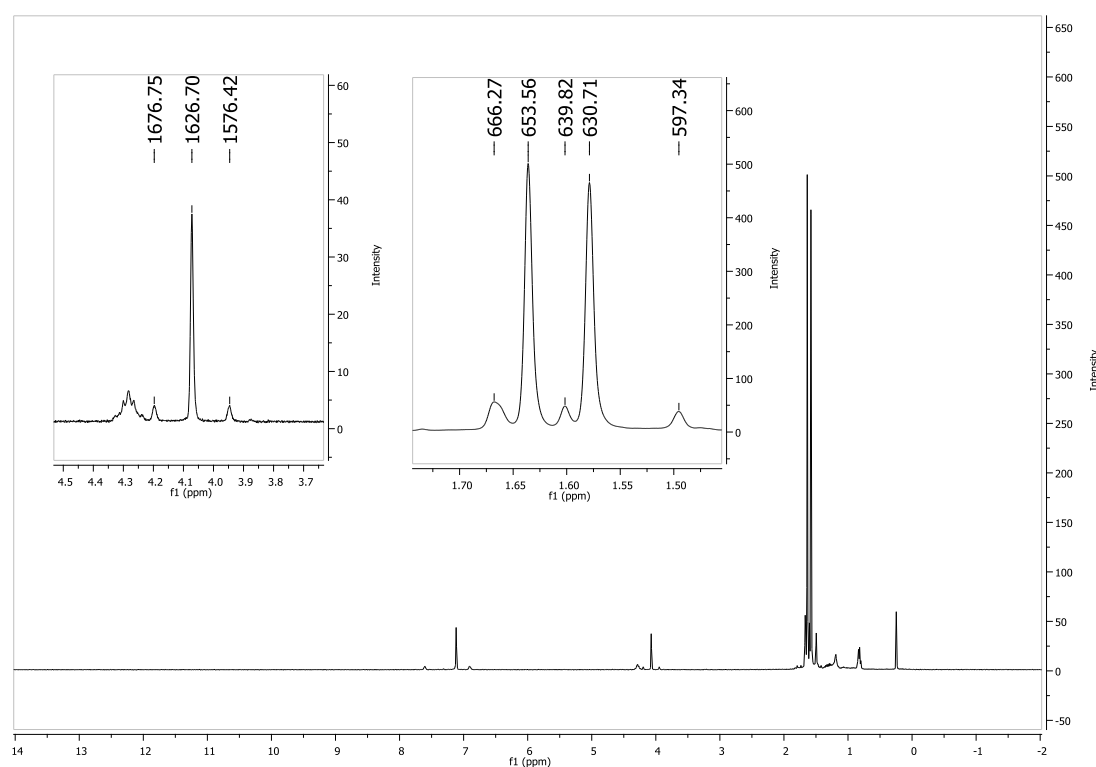


Figure 4.9: ^1H NMR spectrum of $\text{Cp}^{\text{Me}^4}\text{SnI}_2$

Chemical Shift	Relative Integral	$J^{1\text{H-Sn}}$
4.07	1	166
1.64	6	27
1.58	6	67

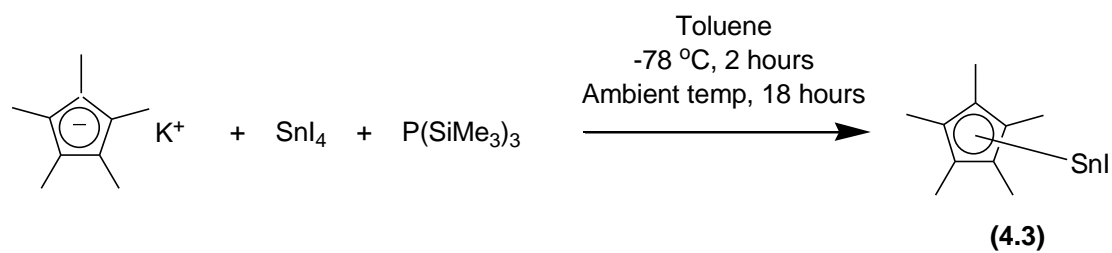
Table 4.1: ^1H NMR spectroscopic data for $\text{Cp}^{\text{Me}^4}\text{SnI}_2$

This indicated that even in solution, the Sn centre does not move evenly across all five carbons of the ring. If, as observed with Cp^* , the structure was fluxional, then an average of the positions would be seen which would result in the two Me resonances having similar values of coupling constant to the Sn centre. The reality that one of the Me resonances has a $^{117/119}\text{Sn}$ coupling constant value more than twice the magnitude of the other indicates a localisation of the Sn centre on the non-methylated C of the ring.

Reactions between SnI_4 and the alkali metal salts of bulkier Cp rings including LiCp^{S} and KCpPh_5 failed to yield any identifiable products, often just returning samples of SnI_4 . As the Cp^*SnI_3 was the only confirmed product of the desired form at this point it was used as the basis for the next stage of the process, addition of a PR_2 group.

Reaction between KCp^* , SnI_4 and $\text{P}(\text{SiMe}_3)_3$

In order to investigate the product of a one-pot synthesis, a reaction was carried out combining $\text{P}(\text{SiMe}_3)_3$, SnI_4 and KCp^* in a 1:1:1 ratio in toluene at $-78\text{ }^\circ\text{C}$ and stirring for two hours before warming to ambient temperature and stirring for a further eighteen hours. The result, however, was not the formation of a SnP bond, but instead the reduction of the Sn centre and the production of Cp^*SnI . (Scheme 4.11)



*Scheme 4.11: Synthesis of Cp*SnI*

The product was crystallised as pale yellow needles which were used for X-ray diffraction. (Figure 4.10)

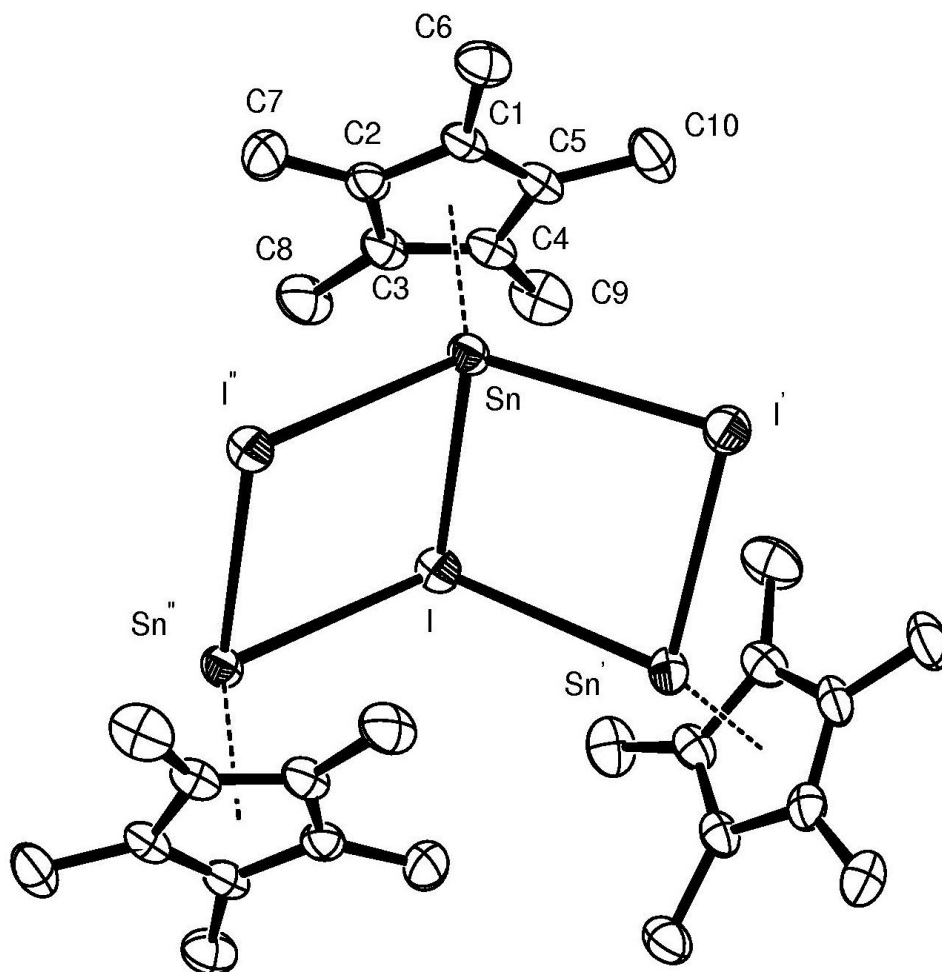


Figure 4.10: ORTEP molecular structure of $(\text{Cp}^*\text{SnI})_3$, (**4.3**) representing part of a longer $(\text{Cp}^*\text{SnI})_n$ chain (H atoms omitted for clarity)

Selected Bond Lengths [\AA]	
Sn-C1	2.653(3)
Sn-C2	2.597(3)
Sn-C3	2.473(3)
Sn-C4	2.467(3)
Sn-C5	2.577(3)
Sn-I	3.1901(3)
Sn-I'	3.4997(3)
Sn-I''	3.5622(3)

Selected Bond Angles [$^\circ$]	
I-Sn-I'	87.087(7)
I-Sn-I''	83.491(7)
I'-Sn-I'	126.929(7)
Sn-I-Sn'	90.291(7)
Sn-I-Sn''	96.509(7)
Sn''-I-Sn'	111.102(7)
I-Sn-M	117.25(7)
I'-Sn-M	113.31(7)
I''-Sn-M	117.38(7)

The X-ray diffraction analysis showed that the ring is in the η^5 position typical of Sn(II) species, albeit slightly shifted towards the C3-C4 bond, and that in the solid state the molecules form a ladder-like chain. This chain adopts what can be described as a boat form (with alternating *cis*- and *trans*- rings) rather than a chair form (with only *trans*- rings) in order to provide the maximum separation for the bulky Cp* groups. (Figure 4.11)

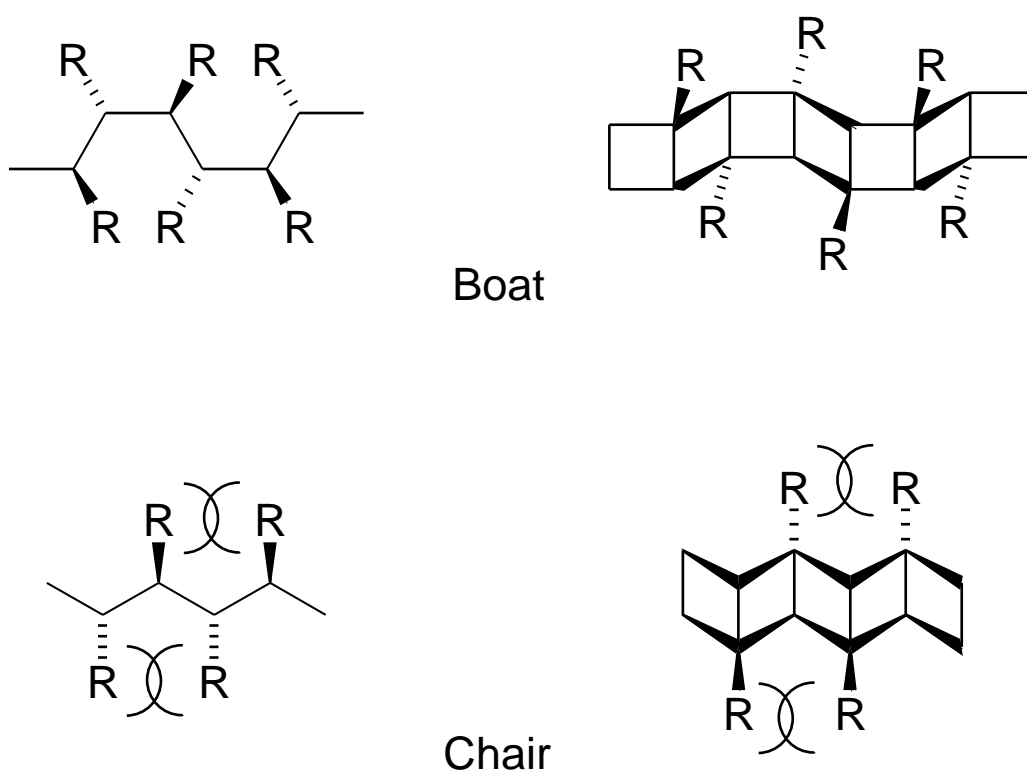
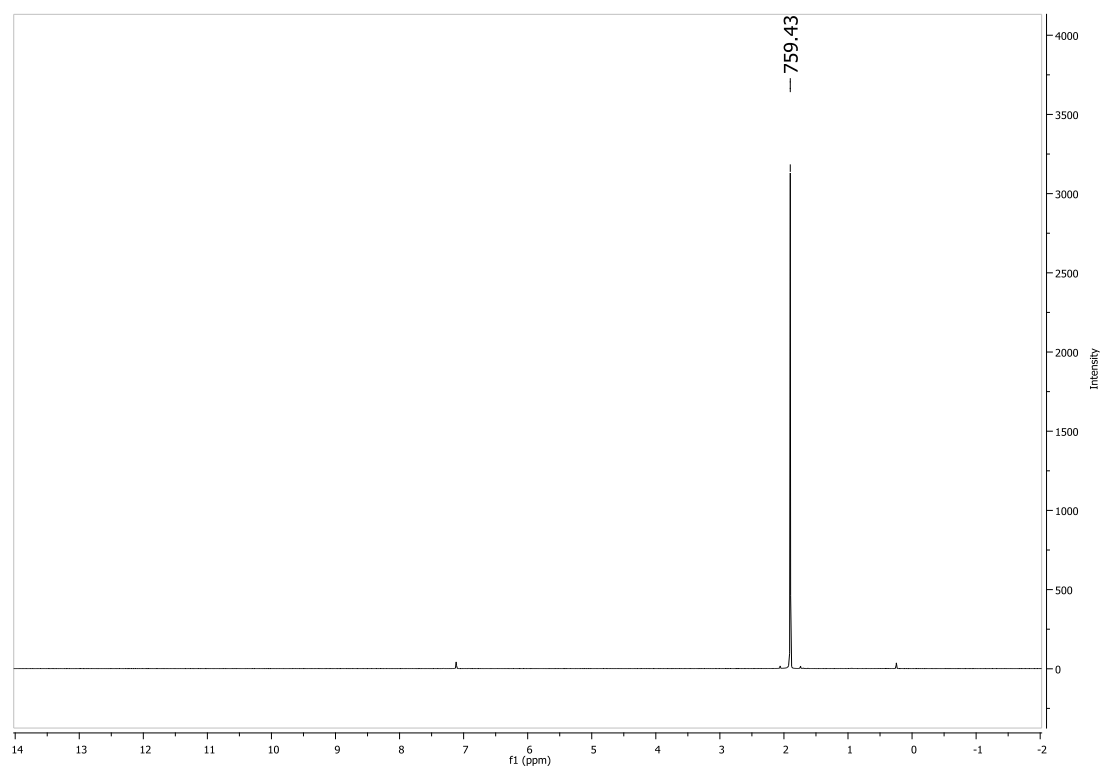


Figure 4.11: “Boat” and “Chair” arrangements of Cp*SnI (Sn and I labels omitted for clarity)

In terms of the X-ray data displayed in Figure 4.10, the Sn-I-Sn'-I' ring represents one of the *cis*- linkages (parallel to the chain) whilst the Sn-I-Sn''-I'' ring represents one of the *trans*- linkages (oblique to the chain).

The ^1H NMR spectroscopic analysis showed the expected single resonance from the five equivalent Me groups, but without any Sn satellites. (Figure 4.12)



*Figure 4.12: ^1H NMR spectrum of Cp^*SnI*

The ^{119}Sn NMR spectrum displayed just one singlet. (Figure 4.13) The chemical shift is found to be at a low frequency of δ -1537 which is in the region typical for Sn(II) compounds. The resonance was also significantly broadened with $\nu_{1/2} = 515$ Hz.

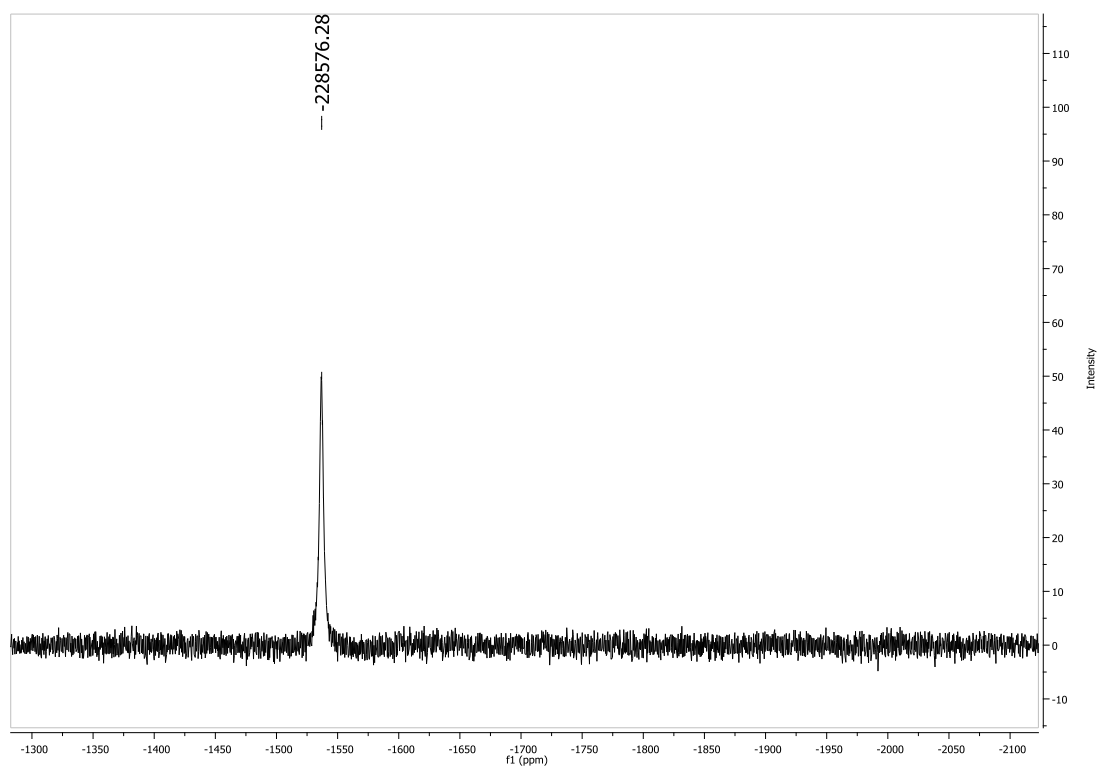
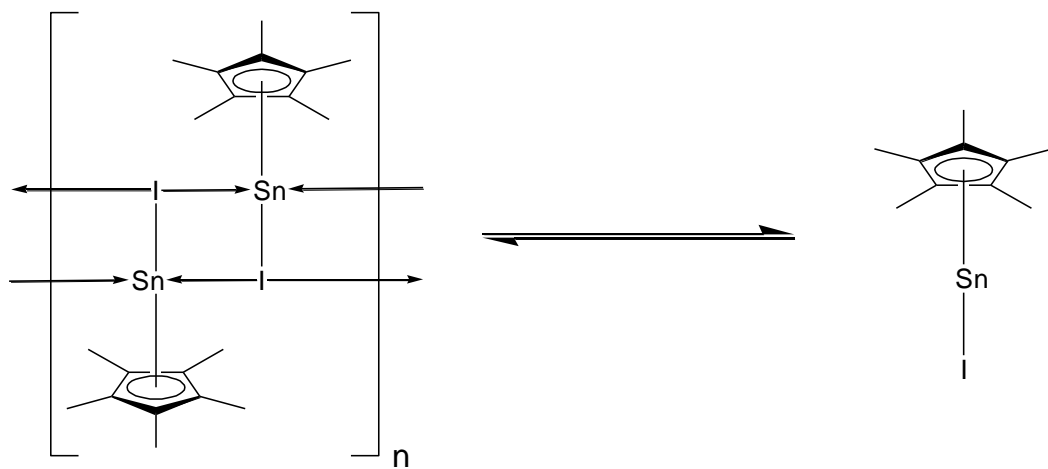


Figure 4.13: $^{119}\text{Sn}\{^1\text{H}\}$ NMR spectrum of Cp^*SnI

A possible cause for broadness may be a fluxional equilibrium process whereby the Cp^*SnI units are coordinating as shown in the crystal structure and dissociating into monomers. (Scheme 4.12)

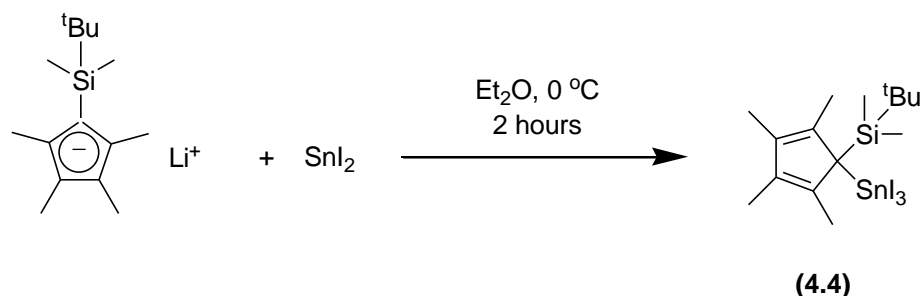


Scheme 4.12: Proposed polymer/monomer equilibrium of Cp^*SnI

Attempts to synthesise Cp^*SnI directly from KCp^* and SnI_2 only succeeded in producing Cp^*SnI_3 . From this it was concluded that the phosphine is essential in the reduction of the Sn centre and that without the presence of a reducing agent the Sn reagent will disproportionate.

Synthesis of Cp^sSnI_3 (4.4)

The formation of Cp^sSnI_3 from the SnI_2 offered a potential route to the production of bulkier Cp analogues by removing the steric hindrance of the additional iodine atoms. Using this method a reaction between lithium Cp^s and an excess of SnI_2 was performed in Et_2O at $0\text{ }^\circ\text{C}$ for two hours. The result was the formation of the Cp^sSnI_3 . (Scheme 4.12) The by-products of this reaction could not be identified.



Scheme 4.13: Synthesis of Cp^sSnI_3

This was shown by X-ray diffraction of a single, dark-red crystal. (Figure 4.14)

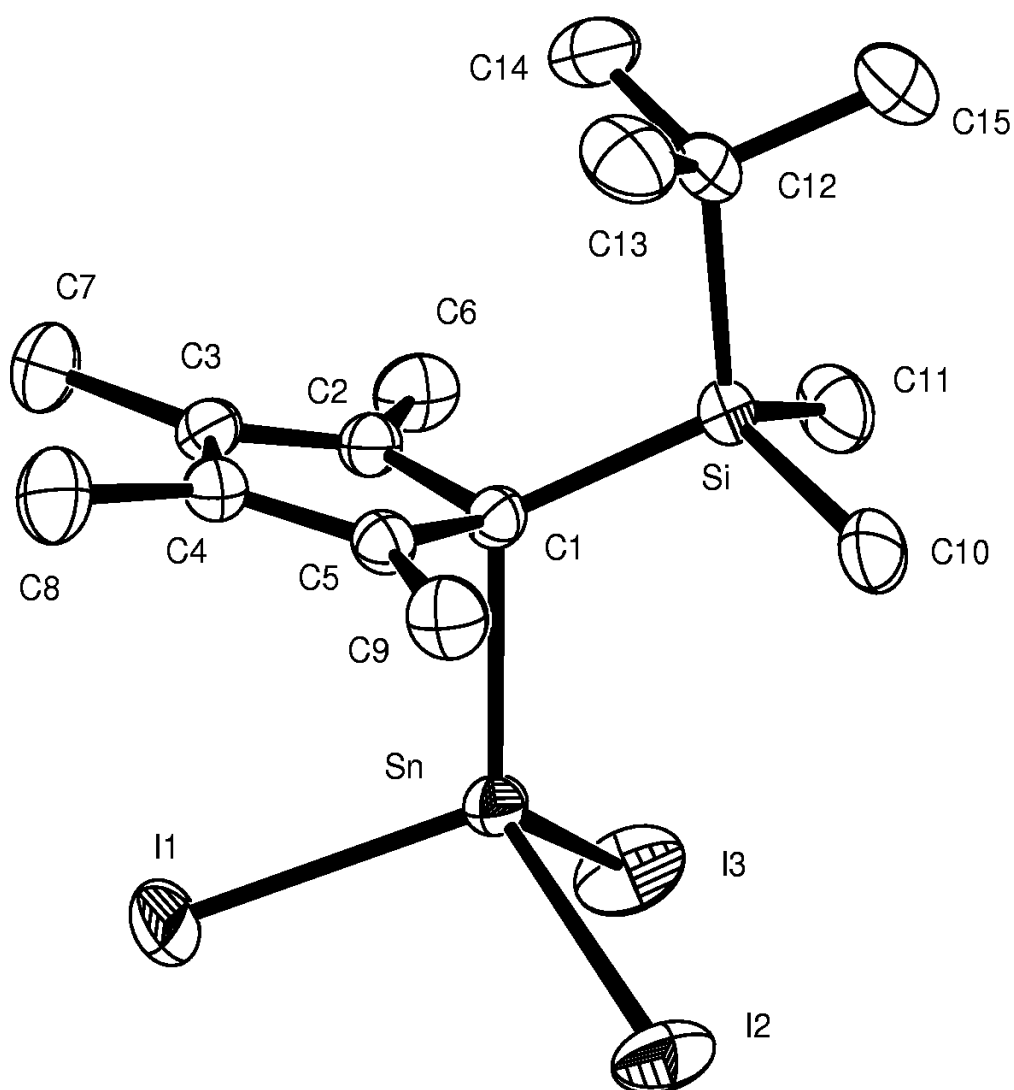


Figure 4.14: ORTEP molecular structure of $\text{Cp}^{\text{S}}\text{SnI}_3$ (H atoms omitted for clarity)

Selected Bond Lengths [\AA]	
C1-Sn	2.207(4)
C1-C2	1.505(6)
C2-C3	1.366(6)
C3-C4	1.446(7)
C4-C5	1.360(6)
C5-C1	1.509(6)
C1-Si	1.922(4)
Si-C12	1.900(5)
Sn-I1	2.6806(5)
Sn-I2	2.6956(4)
Sn-I3	2.6962(6)

Selected Bond Angles [$^\circ$]	
Sn-C1-C2	98.4(3)
Sn-C1-C5	96.9(3)
Sn-C1-Si	114.04(19)
C2-C1-C5	103.7(3)
C1-C2-C3	108.5(4)
C2-C3-C4	109.1(5)
C3-C4-C5	110.3(5)
C4-C5-C1	107.9(5)
C1-Sn-I1	108.88(11)
C1-Sn-I2	111.62(15)
C1-Sn-I3	113.18(16)
C1-Si-C12	108.92(19)

These values for the bond lengths and angles are very close to the applicable equivalents in the previous Sn(IV) examples, and again the ring is shown to coordinate in an η^1 fashion through C1. The ^1H NMR spectrum showed the four resonances associated with the Cp^{S} group, with those corresponding to the Me groups bound to the ring showing $^{117/119}\text{Sn}$ satellites. (Figure 4.15) The ^1H NMR spectroscopic data is shown in Table 4.2.

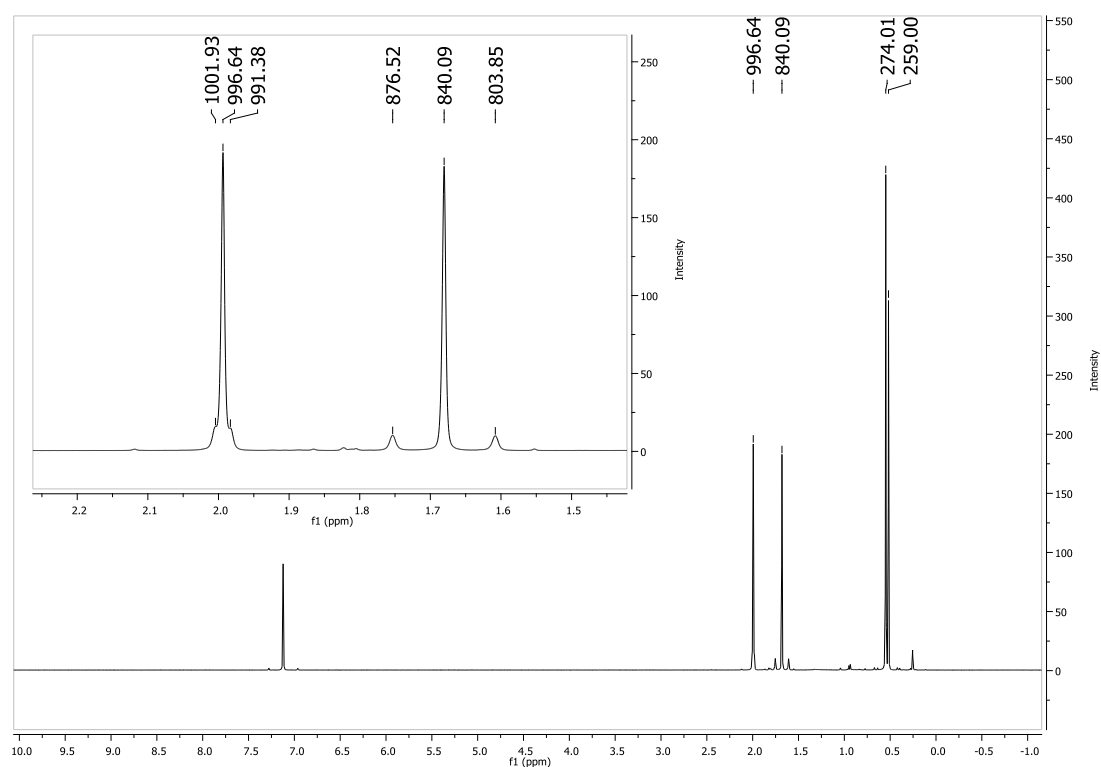


Figure 4.15: ^1H NMR spectrum of $\text{Cp}^{\text{S}}\text{SnI}_3$

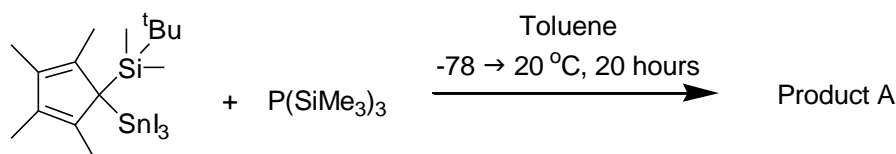
Chemical Shift	Relative Integral	J ^1H -Sn
1.99	6	11
1.68	6	73
0.55	9	-
0.52	6	-

Table 4.2: ^1H NMR spectroscopic data for $\text{Cp}^{\text{S}}\text{SnI}_3$

The $^{117/119}\text{Sn}$ satellites of the resonance at δ 1.68 displayed a far greater coupling constant value than those of the resonance at δ 1.99, which appeared only as shoulders on the main peak. As observed for $\text{Cp}^{\text{Me}_4}\text{SnI}_2$, this difference indicates that in solution the Sn centre remains localised over C1. Whilst the 4J and 5J couplings of the Sn atom to the Me groups bound to the ring were clearly visible in the ^1H NMR spectrum, no 4J and 5J couplings could be observed on the resonances of the SiMe_2^tBu group. It has been shown that long-range couplings can be strengthened by the presence of a conjugated π -electron system²⁷ such as that found in the Cp ring. In essence the conjugated system can be thought of as one elongated bond and, although the coupling interaction through π -system decreases exponentially with increasing path length, the decrease is much less than through several separate bonds the σ -bonded structures, enabling couplings over longer distances. The angle of the Sn-C bond at 77.59° from the plane of the ring indicates that it has a high degree of p-orbital character from the C atom, which would align the bonding orbital with the π -system and allow a significant interaction.²² Effectively this enables a direct, if somewhat diminished, coupling interaction between the Sn and the remote C atoms of the ring. This is proposed as the reason why there is evidence of coupling to the Me groups of the ring whilst not for the SiMe_2^tBu group through the entirely σ -bond based system.

Reaction Between $\text{Cp}^{\text{S}}\text{SnI}_3$ and $\text{P}(\text{SiMe}_3)_3$

Once synthesised, the $\text{Cp}^{\text{S}}\text{SnI}_3$ was combined in a reaction with one equivalent of $\text{P}(\text{SiMe}_3)_3$ in toluene at -78°C before warming to ambient temperature and stirring for twenty hours, resulting in a yellow solution. (Scheme 4.14)



Scheme 4.14: Reaction of $\text{Cp}^{\text{S}}\text{SnI}_3$ and $\text{P}(\text{SiMe}_3)_3$

The ^1H NMR spectroscopic data for this product shows the resonances of the Cp^{S} group with no visible $^{117/119}\text{Sn}$ satellites and no SiMe_3 resonances. The absence of any $\text{P}(\text{SiMe}_3)_2$ groups was corroborated by the ^{31}P NMR spectrum showing that the sample contained no phosphorus atoms at all. This implies that any reaction undergone by the phosphine has not resulted in the P being bound to the Sn centre, but being lost as part of a volatile molecule *in vacuo* with the solvent. When cooled to $-30\text{ }^\circ\text{C}$, the solution changed from yellow to a pale blue-green, with the blue colour becoming more predominant as the temperature was lowered further. When stored at *circa* $-80\text{ }^\circ\text{C}$ a dark blue precipitate was formed. Upon warming back to ambient temperature the yellow colour was regained. This kind of thermochromic response indicated a possible monomer-dimer (or higher oligomer) equilibrium. This data would be consistent with product A being a Sn(II) product analogous to the Cp^*SnI complex reported earlier, but as no crystals were available for X-ray diffraction there was insufficient evidence to confirm this. (Figure 4.16) The ^1H NMR spectroscopic data is collected in Table 4.3.

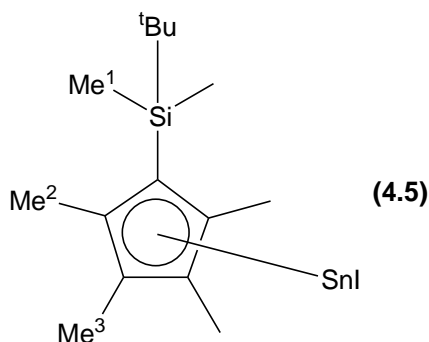


Figure 4.16: Possible molecular structure of product A (4.5)

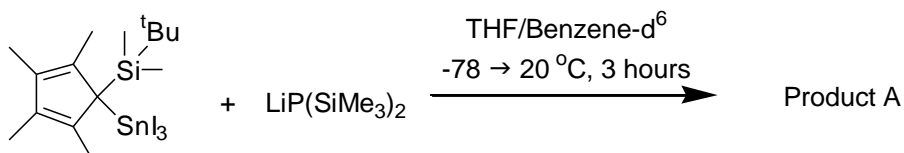
Cp ^S SnI ₃ + P(SiMe ₃) ₃ (Benzene-d ⁶)		
Chemical Shift	Relative Integral	Proposed assignment
2.01	6	Me ³
1.89	6	Me ²
0.84	9	^t Bu
0.35	6	Me ¹

Table 4.3: ¹H NMR spectroscopic data of the reaction product of Cp^SSnI₃ with P(SiMe₃)₃

Attempts were made to obtain a ¹¹⁹Sn NMR spectrum of this sample but proved unsuccessful.

Reaction Between Cp^SSnI₃ and LiP(SiMe₃)₂

The use of LiP(SiMe₃)₂ offered an alternative route to the formation of the Sn-P bond, through the elimination of LiI. LiP(SiMe₃)₂ and Cp^SSnI₃ were combined in a 1:1 ratio in an NMR tube and dissolved in a mixture of THF and benzene-d⁶ at -78 °C. Upon warming to ambient temperature the mixture was left for 3 hours, causing the colour to change from dark red to yellow.



Scheme 4.15: Reaction of Cp^SSnI₃ and LiP(SiMe₃)₂

The ¹H NMR spectrum of the product was similar to that seen in the reaction of P(SiMe₃)₃, showing resonances corresponding to the Cp^S group without any ^{117/119}Sn

satellites. (Figure 4.17) Also present were three resonances between δ 0.2 and δ -0.2 attributed to unidentified SiMe_3 groups. None of these resonances corresponded to an integer number of SiMe_3 groups when integrated against the Cp^{S} resonances and so were thought to correspond to by-products of the reaction.

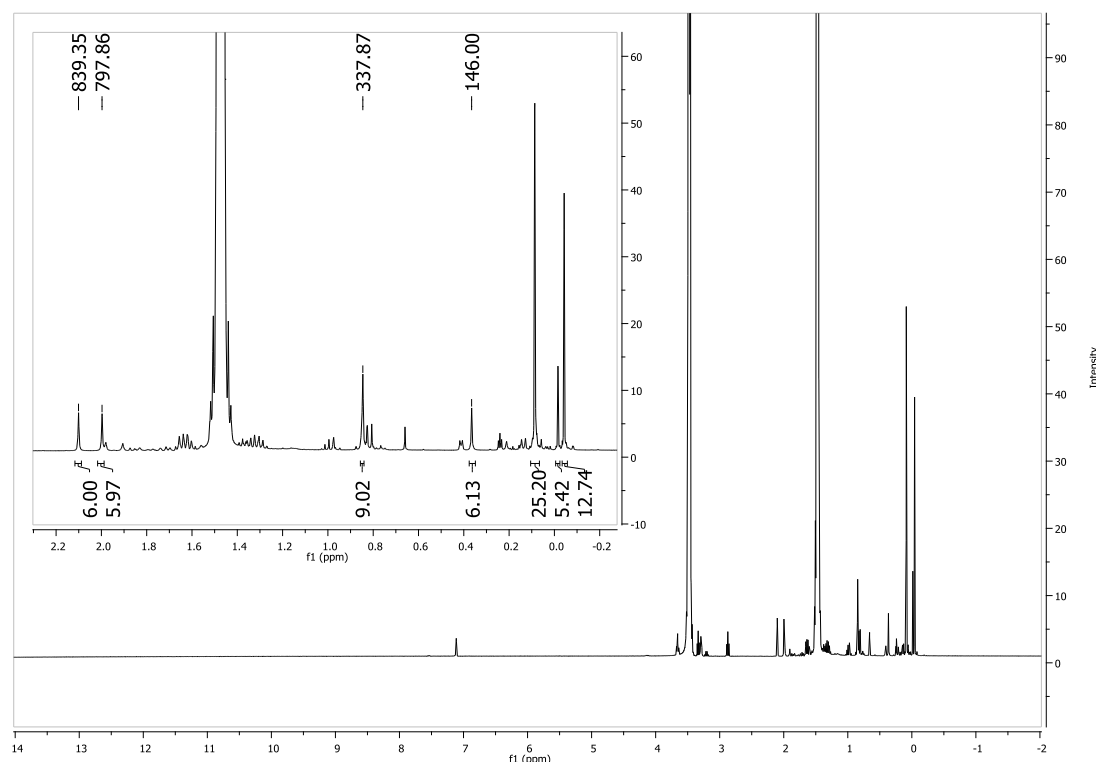


Figure 4.17: ^1H NMR spectrum of the products of the reaction of $\text{Cp}^{\text{S}}\text{SnI}_3$ and $\text{LiP}(\text{SiMe}_3)_2$

The chemical shifts of the Cp^{S} group in this reaction mixture do not match exactly with those reported from the reaction between $\text{Cp}^{\text{S}}\text{SnI}_3$ and $\text{P}(\text{SiMe}_3)_3$, but the greatest difference is only 0.11 ppm and could be due to the change in solvent. The ^1H NMR spectroscopic data for this product is outlined in Table 4.4, along with proposed assignments based on the proposed $\text{Cp}^{\text{S}}\text{SnI}$ structure depicted in Figure 4.16

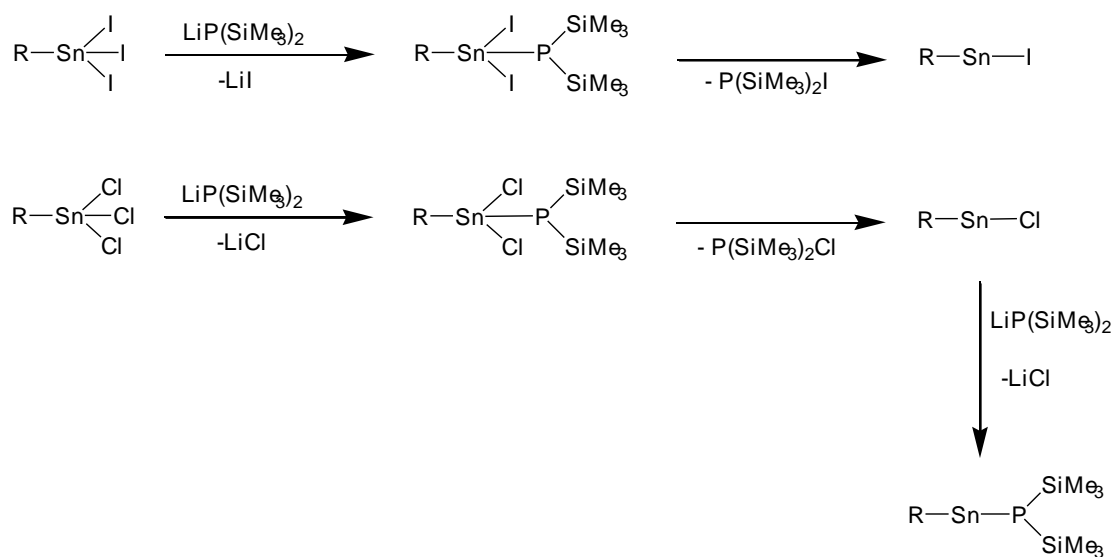
Cp ^S SnI ₃ + LiP(SiMe ₃) ₂ (THF, Benzene-d ⁶)		
Chemical Shift	Chemical Shift	Proposed assignment
2.10	6	Me ³
2.00	6	Me ²
0.85	9	^t Bu
0.37	6	Me ¹

Table 4.4: ¹H NMR spectroscopic data of the reaction product of Cp^SSnI₃ with LiP(SiMe₃)₂

A ³¹P{¹H} NMR spectrum of the reaction products displayed two singlets at δ -174 and δ -217. The identity of the compounds to which these resonances correspond was not determined, but as neither exhibited any ^{117/119}Sn satellites it was thought unlikely that the products of this reaction contained a Sn-P bond.

The similarity of the ¹H NMR spectroscopic data suggests the products of the two reactions could be the same proposed species, and the known reducing property of LiP(SiMe₃)₂²⁸ makes the formation of Cp^SSnI a distinct possibility. If the reaction with LiP(SiMe₃)₂ has formed Cp^SSnI, the mechanism is proposed to be through the formation of the SnP bond, followed by a reductive elimination of P(SiMe)₂I, although these by-products have yet to be detected.

An article detailing reactions similar to this was published earlier this year,²⁹ in which RSnCl₃ (R = 2,6-(2,4,6-ⁱPr₃C₆H₂)₂C₆H₃) was observed to undergo a reduction in a reaction with LiP(SiMe₃)₂. The result, however, was not RSnCl, but instead RSnP(SiMe₃)₂. A possible reason for this is that after an initial reduction the RSnCl was attacked by a second equivalent of LiP(SiMe₃)₂, whereas the iodides were not. (Scheme 4.16)



Scheme 4.16: Variation in reduction products of RSnX_3 species by $\text{LiP}(\text{SiMe}_3)_2$

4.3: Conclusions

The production of the Sn(II) centred Cp*SnI in the reaction between KCp*, SnI₄ and P(SiMe₃)₃ is taken as evidence of the ability of the phosphine to reduce the Sn(IV) to Sn(II). Given the fact that an oxidation from P(III) to P(V) would require the addition of two iodine atoms to the already crowded P of P(SiMe₃)₃, it is thought more probable that an initial reaction occurs in which SiMe₃I is eliminated forming a Sn-P bond, followed by a reductive elimination of P(SiMe₃)₂I, although these by-products have not been identified. A reaction such as this would be in keeping with the results reported in Chapter 2 of this work in which it was proposed that the Sn-P bond was highly susceptible to radical cleavage which, in turn, was seen to promote reductive elimination.

Conversely, it was observed that in the reactions SnI₂ with KCp* or LiCp^S, the product would be the respective alkyl tin triiodide. Although the by-products were not identified, the transfer of iodine atoms from one Sn centre to another could possibly suggest a disproportionation, also producing colloidal Sn(0).

References

1. Gier, T. E. *J. Am. Chem. Soc.*, 1961, **83**, 1769
2. Power, P. P. *Chem. Rev.* 1999, **99**, 3463 (and references therein)
3. Drago, R. S., *J. Phys. Chem.*, 1958, **62**, 353
4. Jutzi, P., *Angew. Chem. Int. Ed. Engl.*, 1975, **14**, 292
5. Regitz, M. *Chem. Rev.*, 1990, **90**, 191 (and references therein)
6. Haber, S., Le Floch, P., Mathey, F., *J. Chem. Soc., Chem. Commun.*, 1992, 1799
7. Hopkinson, M. J., Kroto, H. W., Nixon, J. F., Simmons, N. P. C., *J. Chem. Soc., Chem. Commun.*, 1976, 513
8. Guillemin, J-C., Janati, T., Guenot, P., Savignac, P., Denis, J-M., *Angew. Chem., Int. Ed. Engl.*, 1991, **30**, 196
9. Appel, R., Maier, G., Reisenhauer, H. P., Westerhaus, A., *Angew. Chem., Int. Ed. Engl.*, 1981, **20**, 197
10. Fiedler, W., Löber, O., Bergsträßer, U., Regitz, M., *Eur. J. Org. Chem.*, 1999, 363.
11. Guillemin, J-C., Janati, T., Denis, J-M., *J. Chem. Soc., Chem. Commun.*, 1992, 415
12. Becker, G., Gresser, G., Uhl, W., *Z. Naturforsch., B*, 1981, **36**, 16
13. Allspach, T., Regitz, M., Becker, G., Becker W., *Synthesis*, 1986, 31.
14. Mack, A., Pierron, E., Allspach, T., Bergsträßer, U., Regitz M., *Synthesis*, 1998, 1305
15. Märkl, G. Sejpka, H., *Angew. Chem., Int. Ed. Engl.*, 1986, **25**, 286.
16. Metail, V., Serio, A., Lasalle, L., Guillemin, JC., Pfitzner-Guillozo, G., *Organometallics*, 1995, **14**, 4732.

17. Lassalle, L., Legoupy, S., Guillemin, J.C., *Inorg. Chem.*, 1995, **34**, 5694
18. Finze, M., Bernhardt, E., Willner, H., Lehmann, C.W., *Angew. Chem., Int. Ed. Engl.*, 2004, **43**, 4160
19. Lai, C.H., Su, M.D., Chu, S.Y., *J. Phys. Chem. A*, 2002, **106**, 575
20. Hu, Y.H., Su, M.D., *Chem. Phys. Lett.*, 2003, **378**, 289
21. Stone, F. G. A., West, R., Connolly, J. W., Hoff, C., *Advances in Organometallic Chemistry*, 1981, **19**, 123
22. Davis, A. G., Housecroft, C. E., Crabtree, R. H., Mingos, D. M. P., *Comprehensive Organometallic Chemistry III*, 2007, **3**, 809
23. Gómez-Ruiz, S., Prashar, S., Fajardo, M., Antiñolo, A., Otero, A., *J. Organomet. Chem.*, 2007, **692**, 3057
24. Jutzi, P., Reumann, G., *J. Chem. Soc., Dalton Trans.*, 2000, 2237
25. Luo, Y.R., Lide, D. R., *Handbook of Chemistry and Physics*, 89TH Ed., 2008, 9-64
26. Jutzi, P.; Kohl, F. *J. Organomet. Chem.*, 1979, **164**, 141.
27. Gräfenstein, J., Tuttle, T., Cremer, D., *Phys. Chem. Chem. Phys.*, 2005, **7**, 452
28. Blake, P. C., Hey, E., Lappert, M. F., Atwood, J. L., Zhang, H., *J. Organomet. Chem.*, 1988, **353**, 307
29. Johnson, B. P., Almstätter, S., Dielmann, F., Bodensteiner, M., Scheer, M., Z. *Anorg. Allg. Chem.*, 2010, **636**, 1275

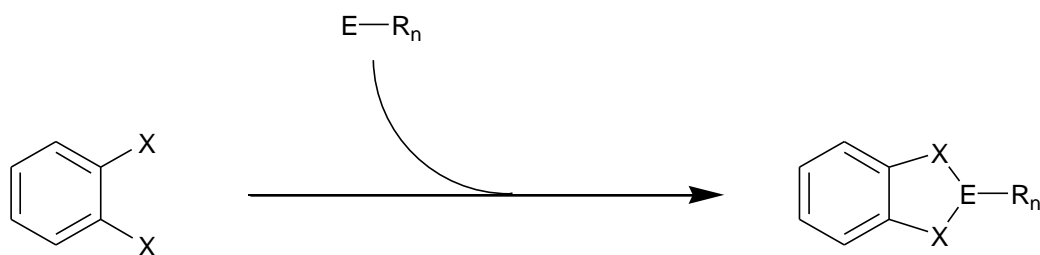
Chapter 5

Using Bis(phosphino)benzene to Produce New

Group 14 Heterocycles

5.1: Introduction

For many years now *ortho*-substituted benzene rings have been a useful reagent for the synthesis of novel heteroatomic bicyclic ring systems. The rigid ring structure holds the substituents in the plane and so provides a ready made template into which a final atom or group can be inserted to produce bicyclic ring systems.¹ (Scheme 5.1)



Scheme 5.1: Generalised formation of a heteroatomic ring system from a substituted benzene

A multitude of compounds of this form have been reported with a variety of groups in the X and E positions, as both neutral and charged species.²⁻⁴ (Figure 5.1)

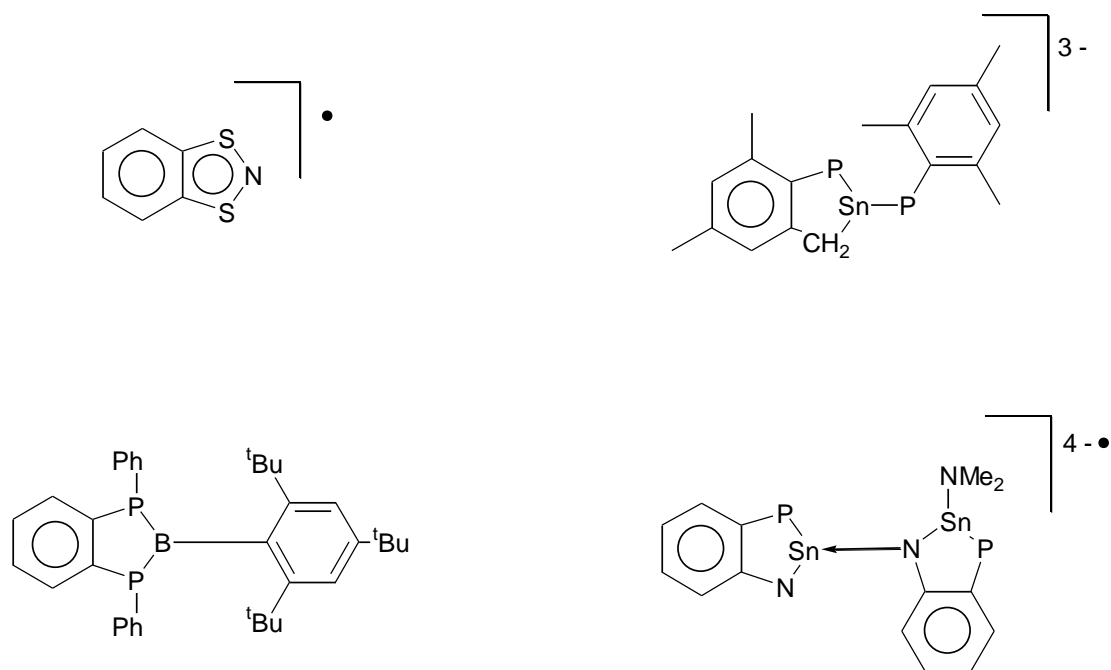


Figure 5.1: Examples of heteroatomic ring systems derived from substituted benzenes

One such species of interest is the $C_6H_4-1,2-(PH_2)_2$ molecule and its derivatives. A large amount of the early work reported with this system dealt principally with $C_6H_4-1,2-(PHLi)_2$ and its reactions with chlorides of C, P and As.¹ Several new bicyclic molecules were synthesised of the [4.3.0] fused ring form depicted in Scheme 5.1, including those with CH_2 , PMe, PEt, AsMe or AsPh moieties bound between the P atoms. (Figure 5.2)

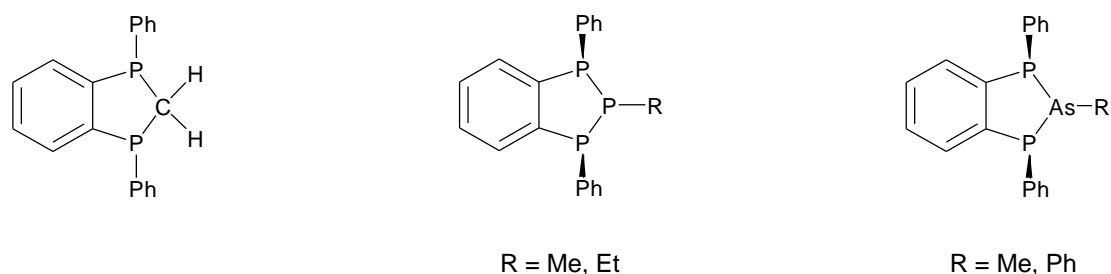
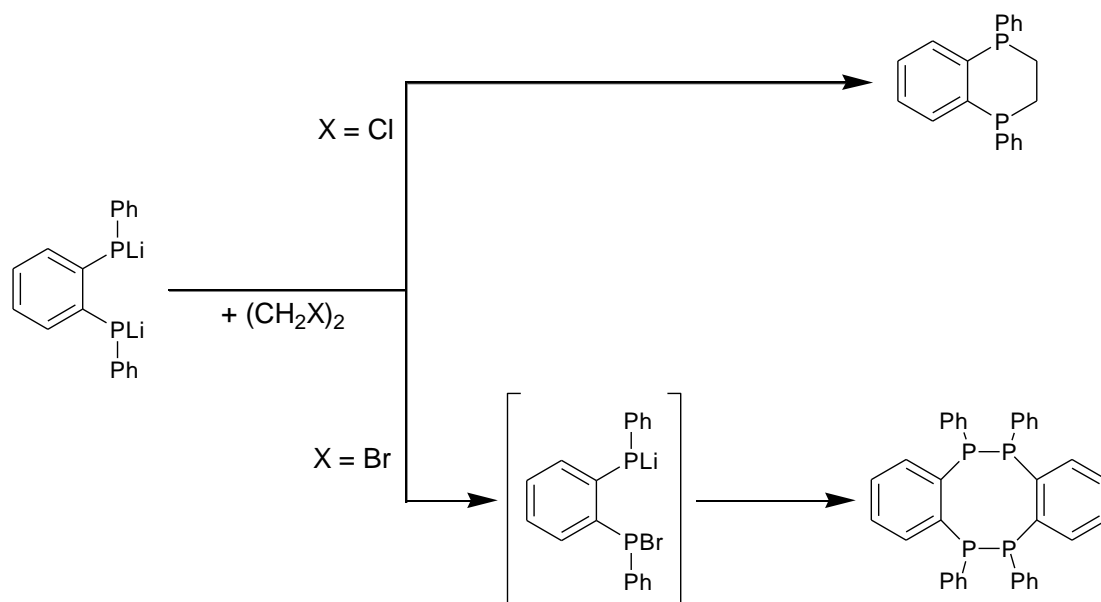


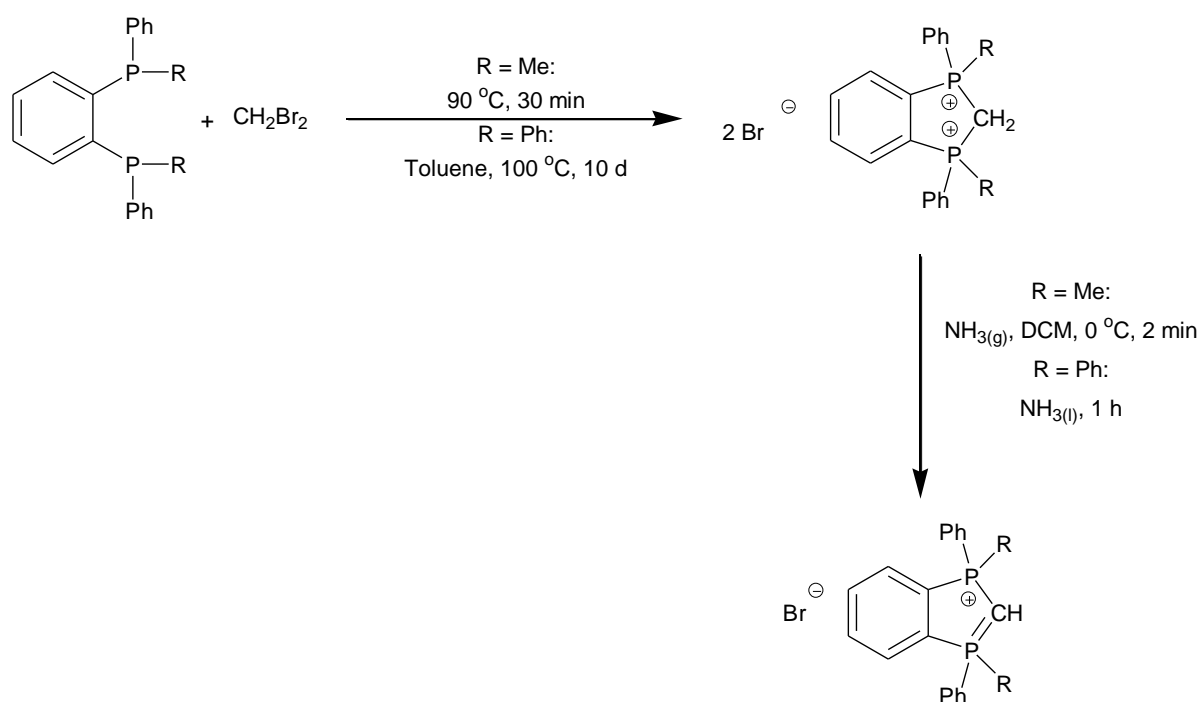
Figure 5.2: Products of early reactions using $C_6H_4-1,2-(PPhLi)_2$

The same article detailed reactions between $C_6H_4-1,2-(P^HLi)_2$ and 1,2-dihaloethanes, the results of which differed depending on the halide employed. (Scheme 5.2) The reaction with $C_2H_4Cl_2$ was shown to afford a [4.4.0] fused ring system in which the ethylene moiety bridged between the two P atoms. When the reaction was performed with $C_2H_4Br_2$, the ethylene moiety was not present in the product. Instead two of the bis(phosphino)benzene derivatives coupled to produce a new P_4C_4 ring. The mechanism for this reaction was postulated to involve a halogen exchange with the $C_2H_4Br_2$ to produce $C_6H_4-1,2-(P^HLi)(P^HBr)$ which then dimerised, eliminating two equivalents of LiBr.



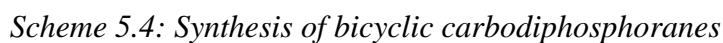
Scheme 5.2: Reactions of $C_6H_4-1,2-(P^HPhLi)_2$ and 1,2-dihaloethanes

Subsequent reports detailed reactivity other than the lithium halide eliminations. It was reported that $C_6H_4-1,2-(P^HPhMe)_2$ and $C_6H_4-1,2-(P^HPh)_2$ were used as precursors in the formation of strained carbodiphosphanes.⁵ By performing a reaction between the bisphosphine and CH_2Cl_2 a diphosponium ion was formed with the P atoms oxidised from P(III) to P(V). The dication was then deprotonated with NH_3 to generate a semi-ylide phosphonium species. (Scheme 5.3)



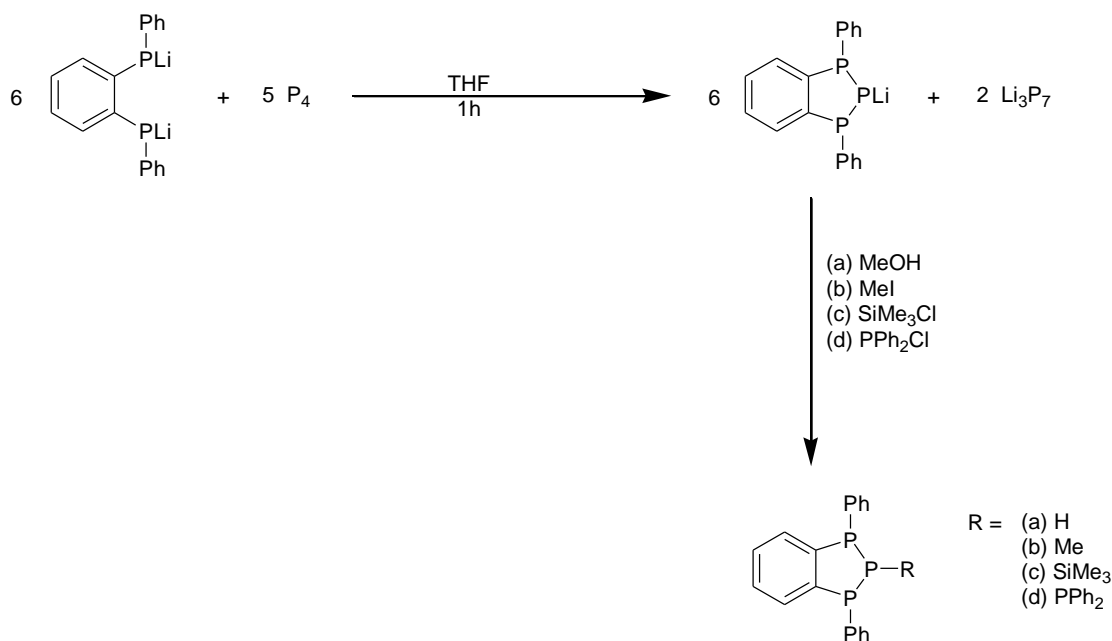
Scheme 5.3: Reactions of substituted bis(phosphino)benzenes with CH_2Br_2 and NH_3 to form semi-ylid phosphonium salts

The same reaction pathways were followed regardless of whether the second phosphine substituent is a Me or Ph group, although the conditions for the reactions of the Ph analogues were somewhat harsher. This was not the case, however, when attempting the final step to form the carbodiphosphorane. (Scheme 5.4) In the Ph substituted example, deprotonation using $\text{Et}_3\text{P}=\text{CHMe}$ in THF resulted in formation of the desired carbodiphosphorane, but when Me groups were present on the phosphines, these were deprotonated instead of the central carbon, giving rise to an asymmetrical double ylide. The Me substituted carbodiphosphorane was formed directly from the diphosponium anion by reaction $^n\text{BuLi}$ and isolated as an adduct of the LiBr by-product.


$$\text{C}_6\text{H}_4(\text{PCl}_2)_2 + \text{H}_2\text{O} \xrightarrow[\text{Et}_2\text{O}]{\Delta} \text{C}_6\text{H}_4(\text{PCl}_2)(\text{OPCl}_2)$$

Scheme 5.5: Formation of C₆H₄-1,2-(PCL)₂O

Further reports showed that $C_6H_4-1,2-(P^H Li)_2$ could be employed to instigate a disproportionation of white phosphorus by removing P^+ and affording P_7^{3-} .⁷ The product of this reaction was a benzotriphosphole anion which was then treated with a number of different nucleophiles. (Scheme 5.6)



Scheme 5.6: Reaction of $C_6H_4-1,2-(P^H Li)_2$ with P_4

More recently research has returned to focus on the Li salts of bis(phosphino)benzene derivatives and their reactions with main group chlorides. $C_6H_4-1,2-(PH_2)_2$ can be deprotonated by anywhere from one to all four protons (with the alkylated phosphines being deprotonated as far as they are able) to potentially give a variety of reagents tailored towards different products. (Figure 5.3)

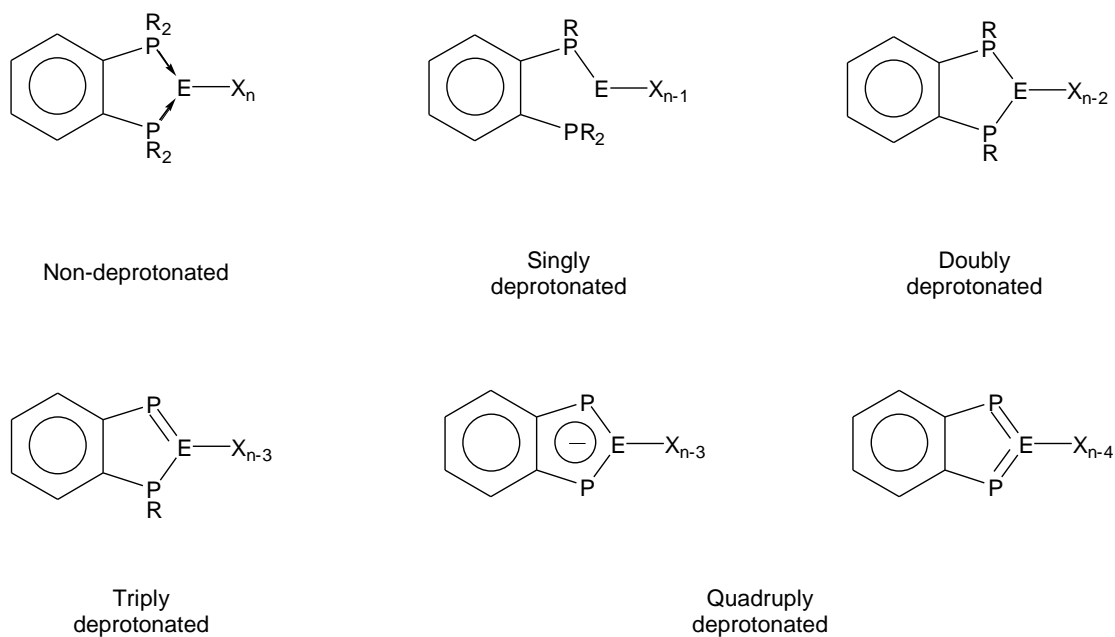
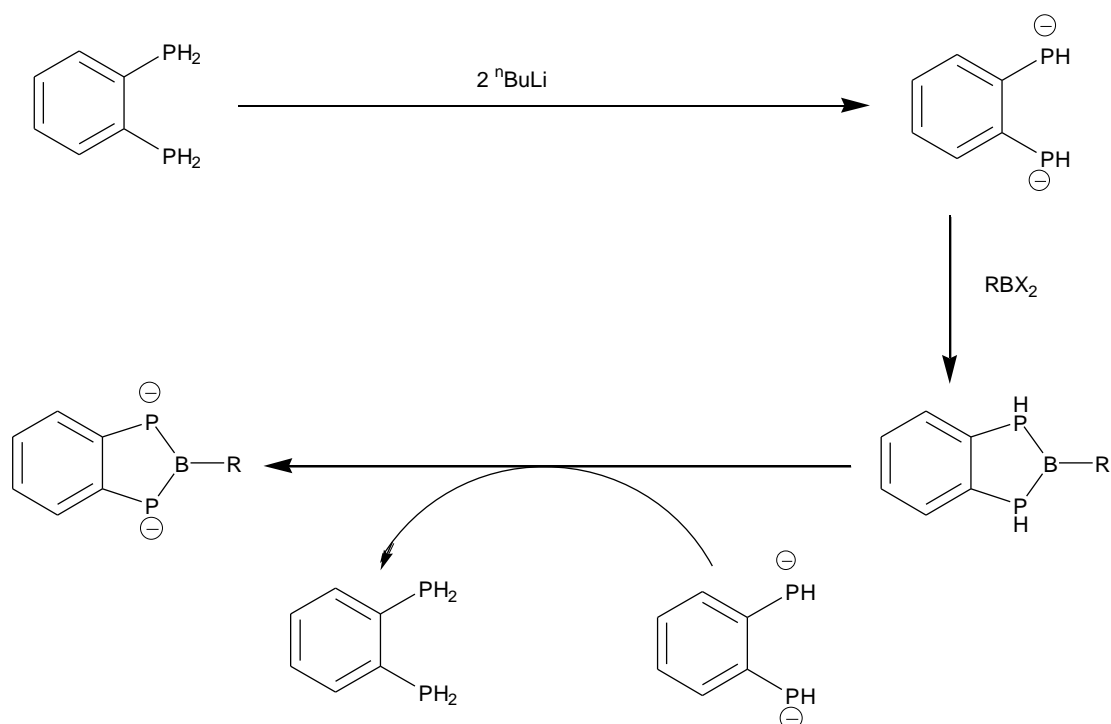


Figure 5.3: Products of increasingly deprotonated $C_6H_4-1,2-(PH_2)_2$

All of these structures have been observed with main group elements.^{3,5,8-11}

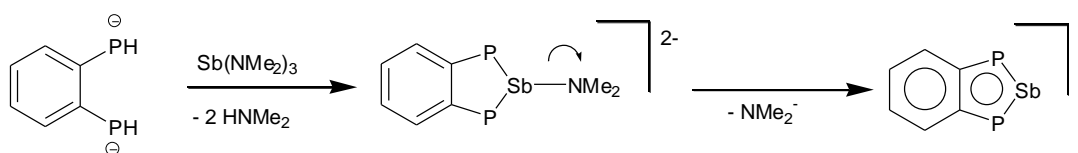
Although $C_6H_4-1,2-(PH_2)_2$ can be converted entirely to $C_6H_4-1,2-(PHLi)_2$ using two equivalents of nBuLi , it has been reported that in the reaction between $C_6H_4-1,2-(PHLi)_2$ and $BRCI_2$, the desired benzodiphosphaborolane once formed was further deprotonated by remaining unreacted $C_6H_4-1,2-(PHLi)_2$. (Scheme 5.7) The result was the regeneration of $C_6H_4-1,2-(PH_2)_2$ and the production of a new dilithiated benzodiphosphaborolane.³



Scheme 5.7: Regeneration of bis(phosphino)benzene during the reaction between C_6H_4 -1,2-($PHLi$)₂ and an alkyl boron dihalide

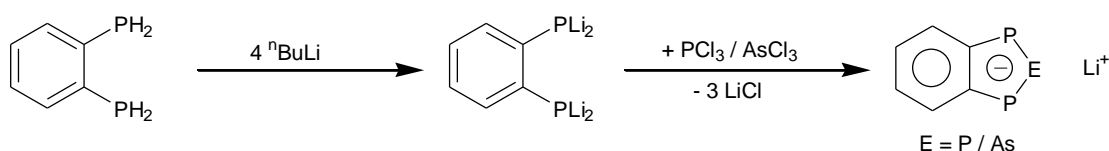
The formation of this side product was suppressed by adding the lithium salt slowly to the dihalide, thus ensuring that the latter was always in excess.

Phosphorus has been shown to act as a ready substitute for a CH group and as such has already found use in a number of aromatic molecules,¹² making C_6H_4 -1,2-(PH_2)₂ a useful starting material in the formation of [4.3.0] heteroatomic aromatic systems and in recent years a number of such compounds have been produced. A reaction has been reported between C_6H_4 -1,2-($PHLi$)₂ and $Sb(NMe_2)_3$ which afforded the aromatic $C_6H_4P_2Sb^-$ anion.¹³ (Scheme 5.8) During the reaction two equivalents of $NHMe_2$ are eliminated to form the C_2P_2Sb cycle, followed by the loss of a final NMe_2^- which enables the aromaticity.



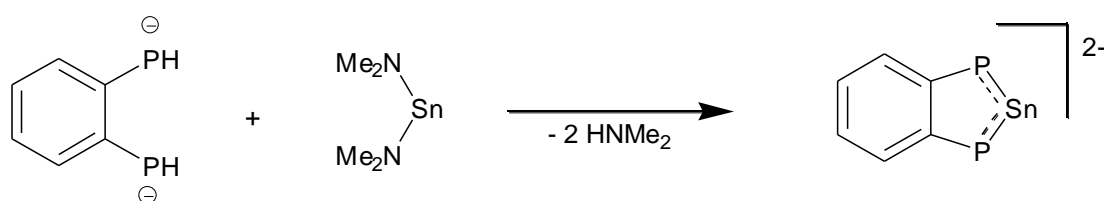
Scheme 5.8: Formation of an aromatic C_6H_4 -1,2- P_2Sb anion

The synthesis of the analogous P and As compounds has also been reported.¹⁴ In these reactions C_6H_4 -1,2- P_2^{4+} was combined with PCl_3 or $AsCl_3$, eliminating three equivalents of LiCl and affording the aromatic system. (Scheme 5.9)



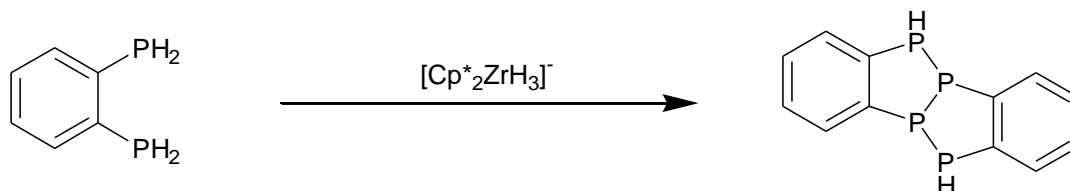
Scheme 5.9: Formation of aromatic systems containing P and As

To date none of the heavy group 14 elements have been reported as forming an equivalent aromatic structure, although a similar structure has been produced incorporating a Sn centre. In an analogous procedure to that used in the production of the Sb species depicted in Figure 5.8, C_6H_4 -1,2-(PHLi)₂ underwent a reaction with $Sn(NMe_2)_2$ to produce a compound with the formula $C_6H_4P_2Sn^{2-}$.¹⁵ (Scheme 5.10) Whilst this product does possess 10 π -electrons across the molecule, it appears to be closer to an Arduengo carbene than a fully delocalised aromatic system.



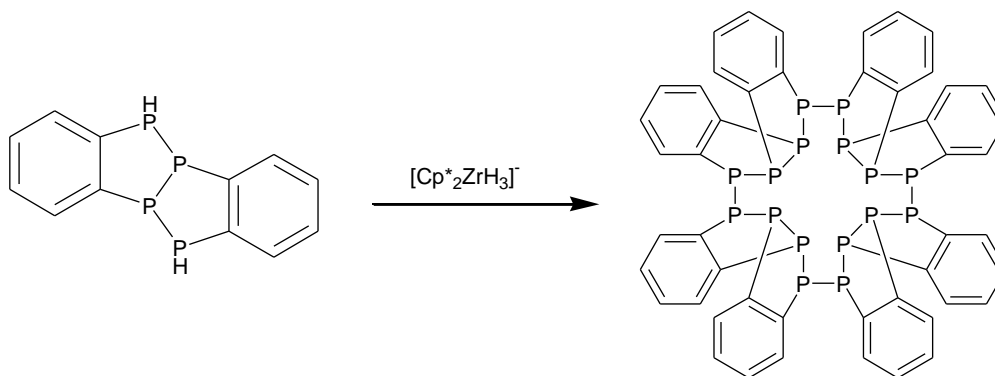
Scheme 5.10: Formation of a Sn-P Arduengo carbene analogue

In the reaction between 20 equivalents of $\text{C}_6\text{H}_4\text{-1,2-(PH}_2)_2$ and $[\text{Cp}^*_2\text{ZrH}_3][\text{K}(\text{THF})_2]$ in a mixture of toluene and THF at 90 °C for 12 hours, the initial product formed within the first 30 minutes is a dehydrogenated dimer of $\text{C}_6\text{H}_4\text{-1,2-(PH}_2)_2$ bonding *via* the P atoms.¹⁶ (Scheme 5.11)



Scheme 5.11: Reductive coupling of bis(phosphino)benzene

Over the following hours these dimers themselves are subject to further dehydrocouplings resulting in an overall cyclic octomer of $\text{C}_6\text{H}_4\text{-1,2-P}_2$. (Scheme 5.12)



Scheme 5.12: Formation of the $\text{C}_6\text{H}_4\text{-1,2-P}_2$ octomer

5.2: Results and Discussion

Initial attempts to create a C_2P_2Sn ring system from $C_6H_4-1,2-(PH_2)_2$ were unsuccessful. A wide variety of reagents and reaction conditions were employed, but the vast majority afforded the known, coupled bis(phosphino)benzene compound depicted in Scheme 5.11,¹⁶ as was evident from the ^{31}P NMR spectra. (Figure 5.4)

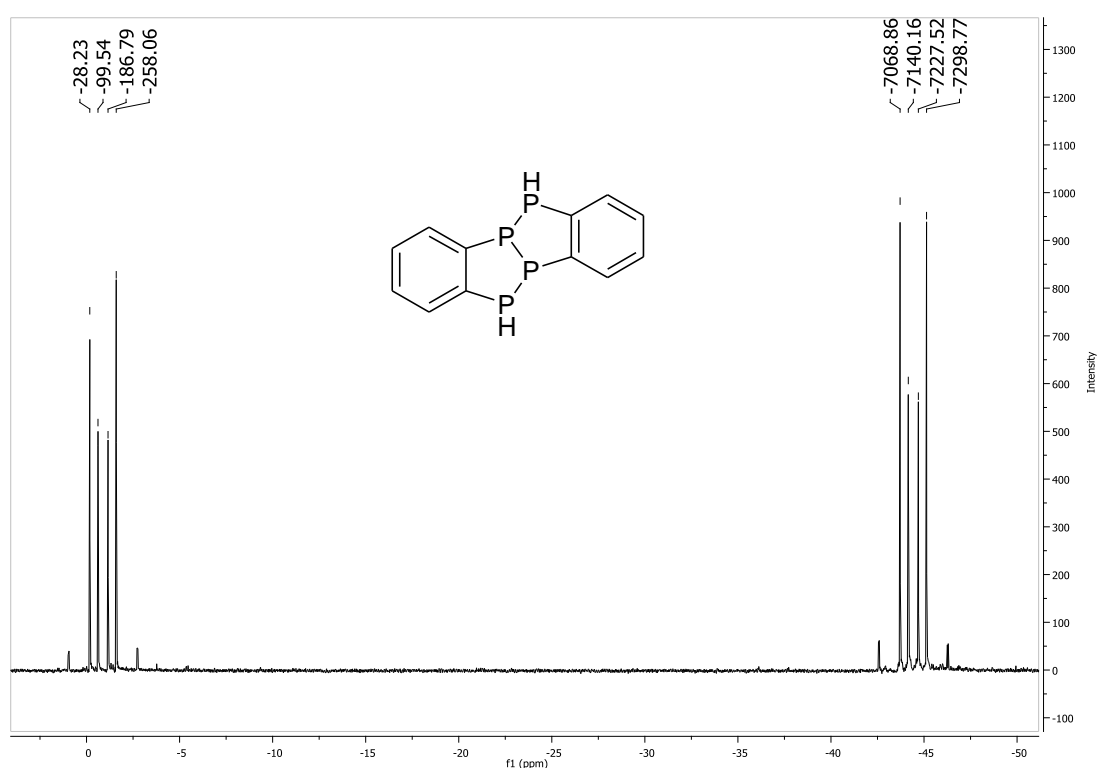
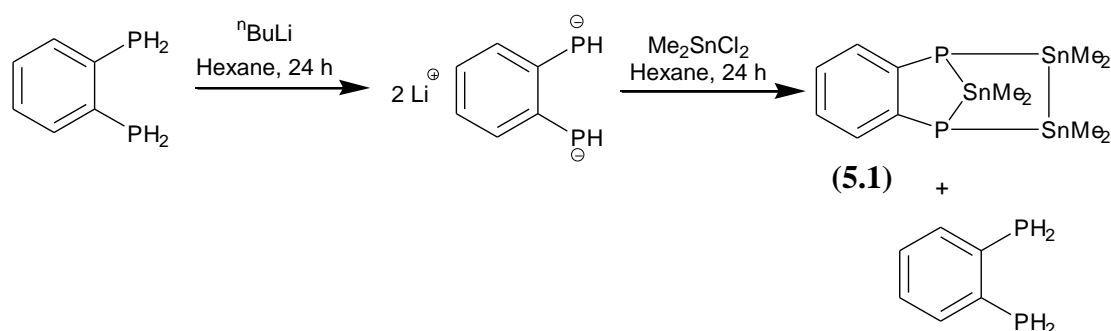


Figure 5.4: $^{31}P\{^1H\}$ NMR spectrum of the coupled bis(phosphino)benzene

This was the result of all reactions involving alkyl tin trihalides or those performed in THF, but many different combinations of solvents, substituents and temperatures resulted in the same product.

Synthesis of $C_6H_4-1,2-P_2(\mu-SnMe_2)(\mu^2-Sn_2Me_4)$ (5.1)

A sample of $C_6H_4-1,2-(PH_2)_2$ was combined with two equivalents of $nBuLi$ in hexane at ambient temperature and stirred for twenty four hours, generating a bright yellow precipitate. One equivalent of Me_2SnCl_2 was then added as a solution in hexane and the mixture stirred for a further twenty four hours, forming a white precipitate. (Scheme 5.13)



Scheme 5.13: Synthesis of $C_6H_4-1,2-P_2(\mu-SnMe_2)(\mu^2-Sn_2Me_4)$

The product of this reaction displayed a singlet resonance in the $^{31}P\{^1H\}$ NMR spectrum at δ -158.2 along side that of $C_6H_4-1,2-(PH_2)_2$ at δ 125. (Figure 5.5) A minor side product was also visible at δ -139 which will be fully discussed later. The $^{31}P\{^1H\}$ and $^{119}Sn\{^1H\}$ NMR spectroscopic data for both products is compared in Table 5.1.

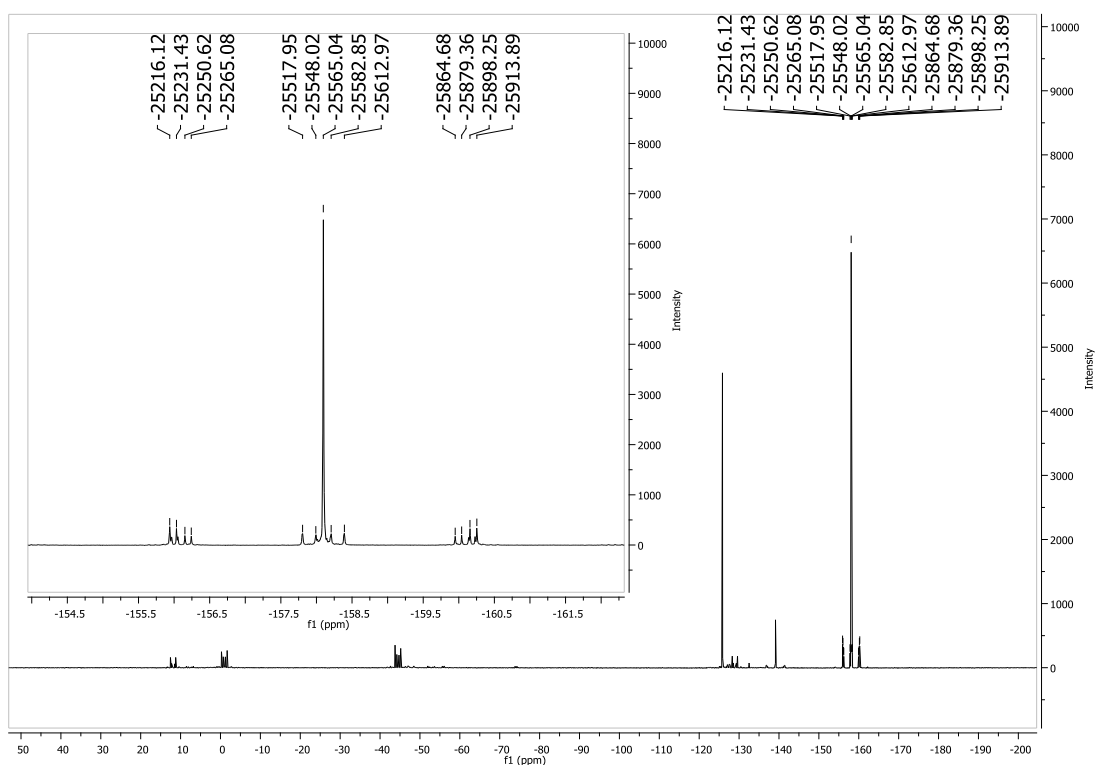


Figure 5.5: $^{31}\text{P}\{^1\text{H}\}$ NMR spectrum of the reaction products of $\text{C}_6\text{H}_4\text{-1,2-(PHLi)}_2$ and Me_2SnCl_2

Product	Sn^{i}			Sn^{ii}				^{31}P δ
	δ	Relative Integral	$J^{31}\text{P-}^{119}\text{Sn}$ /Hz	δ	Relative Integral	$J^{31}\text{P-}^{119}\text{Sn}$ /Hz	$J^{119}\text{Sn-}^{117}\text{Sn}$ /Hz	
$\text{C}_6\text{H}_4\text{-1,2-P}_2(\mu\text{-SnMe}_2)(\mu^2\text{-Sn}_2\text{Me}_4)$	126	1	698	-55	2	659 66	2724	-158.2
Side product	58	0.06	750	-78	0.12	707 7	-	-139.1

Table 5.1: NMR spectroscopic data for $\text{C}_6\text{H}_4\text{-1,2-P}_2(\mu\text{-SnMe}_2)(\mu^2\text{-Sn}_2\text{Me}_4)$ and side product

The resonance for $\text{C}_6\text{H}_4\text{-1,2-P}_2(\mu\text{-SnMe}_2)(\mu^2\text{-Sn}_2\text{Me}_4)$ was a singlet in the ^{31}P NMR spectrum, (Figure 5.6) indicating that whilst the P atoms of the $\text{C}_6\text{H}_4\text{-1,2-(PHLi)}_2$ precursor were protonated, this was no longer the case.

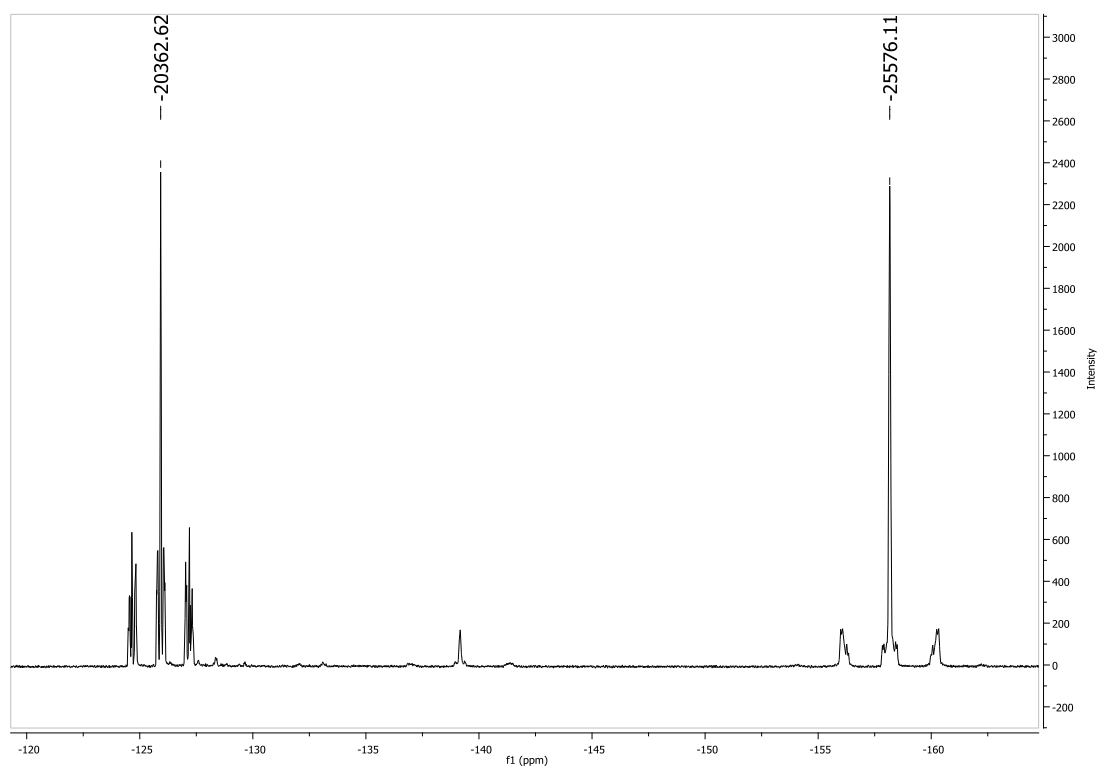


Figure 5.6: ^{31}P NMR spectrum of reaction products of $\text{C}_6\text{H}_4\text{-1,2-(PHTLi)}_2$ and Me_2SnCl_2

Further inspection of the $^{31}\text{P}\{^1\text{H}\}$ NMR spectrum revealed the presence of $^{117}\text{Sn}/^{119}\text{Sn}$ satellites. There were, in total, three sets of $^{117}\text{Sn}/^{119}\text{Sn}$ satellites, all with some 2nd order complexity. The presence of three Sn centres was corroborated by the $^{119}\text{Sn}\{^1\text{H}\}$ NMR spectroscopic data which showed two resonances, at δ 126 and -55, in a 1:2 ratio. (Figures 5.7 and 5.8)

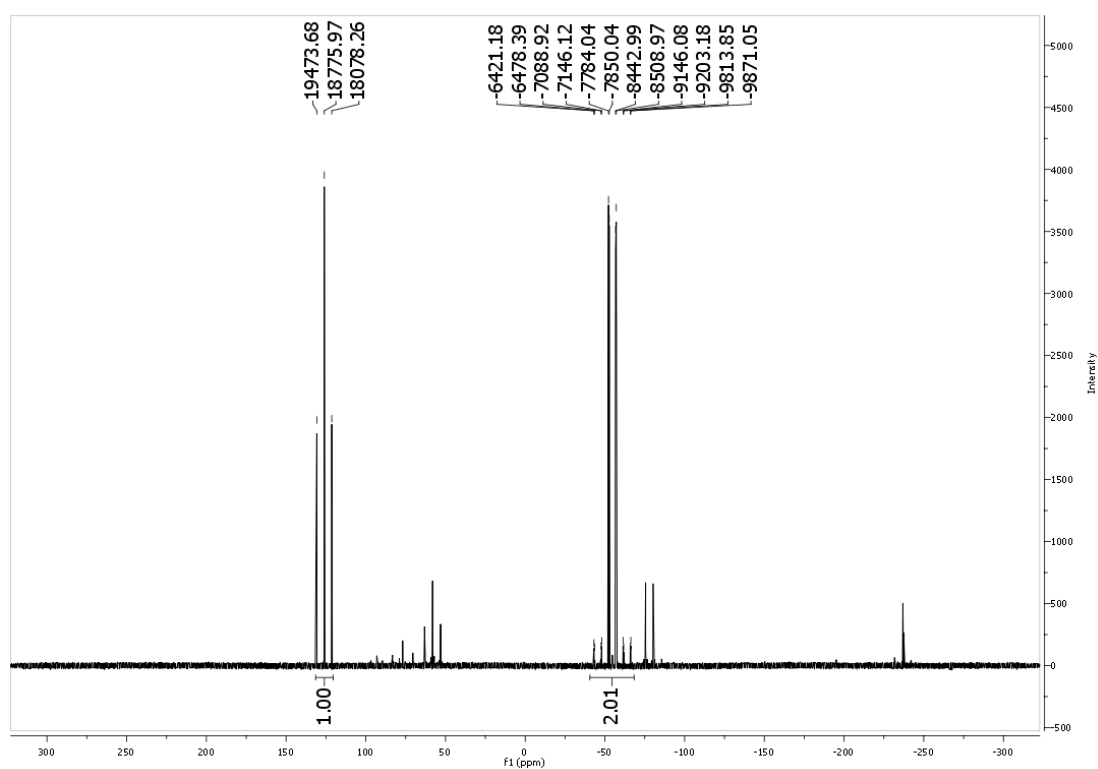


Figure 5.7: $^{119}\text{Sn}\{^1\text{H}\}$ NMR spectrum of reaction products of $\text{C}_6\text{H}_4\text{-1,2-(PHTi)}_2$ and Me_2SnCl_2

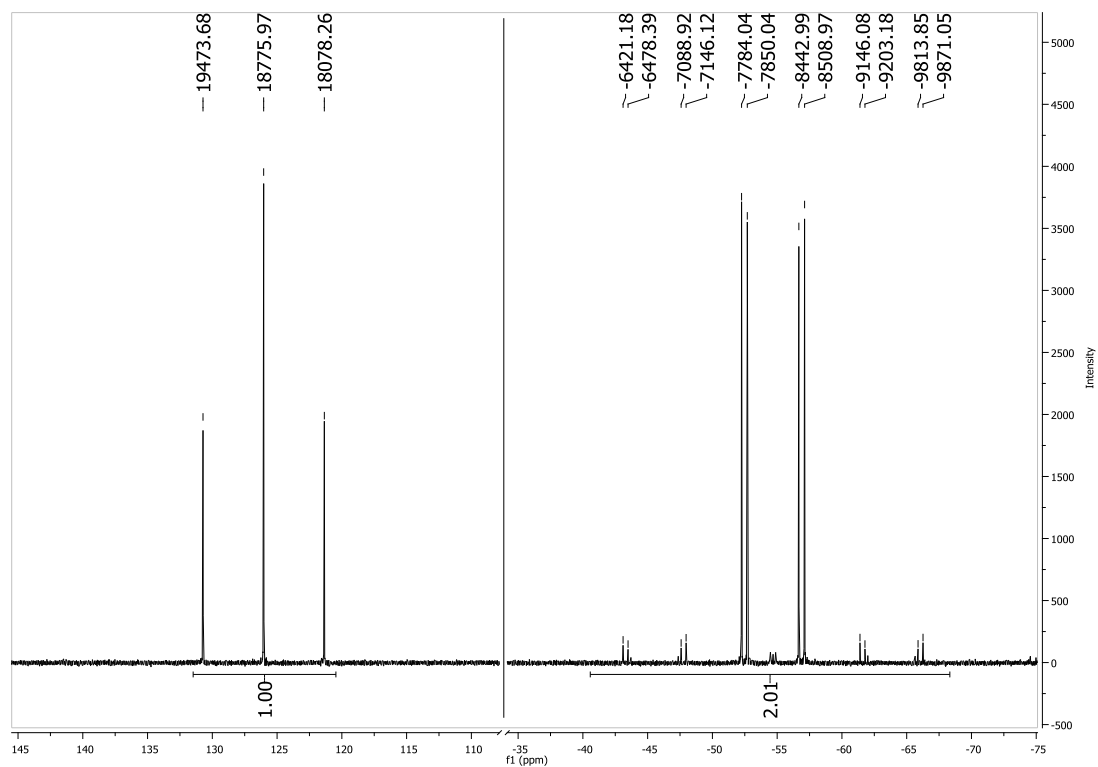


Figure 5.8: Expansion of $^{119}\text{Sn}\{^1\text{H}\}$ NMR spectrum of major reaction product of $\text{C}_6\text{H}_4\text{-1,2-(PHTi)}_2$ and Me_2SnCl_2

The $^{119}\text{Sn}\{^1\text{H}\}$ NMR spectroscopic data also provided a clearer view of the coupling constants to the P atoms. The higher frequency resonance appeared as a triplet with a coupling constant value of 698 Hz, The lower frequency resonance was a doublet of doublets, with a large coupling constant value of 659 Hz and a small coupling constant value of 66 Hz, and showed ^{117}Sn satellites with a coupling constant value of 2724 Hz. Subsequent single-crystal, X-ray diffraction data, showed the product to be $\text{C}_6\text{H}_4\text{-1,2-P}_2(\mu\text{-SnMe}_2)(\mu^2\text{-Sn}_2\text{Me}_4)$. (Figure 5.9)

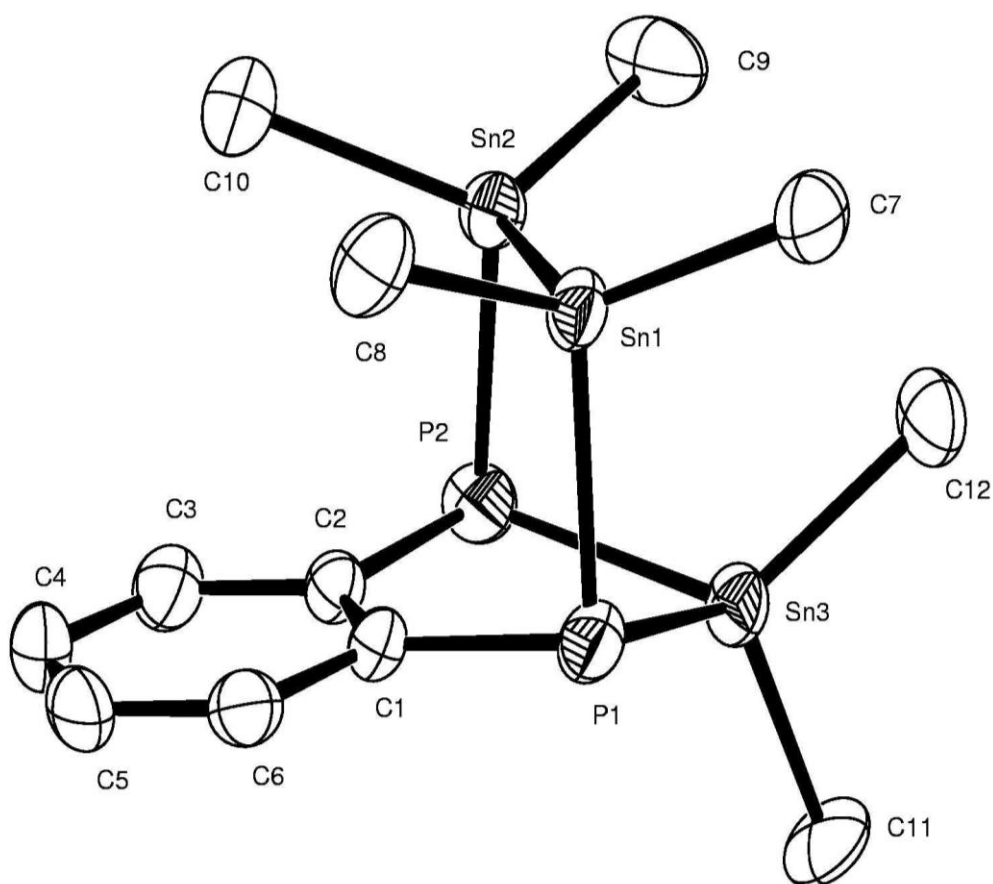


Figure 5.9: ORTEP molecular structure of $C_6H_4-1,2-P_2(\mu-SnMe_2)(\mu^2-Sn_2Me_4)$ (*H atoms omitted for clarity*)

Selected Bond Lengths [Å]	
P1-Sn1	2.5408(17)
P2-Sn2	2.5413(16)
P1-Sn3	2.5089(17)
P2-Sn3	2.5070(18)
Sn1-Sn2	2.7779(6)
P1-C1	1.859(6)
P2-C2	1.860(6)
C1-C2	1.405(8)
C1-C6	1.423(8)
C2-C3	1.403(8)
Sn1-C7	2.143(6)
Sn1-C8	2.164(7)
Sn2-C9	2.146(6)
Sn2-C10	2.147(7)
Sn3-C11	2.157(7)
Sn3-C12	2.142(7)

Selected Bond Angles [°]	
C1-P1-Sn1	91.89(18)
C2-P2-Sn2	91.85(18)
C1-P1-Sn3	95.06(19)
C2-P2-Sn3	95.56(19)
P1-Sn3-P2	91.80(5)
Sn1-P1-Sn3	92.60(6)
Sn2-P2-Sn3	92.63(6)
P1-Sn1-Sn2	99.64(4)
P2-Sn2-Sn1	99.02(4)
C1-C2-P2	125.8(4)
C2-C1-P1	126.6(4)
C1-C2-C3	119.0(5)
C6-C1-C2	118.6(5)
P1-C1-C6	114.8(4)
P2-C2-C3	115.2(5)
C8-Sn1-C7	110.3(3)
C9-Sn2-C10	111.6(3)
C11-Sn3-C12	109.7(3)

The $^{119}\text{Sn}\{^1\text{H}\}$ NMR spectroscopic data was in good agreement with the X-ray crystal diffraction data. The triplet splitting of the resonance at δ 126 indicated that it corresponded to the Sn centre is bound directly to both P atoms. The magnitude of larger value ^{31}P coupling constant of the resonance at δ -55 indicated $^1J_{\text{Sn-P}}$, corresponding to the second Sn atom bound directly to the P, with the smaller value ^{31}P coupling constant of the resonance at δ -55 is due to a 2J interaction with the P atom on the opposite side of the molecule. The coupling constant value of the ^{117}Sn satellites present on the resonance at δ -55 showed the presence of a Sn-Sn bond. The coupling constant values of the ^{31}P and ^{119}Sn resonances were relatively low for 1J and 2J couplings, (*cf.* Table 2.1) but the explanation for this became apparent when examining the structural properties from the X-ray diffraction data. All of the angles between the Sn-P, Sn-Sn and P-C bonds of the molecule were close to 90° , suggesting that the bonding orbitals of the Sn-P bonds are high in p-orbital character. Because the p-orbital possesses a nodal plane at the nucleus, the nuclear spin has a greatly reduced affect on the electrons and so the coupling interaction with other nuclei through the bonds is lessened.¹⁷

Along with $\text{C}_6\text{H}_4\text{-1,2-P}_2(\mu\text{-SnMe}_2)(\mu^2\text{-Sn}_2\text{Me}_4)$, the $^{31}\text{P}\{^1\text{H}\}$ and $^{119}\text{Sn}\{^1\text{H}\}$ NMR spectra showed a second set of resonances at approximately 5% of the intensity, with very similar characteristics. A resonance appeared at δ -139 in the $^{31}\text{P}\{^1\text{H}\}$ NMR spectrum (Figure 5.10) with a pattern of $^{117}\text{Sn}/^{119}\text{Sn}$ satellites closely resembling those observed for $\text{C}_6\text{H}_4\text{-1,2-P}_2(\mu\text{-SnMe}_2)(\mu^2\text{-Sn}_2\text{Me}_4)$ resonance at δ -158. The $^{119}\text{Sn}\{^1\text{H}\}$ NMR spectrum (Figure 5.11) showed a second triplet and doublet of doublets at δ 58 and -77 respectively, again in a 1:2 ratio. Although the NMR spectroscopic data of the two compounds displayed many of the same features, notable differences could be seen in the values of $J_{\text{P-Sn}}$. The value of $J_{\text{P-Sn}}$ for the triplet resonance in the $^{119}\text{Sn}\{^1\text{H}\}$ NMR

spectrum of the minor side product is 750 Hz compared to 698 Hz for the equivalent in $\text{C}_6\text{H}_4\text{-1,2-P}_2(\mu\text{-SnMe}_2)(\mu^2\text{-Sn}_2\text{Me}_4)$ and the larger coupling in the doublet of doublets is similarly greater at 706 Hz as opposed to 659 Hz. The small coupling, however, is only 7 Hz, far less than the 66 Hz equivalent observed for $\text{C}_6\text{H}_4\text{-1,2-P}_2(\mu\text{-SnMe}_2)(\mu^2\text{-Sn}_2\text{Me}_4)$.

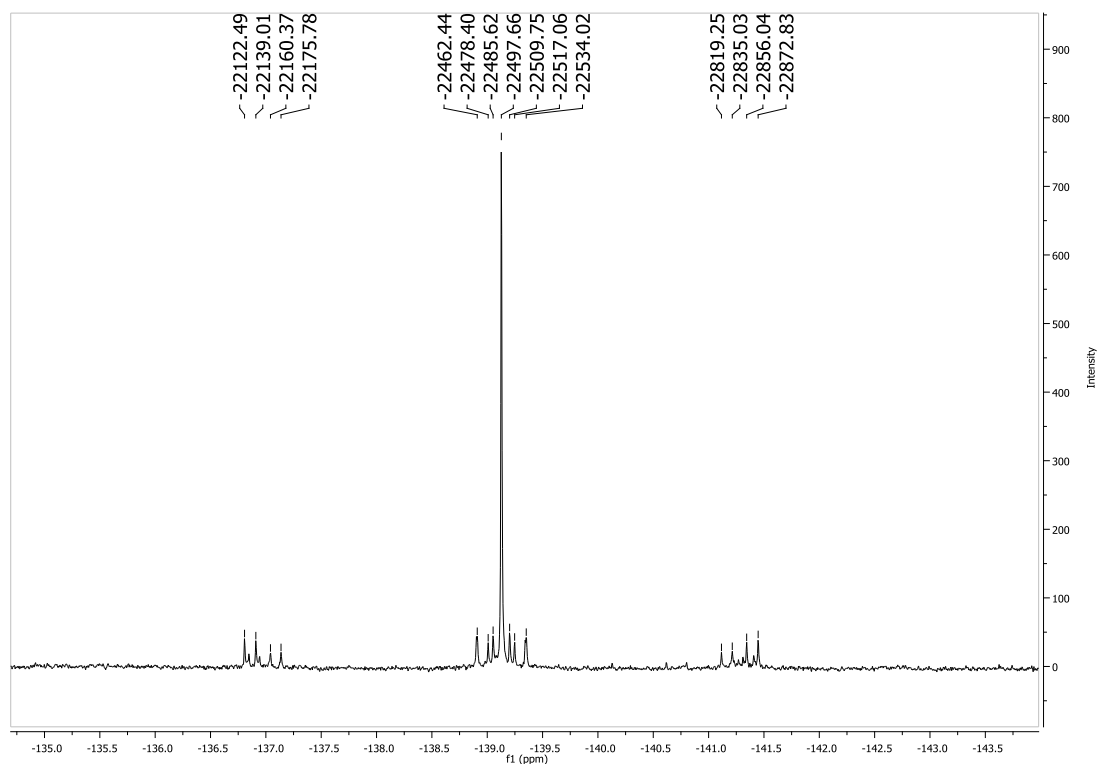


Figure 5.10: $^{31}\text{P}\{^1\text{H}\}$ NMR spectrum of the minor reaction product of $\text{C}_6\text{H}_4\text{-1,2-(PHLi)}_2$ and Me_2SnCl_2

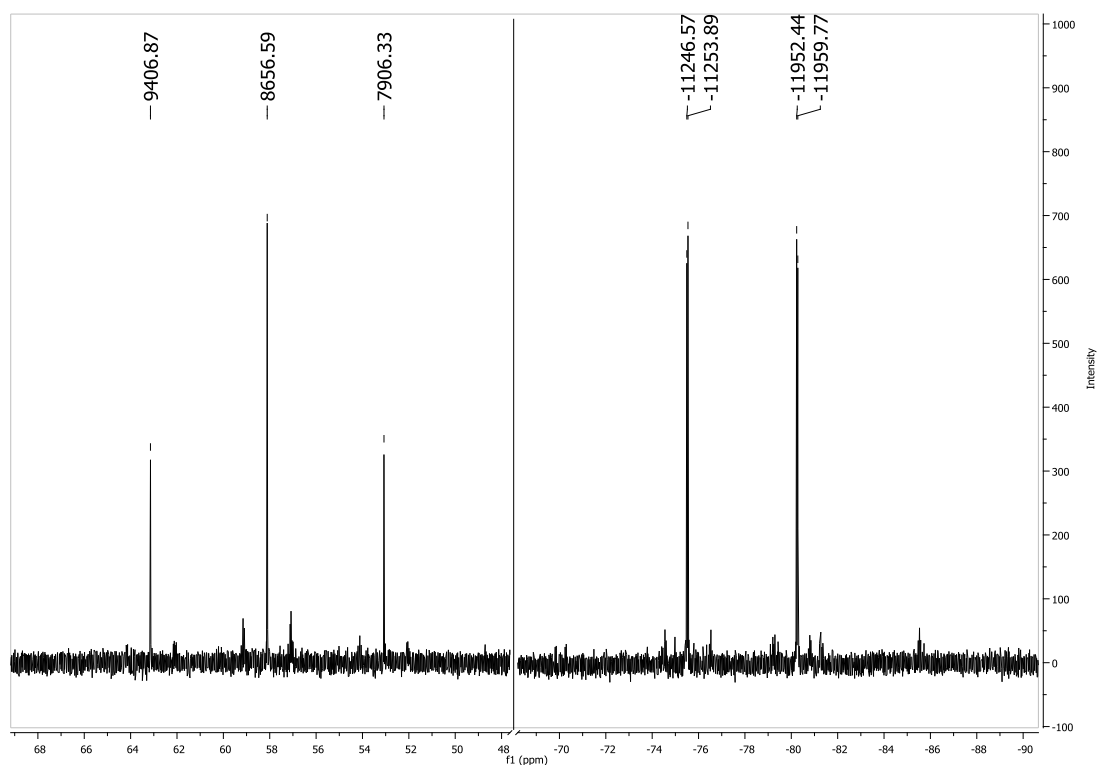


Figure 5.11: $^{119}\text{Sn}\{^1\text{H}\}$ NMR spectrum of the minor reaction product of C_6H_4 -1,2-($\text{P}(\text{H})\text{Li}$) $_2$ and Me_2SnCl_2

The minor side product was proposed to be to an intermediate in the synthesis of C_6H_4 -1,2- $\text{P}_2(\mu\text{-SnMe}_2)(\mu^2\text{-Sn}_2\text{Me}_4)$ in which the Sn-Sn bond has not been formed and the two related Sn atoms each retain one chloride. (Figure 5.12) Because these Me_2SnCl groups would be terminal, some of the steric forces responsible for the *circa* 90° bond angles in C_6H_4 -1,2- $\text{P}_2(\mu\text{-SnMe}_2)(\mu^2\text{-Sn}_2\text{Me}_4)$ would not be experienced and so the bonding orbitals are likely to possess a slightly higher degree of s-orbital character, resulting in the increased value of the 1J coupling constants. Without the Sn-Sn bond, however, the 2J pathway is unavailable for the small ^{31}P - ^{119}Sn coupling between opposite sides of the molecule. Instead the minimum through-bond distance would be the 3J coupling through the ring system, accounting for a much smaller value of coupling constant. The lack of a Sn-Sn bond also explains the absence of 1J ^{117}Sn satellites on the δ -77.9 resonance in the $^{119}\text{Sn}\{^1\text{H}\}$ NMR spectrum.

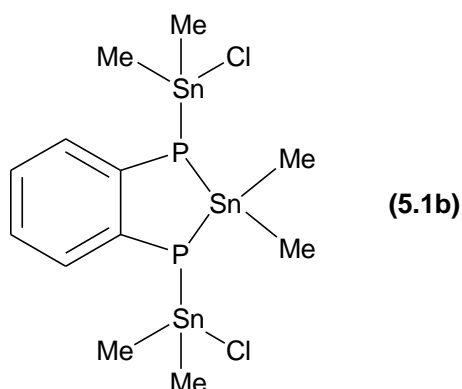
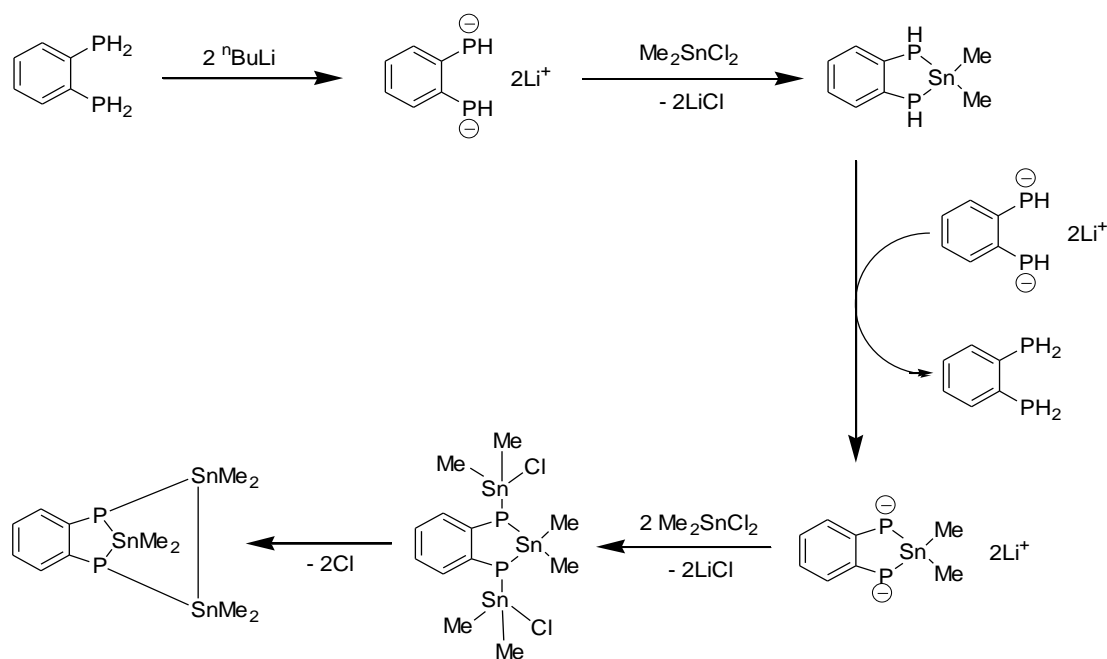


Figure 5.12: Proposed side product of $C_6H_4-1,2-P_2(\mu-SnMe_2)(\mu^2-Sn_2Me_4)$ synthesis (5.1b)

The proposed mechanism by which $C_6H_4-1,2-P_2(\mu-SnMe_2)(\mu^2-Sn_2Me_4)$ is formed firstly involves the elimination of two equivalents of LiCl to form the central P-Sn-P bonds. This intermediate then undergoes a reaction with a second equivalent of $C_6H_4-1,2-(PHLi)_2$, losing the two remaining protons and regenerating a molecule of $C_6H_4-1,2-(PH_2)_2$ as a by-product, as has been observed in an analogous reaction with boron halides.³ Further metathesis reactions then occur to bond the second and third Sn groups to the P atoms resulting in the proposed structure of the observed side product. Finally a reduction, most likely by remaining $C_6H_4-1,2-(PHLi)_2$,¹⁸ removes the chlorine atoms and affords the Sn-Sn bond. (Scheme 5.14)

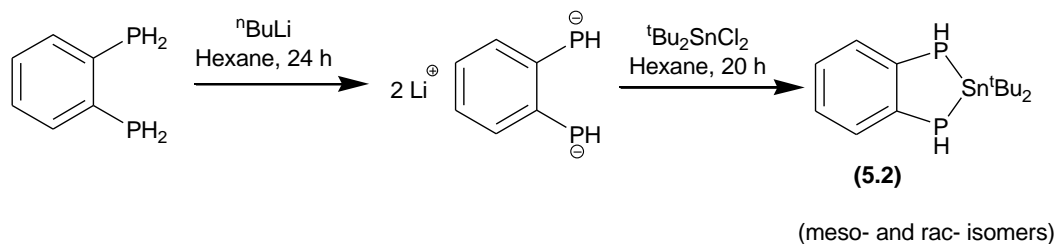


Scheme 5.14: Proposed mechanism for the formation of $C_6H_4-1,2-P_2(\mu-SnMe_2)(\mu^2-Sn_2Me_4)$

Synthesis of $C_6H_4-1,2-(PH)_2(\mu-Sn^tBu_2)$ (5.2)

By increasing the bulk of the alkyl groups on the Sn atoms, it was observed that the addition of the second and third Sn groups could be sterically prevented.

A sample of $C_6H_4-1,2-(PH_2)_2$ was combined with two equivalents of $n-BuLi$ in hexane at ambient temperature and stirred for twenty four hours, generating a bright yellow precipitate. One equivalent of tBu_2SnCl_2 was then added as a solution in hexane and the mixture stirred for a further twenty hours, causing the mixture to turn orange. (Scheme 5.15)



Scheme 5.15: Synthesis of $C_6H_4-1,2-(PH)_2(\mu-Sn^tBu_2)$

The $^{31}P\{^1H\}$ NMR spectrum of the product showed two singlet resonances at δ -143.0 and -146.8 with a relative intensity ratio of approximately 1:1.36, each with a single set of $^{117}Sn/^{119}Sn$ satellites with coupling constant values of *circa* 680 Hz. (Figure 5.13)

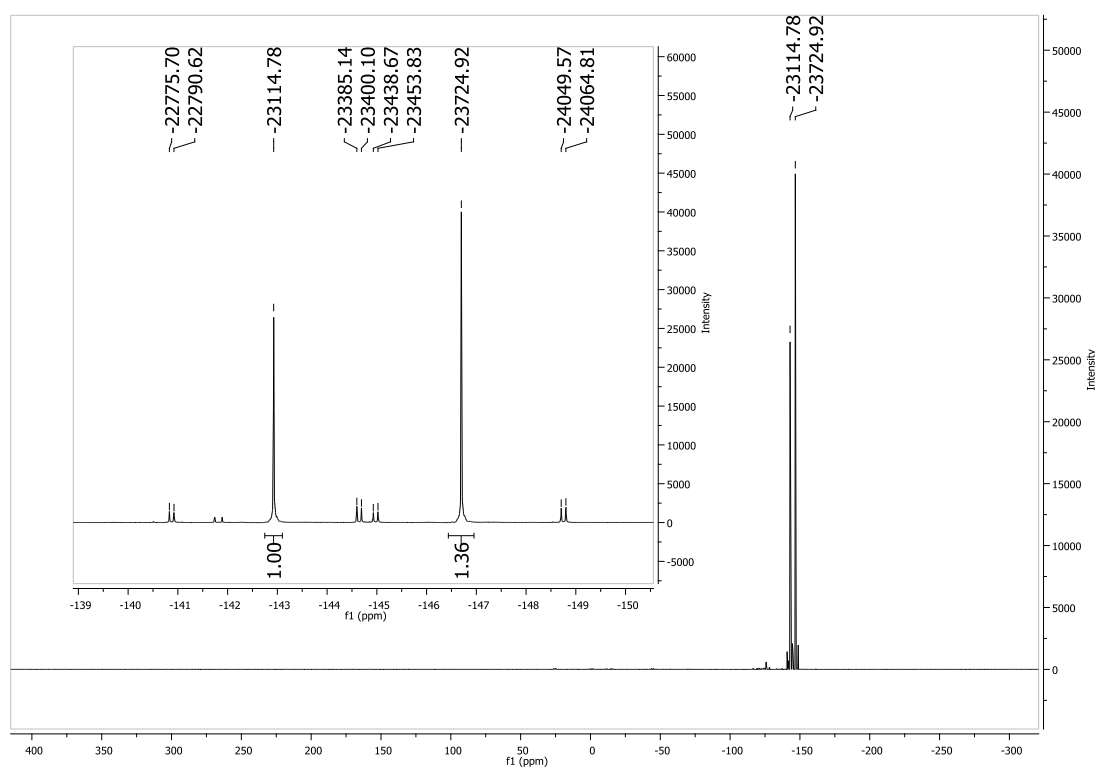


Figure 5.13: $^{31}P\{^1H\}$ NMR spectrum of $C_6H_4-1,2-(PH)_2(\mu-Sn^tBu_2)$

In the proton coupled ^{31}P NMR spectrum, both of the signals were split into doublets with coupling constant values *circa* 175 Hz (with some additional long range

multiplicity) demonstrating that the phosphorus atoms had retained their single protons.
(Figure 5.14)

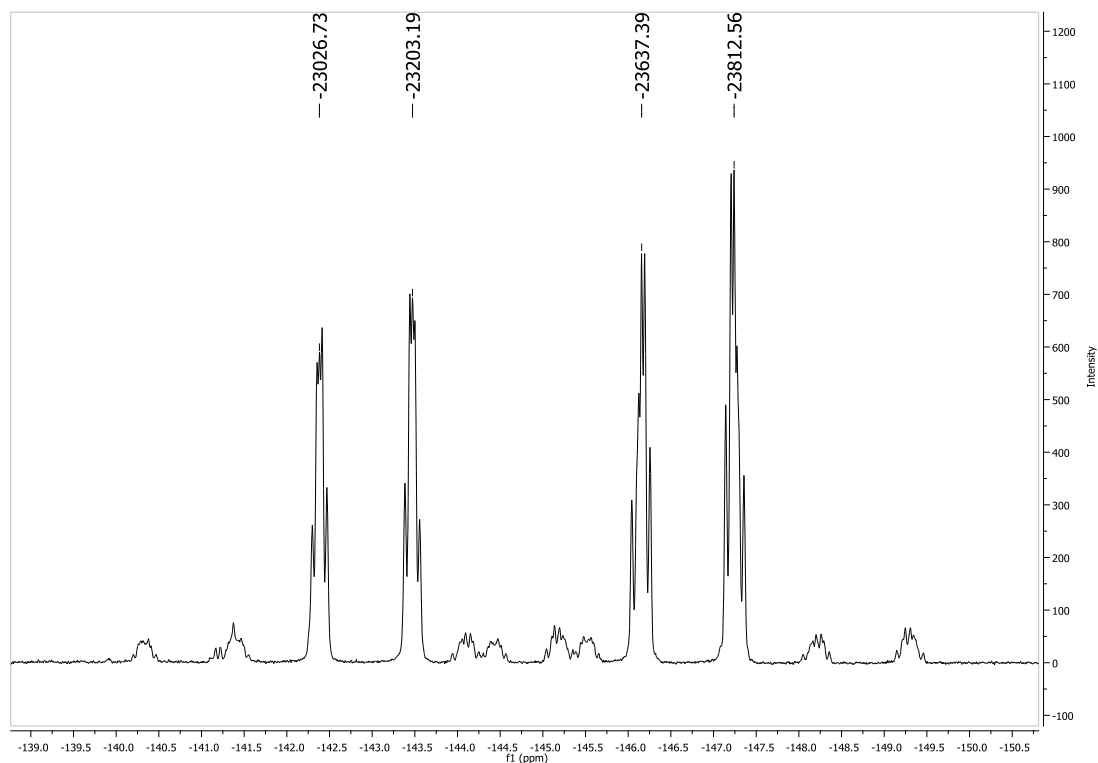


Figure 5.14: ^{31}P NMR spectrum of $\text{C}_6\text{H}_4\text{-1,2-(PH)}_2(\mu\text{-Sn}^t\text{Bu}_2)$

The $^{119}\text{Sn}\{^1\text{H}\}$ NMR spectrum showed two triplet resonances at δ 147 and δ 136 with the same relative integrals and coupling constant values as the resonances observed in the $^{31}\text{P}\{^1\text{H}\}$ NMR spectrum. (Figure 5.15)

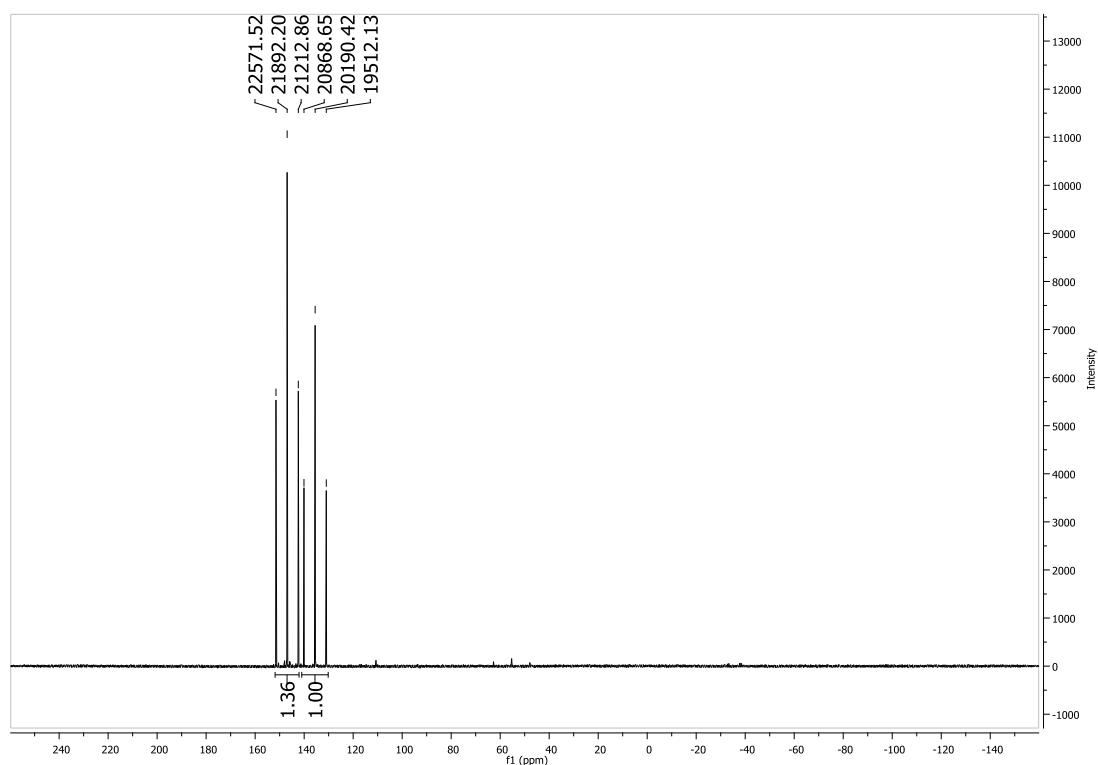


Figure 5.15: $^{119}\text{Sn}\{^1\text{H}\}$ NMR spectrum of $\text{C}_6\text{H}_4\text{-1,2-(PH)}_2(\mu\text{-Sn}^t\text{Bu}_2)$

The fact that the two products of this reaction showed such incredibly similar NMR spectra suggested that they may be a pair of stereoisomers. As observed for the central Sn atom of $\text{C}_6\text{H}_4\text{-1,2-P}_2(\mu\text{-SnMe}_2)(\mu^2\text{-Sn}_2\text{Me}_4)$, the triplet splitting and 1J coupling in the $^{119}\text{Sn}\{^1\text{H}\}$ NMR spectrum indicated that the Sn centre is bound directly between the P atoms. The presence of a single Sn centre and the fact that the P atoms are each bonded to a single proton are consistent with $\text{C}_6\text{H}_4\text{-1,2-(PH)}_2(\mu\text{-Sn}^t\text{Bu}_2)$. The two isomers would be a result of the chiral phosphorus centres, with the relative positions of the associated protons giving rise to *rac*- and *meso*- forms of the molecule. (Figure 5.16)

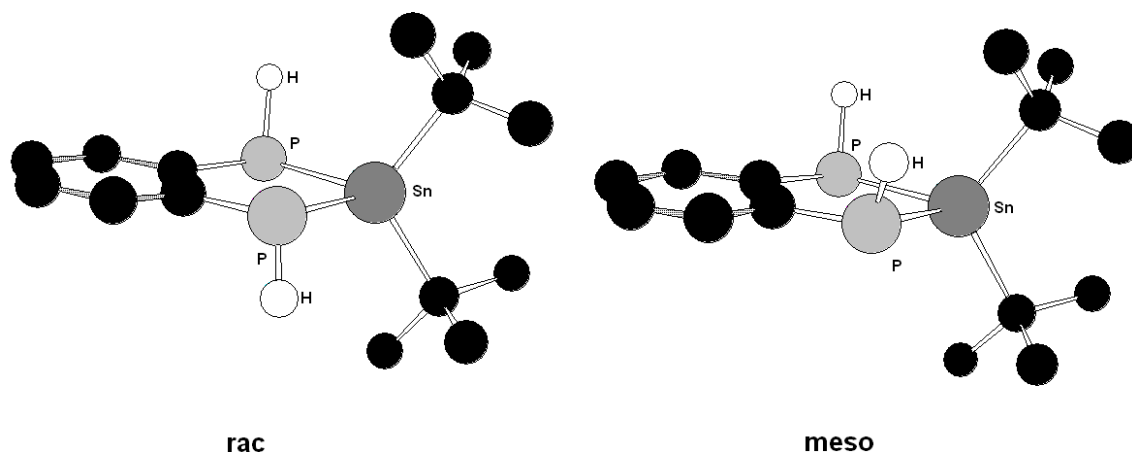


Figure 5.16: *Rac*- and *meso*- isomers of C_6H_4 -1,2- $(PH)_2(\mu\text{-}Sn^tBu_2)$

Whilst the presence of the two isomers could be observed in the $^{119}Sn\{^1H\}$ and $^{31}P\{^1H\}$ NMR spectra, the symmetry of the molecule meant that they offered no way to determine which isomer corresponds to which resonance. The 1H NMR spectrum, however, provided some insight into the geometry of the molecules. (Figure 5.17) In the *rac*- form the molecule has C_2 symmetry, with the rotational axis passing through the centre of the aromatic ring and the Sn atom. As a result, the tBu groups are chemically equivalent and would only give one resonance in the 1H NMR spectrum. In contrast, the *meso*- form has C_s symmetry with the mirror plane running through the Sn atom and the central carbons of both tBu groups. In this instance the tBu groups are chemically inequivalent, one on the same face of the molecule as the protons and one on the opposite, therefore generating two separate resonances in the 1H NMR spectrum. Comparing the intensities of the three tBu resonances showed that the *rac*- isomer is the slightly more abundant form, with its single tBu resonance possessing an integral 1.36 times the size of the two others combined. (Figure 5.18) Selected NMR spectroscopic data for these isomers is shown in Table 5.2.

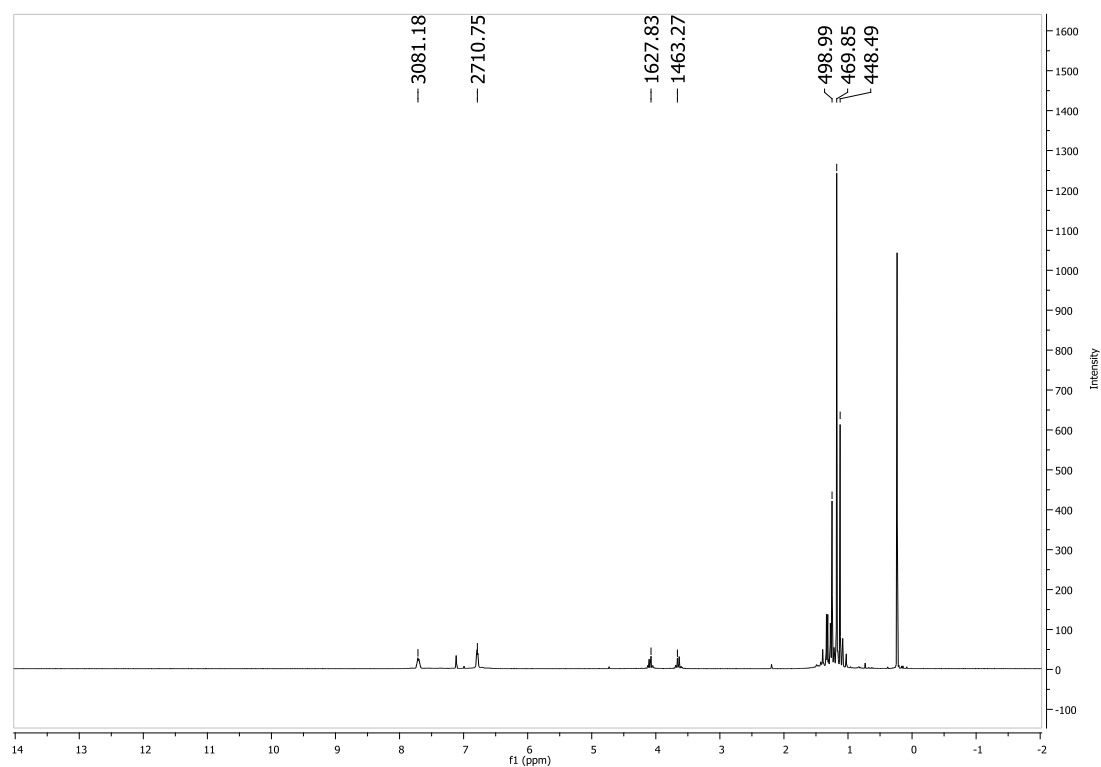


Figure 5.17: ^1H NMR spectrum of $\text{C}_6\text{H}_4\text{-1,2-(PH)}_2(\mu\text{-Sn}^t\text{Bu}_2)$

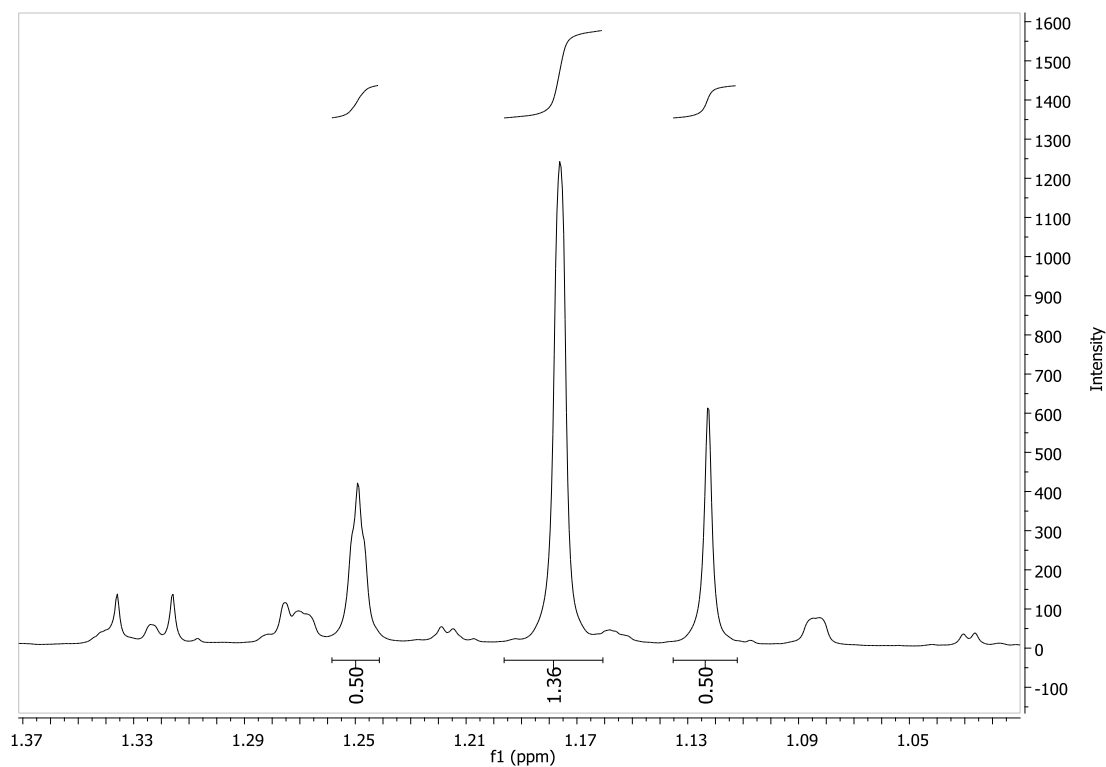


Figure 5.18: Expanded ^1H NMR spectrum of $\text{C}_6\text{H}_4\text{-1,2-(PH)}_2(\mu\text{-Sn}^t\text{Bu}_2)$

Isomer	Relative Integral	$^{119}\text{Sn } \delta$	$^{31}\text{P } \delta$	$^t\text{Bu } ^1\text{H, } \delta$	$^1\text{J } ^{119}\text{Sn}-^{31}\text{P}$	$^1\text{J } ^{31}\text{P}-^1\text{H}$
<i>Rac</i> -	1.36	147	-146.8	1.18	679	175
<i>Meso</i> -	1.00	136	-143.0	1.25 1.12	678	176

Table 5.2: Selected NMR spectroscopic data for C_6H_4 -1,2-(PH) $_2(\mu\text{-Sn}^t\text{Bu}_2)$

Because the structural difference between these two isomers was only the reversed positioning of a proton and a lone pair of electrons, the energetic difference between them was incredibly small. The result of this was that attempts to synthesise just one isomer, or separate them once formed, proved impossible. The difference in the structures was, however, sufficient to prevent an ordered packing of the molecules. This meant that the product could only be obtained as an oil, rather than a solid, and all attempts to produce crystals of the product for X-ray diffraction were unsuccessful. Without any X-ray diffraction data it was obviously difficult to determine the exact geometry of the molecules, but the NMR spectroscopic data did provide some information. The Sn-P coupling constants in these molecules are very close to the values observed for the equivalent phosphorus and tin atoms in C_6H_4 -1,2-P $_2(\mu\text{-SnMe}_2)(\mu^2\text{-Sn}_2\text{Me}_4)$. If the justification for the low coupling constant is correct (*i.e.* the bonds are high in p-orbital character) it can therefore be inferred from this data that the ring angles of the Sn and P atoms were all close to 90°.

A single hexagonal crystal was obtained from the reaction mixture but the X-ray analysis showed that it was a trace side product. Instead of a single $^t\text{Bu}_2\text{Sn}$ group bound between the two P atoms, two equivalents had formed a Sn-Sn bond, resulting in a six membered, P $_2\text{C}_2\text{Sn}_2$ ring. (Figure 5.19)

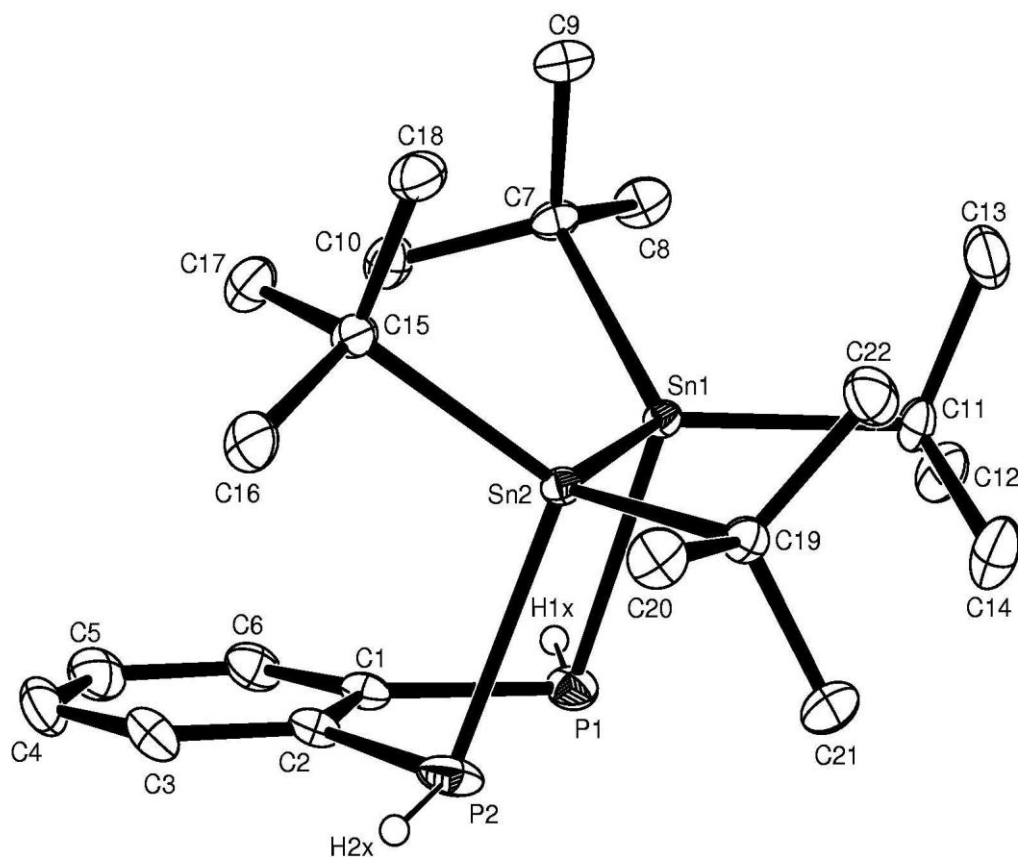


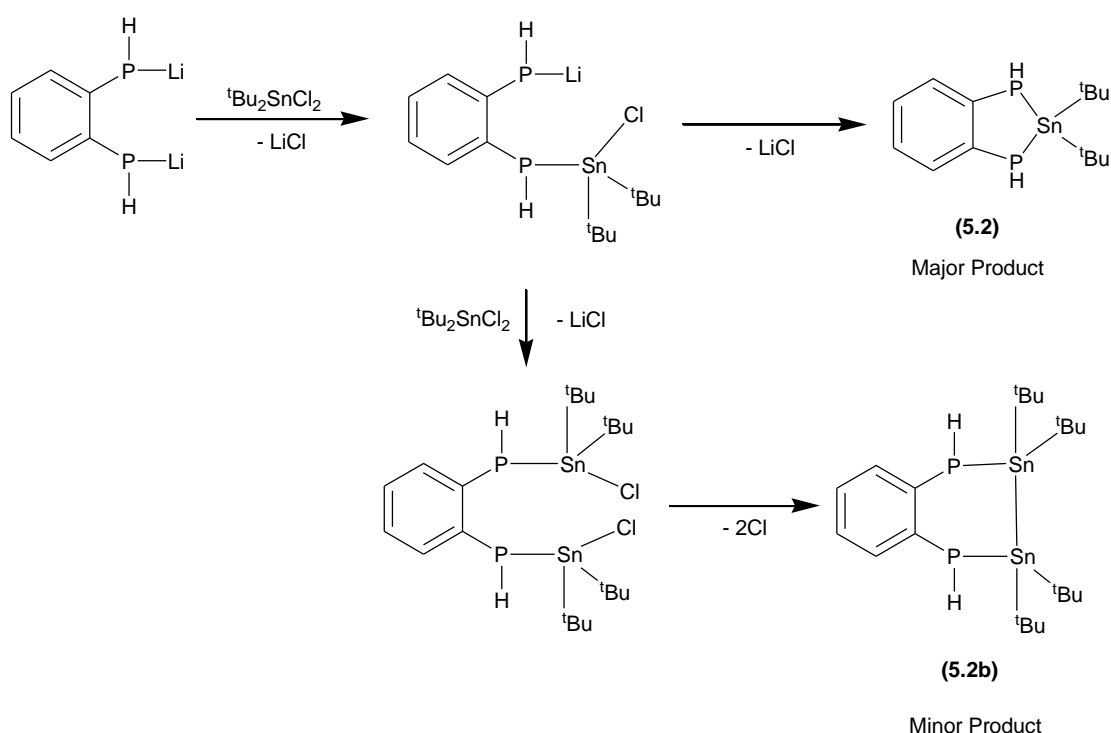
Figure 5.19: ORTEP molecular structure of C_6H_4 -1,2- $(PH)_2(\mu^2-Sn_2^tBu_4)$ (**5.2b**) (H atoms omitted for clarity)

Selected Bond Lengths [Å]	
P1-Sn1	2.5434(7)
P2-Sn2	2.5353(7)
P1-C1	1.840(3)
P2-C2	1.829(3)
Sn1-Sn2	2.8254(2)
C1-C2	1.412(3)
C1-C6	1.396(4)
C2-C3	1.397(4)
Sn1-C7	2.213(2)
Sn1-C11	2.211(2)
Sn2-C15	2.212(2)
Sn2-C19	2.225(2)

Selected Bond Angles [°]	
C1-P1-Sn1	101.83(7)
C2-P2-Sn2	100.20(8)
P1-Sn1-Sn2	94.920(17)
P2-Sn2-Sn1	97.875(19)
C1-C2-P2	121.2(2)
C2-C1-P1	124.1(2)
C2-C1-C6	118.3(2)
C1-C2-C3	118.6(2)
P1-C1-C6	120.4(2)
P2-C2-C3	113.3(5)
C7-Sn1-C11	110.18(9)
C15-Sn2-C19	112.09(9)

The formation of this distannylated product occurs far less readily than the monostannylated due to the fact that once the first Sn group has bonded to the P atom,

the ring closure is vastly favoured over the introduction of a second Sn centre due to the proximity of the eliminating groups. Although the crystal data clearly shows that the distannylated product will form independently alongside the monostannylated, the fact that its presence was so small that its NMR spectroscopic resonances were not observed is a testament to how infrequently a second Sn group has the opportunity to react with the remaining phosphide before the ring is closed. (Scheme 5.16) If the second equivalent of $^t\text{Bu}_2\text{SnCl}_2$ does react with the lithium salt it is postulated that a second molecule of dilithiobis(phosphine)benzene is responsible for the removal of the Cl atoms and thus the reductive coupling of the Sn groups.

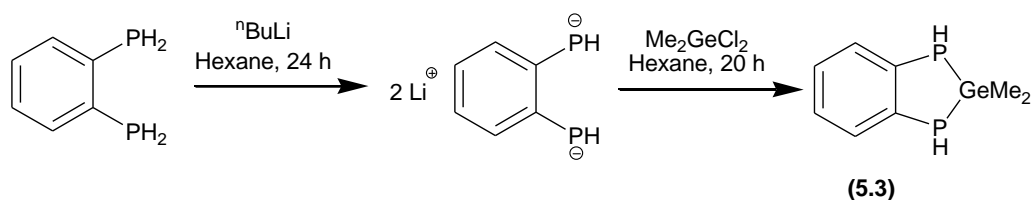


Scheme 5.16: Synthesis of $\text{C}_6\text{H}_4\text{-1,2-(PH)}_2(\mu\text{-Sn}^t\text{Bu}_2)$ and $\text{C}_6\text{H}_4\text{-1,2-(PH)}_2(\mu^2\text{-Sn}_2^t\text{Bu}_4)$

Once it had been established that increasing the size of the organic groups on the metal could prevent subsequent additions, the effect of changing the metal itself was investigated.

Synthesis of $C_6H_4-1,2-(PH)_2(\mu-GeMe_2)$ (5.3)

A sample of $C_6H_4-1,2-(PH_2)_2$ was combined with two equivalents of $nBuLi$ in hexane at ambient temperature and stirred for twenty four hours, generating a bright yellow precipitate. One equivalent of Me_2GeCl_2 was then added as a solution in hexane and the mixture stirred for a further twenty hours, causing the mixture to turn white. (Scheme 5.17)



Scheme 5.17: Synthesis of $C_6H_4-1,2-(PH)_2(\mu-GeMe_2)$

The product was a colourless solid which, as observed in the case of $C_6H_4-1,2-(PH)_2(\mu-Sn^tBu_2)$ compound, contained a mixture of isomers. Again, the $^{31}P\{^1H\}$ NMR spectrum shows two singlet resonances at δ -101.7 and -108.9 with relative integrals in a 1:1.5 ratio. (Figure 5.20) These resonances are split into doublets with coupling constant values *circa* 180 Hz with proton coupling, indicating P-H bonds. (Figure 5.21)

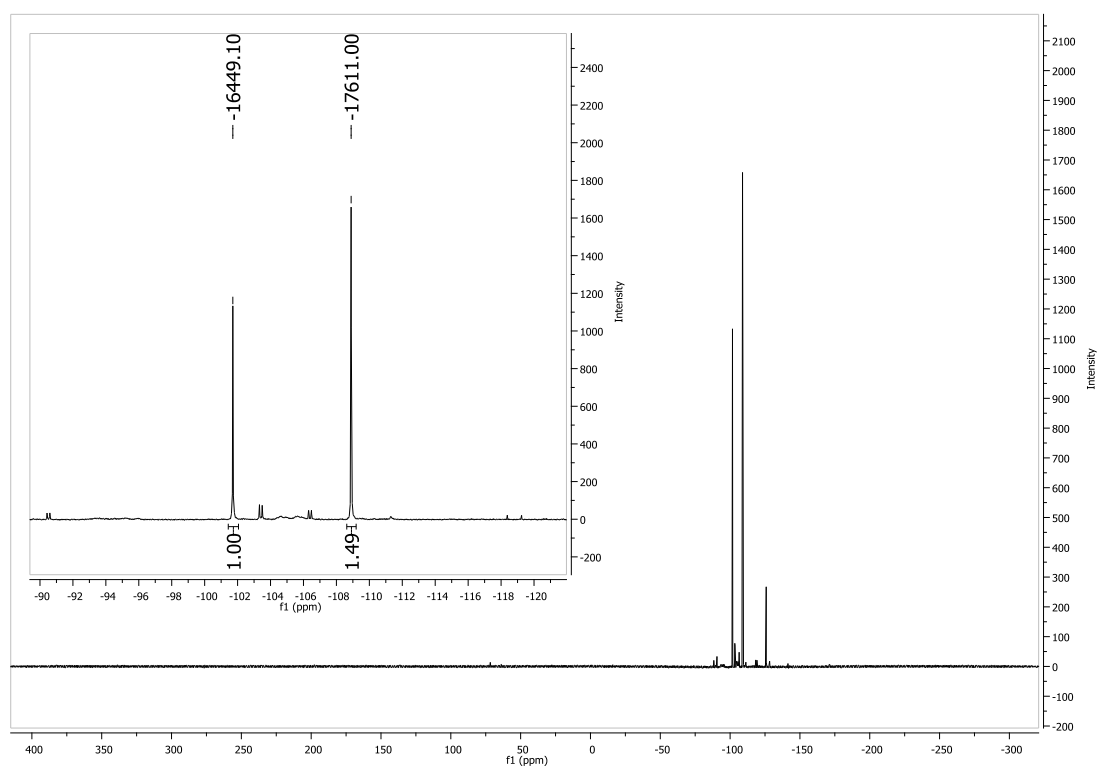


Figure 5.20: $^{31}\text{P}\{^1\text{H}\}$ NMR spectrum of $\text{C}_6\text{H}_4\text{-1,2-(PH)}_2(\mu\text{-GeMe}_2)$
($\text{C}_6\text{H}_4\text{-1,2-(PH)}_2$) visible at δ -125)

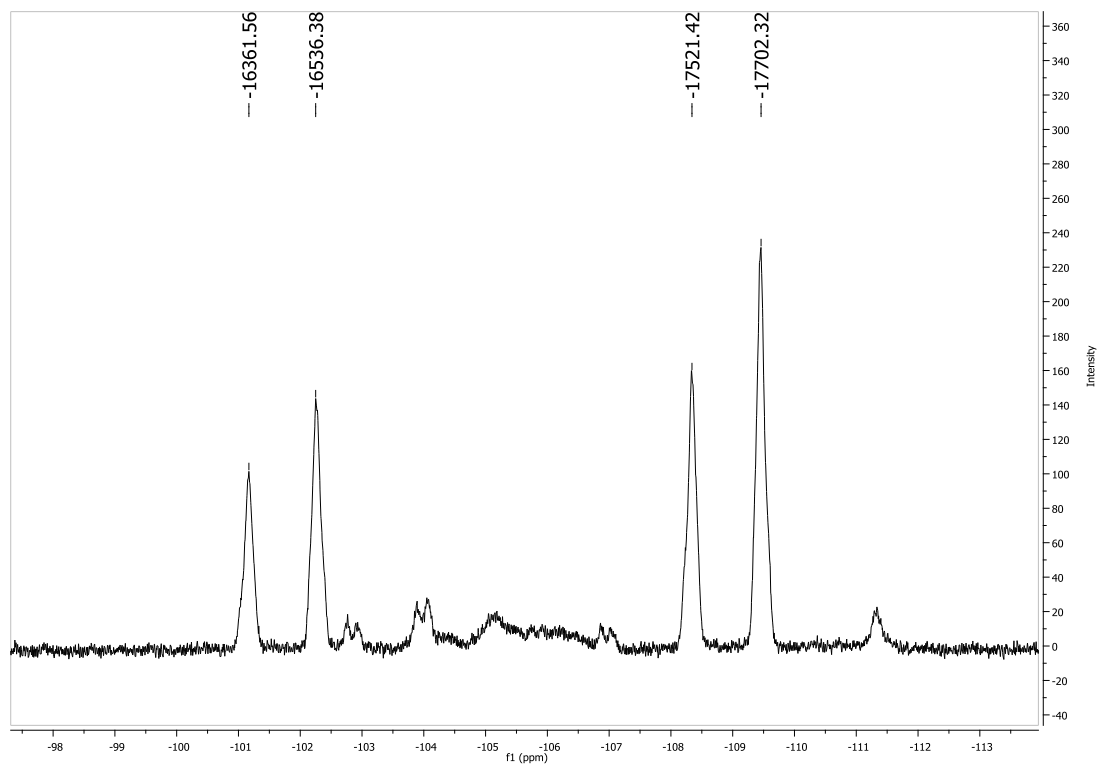


Figure 5.21: ^{31}P NMR spectrum of $\text{C}_6\text{H}_4\text{-1,2-(PH)}_2(\mu\text{-GeMe}_2)$
(plus several trace impurities)

The use of Ge instead of Sn made characterisation of the product slightly more difficult due to the fact that it has no isotope suitable for NMR spectroscopic analysis, but the close resemblance of the $^{31}\text{P}\{^1\text{H}\}$ NMR spectrum to that of the $^t\text{Bu}_2\text{Sn}$ analogue implied a similar structure.

As with the $^t\text{Bu}_2\text{Sn}$ analogue, the organic substituents bound to the metal centre were used to ascertain which of the isomers is more abundant. The ^1H NMR spectrum (Figure 5.22) for the Me groups of this compound displayed broad peaks, possibly due to unresolved 3J coupling to the P atoms, but seemed to show two slightly overlapping resonances at δ 0.59 and 0.54 attributed to the two inequivalent Me groups of the *meso*-isomer and a third resonance at δ 0.38 attributed to the *rac*- isomer. (Figure 5.23)

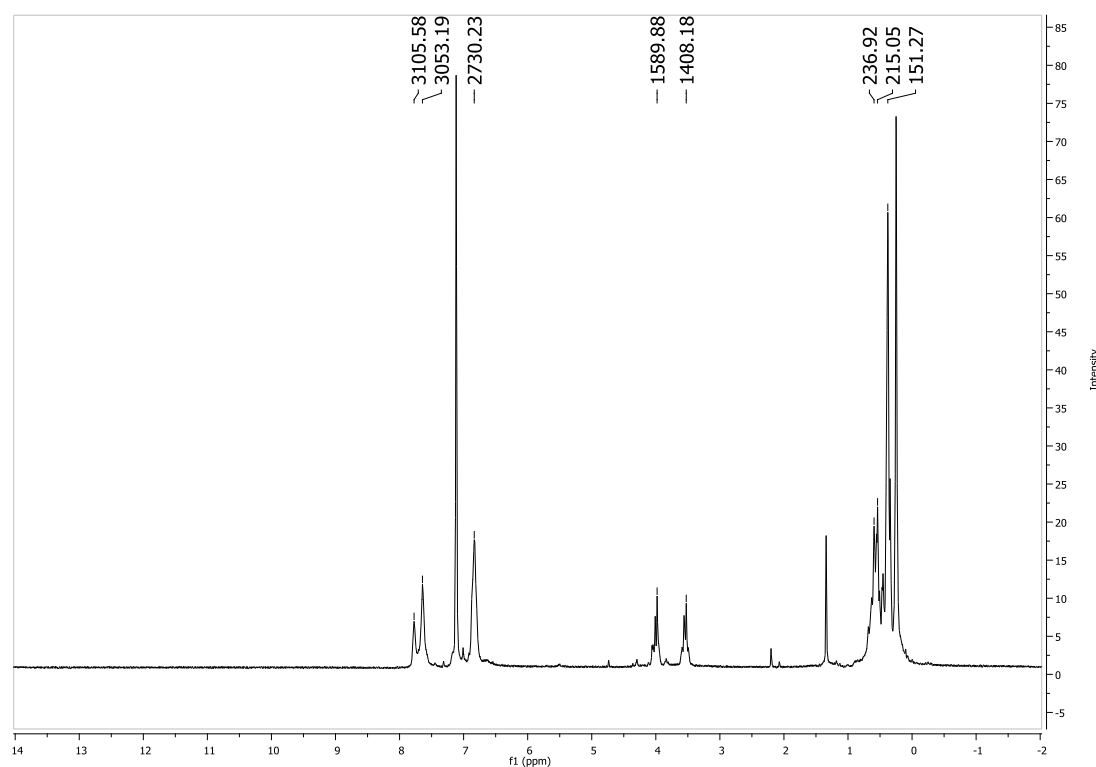


Figure 5.22: ^1H NMR spectrum of C_6H_4 -1,2- $(\text{PH})_2(\mu\text{-GeMe}_2)$

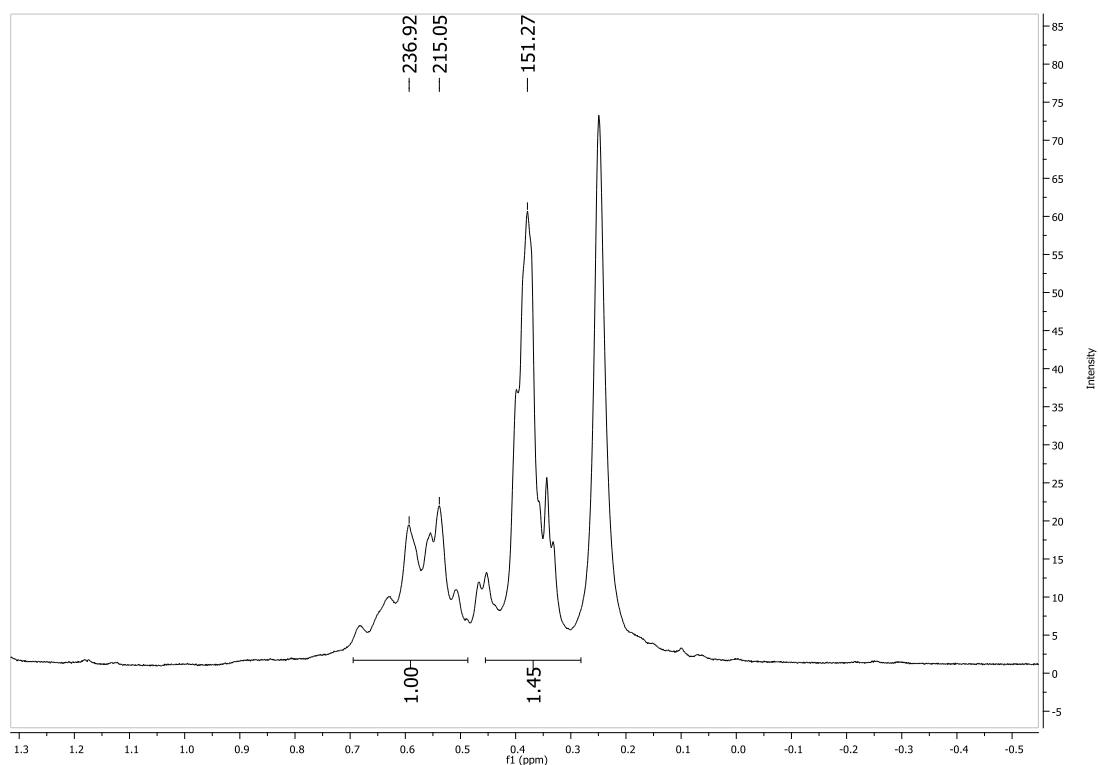


Figure 5.23: Expanded ^1H NMR spectrum of $\text{C}_6\text{H}_4\text{-1,2-(PH)}_2(\mu\text{-GeMe}_2)$ (PDMS contaminant at δ 0.24)

Isomer	Relative Integral	^{31}P δ	Me ^1H , δ	$^1\text{J } ^{31}\text{P-}^1\text{H}$
<i>Rac</i> -	1.5	-108.9	0.38	181
<i>Meso</i> -	1.0	-101.7	0.59 0.54	175

Table 5.3: Selected NMR spectroscopic data for $\text{C}_6\text{H}_4\text{-1,2-(PH)}_2(\mu\text{-GeMe}_2)$

The relative intensities of these resonances approximately matched with the 1:1.49 ratio of those observed in the $^{31}\text{P}\{^1\text{H}\}$ NMR spectrum and indicated that, as in the case of $\text{C}_6\text{H}_4\text{-1,2-(PH)}_2(\mu\text{-Sn}^t\text{Bu}_2)$, the *rac*- isomer was the more abundant of the two.

5.3: Conclusions

The initial reactions of this chapter further illustrates the difficulty of forming Sn-P bonds, with the result being almost ubiquitously the coupled bis(phosphino)benzene product. This was avoided with the use of Me_2SnCl_2 which succeeded in forming a polycyclic compound containing three Sn centres. The fact that the problem was overcome by switching to Me substituents just as observed in Chapter 2 suggests the possibility that the coupling of bis(phosphino)benzene molecules may also have arisen as a result of radical cleavage of the Sn-P bond, although this is currently speculative.

Investigation of the analogous reaction using $^t\text{Bu}_2\text{SnCl}_2$ showed that the formation of multiple heterocycles could be prevented by increasing the steric bulk of the organic substituents. As a result a single Sn centre was bound between the P atoms, with the PH groups exhibiting both *meso*- and *rac*- isomers. The complete absence of any uncyclised *rac*- isomer in the Me_2SnCl_2 reaction suggests that the addition of at least the third Sn centre may have been directed in some way.

Reactions using Ge reagents showed that Me groups were sufficient to prevent the addition of more than one Ge centre.

References

1. Mann, F. G., Mercer, A., J., H., *J.C.S. Perkin I*, 1972, 1631
2. Rawson, J. M., Alberola, A., Whalley, A., *J. Mater. Chem.*, 2006, **16**, 2560.
3. Kaufmann, B., Jetzfellner, R., Leissring, E., Issleib, K., Nöth, H., Schmidt, M., *Chem. Ber./Recueil.*, 1997, **130**, 1677.
4. García, F., Humphrey, S. M., Kowenicki, R. A., McInnes, E. J. L., Pask, C. M., McPartlin, M., Rawson, J. M., Stead, M. L., Woods, A. D., Wright D. S., *Angew. Chem. Int. Ed. Engl.*, 2005, **44**, 3456
5. Bowmaker, G. A., Herr, R., Schmidbaur, H., *Chem. Ber.*, 1983, **116**, 3567
6. Woerz, HJ., Quien, E., Latscha, H. P., *Z. Naturforsch. B.*, 1984, **39**, 1706
7. Schmidpeter, A., Burget, G., Sheldrick W. S., *Chem. Ber.*, 1985, **118**, 3849
8. Davis, M., F., Levason, W., Reid, G., Webster, M., *Dalton Trans.*, 2008, 2261
9. Issleib, K., Leissring, E., Riemer, M., *Z. Anorg. Allg. Chem.*, 1984, **519**, 75
10. Issleib, K., Schmidt, H., Leissring, E., *J. Organomet. Chem.*, 1990, **382**, 53
11. García, F., Less, R. J., Naseri, V., McPartlin, M., Rawson, J. M., Tomas, M. S., Wright D. S., *Chem. Commun.*, 2008, 859
12. Dillon, K. B., Mathey, F., Nixon, J. F., *Phosphorus: The Carbon Copy* 1998
13. García, F., Less, R. J., Naseri, V., McPartlin, M., Rawson, J. M., Wright, D. S., *Angew. Chem. Int. Ed. Engl.*, 2007, **46**, 7827
14. Butts, C. P., Green, M., Hooper, T. N., Kilby, R. J., McGrady, J. E., Pantazis, D. A., Russell, C. A., *Chem. Commun.*, 2008, 856
15. Eisler, D. J., Less, R. J., Naseri, V., McPartlin, M., Rawson, J. M., Wright, D. S., *Dalton Trans.*, 2008, 2382–2384
16. Etkin, N., Fermin, M. C., Stephen, D. W., *J. Am. Chem. Soc.*, 1997, **119**, 2954

17. Mosher, M. D., Ojha, S., *J. Chem. Educ.*, 1998, **75**, 888
18. Blake, P. C., Hey, E., Lappert, M. F., Atwood, J. L., Zhang, H., *J. Organomet. Chem.*, 1988, **353**, 307

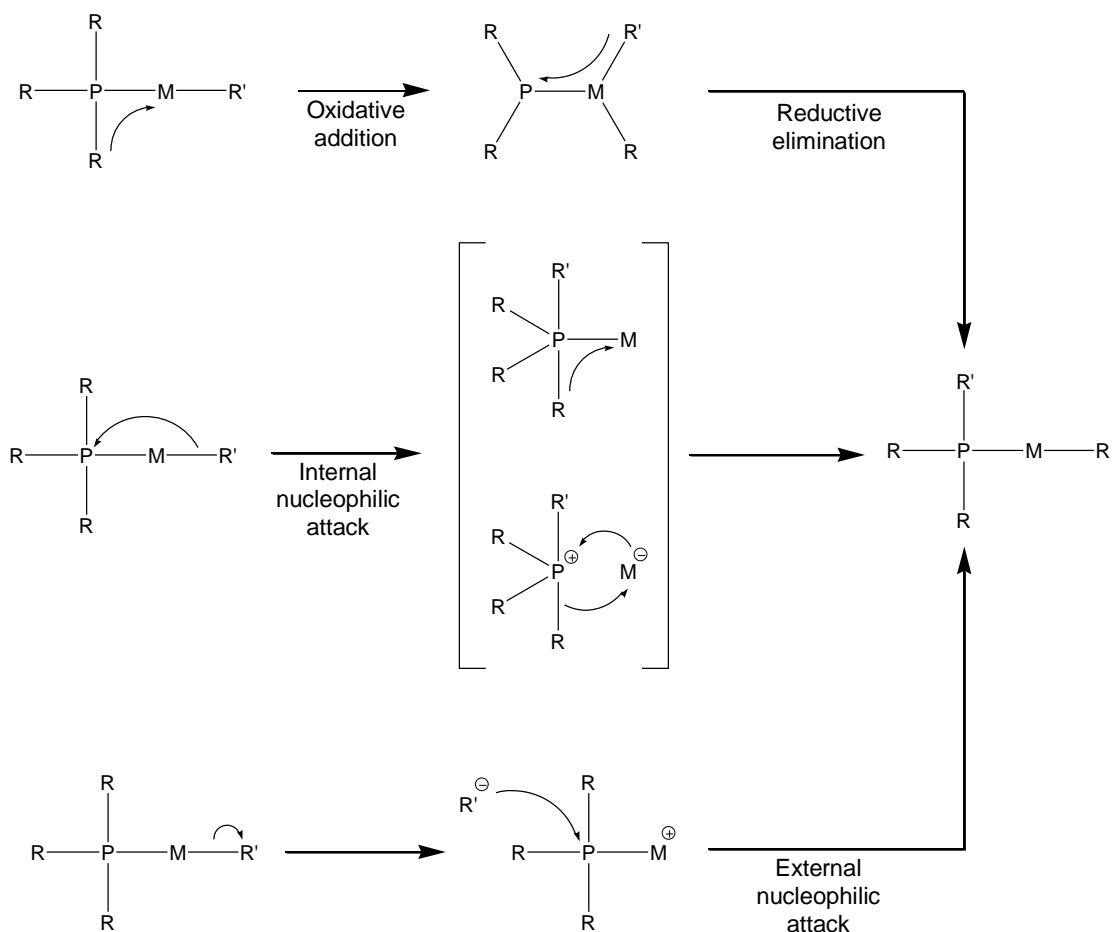
Chapter 6

The Exchange of Protons and Trimethylsilyl

Groups Between Phosphines

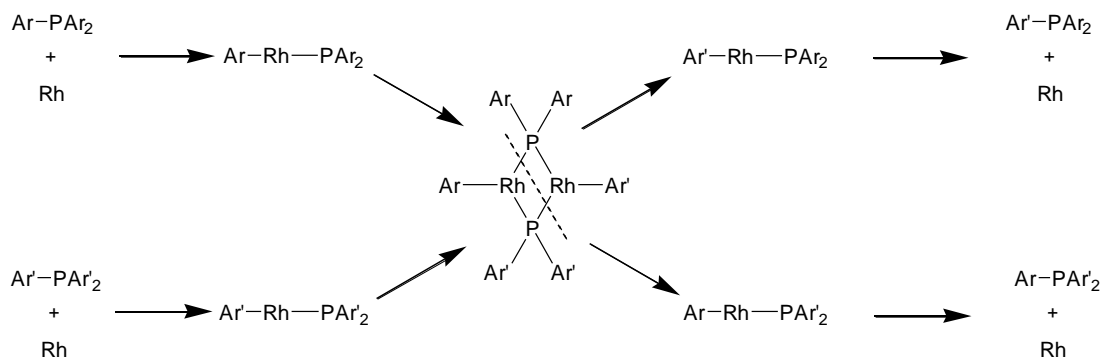
6.1: Introduction

Substituent exchange reactions of phosphines with transition metals have been studied for several years, often as undesirable complications in reactions which use phosphines as ancillary ligands. A variety of different aryl/aryl and aryl/alkyl exchanges have been observed and attributed to several different mechanisms.¹ (Scheme 6.1)



Scheme 6.1: Substituent exchange pathways for coordinated phosphines

Many late transition metal complexes have been shown to catalyse the exchange of phenyl and *p*-tolyl groups between the respective tertiary phosphines when heated. This was initially reported for the Rh based hydroformylation catalyst $[\text{Rh}(\text{H})(\text{CO})(\text{PPh}_3)_3]$ and was proposed to occur *via* an oxidative addition, phosphide exchange and reductive elimination.² (Scheme 6.2)

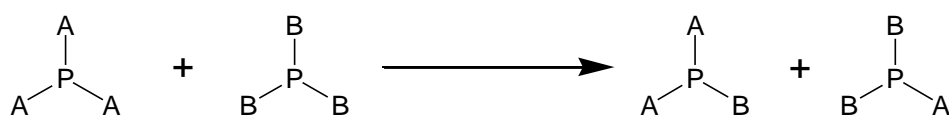


Scheme 6.2: Rhodium catalysed substituent scrambling on phosphines

Reactions similar to this have also been reported for certain Pd reagents when used in cross coupling reactions.³ Heating the complex *trans*-[Pd(Ar)I(PPh₃)₂] (Ar = *p*-tolyl) to 60 °C in THF yielded a mixture of *trans*-[Pd(Ph)I(PPh₂Ar)₂] and *trans*-[Pd(Ph)I(PPh₃)₂]. These were most likely formed through a scrambling of the phosphines following the formation of the initial exchange product *trans*-[Pd(Ph)I(PPh₂Ar)(PPh₃)].

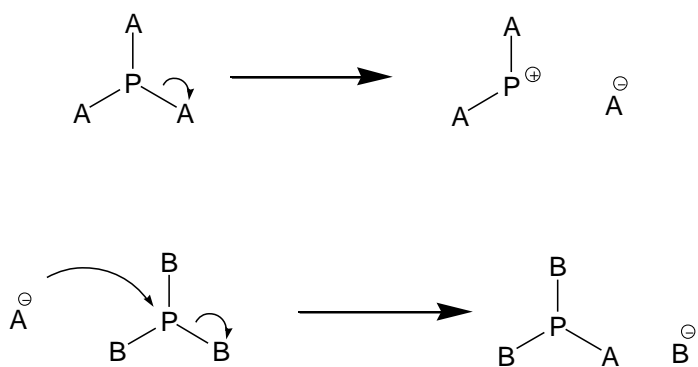
Aryl/Alkyl exchanges have been observed in similar systems but with some notably different results.⁴ Heating *trans*-[Pd(Me)I(PPh₃)₂] to 75 °C in benzene caused an exchange of Me and Ph groups, but unlike the equilibria which were reached in the aryl/aryl exchanges, the exchange was irreversible.

The exchange of substituents between two phosphines without any activation by a metal centre, however, is not a common reaction. Taking a reaction of the general form shown in Scheme 6.3;



Scheme 6.3: General phosphine substituent exchange reaction

The sum of the bond energies before and after the reaction is identical (3 P-A bonds and 3 P-B bonds) meaning that, in the absence of any steric effects, there is little to no energetic advantage to the reaction. Similarly, neither state is more entropically favourable than the other. However, if one or more of the substituents were extremely labile, such a reaction could proceed *via* a dissociative mechanism. (Scheme 6.3) If, for example, the P-A bond were to spontaneously cleave, the resulting fragments (either charged or radical, depending on the nature of the cleavage) would be far more reactive and thus able to initiate a substitution reaction with the other phosphine.⁵



Scheme 6.4: Proposed exchange reaction initiated through the loss of a labile substituent.

If left for a sufficient period of time, this would result in a statistical redistribution of the substituents. (Figure 6.1)

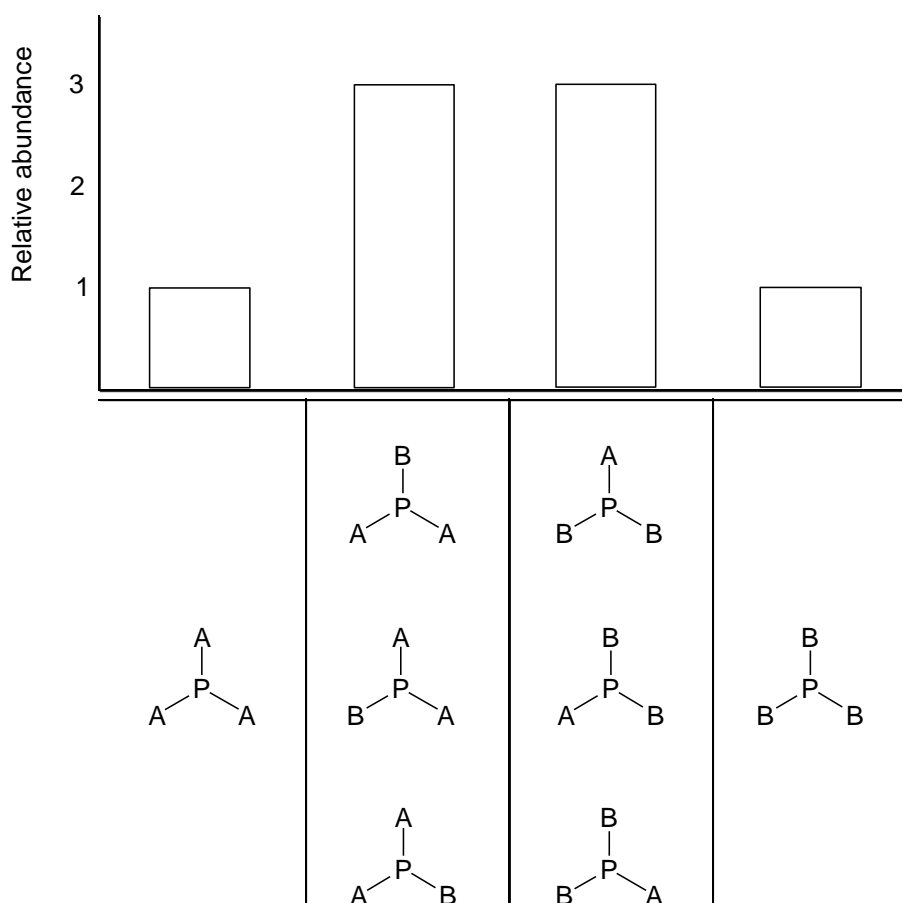


Figure 6.1: Statistical distribution of phosphine substituents

Whilst not as strongly basic as the analogous amines, the basicity of phosphines due to the presence of the lone pair of electrons has been acknowledged for many years.⁶ Multiple studies have been carried out to determine the pKa values of various different phosphines in order to quantify the effect of the substituents. During these experiments it was found that some of the phosphines containing P-H bonds displayed a distinctly acidic character, notably those which also possessed aryl substituents due to the stabilisation of the conjugate base by the aromatic substituents.⁷ (Figure 6.2)

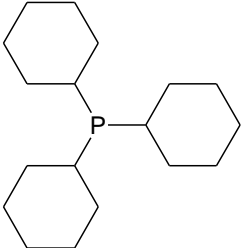
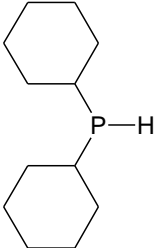
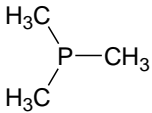
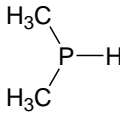
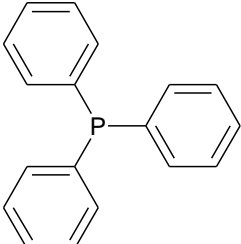
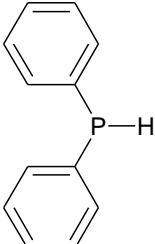
	pKa		pKa
	9.70		4.55
	8.65		3.91
	2.73		0.03

Figure 6.2: pKa values of selected tertiary and secondary phosphines

With this varying acid/base behaviour dependant on the substituents, it would seemingly be possible to combine acidic and basic phosphines and achieve a proton transfer from one to the other. The following step depends largely on the substituents of the newly formed phosphonium ion. If they are bound too strongly or disinclined to support a positive charge then the reaction will not proceed. If, however, appropriate leaving groups are employed there is the potential for them to transfer on to the phosphide thus complete the exchange.

6.2: Results and Discussion

When $C_6H_4-1,2-(PH_2)_2$ and $P(SiMe_3)_3$ were combined in a 1:1 ratio in an NMR tube with benzene- d^6 at ambient temperature there were no immediate signs of reaction. However, over the course of *circa* eight weeks, new resonances began to emerge in the $^{31}P\{^1H\}$ NMR spectra. The new resonances appeared as a singlet at δ -236 and coupling doublets at δ -121 and δ -124. As the reaction progressed, additional resonances were observed indicating the generation of further products. After *circa* twenty weeks an equilibrium appeared to have been reached. The chemical shifts of the products seemed to fall in localised regions around those of the two reagents, $C_6H_4-1,2-(PH_2)_2$ at δ -125.4 and $P(SiMe_3)_3$ at δ -251.8. (Figures 6.3 – 6.5) The $^{31}P\{^1H\}$ NMR spectroscopic data is listed in Table 6.1.

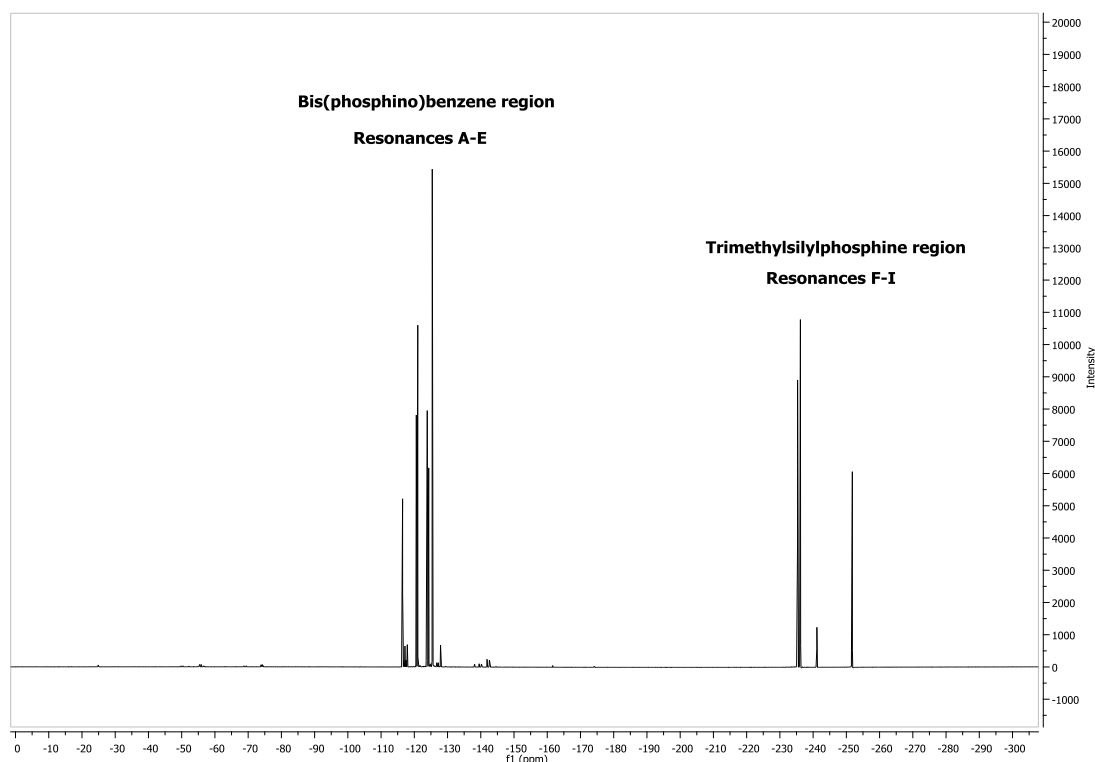


Figure 6.3: $^{31}P\{^1H\}$ NMR spectrum of the reaction of $C_6H_4-1,2-(PH_2)_2$ with $P(SiMe_3)_3$

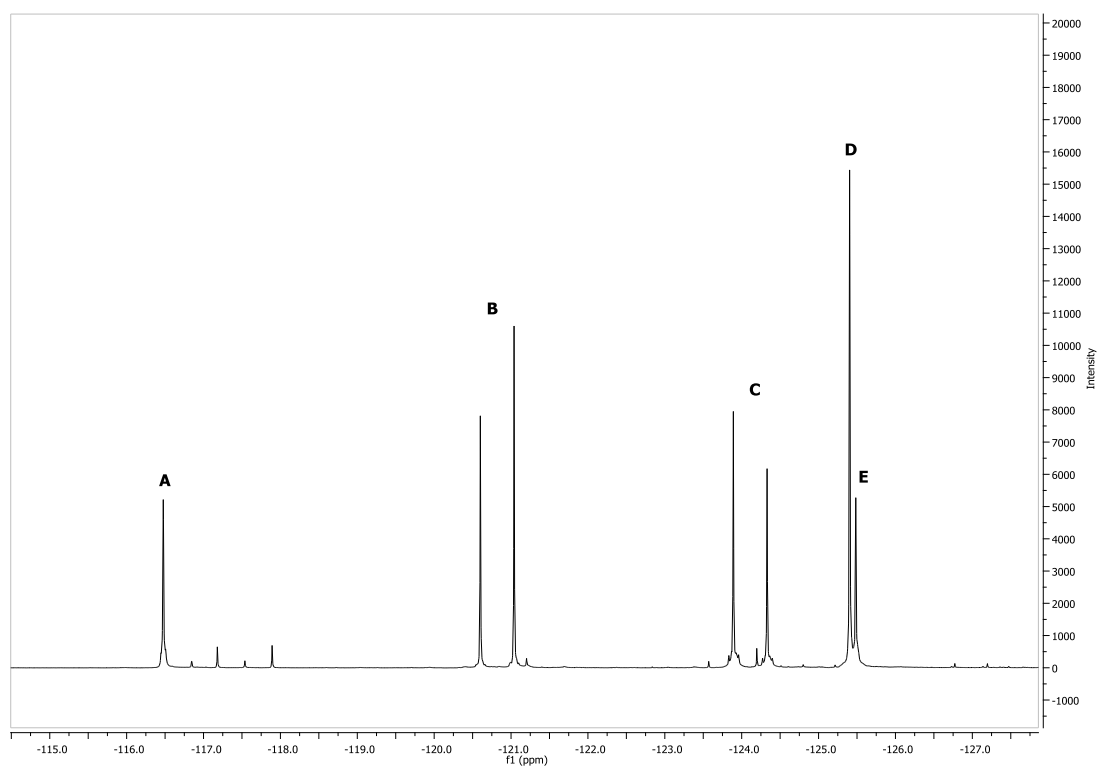


Figure 6.4: Expanded $\text{C}_6\text{H}_4\text{-1,2-(PH}_2)_2$ region of $^{31}\text{P}\{^1\text{H}\}$ NMR spectrum of the reaction of $\text{C}_6\text{H}_4\text{-1,2-(PH}_2)_2$ with $\text{P(SiMe}_3)_3$

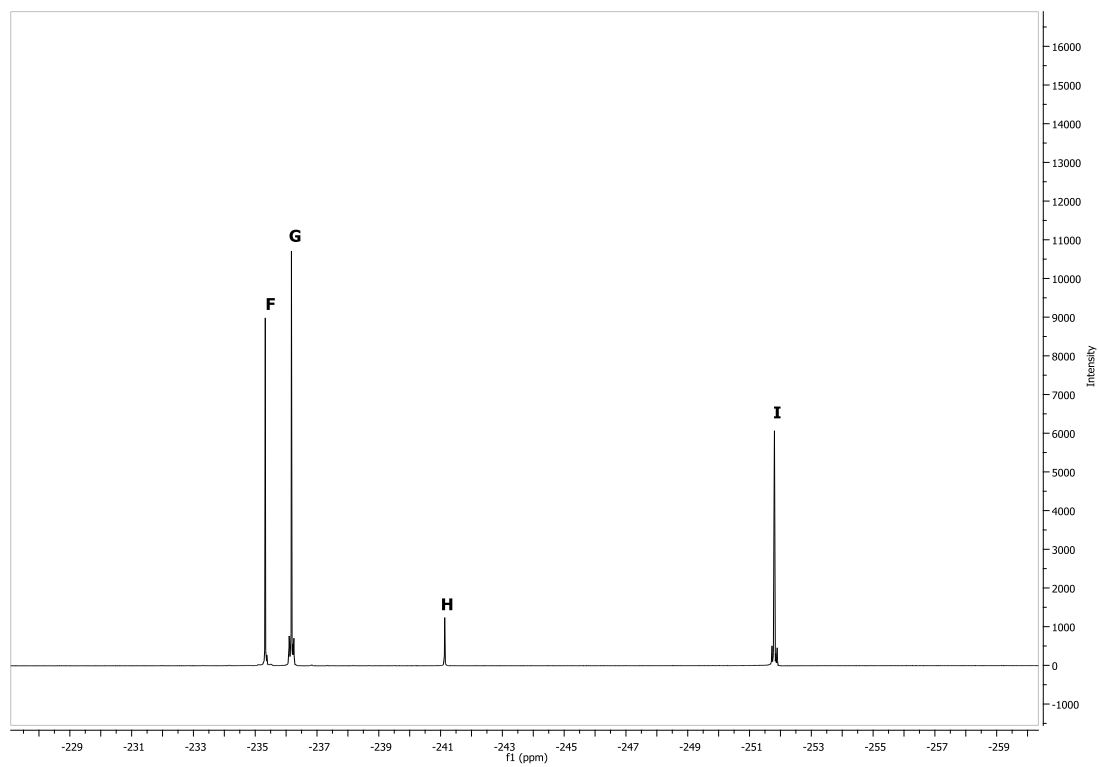


Figure 6.3: Expanded $\text{P(SiMe}_3)_3$ region of $^{31}\text{P}\{^1\text{H}\}$ NMR spectrum of the reaction of $\text{C}_6\text{H}_4\text{-1,2-(PH}_2)_2$ with $\text{P(SiMe}_3)_3$

Resonance	Chemical Shift	$J^{31}\text{P}-^{31}\text{P}$
A	-116.5	-
B	-120.8	71
C	-124.1	71
D	-125.4	-
E	-125.5	-
F	-235.3	-
G	-236.2	-
H	-241.1	-
I	-251.8	-

Table 6.1: $^{31}\text{P}\{^1\text{H}\}$ NMR spectroscopic data from the reaction of C_6H_4 -1,2-(PH_2)₂ with $\text{P}(\text{SiMe}_3)_3$

Resonances **D** and **I** correspond to the reagents, C_6H_4 -1,2-(PH_2)₂ and $\text{P}(\text{SiMe}_3)_3$, respectively. The products were positively identified using proton coupled ^{31}P NMR spectroscopy, which showed $J_{\text{P-H}}$ values of approximately 180-200 Hz attributed to $^1J_{\text{P-H}}$ couplings as well as in some cases the smaller values of <10 Hz which were attributed $^3J_{\text{P-H}}$ arising from the P-SiMe₃ groups. (Figures 6.6 to 6.8)

The ^{31}P NMR spectrum of the C_6H_4 -1,2-(PH_2)₂ region showed that the resonance **A**, which was a singlet without proton coupling, now appeared as a second order doublet of doublets. This data is consistent with the literature data for *meso*- C_6H_4 -1,2-(PHSiMe_3)₂.⁸ Comparison of the relative integrals showed that the resonance **E** visible in the proton coupled spectrum was only half of the total signal observed in the proton decoupled spectrum and thus it may well have been split into a doublet with the other half lost among the overlapping signals around δ -125. This, along with the

reasonable agreement of the chemical shift with published data⁸ and the appearance alongside the *meso*- form make the assignment of **E** to *rac*-C₆H₄-1,2-(PHSiMe₃)₂ a logical inference. The pair of doublets, **B** and **C**, indicated an asymmetric bis(phosphino)benzene derivative and were split into a triplet of doublets and a doublet of doublets respectively in the proton coupled spectrum. The triplet and doublet splitting are indicative of PHR and PH₂ groups respectively, suggesting that these resonances correspond to C₆H₄-1,2-(PHSiMe₃)(PH₂).

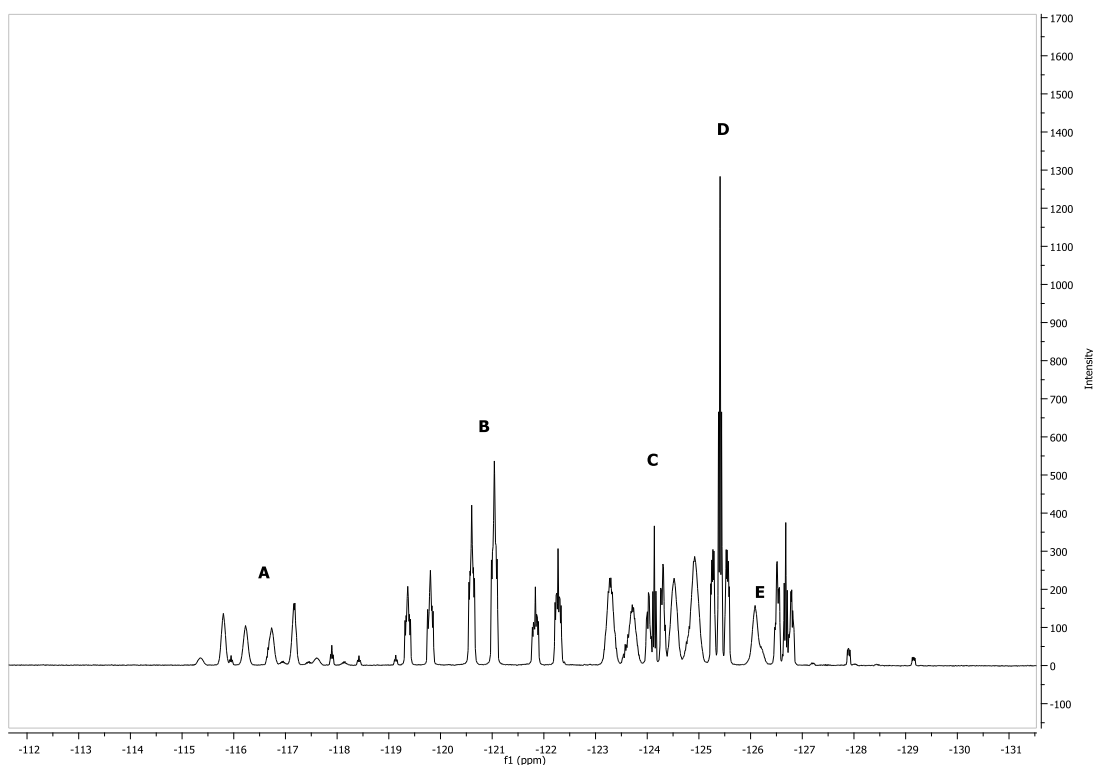


Figure 6.6: Expanded *Bn*(PH₂)₂ region of ³¹P NMR spectrum of the reaction of C₆H₄-1,2-(PH₂)₂ with P(SiMe₃)₃

The region of the ³¹P NMR spectrum between δ -230 and δ -260 displayed the resonances of three products along with that of P(SiMe₃)₃. The products were easily assigned using the *J*_{P-H} couplings obtained from the ³¹P NMR spectrum for which even the long range couplings were well defined. The resonance **F** changed from a singlet

into a triplet (182 Hz), indicating two H atoms bound to the P. The long range coupling (4 Hz) produced a decet which indicated nine SiMe₃ protons. Combined, these data suggested the product to be PH₂(SiMe₃). The resonance **G** was observed as a large doublet splitting (187 Hz) and its multiplicity arising from the long range coupling (4 Hz), indicated it to arise from a PH(SiMe₃)₂ (the long range coupling should give a nonadecet, but at best *circa* 15 peaks were detected, the four outermost being too small to be observable). The resonance **H** was split into a simple quartet in the proton coupled spectrum. The value of the coupling constant (186 Hz) is consistent with ¹J_{P-H}, thus the resonance was attributed to PH₃.

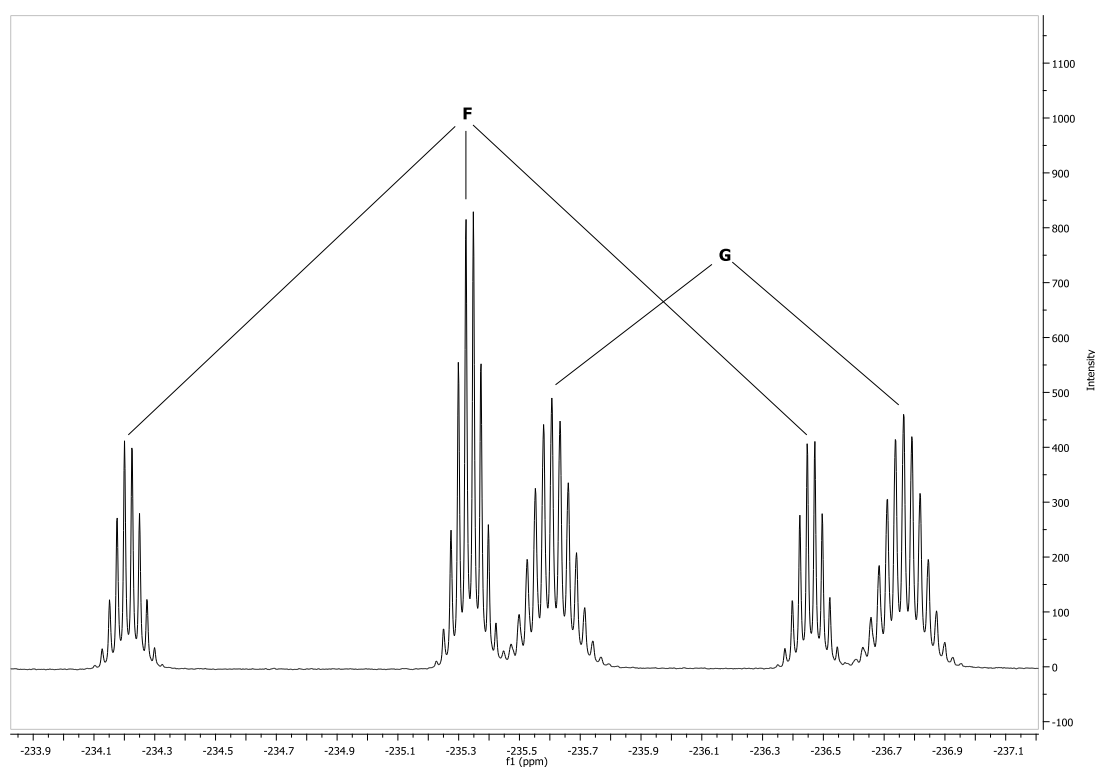


Figure 6.7: Expanded PH(SiMe₃)₂ and PH₂(SiMe₃) ³¹P NMR spectroscopic resonances from the reaction of C₆H₄-1,2-(PH₂)₂ with P(SiMe₃)₃

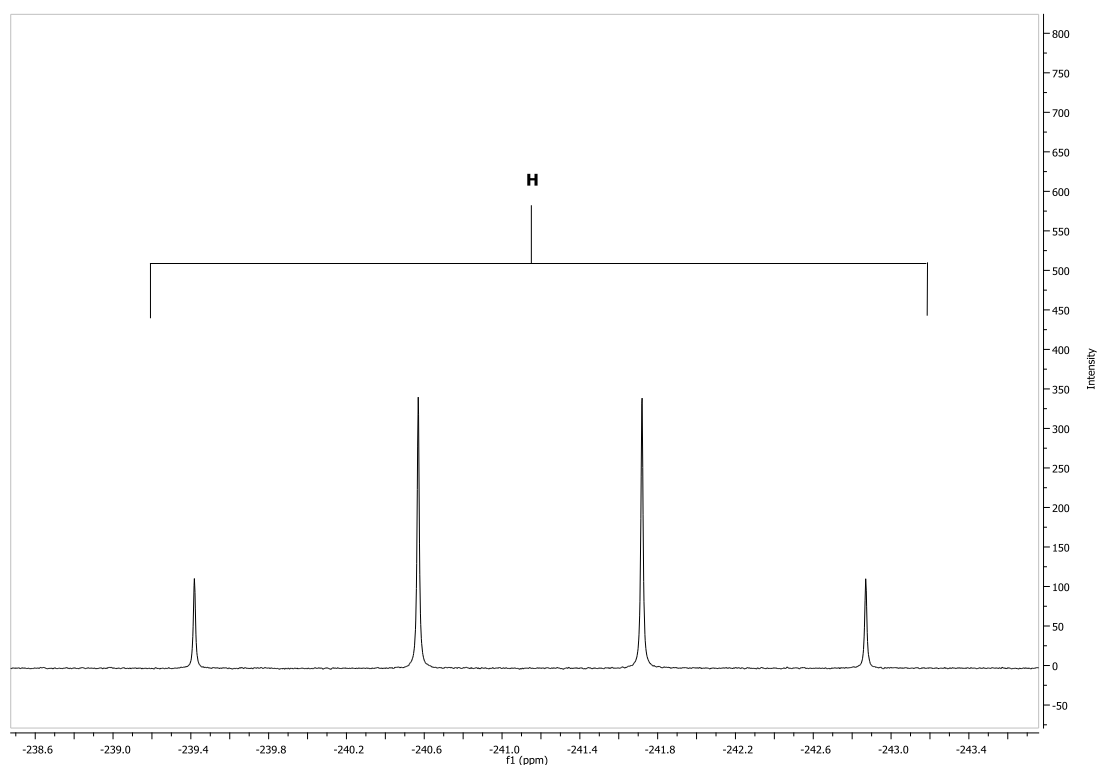
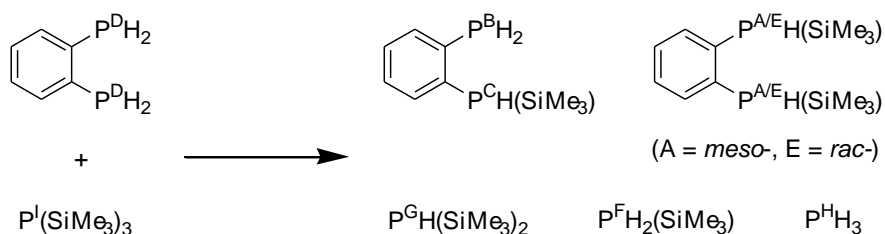


Figure 6.8: Expanded PH_3 ^{31}P NMR spectroscopic resonance from the reaction of C_6H_4 -1,2- $(\text{PH}_2)_2$ with $\text{P}(\text{SiMe}_3)_3$

These assignments indicated that the C_6H_4 -1,2- $(\text{PH}_2)_2$ and $\text{P}(\text{SiMe}_3)_3$ were undergoing a reaction in which the H atoms and SiMe_3 groups were exchanged between the P atoms. (Scheme 6.5)



Scheme 6.5: Substituent exchange reaction between C_6H_4 -1,2- $(\text{PH}_2)_2$ and $\text{P}(\text{SiMe}_3)_3$ (P atoms labelled corresponding to $^{31}\text{P}\{^1\text{H}\}$ NMR assignments)

A mechanism by which this exchange occurs could be initiated by the donation of the acidic protons of the $\text{C}_6\text{H}_4\text{-1,2-(PH}_2)_2$ to the $\text{P}(\text{SiMe}_3)_3$ to create a phosphonium ion. This would then release a SiMe_3 cation to the deprotonated $\text{C}_6\text{H}_4\text{-1,2-(PH}_2)_2$. In order to test this theory, two simultaneous reactions were performed. A 1:1 reaction mixture of $\text{C}_6\text{H}_4\text{-1,2-(PH}_2)_2$ and $\text{P}(\text{SiMe}_3)_3$ in benzene- d^6 was divided between two NMR tubes, to one of which was added 0.2 equivalents of NEt_3HCl to act as a catalytic proton source. The tubes were then heated to $50\text{ }^\circ\text{C}$ and the progress of both reactions was monitored regularly by $^{31}\text{P}\{^1\text{H}\}$ NMR spectroscopy. It was observed that the initial production of both $\text{PH}(\text{SiMe}_3)_2$ and $\text{PH}_2(\text{SiMe}_3)$ occurred much faster in the acid catalysed reaction, supporting the proposed mechanism. (Figure 6.9)

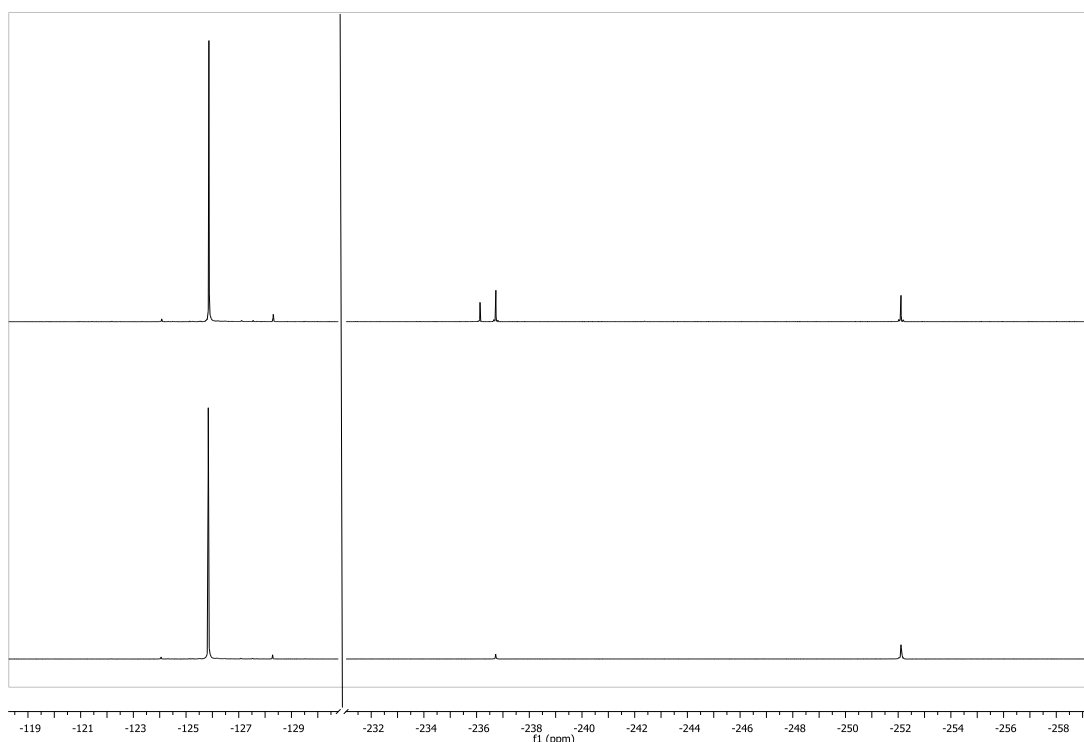


Figure 6.9: $^{31}\text{P}\{^1\text{H}\}$ NMR spectra of the catalysed (top) and uncatalysed (bottom) reaction of $\text{C}_6\text{H}_4\text{-1,2-(PH}_2)_2$ with $\text{P}(\text{SiMe}_3)_3$ at 40 hours

The relative concentrations of both reagents and two of the products $\text{PH}(\text{SiMe}_3)_2$ and $\text{C}_6\text{H}_4\text{-1,2-(PHSiMe}_3\text{)(PH}_2\text{)}$, were determined from their relative integrals of the ^{31}P NMR spectra over the course of the reaction. A series of graphs showing the consumption of the reagents and the generation of the products over time are displayed in the following four figures. (Figures 6.10 to 6.13) (*N.B.* Values quoted as $<0\%$ or $>100\%$ are due to random errors of integration).

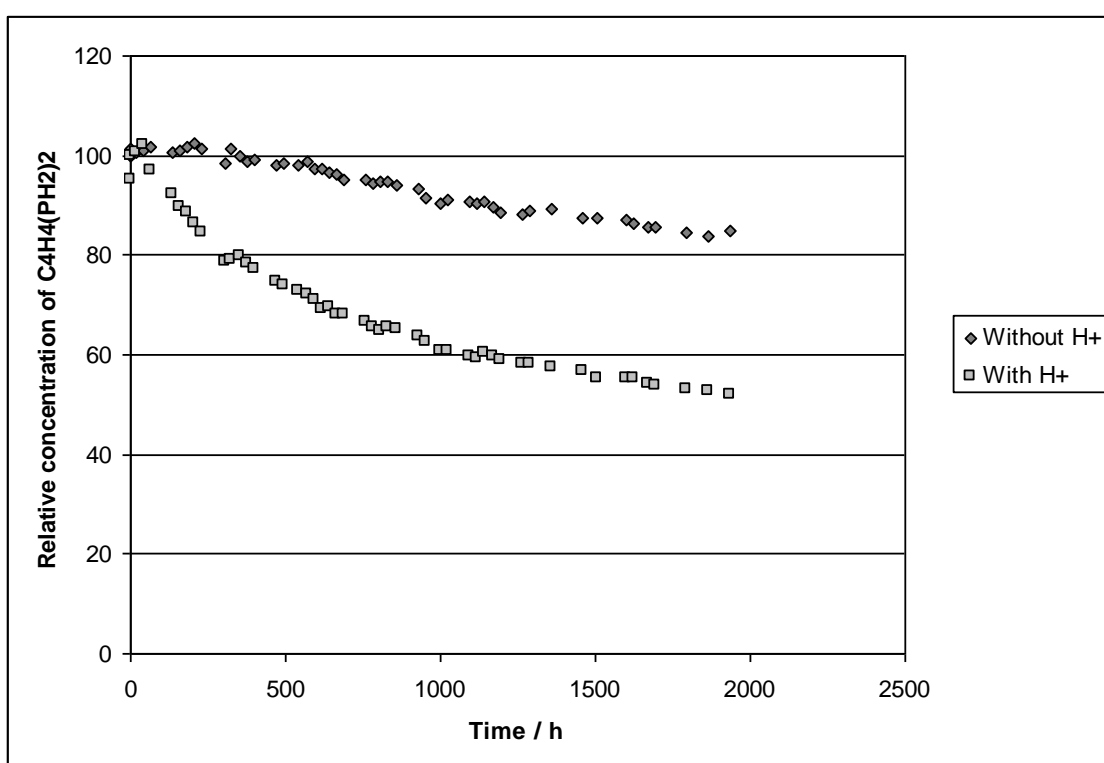


Figure 6.10: Relative concentration of $\text{C}_6\text{H}_4\text{-1,2-(PH}_2\text{)}_2$ vs. time

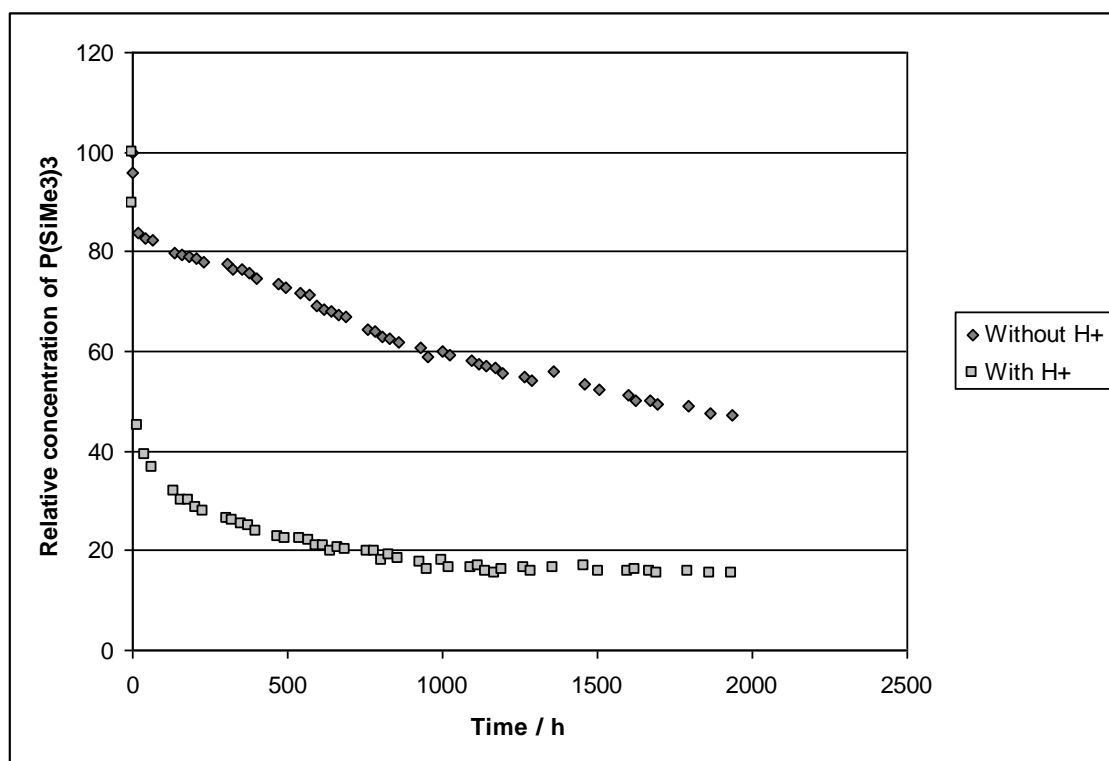


Figure 6.11: Relative concentration of $P(SiMe_3)_3$ vs. time

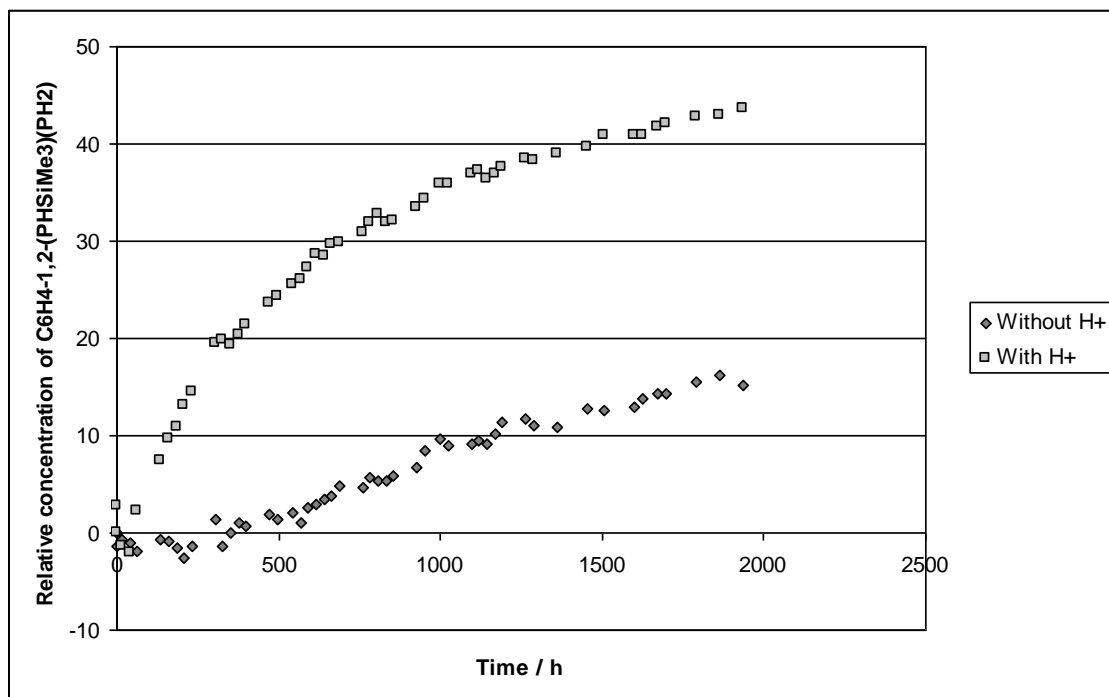


Figure 6.12: Relative concentration of $C_6H_4-1,2-(PHSiMe_3)(PH_2)$ vs. time

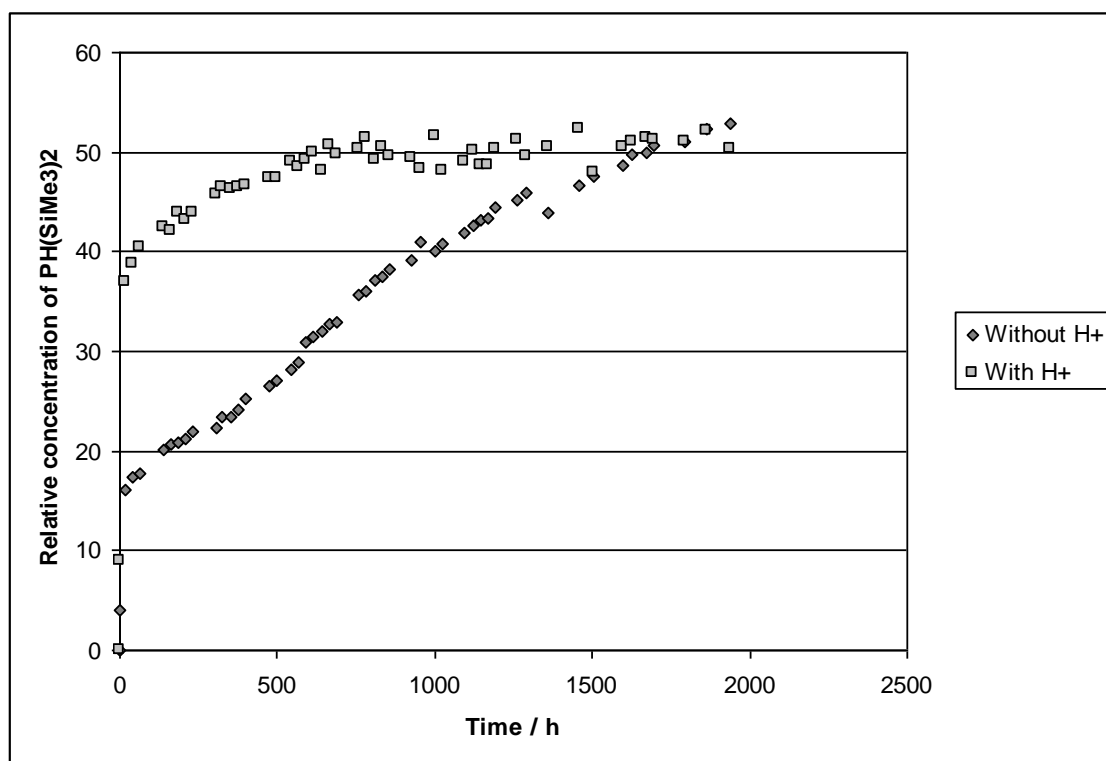


Figure 6.13: Relative concentration of $\text{PH}(\text{SiMe}_3)_2$ vs. time

A direct comparison revealed that the acid catalysed reaction proceeded more quickly than the uncatalysed reaction. The graph showing the percentage of $\text{PH}(\text{SiMe}_3)_2$ appeared to show that between 1500 and 2000 hours the uncatalysed reaction had caught up with and possibly overtaken the catalysed exchange. This was due to the steady state conversion of $\text{PH}(\text{SiMe}_3)_2$ to $\text{PH}_2(\text{SiMe}_3)$ and PH_3 . These products were not seen in the uncatalysed reaction, in which the amount of $\text{PH}(\text{SiMe}_3)_2$ continued to increase at a steady rate. Interestingly, this seemed to imply that although it is much slower, the uncatalysed reaction was, up to this point at least, more controlled and selective. This could clearly be seen the $^{31}\text{P}\{^1\text{H}\}$ NMR spectra, which showed that after over 1900 hours the uncatalysed reaction still contained almost no evidence of the multiple exchange products, with only $\text{C}_6\text{H}_4\text{-1,2-(PHSiMe}_3\text{)(PH}_2\text{)}$ and $\text{PH}(\text{SiMe}_3)_2$

being produced while the catalysed reaction showed the full range of exchange products. (Figure 6.14)

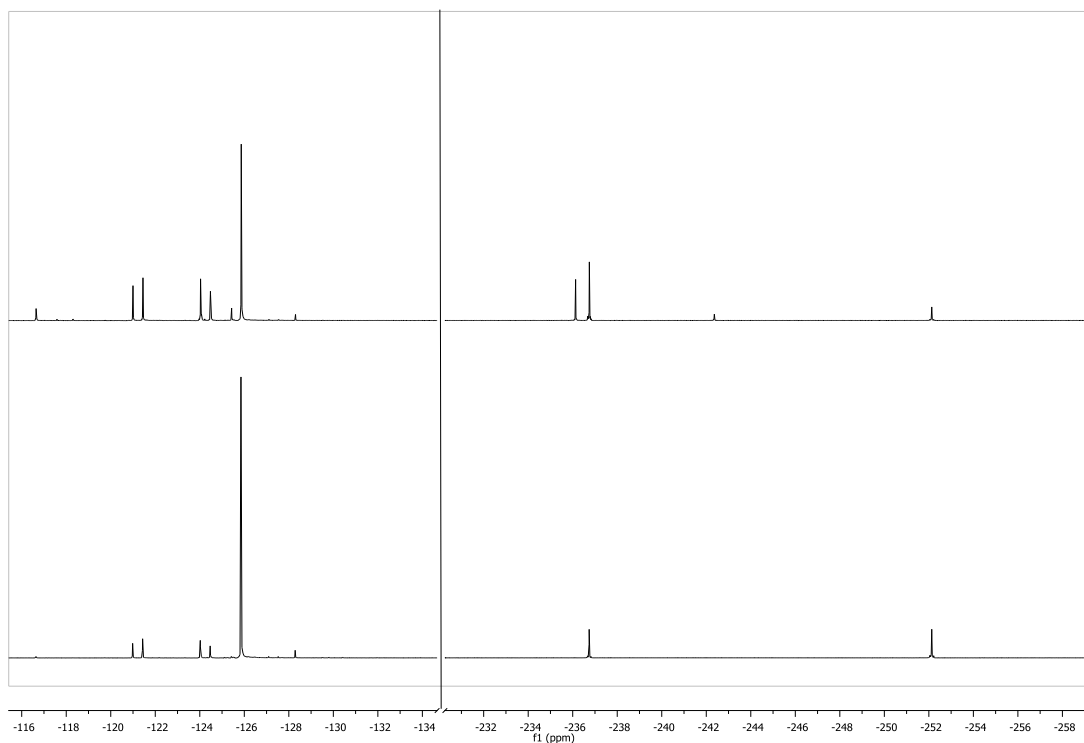


Figure 6.14: $^{31}\text{P}\{^1\text{H}\}$ NMR spectra of the catalysed (top) and uncatalysed (bottom) reaction of $\text{C}_6\text{H}_4\text{-1,2-(PH}_2\text{)}_2$ with $\text{P}(\text{SiMe}_3)_3$ at 1936 hours

Although still faster than the uncatalysed reaction, the catalysed reaction displayed a induction period before the production of $\text{C}_6\text{H}_4\text{-1,2,}(\text{PHSiMe}_3)(\text{PH}_2)$ was observed. The reason for this was revealed when examination of the ^1H NMR spectrum of the reaction mixture showed a singlet at δ 0.14 indicating the presence of SiMe_3Cl , alongside the ^{31}P coupled resonances corresponding to the SiMe_3 groups of $\text{PH}(\text{SiMe}_3)_2$ and $\text{PH}_2(\text{SiMe}_3)_2$. (Figure 6.15)

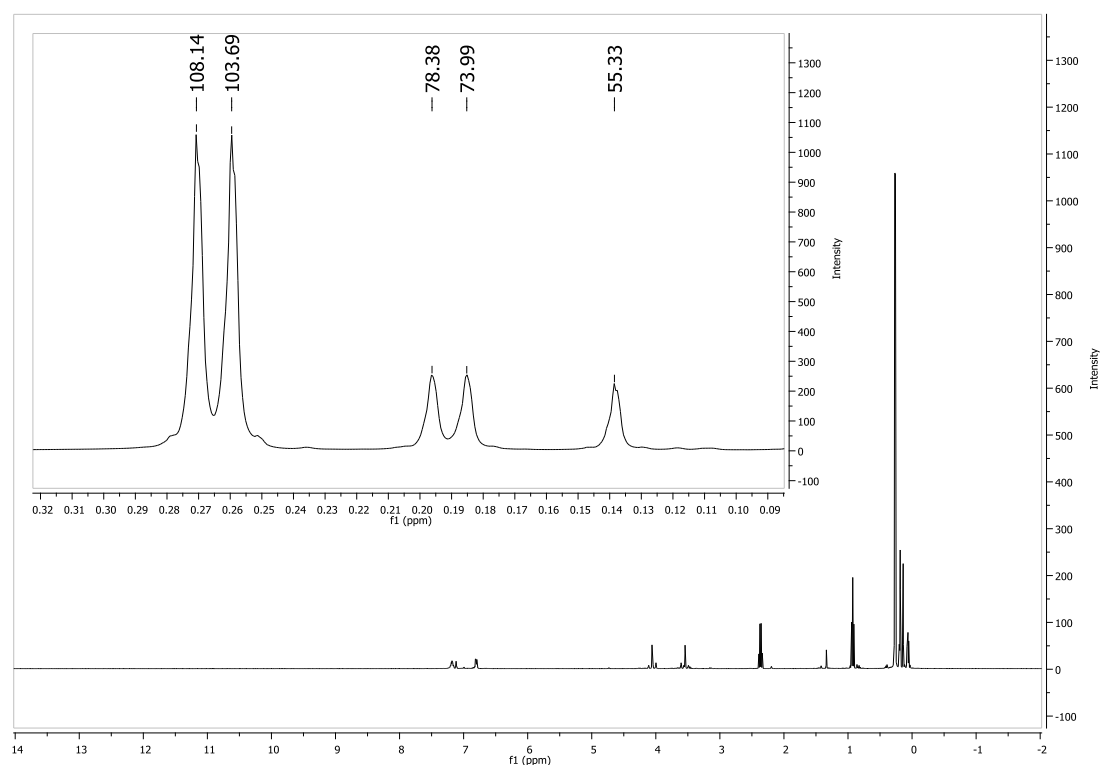
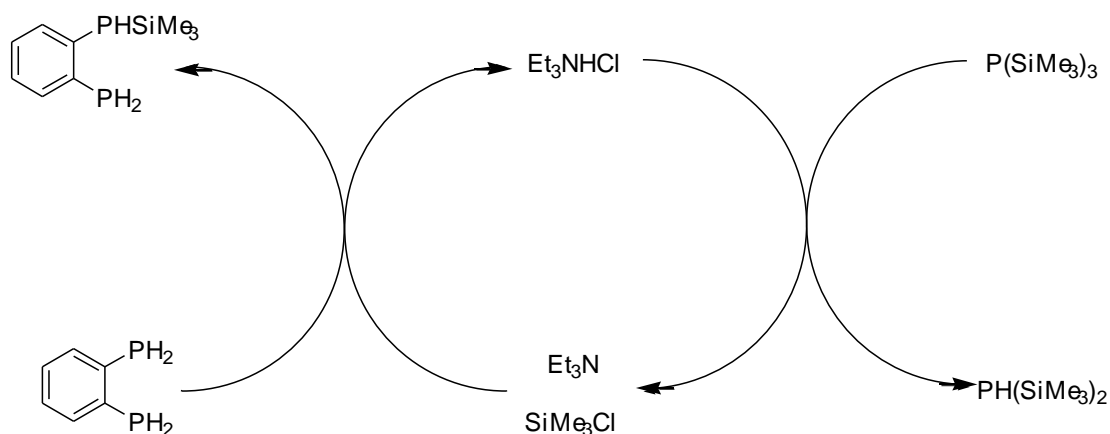


Figure 6.15: ^1H NMR spectrum of the reaction of $\text{C}_6\text{H}_4\text{-1,2-(PH}_2)_2$ with $\text{P(SiMe}_3)_3$ at 184 hours.

This indicated that the NEt_3HCl firstly protonated the $\text{P(SiMe}_3)_3$ which caused the loss of a SiMe_3 group, affording SiMe_3Cl and NEt_3 . The basic NEt_3 then facilitated the loss of a proton from the $\text{C}_6\text{H}_4\text{-1,2-(PH}_2)_2$, the conjugate base of which in turn reacted with the SiMe_3Cl to form $\text{C}_6\text{H}_4\text{-1,2, (PHSiMe}_3\text{)(PH}_2)$ and regenerate the catalyst. (Scheme 6.7)



Scheme 6.7: Catalysis of substituent exchange by a proton source, Et_3HCl

The absolute values for the conversion of $\text{P}(\text{SiMe}_3)_3$ to its various derivatives could not be obtained from the ^{31}P integrals due to the unusually long relaxation time of the phosphorus nuclei causing some resonances to appear with a deceptively low intensity. For example the value of T_1 determined for the P atom of $\text{P}(\text{SiMe}_3)_3$ was 44.6 s with an error of circa 4.84 s. The major reason for this large value is attributed to the nuclear magnetic dipole coupling (a significant contributing factor in spin-spin relaxation) and its dependence on internuclear distance. The dipole-dipole coupling constant is given by equation 6.1.

$$b = - \frac{\mu_o}{4\pi} \frac{\hbar \gamma_a \gamma_b}{r^3} \quad \text{eq 6.1}$$

Where γ_a and γ_b are the magnetogyric ratios of the two nuclei and r is the distance through space between them.⁹

Because spin active C and Si have relatively low magnetogyric ratios and natural abundances, the only other nuclei of any consequence that the P has available to couple

to are the protons. These protons though are on average approximately 3.7 Å away from the phosphorus¹⁰ in comparison with, for example, PH₃ with P-H separations of around 1.42 Å¹¹ and a relaxation time less than 1 s.¹² Because of the inverse cube relationship, the fact that the protons are 2.61 times further away from the phosphorus in the case of P(SiMe₃)₃ means that the dipole-dipole coupling is 17.7 times weaker, greatly increasing the relaxation time. Clearly the weak dipole-dipole coupling alone does not account for the long relaxation time but this is the predominant contributor.

6.3: Conclusions

The reaction between $\text{P}(\text{SiMe}_3)_3$ and $\text{C}_6\text{H}_4\text{-1,2-(PH}_2)_2$ was shown to result in an exchange of SiMe_3 and H groups over an extended time period to produce several different products. Further investigation of this reaction revealed that a catalytic amount of $\text{NEt}_3(\text{HCl})$ greatly increased the rate of exchange, indicating that the reaction proceeds via an ionic mechanism which was aided by the introduction of an additional proton source.

The observation that the resonance of $\text{P}(\text{SiMe}_3)_3$ in the ^{31}P NMR spectrum was smaller than expected prompted an investigation of its relaxation time, which was observed to be 44.6 seconds. The reason for this incredibly slow relaxation was attributed primarily to the low nuclear magnetic dipole coupling due to the distance between the P and the H atoms (the closest available spin-active nuclei).

References

1. Macgregor, S. A., *Chem. Soc. Rev.*, 2007, **36**, 67
2. A. G. Abatjoglou and D. R. Bryant, *Organometallics*, 1984, **3**, 932
3. K.-C. Kong and C.-H. Cheng, *J. Am. Chem. Soc.*, 1991, **113**, 6313
4. D. K. Morita, J. K. Stille and J. R. Norton, *J. Am. Chem. Soc.*, 1995, **117**, 8576
5. Kyba, E. P., *J. Am. Chem. Soc.*, 1976, **98**, 4805
6. Li, JN., Liu, L., Fu, Y., Gou, QX., *Tetrahedron*, 2006, **62**, 4453
7. Henderson Jr, W.A., Streuli, C. A., *J. Am. Chem. Soc.*, 1960, **82**, 5791
8. Hitchcock, P. B., Lappert, M. F., Leung, W. P., Yin, P., *J. Chem. Soc. Dalton Trans.*, 1995, 3925
9. Levitt, M. H., *Spin Dynamics*, 2001, 527
10. Bruckmann, J., Krüger, C., *Acta. Crystallogr. C.*, 1995, **51**, 1152
11. Lide, D. R., *Handbook of Chemistry and Physics*, 89TH Ed., 2008, 9-48
12. Dixon, K. R., Mason. J., *Multinuclear NMR*, 1987, 369

Experimental

General Details

All work was carried out under argon using standard Schlenk-line and cannula techniques, or in a dry nitrogen-filled glovebox. Glassware was dried in an oven at around 130 °C prior to use. Solvents were dried by heating to reflux over the appropriate drying agents (sodium, potassium or NaK), stored over potassium mirror or molecular sieves and degassed prior to use.

NMR spectra were recorded on either a Bruker Avance DPX 300 MHz spectrometer, or a Varian Direct Drive 400, 500 or 600 MHz spectrometer. All shifts are reported in ppm, proton and carbon shifts are referenced to the residual proton and ^{13}C chemical shifts respectively of the internal solvent, phosphorus shifts are referenced to $\text{H}_3\text{PO}_{4(\text{aq})}$, tin shifts are referenced to SnMe_4 , silicon shifts are referenced to SiMe_4 . Coupling constants are quoted in Hertz (Hz). The spectrometer frequencies (in MHz) for the various nuclei observed were as follows;

	Advance DPX 300	Direct Drive 400	Direct Drive 500	Direct Drive 600
^1H	300.13	399.50	499.91	599.69
^{13}C	75.47	100.46	125.71	150.81
^{29}Si	-	79.73	-	119.14
^{31}P	121.49	161.71	-	242.78
^{119}Sn	-	148.99	-	223.63

NMR spectra performed on the 600 MHz spectrometer were carried out by Dr I. J. Day. Crystals for X-ray diffraction were covered in an inert oil and suitable single crystals were selected under a microscope and mounted on a Kappa CCD diffractometer. Data was collected at 173(2) K using Mo K α radiation at 0.71073 Å. The structures were refined with SHELXL-97.¹ Structural determinations were carried out by Dr. P. B. Hitchcock and Dr M. P. Coles.

Mass spectrometry (EI) was performed using a Fisons Instruments VG Autospec mass spectrometer at 70 eV. Measurements were carried out by Dr A. K. Abdul-Sada.

Elemental analyses were performed by Stephen Boyer at London Metropolitan University.

Starting materials

The following materials were synthesised using published preparations;



$\text{P}(\text{SiMe}_3)_3$ was synthesised *via* a preparation adapted from the literature; ⁴

Red phosphorus (62 g, 2.0 mol), sodium (140 g, 6.1 mol) and naphthalene (3.0 g, 0.023 mol) were stirred in refluxing DME for 3 days causing a colour change from red to grey. Trimethylsilyl chloride (787 ml, 674 g, 6.2 mol) was added slowly and the mixture was stirred for one more day. The resulting off white slurry was diluted with further DME and filtered through celite. The solvent was distilled off at atmospheric pressure, followed by distillation of the phosphine at 6 mmHg and $\approx 87^\circ\text{C}$. Product collected as a colourless liquid.

Yield = 225-380 g, 45-76 %

Cp^*SnI_3 (**4.1**) was synthesised *via* an unpublished method;

Pentamethylcyclopentadienyl potassium (0.44 g, 2.5 mmol) was dissolved in diethyl ether and cooled to 0°C . The solution was added dropwise to a stirring solution of tin tetraiodide, also in diethyl ether at 0°C . This caused a change from yellow to dark orange and the production of a precipitate. The mixture was stirred at 0°C for 2 h before warming to ambient temperature and being left stirring overnight, after which the

solution had become dark red. The solvent was removed *in vacuo* and the product was extracted with hexane. The product was crystallised as dark red needles at -30 °C.

Yield = 1.42 g, 89 %

The following materials were purchased from Sigma-Aldrich;

SnI₂

Cp^{Me4}H

ⁿBuLi

Me₂SnCl₂

SnCl₂

TiCp₂Cl₂

Mg

FeCl₂

^tBu₂SnCl₂

Me₂GeCl₂

AdCP

Bn(PH₂)₂ was purchased from Strem Chemicals Inc.

The following materials were kindly donated by other lab users;

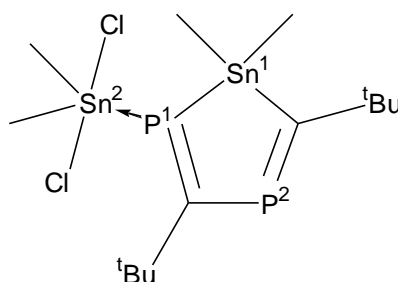
SnI₄

Cp*K

^tBuCp

Experimental Procedures

Synthesis of $\text{Me}_2\text{Sn}(\text{P}_2\text{C}_2^t\text{Bu}_2)\text{SnMe}_2\text{Cl}_2$ (2.1)



An NMR tube was charged with $\text{Cp}_2\text{Zr}(\text{P}_2\text{C}_2^t\text{Bu}_2)$ (0.029 g, 0.069 mmol) and dimethyltin dichloride (0.031 g, 0.14 mmol). The mixture was then dissolved in a combination of THF and d_6 -benzene (approximately 1:10), degassed and heated to 50 °C in the dark for seven days, over which time the colour had changed from the initial orange, becoming pale yellow. The solution was placed in a -30 °C freezer.

Yield = approx 85 % by ^{31}P NMR spectroscopy

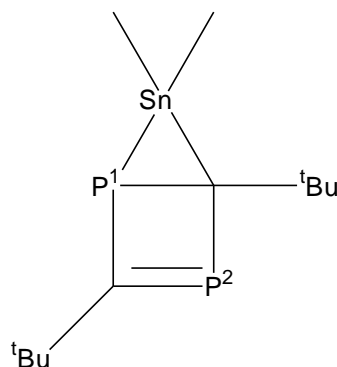
^1H NMR: δ = 1.32 [s, 9H, ^tBu], 1.22 [s, 9H, ^tBu], 0.89 [d, 6H, $^3J(^{31}\text{P}, ^1\text{H}) = 4$ Hz, $^2J(^{117/119}\text{Sn}, ^1\text{H}) = 57$ Hz, Sn^1Me_2], 0.58 [s, 6H, $^2J(^{119}\text{Sn}, ^1\text{H}) = 58$ Hz, Sn^2Me_2]

$^{31}\text{P}\{^1\text{H}\}$ NMR: δ = 311.2 [d, broad, 1P, $^2J(^{31}\text{P}, ^{31}\text{P}) = 80$ Hz, $^2J(^{117/119}\text{Sn}, ^{31}\text{P}) = 124$ Hz, P^2], 21.4 [d, 1P, $^2J(^{31}\text{P}, ^{31}\text{P}) = 80$ Hz, $^1J(^{119}\text{Sn}, ^{31}\text{P}) = 1635$ Hz, $^1J(^{117}\text{Sn}, ^{31}\text{P}) = 1560$ Hz, Dative $^1J(^{117/119}\text{Sn}, ^{31}\text{P}) = 37$ Hz, P^1]

$^{119}\text{Sn}\{^1\text{H}\}$ NMR: δ = 101 (s, 1Sn, Sn^2), 10 [dd, 1Sn, $^1J(^{119}\text{Sn}, ^{31}\text{P}) = 1635$ Hz, $^2J(^{119}\text{Sn}, ^{31}\text{P}) = 124$ Hz, Sn^1]

Elemental analysis unavailable due to mixed products.

Synthesis of $\text{Me}_2\text{Sn}(\text{P}_2\text{C}_2^t\text{Bu}_2)$ (2.2)



An NMR tube was charged with $\text{Cp}_2\text{Zr}(\text{P}_2\text{C}_2^t\text{Bu}_2)$ (0.028 g, 0.067 mmol) and dimethyltin dichloride (0.015 g, 0.067 mmol). The mixture was then dissolved in a combination of THF and d_6 -benzene (approximately 1:10), degassed and heated to 65 °C for five days, over which time the colour had changed from the initial orange, becoming slightly more yellow. (Product formed in a mixture with the $\text{Me}_2\text{Sn}(\text{P}_2\text{C}_2^t\text{Bu}_2)\text{SnMe}_2\text{Cl}_2$ and $\text{Me}_2\text{SnCl}(\text{P}_2\text{C}_2^t\text{Bu}_2)\text{H}$ which could not be separated).

^1H NMR: $\delta = 1.04$ (s, 9H, ^tBu), 0.99 (s, 9H, ^tBu), 0.82 [d, 3H, $^3J(^{31}\text{P}, ^1\text{H}) = 2$ Hz,

$^2J(^{117/119}\text{Sn}, ^1\text{H}) = 57$ Hz, SnMe], 0.65 [d, 3H, $^3J(^{31}\text{P}, ^1\text{H}) = 2$ Hz,

$^2J(^{117/119}\text{Sn}, ^1\text{H}) = 56$ Hz, SnMe]

$^{31}\text{P}\{^1\text{H}\}$ NMR: $\delta = 355.8$ [d, 1P, $^2J(^{31}\text{P}, ^{31}\text{P}) = 43$ Hz, $^2J(^{119}\text{Sn}, ^{31}\text{P}) = 242$ Hz, $^2J(^{117}\text{Sn},$

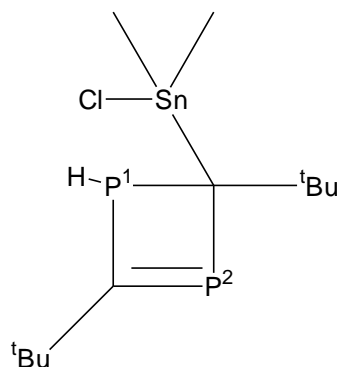
$^{31}\text{P}) = 231$ Hz, P^2], 4.6 [d, 1P, $^2J(^{31}\text{P}, ^{31}\text{P}) = 43$ Hz, $^1J(^{119}\text{Sn}, ^{31}\text{P}) = 1310$

Hz, $^1J(^{117}\text{Sn}, ^{31}\text{P}) = 1252$ Hz, P^1]

$^{119}\text{Sn}\{^1\text{H}\}$ NMR: $\delta = 67$ [dd, $^1J(^{119}\text{Sn}, ^{31}\text{P}) = 1310$ Hz, $^2J(^{119}\text{Sn}, ^{31}\text{P}) = 242$ Hz]

Elemental analysis unavailable due to mixed products.

Synthesis of $\text{Me}_2\text{SnCl}(\text{P}_2\text{C}_2^t\text{Bu}_2)\text{H}$ (2.3)



An ampoule was charged with $\text{Cp}_2\text{Zr}(\text{P}_2\text{C}_2^t\text{Bu}_2)$ (0.200 g, 0.47 mmol) and dimethyltin dichloride (0.104 g, 0.47 mmol). The mixture was then dissolved in THF, degassed and heated to 55 °C for seven days, over which time the colour had changed from the initial orange, becoming slightly more yellow. The THF was removed *in vacuo* and while in the solid state the compound turned a bright yellow. The product was extracted with cold hexane, concentrated and placed in a -30 °C freezer, where it crystallised as yellow needles.

Yield = 0.11 g, 65 %

^1H NMR: δ = 6.70 [dd, 1H, $^1J(^{31}\text{P}, ^1\text{H})$ = 165 Hz, $^3J(^{31}\text{P}, ^1\text{H})$ = 20 Hz, P^1H], 1.27 (s, 9H, ^tBu), 1.08 (s, 9H, ^tBu), 0.51 [s, 3H, $^2J(^{117/119}\text{Sn}, ^1\text{H})$ = 54 Hz, SnMe], 0.48 [s, 3H, $^2J(^{117/119}\text{Sn}, ^1\text{H})$ = 54 Hz, SnMe]

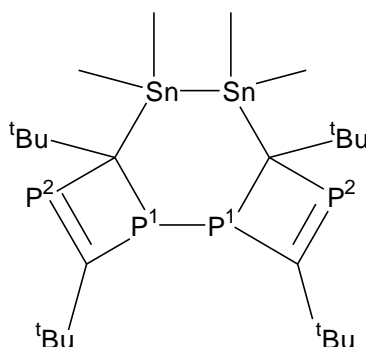
$^{31}\text{P}\{^1\text{H}\}$ NMR: δ = 362.5 [d, 1P, $^2J(^{31}\text{P}, ^{31}\text{P})$ = 42 Hz, P^2], -8.2 [d, 1P, $^2J(^{31}\text{P}, ^{31}\text{P})$ = 42 Hz, $^2J(^{117/119}\text{Sn}, ^{31}\text{P})$ = 17 Hz, P^1]

$^{119}\text{Sn}\{^1\text{H}\}$ NMR: δ = 112 (s, broad)

MS(EI): $[\text{M}^+] = 386$, $[\text{M}^+ - \text{Cl}] = 351$, $[\text{P}_2\text{C}_2^t\text{Bu}_2\text{H}^+] = 201$, $[\text{PC}_2^t\text{Bu}_2^+] = 169$, $[\text{P}_2\text{C}^t\text{BuH}^+] = 131$, $[\text{PC}^t\text{BuH}^+] = 101$

Elemental analysis unavailable due to time constraints.

Synthesis of $[\text{Me}_2\text{Sn}(\text{P}_2\text{C}_2^t\text{Bu}_2)]_2$ (2.4)



A sample of $\text{Me}_2\text{Sn}(\text{P}_2\text{C}_2^t\text{Bu}_2)$ in THF and benzene- d^6 (approximately 1:10) was exposed to sunlight for 14 days, causing an approximate 1/3 conversion to the product (measured by ^{31}P NMR spectroscopy). Crystals were obtained as yellow blocks from hexane at -30°C .

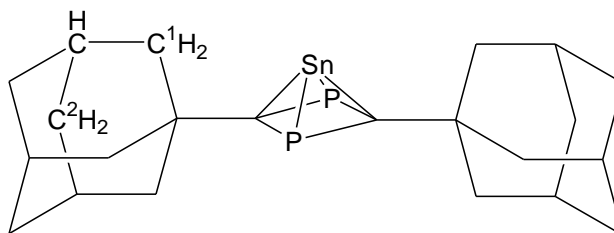
^1H NMR: $\delta = 1.48$ (s, 9H, ^tBu), 1.26 (s, 9H, ^tBu), 0.35 [s, 6H, $^2J(^{117/119}\text{Sn}, ^1\text{H}) = 44$ Hz, SnMe], 0.32 [s, 6H, $^2J(^{117/119}\text{Sn}, ^1\text{H}) = 45$ Hz, SnMe]

$^{31}\text{P}\{^1\text{H}\}$ NMR: $\delta = 297.8$ [dd, 2P, $^2J(^{31}\text{P}, ^{31}\text{P}) = 46$ Hz, $^3J(^{31}\text{P}, ^{31}\text{P}) = 42$ Hz, $^2J(^{117/119}\text{Sn}, ^{31}\text{P}) = 23$ Hz, $^3J(^{117/119}\text{Sn}, ^{31}\text{P}) = 10$ Hz, P^1], 49.2 [dd, 2P, $^2J(^{31}\text{P}, ^{31}\text{P}) = 46$ Hz, $^3J(^{31}\text{P}, ^{31}\text{P}) = 42$ Hz, $^2J(^{117/119}\text{Sn}, ^{31}\text{P}) = 15$ Hz, P^2]

$^{119}\text{Sn}\{^1\text{H}\}$ NMR: $\delta = -67$ [m, , $^2J(^{119}\text{Sn}, ^{31}\text{P}) = 23$ Hz, $^2J(^{119}\text{Sn}, ^{31}\text{P}) = 15$ Hz, $^3J(^{119}\text{Sn}, ^{31}\text{P}) = 10$ Hz, $^1J(^{119}\text{Sn}, ^{117}\text{Sn}) = 3495$ Hz]

Elemental analysis unavailable due to mixed products.

Synthesis of $\text{Sn}(\text{P}_2\text{C}_2\text{Ad}_2)$ (2.5)



An ampoule was charged with $\text{Cp}_2\text{Zr}(\text{P}_2\text{C}_2\text{Ad}_2)$ (0.152 g, 0.26 mmol) and tin dichloride (0.05 g, 0.26 mmol). The mixture was then dissolved in THF, degassed and heated to approximately 60 °C. The reaction mixture was stirred at this temperature for seven days, over which time the colour had changed from orange to pale yellow. The solvent was removed under vacuum and the product was extracted with hexane. The solution was cooled to -30 °C causing the product to crash out as a yellow powdery solid.

Yield = 0.072 g, 58 %

^1H NMR: δ = 1.75 (s, broad, 6H, CH), 1.51 (s, broad, 12H, CH_2), 1.44 [d, 6H, $^2J(^1\text{H}, ^1\text{H})$ = 48 Hz, C^2H], 1.42 [d, 6H, $^2J(^1\text{H}, ^1\text{H})$ = 48 Hz, C^2H]

$^{31}\text{P}\{^1\text{H}\}$ NMR: δ = 140.2 [s, $^1J(^{119}\text{Sn}, ^{31}\text{P})$ = 305 Hz, $^1J(^{117}\text{Sn}, ^{31}\text{P})$ = 291 Hz]

$^{119}\text{Sn}\{^1\text{H}\}$ NMR: δ = -2405 [t, $^1J(^{119}\text{Sn}, ^{31}\text{P})$ = 305 Hz]

Anal. Calc. for $\text{C}_{22}\text{H}_{30}\text{P}_2\text{Sn}$ (475.13 u): C = 55.61 %, H = 6.36 %. Found: C = 55.62 %, H = 6.36 %

Synthesis of $\text{TiCp}_2(\text{AdCP})_3$ (3.1)

Titanocene dichloride (0.10 g, 0.40 mmol) was dissolved in THF and stirred over activated magnesium. Once the colour had changed the mixture was cooled to -78

°C and filtered into a solution of AdCP (0.144 g, 0.080 mmol) in THF, also cooled to -78 °C. The reaction mixture was allowed to warm to ambient temperature and stirred for an hour before the solvent was removed *in vacuo* to give a dark green solid. The product was extracted with cold pentane and transferred to a -30 °C freezer.

^1H NMR: δ = 5.85-6.80 (m, 10H, Cp), 1.20-2.35 (m, 45H, Ad)

$^{31}\text{P}\{^1\text{H}\}$ NMR: δ = -50.4 [d, 1P, $^1J(^{31}\text{P}, ^{31}\text{P}) = 297$ Hz], -129.5 (s, 1P), -191.0 [d, 1P, $^1J(^{31}\text{P}, ^{31}\text{P}) = 297$ Hz]

MS(EI): $[\text{M}^+] = 714$, $[\text{M}^+ - \text{TiCp}] = 602$, $[\text{M}^+ - \text{AdCP}] = 536$, $[\text{Cp}(\text{AdCP})_2^+] = 422$

Elemental analysis unavailable due to mixed products.

Synthesis of $\text{ZrCp}(\text{P}_2\text{C}_2\text{Ad}_2)\text{Cl}_2\text{Fe}(\text{P}_2\text{C}_2\text{Ad}_2)$ (3.3)

An ampoule was charged with $\text{Cp}_2\text{Zr}(\text{P}_2\text{C}_2\text{Ad}_2)$ (0.1 g, 0.17 mmol) and iron (II) chloride (0.022 g, 0.17 mmol). The mixture was then dissolved in THF, degassed and heated to approximately 55 °C. The reaction mixture was stirred at this temperature for five days. The solvent was removed under vacuum and the product was extracted with hexane giving an orange-brown solution. The solution was cooled to -80 °C causing the product to crystallise as very dark purple, square plates.

Yield = 0.0125 g 7 %

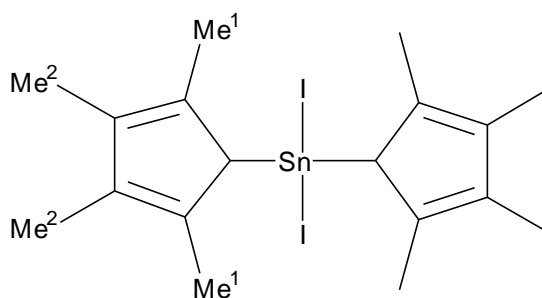
No NMR could be obtained due to the paramagnetic nature of the compound.

Elemental analysis unavailable due to time constraints.

Evans' Method NMR Spectroscopic Study of $\text{CpZr}(\text{P}_2\text{C}_2\text{Ad}_2)\text{Cl}_2\text{Fe}(\text{P}_2\text{C}_2\text{Ad}_2)$

A solvent mixture of benzene- d^6 and TMS (25:1) was used to make up a 0.25 cm^3 solution of 3.0 mg of the product. A sample of the same benzene- d^6 /TMS mixture without the dissolved product was sealed in a capillary tube and placed inside the NMR tube containing the solution. The ^1H NMR spectrum showed two resonances corresponding to the TMS protons in the two different solutions (as well as two benzene resonances). The difference in frequency caused by the paramagnetic compound was 35.51 Hz. This value was used to determine the magnetic moment, μ and subsequently the number of unpaired electrons in the complex.⁵ The result of this calculation was a value of $\mu = 3.89 \text{ BM}$ which corresponds to the presence of three unpaired electrons.

Synthesis of $\text{Cp}^{\text{Me}4}_2\text{SnI}_2$ (4.2)



Tin tetraiodide (0.506 g, 0.8 mmol) was dissolved in diethyl ether and cooled to 0°C . $\text{LiCp}^{\text{Me}4}$ (0.1 g, 0.8 mmol) in ether was added dropwise *via* a cannula, turning the mixture a deep orange. The reaction was stirred for 2 h before being allowed to reach ambient temperature and stirred overnight. The solvent was removed under vacuum and

the residue was extracted with cold pentane, giving a dark red-orange solution. The product was recrystallised at -80 °C as dark red needles.

Yield = 0.325 g, 66 %

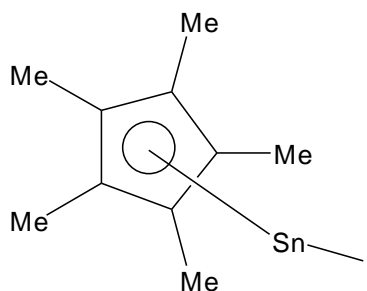
^1H NMR: δ = 4.07 [s, 2H, $^2J(^{117/119}\text{Sn}, ^1\text{H})$ = 166 Hz, C 1 H], 1.64 [s, 12H, $^5J(^{117/119}\text{Sn}, ^1\text{H})$ = 27 Hz, Me 2], 1.58 [s, 12H, $^4J(^{119}\text{Sn}, ^1\text{H})$ = 67 Hz, Me 1]

^{13}C NMR: δ = 139.9 (s, Cp), 122.6 (s, Cp), 84.1 (s, Cp), 13.3 (s, Me), 11.0 (s, Me)

$^{119}\text{Sn}\{^1\text{H}\}$ NMR: δ = -515 (s)

Elemental analysis unavailable due to time constraints.

Synthesis of Cp*SnI (4.3)



Tris(trimethylsilyl)phosphine (2.90 ml, 2.50 g, 0.01 mol) was dissolved in toluene and cooled to -78 °C. Tin tetraiodide (6.28 g, 0.01 mol) was added slowly as a solid, resulting in a yellow solution. Pentamethylcyclopentadienyl potassium (1.74 g, 0.01 mol) was added gradually to the reaction mixture, causing it to turn brown and opaque. The mixture was allowed to warm to ambient temperature and was left stirring for 60 h. When the stirring was ceased a fine precipitate settled out leaving a dark orange solution. The solution was filtered off and the solvent removed under vacuum.

The residue was then extracted with cold pentane to give a pale yellow solution. The product crystallised out at $-30\text{ }^{\circ}\text{C}$ as yellow needles.

Yield = 0.45 g, 12 %

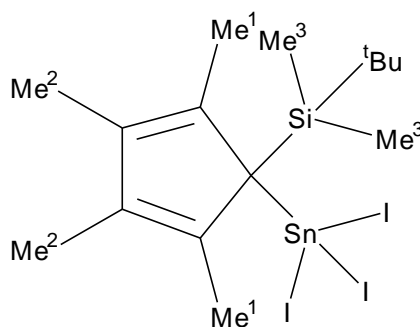
^1H NMR: $\delta = 1.90$ (s, Me)

^{13}C NMR: $\delta = 117.6$ [s, $^1J(^{117/119}\text{Sn}, ^{13}\text{C}) = 31\text{ Hz}$, Cp], 10.0 [s, $^2J(^{117/119}\text{Sn}, ^{13}\text{C}) = 3\text{ Hz}$, Me]

$^{119}\text{Sn}\{^1\text{H}\}$ NMR: $\delta = -1536$ (s, broad)

Anal. Calc. for $\text{C}_{10}\text{H}_{15}\text{SnI}$ (380.82 u): C = 31.54 %, H = 3.97 %. Found: C = 31.55 %, H = 3.89 %

Synthesis of $\text{Cp}^{\text{S}}\text{SnI}_3$ (4.4)



Tin diiodide (0.2 g, 0.54 mmol) was dissolved in diethyl ether and cooled to $0\text{ }^{\circ}\text{C}$. LiCp^{S} (0.13 g, 0.54 mmol) in ether was added dropwise *via* a cannula, turning the mixture a deep orange. The reaction was stirred for 2 h before being allowed to reach ambient temperature and stirred overnight. After about 16 h, the solvent was removed under vacuum. The residue was extracted with cold pentane, giving a dark red-orange solution. The product was recrystallised at $-30\text{ }^{\circ}\text{C}$ as large, dark red needles.

Yield = 0.14 g, 35 % (wrt Cp^{S})

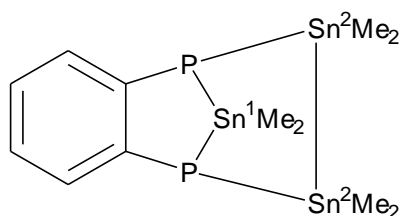
^1H NMR: $\delta = 1.99$ [s, 6H, $^5J(^{117/119}\text{Sn}, ^1\text{H}) = 11$ Hz, Me^2], 1.68 [s, 6H, $^4J(^{117/119}\text{Sn}, ^1\text{H}) = 73$ Hz, Me^1], 0.55 (s, 9H, Me^4), 0.52 (s, 6H, Me^3)

$^{29}\text{Si}\{^1\text{H}\}$ NMR: $\delta = 5.6$ (s)

$^{119}\text{Sn}\{^1\text{H}\}$ NMR: $\delta = -573.2$ (s)

Anal. Calc. for $\text{C}_{15}\text{H}_{27}\text{SiSnI}_3$ (734.85 u): C = 24.52 %, H = 3.70 %. Found: C = 24.41 %, H = 3.79 %

Synthesis of $\text{C}_6\text{H}_4\text{P}_2(\text{SnMe}_2)_3$ (5.1)



1,2-bisphosphinobenzene (0.1 ml, 0.11 g, 0.77 mmol) was dissolved in hexane. A 2.5 M solution of *n*-butyl lithium (0.62 ml, 1.54 mmol) was added dropwise *via* a syringe, instantly forming a bright yellow precipitate. The mixture was then left stirring overnight. Dimethyltin dichloride (0.17 g, 0.77 mmol) was dissolved in hexane and added dropwise to the phosphine mixture at 0 °C causing the colour to fade almost completely. The mixture was stirred for approximately 24 h, after which time the colour had disappeared. The mixture was filtered and the solvent removed under vacuum to leave a powdery white solid. The product was crystallised from hexane as colourless blocks at room temperature by slow evaporation of solvent

Yield = 0.13 g, 77 % (wrt Me_2SnCl_2)

^1H NMR: δ = 7.87 (m, 2H, Bn), 6.75 (m, 2H, Bn), 0.40 [s, 3H, $^2J(^{119}\text{Sn}, ^1\text{H})$ = 46 Hz, Sn^1Me], 0.37 [s, 3H, $^2J(^{119}\text{Sn}, ^1\text{H})$ = 47 Hz, Sn^1Me], 0.24 [s, 6H, $^2J(^{119}\text{Sn}, ^1\text{H})$ = 82 Hz, Sn^2Me], 0.12 [s, 6H, $^2J(^{119}\text{Sn}, ^1\text{H})$ = 48 Hz, Sn^2Me]

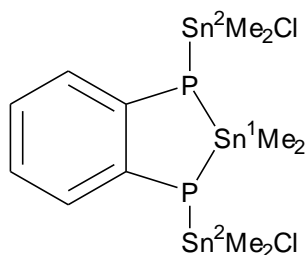
$^{13}\text{C}\{^1\text{H}\}$ NMR: δ = 136 (m, Bn), 126 [t, $J(^{13}\text{C}, ^{31}\text{P})$ = 6 Hz], -8.8 (s, SnMe), -9.7 (s, SnMe), -9.9 (s, SnMe)

$^{31}\text{P}\{^1\text{H}\}$ NMR: δ = -158.2 [s, $^1J(^{119}\text{Sn}, ^{31}\text{P})$ = 698 Hz, $^1J(^{119}\text{Sn}, ^{31}\text{P})$ = 659 Hz, $^2J(^{119}\text{Sn}, ^{31}\text{P})$ = 66 Hz, $^1J(^{117}\text{Sn}, ^{31}\text{P})$ = 629 Hz, $^1J(^{117}\text{Sn}, ^{31}\text{P})$ = 600 Hz, $^2J(^{117}\text{Sn}, ^{31}\text{P})$ = 63 Hz]

$^{119}\text{Sn}\{^1\text{H}\}$ NMR: δ = 126 [t, 1Sn, $^1J(^{119}\text{Sn}, ^{31}\text{P})$ = 698 Hz, Sn^1], -55 [dd, 2Sn, $^1J(^{119}\text{Sn}, ^{31}\text{P})$ = 659 Hz, $^1J(^{119}\text{Sn}, ^{117}\text{Sn})$ = 2724 Hz, Sn^2]

Anal. Calc. for $\text{C}_{12}\text{H}_{22}\text{P}_2\text{Sn}_3$ (584.38 u): C = 24.66 %, H = 3.79 %. Found: C = 22.07 %, H = 3.49 %

Synthesis of $\text{C}_6\text{H}_4\text{P}_2(\text{SnMe}_2)(\text{SnMe}_2\text{Cl})_2$ (5.1b)



Formed as a by product in the synthesis of $\text{C}_6\text{H}_4\text{P}_2(\text{SnMe}_2)_3$.

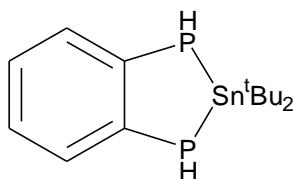
^1H NMR: Not observable beneath $\text{C}_6\text{H}_4\text{P}_2(\text{SnMe}_2)_3$.

$^{31}\text{P}\{^1\text{H}\}$ NMR: δ = -139.1 [s, $^1J(^{119}\text{Sn}, ^{31}\text{P})$ = 750 Hz, $^1J(^{117}\text{Sn}, ^{31}\text{P})$ = 676 Hz, $^1J(^{119}\text{Sn}, ^{31}\text{P})$ = 707 Hz, $^1J(^{117}\text{Sn}, ^{31}\text{P})$ = 644 Hz, $^3J(^{117/119}\text{Sn}, ^{31}\text{P})$ = 7 Hz]

$^{119}\text{Sn}\{^1\text{H}\}$ NMR: $\delta = 58$ [t, 1Sn, $^1J(^{119}\text{Sn}, ^{31}\text{P}) = 750$ Hz, Sn^1], -78 [dd, 2Sn, $^1J(^{119}\text{Sn}, ^{31}\text{P}) = 707$ Hz $^1J(^{119}\text{Sn}, ^{31}\text{P}) = 7$ Hz, Sn^2]

Elemental analysis unavailable due to mixed products.

Synthesis of $\text{C}_6\text{H}_4(\text{PH})_2\text{Sn}^t\text{Bu}_2$ (5.2)



1,2-bisphosphinobenzene (0.1 ml, 0.11 g, 0.77 mmol) was dissolved in hexane. A 2.5 M solution of n-butyl lithium (0.62 ml, 1.54 mmol) was added dropwise *via* a syringe, instantly forming a bright yellow precipitate. The mixture was then left stirring overnight. Di-*tert*-butyltin dichloride (0.24 g, 0.77 mmol) was dissolved in hexane and added dropwise to the phosphine mixture at 0 °C causing the colour to turn slightly orange. The mixture was allowed to warm to ambient temperature and stirred overnight. After approximately 20 h the solution had become completely orange. The mixture was filtered and the solvent removed under vacuum to leave a dark orange oil consisting of a mixture of *meso*- and *rac*- isomers.

Yield = 0.19 g, 68 %

rac- isomer (57.3 %);

^1H NMR: $\delta = 7.71$ (m, 2H, Bn), 6.79 (m, 2H, Bn), 3.86 [d, 2H, $^1J(^1\text{H}, ^{31}\text{P}) = 175$ Hz, PH], 1.18 [s, 18H, $^3J(^{119}\text{Sn}, ^1\text{H}) = 75$ Hz, $^3J(^{117}\text{Sn}, ^1\text{H}) = 72$ Hz, Sn^tBu_2]

$^{13}\text{C}\{^1\text{H}\}$ NMR: $\delta = 136$ (m, Bn), 126.8 [t, $J(^{13}\text{C}, ^{31}\text{P}) = 5$ Hz], 31.4 (s, 6Me), 24.4 (s, CMe_3)

$^{31}\text{P}\{^1\text{H}\}$ NMR: $\delta = -146.8$ [s, $^1J(^{119}\text{Sn}, ^{31}\text{P}) = 679$ Hz, $^1J(^{117}\text{Sn}, ^{31}\text{P}) = 648$ Hz], (d with ^1H coupling $^1J(^1\text{H}, ^{31}\text{P}) = 175$ Hz)

$^{119}\text{Sn}\{^1\text{H}\}$ NMR: $\delta = 147$ [t, $^1J(^{119}\text{Sn}, ^{31}\text{P}) = 679$ Hz]

meso- isomer (42.7 %);

^1H NMR: $\delta = 7.71$ (m, 2H, Bn), 6.79 (m, 2H, Bn), 3.88 [d, 2H, $^1J(^1\text{H}, ^{31}\text{P}) = 176$ Hz, PH], 1.25 [s, 9H, $^3J(^{119}\text{Sn}, ^1\text{H}) = 73$ Hz, $^3J(^{117}\text{Sn}, ^1\text{H}) = 71$ Hz, Sn^tBu], 1.12 [s, 9H, $^3J(^{119}\text{Sn}, ^1\text{H}) = 77$ Hz, $^3J(^{117}\text{Sn}, ^1\text{H}) = 73$ Hz, Sn^tBu]

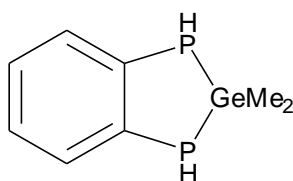
$^{13}\text{C}\{^1\text{H}\}$ NMR: $\delta = 136$ (m, Bn), 126.7 [t, $J(^{13}\text{C}, ^{31}\text{P}) = 5$ Hz], 31.6 (s, CMe_3), 31.0 (s, CMe_3), 23.2 (s, CMe_3), 21.0 (s, CMe_3)

$^{31}\text{P}\{^1\text{H}\}$ NMR: $\delta = -143.0$ [s, $^1J(^{119}\text{Sn}, ^{31}\text{P}) = 678$ Hz, $^1J(^{117}\text{Sn}, ^{31}\text{P}) = 645$ Hz], (d with ^1H coupling $^1J(^1\text{H}, ^{31}\text{P}) = 176$ Hz)

$^{119}\text{Sn}\{^1\text{H}\}$ NMR: $\delta = 136$ [t, $^1J(^{119}\text{Sn}, ^{31}\text{P}) = 678$ Hz]

Elemental analysis unavailable due to oily nature of product.

Synthesis of $\text{C}_6\text{H}_4(\text{PH})_2\text{GeMe}_2$ (5.3)



1,2-bisphosphinobenzene (0.1 ml, 0.11 g, 0.77 mmol) was dissolved in hexane. A 2.5 M solution of n-butyl lithium (0.62 ml, 1.54 mmol) was added dropwise *via* a syringe, instantly forming a bright yellow precipitate. The mixture was then left stirring overnight. Dimethylgermanium dichloride (0.089 ml, 0.13 g, 0.77 mmol) was dissolved in hexane and added dropwise to the phosphine mixture at 0 °C causing the colour to

fade. The mixture was stirred at 0 °C for 2 h before being allowed to warm to ambient temperature and stirred overnight. After approximately 20 h the solution had become completely colourless with a white precipitate. The mixture was cooled back to 0 °C, filtered and the solvent removed under vacuum to leave a sticky white, solid consisting of a mixture of *meso*- and *rac*- isomers.

Yield = 0.14 g, 82 %

rac- isomer (59.8 %);

^1H NMR: δ = 7.64 [s, 2H, Bn], 6.84 [s, 2H, Bn], 3.75 [d, 2H, $^1J(^1\text{H}, ^{31}\text{P}) = 182$ Hz, PH],
0.38 [s, broad, 6H, GeMe₂]

$^{13}\text{C}\{^1\text{H}\}$ NMR: δ = 115.3 (s, Bn), 36.0 (s, 2Me)

$^{31}\text{P}\{^1\text{H}\}$ NMR: δ = -108.9 (s), (d with ^1H coupling $^1J(^1\text{H}, ^{31}\text{P}) = 182$ Hz)

meso- isomer (40.2 %);

^1H NMR: δ = 7.78 [s, 2H, Bn], 6.86 [s, 2H, Bn], 3.78 [d, 2H, $^1J(^1\text{H}, ^{31}\text{P}) = 180$ Hz, PH],
0.59 [s, broad, 3H, GeMe], 0.54 [s, broad, 3H, GeMe]

$^{13}\text{C}\{^1\text{H}\}$ NMR: δ = 128.9 (m, Bn), 47.3 (s, Me), 29.1 (s, Me)

$^{31}\text{P}\{^1\text{H}\}$ NMR: δ = -101.7 (s), (d with ^1H coupling $^1J(^1\text{H}, ^{31}\text{P}) = 180$ Hz)

Anal. Calc. for C₈H₁₂P₂Ge (242.77 u): C = 39.58 %, H = 4.98 %. Found: C = 39.47 %, H = 4.87 %

Substituent exchange between Bn(PH₂)₂ and P(SiMe₃)₃

An NMR tube was charged with 1,2-bis(phosphino)benzene (0.009 ml, 0.01 g, 0.07 mmol), tris(trimethylsilyl)phosphine (0.02 ml, 0.018 g, 0.07 mmol) and benzene-d₆. The mixture was degassed and heated to 50 °C for approximately 16 weeks, after which an equilibrium appeared to have been reached.

³¹P{¹H} NMR:

Meso-Bn(PHSiMe₃)₂ δ = -116.5 (s, 2P)

Bn(PH₂)(PHSiMe₃) δ = -120.8 [d, 1P, ³J(³¹P, ³¹P) = 71 Hz, PH₂],

-124.1 [d, 1P, ³J(³¹P, ³¹P) = 71 Hz, PH]

Rac- Bn(PHSiMe₃)₂ δ = -125.5 (s, 2P)

PH₂(SiMe₃) δ = -235.3 (s, 1P)

PH(SiMe₃)₂ δ = -236.2 (s, 1P)

PH₃ δ = -241.1 (s, 1P)

References

1. Sheldrick, G. M., *SHELX-97, Program for the Refinement of Crystal Structures*, Göttingen, 1997
2. Constantine, S. P., Hitchcock, P. B., Lawless G. A., De Lima, G. M., *Chem. Commun.*, 1996, 1101
3. Wettling, T., Geissler, B., Barth, S., Schneider, R., Binger, P., Regitz, M., *Angew. Chem. Int. Ed. Engl.*, 1992, **31**, 758
4. Becker, G., Holdrich, W., *Chem. Ber.*, 1975, **108**, 2484
5. (a) Evans, D. F., *J. Chem. Soc.*, 1959, 2003 (b) Evans, D. F., Fazakerley, G. V., Phillips, R. F., *J. Chem. Soc. A.*, 1971, 1931 (c) De Buysser, K., Herman, G. G., Bruneel, E., Hoste, S., Van Dreissche, I., *Chem. Phys.*, 2005, **315**, 286